INORGANIC CHEMISTRY
FRONTIERS

REVIEW

View Article Online
View Journal

Check for updates

Cite this: DOI: 10.1039/d6qi00639f

Hydrosilanes. From laboratory curiosity to semiconductors

Daniel Griess,[a,b] Madeleine Heurix,[a,b] Matthias Paris,[a,b] Philomena Vatter[a,b] and Michael Haas *[a,b]

Received 1st April 2026,
Accepted 23rd April 2026

DOI: 10.1039/d6qi00639f

rsc.li/frontiers-inorganic

Hydrosilanes represent a versatile class of silicon compounds that bridge fundamental main-group chemistry with technologically relevant materials science. Since the early discovery of monosilane in the nineteenth century, the chemistry of silicon hydrides has evolved from a laboratory curiosity into a cornerstone of modern semiconductor processing and silicon materials synthesis. This review provides a comprehensive overview of hydrosilane chemistry, focusing on three central aspects: (i) synthetic approaches to mono- and oligohydrosilanes, (ii) their functionalization through silanide intermediates and related transformations, and (iii) their application as molecular precursors for silicon-based materials and deposition technologies.

Introduction

Hydrosilanes are a class of silicon-based compounds that have gained significant attention due to their unique chemical reactivity and broad applications in material science and nanotechnology. Although silicon chemistry shares some conceptual similarities with the more extensively explored realm of carbon chemistry, it boasts its own distinct characteristics and complexities. Unlike their carbon-based counterparts, hydrosilanes exhibit distinctive properties owing to the weaker Si–Si bonds and the polar nature of Si–H bonds. These properties make hydrosilanes highly reactive and suitable for various applications, including silicon deposition, semiconductor processing, hydrogen storage, and the development of next-generation optoelectronic materials. Their role in forming advanced silicon-based nanostructures has also sparked interest in fields such as catalysis and biomedical research.

Recent advances in hydrosilane chemistry have focused on improving their synthetic accessibility, stability, and processability. Methods such as reductive coupling, dehydrogenative coupling, plasma synthesis, and chloride-induced disproportionation have been explored to optimize their production. Additionally, applications in printable electronics, thin-film solar cells, and silicon-based nanostructures have further driven research in this field. Several reviews and reference works have summarized aspects of hydrosilane chemistry over the past decades. Early comprehensive treatments can be found in clas-

[a]Institute of Inorganic Chemistry, Graz University of Technology, Stremayrgasse 9/IV, 8010 Graz, Austria. E-mail: michael.haas@tugraz.at
[b]Christian Doppler Laboratory for New Semiconductor Materials based on Functionalized Hydrosilanes, Stremayrgasse 9/IV, 8010 Graz, Austria

Daniel Griess

Daniel Griess MSc obtained his Master's degree in Chemistry in 2024 under the supervision of Prof. Rolf Breinbauer. He is currently a Ph.D. student in Haas' group at the Institute of Inorganic Chemistry at Graz University of Technology (Austria). His research interests cover mainly the synthesis of aminosilanes.

Madeleine Heurix

DI Madeleine Heurix obtained her Master's degree in Chemistry in 2024 under the supervision of Dr Michael Haas. She is currently a Ph.D. student in Haas' group at the Institute of Inorganic Chemistry at Graz University of Technology (Austria). Her research interests cover mainly the synthesis of oligohydrogermanes and silylgermanes.

Open Access Article. Published on 24 April 2026. Downloaded on 5/15/2026 8:48:04 PM.
This article is licensed under a Creative Commons Attribution 3.0 Unported Licence.

Open Access Article. Published on 24 April 2026. Downloaded on 5/15/2026 8:48:04 PM. This article is licensed under a Creative Commons Attribution 3.0 Unported Licence.

sical sources such as the *Gmelin Handbook of Inorganic Chemistry*, as well as survey articles and encyclopedia entries published during the 1980s and 1990s.[1,2] These works primarily focused on the fundamental properties, preparation, and industrial relevance of simple silanes. Later contributions,[3] including chapters in *Comprehensive Inorganic Chemistry II*,[4] expanded on these topics but remained largely centered on established synthetic methodologies and basic silicon hydride chemistry.

More recently, a review by Gerwig, Böhme, and Friebel has revisited the field with emphasis on hydrosilanes; however, this work mainly addresses hydrosilanes themselves and does not cover the broader chemistry of higher hydrosilanes, their functionalization, and their emerging roles as precursors for modern deposition technologies.[5] Therefore, despite the availability of these valuable contributions, a comprehensive and updated overview connecting classical hydrosilane chemistry with recent developments in functionalization and materials applications remains highly desirable.

Consequently, this review summarizes the broad field of hydrosilanes in terms of their synthesis (i), their functionalization (ii) and, if investigated, their applicability with respect to several deposition techniques (iii).

This review does not deal with hydrosilanes, which have only one hydride R_3SiH (*e.g.*: $(Me_3Si)_3SiH$, Ph_3SiH, or $HPh_2SiSiPh_2H$ *etc.*), as in these cases the organic substituents largely dominate the chemical reactivity. Furthermore, molecular species of the type R_2SiH_2 (*e.g.*: $(Me_3Si)_2SiH_2$, Ph_2SiH_2, or Et_2SiH_2 *etc.*) are likewise excluded for the same reason. However, R_2SiH_2 units within higher silicon hydrides and Si–Si bonded systems are implicitly included in this review. For reviews about hydrosilylation the reader is referred to two very recent publications.[6] For a summary of inorganic tetrylenes the reader is referred to the excellent review of Rivard.[7]

Historical development

The classical approach is the reaction of silicides with diluted acids. The pioneers in this field were F. Wöhler and H. Buff, who synthesized SiH_4 by the reaction of diluted acids with aluminium silicides.[8] In 1902, H. Moissan and S. Smiles identified Si_2H_6 as another product formed by this reaction.[9] Between 1919 and 1921 A. Stock and K. Somieski pioneered the field of organosilanes and aminosilanes with the synthesis of methylsilane[10] and aminosilanes with trisilylamine.[11] In the following years they showed that also higher homologs of the series Si_nH_{2n+2} were formed.[10] G. Fritz was able to obtain the first silylphosphane in 1953 by pyrolysis of PH_3 and SiH_4 [12] and in 1955 B. J. Aylett, H. J. Emeléus and A. G. Maddock were able to obtain evidence of the existence of trisilylphosphane.[13] The next milestone in the synthesis of hydrosilanes was achieved by F. Fehér and co-workers, who used the same methodology and implemented procedures for a targeted isolation up to Si_8H_{18} on a preparative scale. His scientific life is excellently portrayed in M. Baudler's reminiscence.[14] M. A. Ring and D. M. Ritter were the first to report the synthesis of silyl potassium $KSiH_3$.[15] E. Amberger and H. Boeters were the first to isolate and report the properties of trisilylphosphane in 1962.[16]

A change in the paradigm was the targeted synthesis of the first cyclic hydrosilane derivatives by E. Hengge and co-workers in 1973.[17]

In 1993 W. Sundermeyer reported the synthesis of branched silylgermanes, demonstrating the structural diversity accessible in mixed silicon–germanium hydride systems.[18]

13 years later T. Shimoda and co-workers demonstrated that these higher silanes have an application as precursors for liquid phase deposition (LPD).[19] This landmark development resulted in a boom of this chemistry with many groups in academia and industry working on the implementation of solution-based deposition in several industrial processes. In 2015, M. Wagner and co-workers reported the synthesis of silafullerens, expanding the structural landscape of silicon-based cluster chemistry.[20]

In 2017 H. Stueger and co-workers published the synthesis of 2,2,3,3,4,4-hexasilylpentasilane, which is to date the highest isolated hydrosilane on preparative scale.[21] Recently our group pioneered the use of functionalized hydrosilanes as precursors for LPD.[22] In summary this can be seen as a showcase example of an ideal workflow in science. Starting from the very funda-

Matthias Paris

DI Matthias Paris obtained his Master's degree in Chemistry in 2024 under the supervision of Dr Michael Haas. He is currently a Ph.D. student in Haas' group at the Institute of Inorganic Chemistry at Graz University of Technology (Austria). His research interests cover mainly the synthesis of silanides.

Philomena Vatter

Philomena Vatter BSc obtained her Bachelor's degree in Chemistry in 2024 from Karl Franzens University Graz with thesis supervison from Prof. Tremel at JGU Mainz. She is currently a Master's student in Haas' group at the Institute of Inorganic Chemistry at Graz University of Technology (Austria). Her research interests cover mainly the liquid phase deposition of functionalized hydrosilanes.

This journal is © the Partner Organisations 2026

Open Access Article. Published on 24 April 2026. Downloaded on 5/15/2026 8:48:04 PM.
This article is licensed under a Creative Commons Attribution 3.0 Unported Licence.

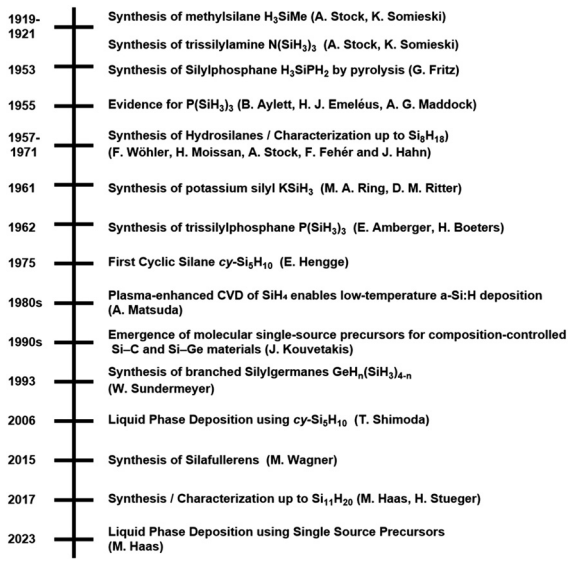

Fig. 1 Historical development.

mental studies to the several applications. In Fig. 1 the historical development of this research topic is summarized.

Silane synthesis

Hydrolysis of silicides

The hydrolytic decomposition of silicides with aqueous acids was first observed by Wöhler and Buff in 1857, marking the first documented formation of a silicon- and hydrogen-containing compound.[8] Subsequently, in 1902, Moissan and Smiles were the first to characterize SiH_4 along with higher hydrosilanes following the decomposition of magnesium silicide with aqueous HCl.[9] This discovery laid the foundation for the use of silicide hydrolysis as a commonly applied method for silane synthesis. The reaction produces monosilane (SiH_4) alongside disilane (Si_2H_6) and minor amounts of higher hydrosilanes. The yield and product distribution are highly dependent on factors like purity of Mg_2Si, the solvent and acid used, and overall reaction conditions. Stock implemented extensive studies on this topic and successfully isolated and characterized higher silanes, including tetrasilane (Si_4H_{10}), pentasilane (Si_5H_{12}) and hexasilane (Si_6H_{14}) (see Scheme 1). The application of preparative gas chromatography further enabled the separation and identification of both linear and branches silanes up to octasilane (Si_8H_{18}).[23–25] Fehér expanded upon these studies by investigating the hydrolysis of Mg_2Si using sulfuric and phosphoric acid, leading to the formation and identification of silanes up to pentadecasilane ($Si_{15}H_{32}$). Moreover, distinct linear silanes up to heptasilane (Si_7H_{16}), as well as branched species such as 2-silyltrisilane, 2-silyltetrasilane and 2-silylpentasilane, were isolated and characterized.[26]

Johnson reported that using ammonium bromide (NH_4Br) in liquid ammonia instead of aqueous HCl increased silane yields to 80–90%.[27]

Hydrogenation of chlorosilanes

The hydrogenation of chlorosilanes with mild reducing agents such as lithium aluminium hydride ($LiAlH_4$) or diisobutylaluminium hydride (i-Bu_2AlH) is a well-established method for synthesizing hydrosilanes on a laboratory scale (see Scheme 2). However, this approach is limited by the availability of chlorosilane precursors and side reactions involving Si–Si bond cleavage (especially $LiAlH_4$ results in the cleavage of silyl groups).

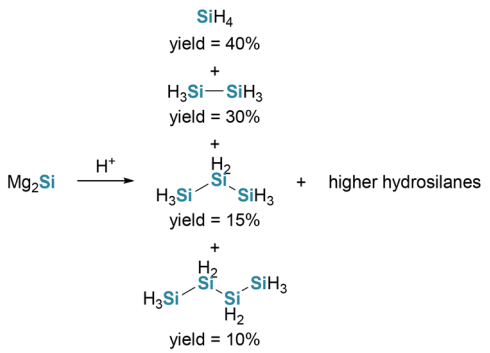

Scheme 1 Synthesis of monosilane and oligohydrosilanes with product distribution according to the work of Stock *et al.*

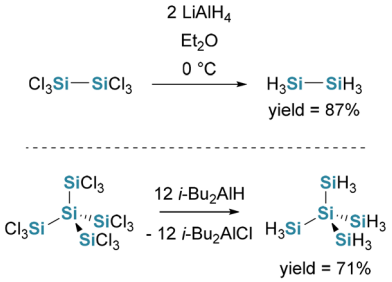

Scheme 2 Formation of oligohydrosilanes *via* the hydrogenation of chlorosilanes.

Michael Haas

Prof. Michael Haas received his Ph.D. under the supervision of Prof. H. Stueger. He subsequently carried out postdoctoral research at Monash University (Australia) in the group of Prof. C. Jones. He is currently a group leader at Graz University of Technology (Austria). His research interests include the enolate chemistry of heavier carbon homologues, silane chemistry, liquid-phase deposition of silicon heterostructures, and the design of new group 14 photoinitiators.

Open Access Article. Published on 24 April 2026. Downloaded on 5/15/2026 8:48:04 PM. This article is licensed under a Creative Commons Attribution 3.0 Unported Licence.

Finholt *et al.* first reported this reaction in 1947, demonstrating the formation of disilane (Si_2H_6) *via* the reduction of hexachlorosilane (Si_2Cl_6) with $LiAlH_4$ (see Scheme 2). The yield of hydrosilanes varies significantly depending to reaction conditions and chlorosilane employed.[28] In 1973, Höfler reported the formation of neopentasilane, short NPS, (*neo*-Si_5H_{12}) *via* the hydrogenation of dodecachloroneopentasilane (*neo*-Si_5Cl_{12}) with $LiAlH_4$, though low yields were observed due to Si–Si bond cleavage. The use of i-Bu_2AlH instead of $LiAlH_4$ improved selectivity and increased product yields.[29]

The Litz–Ring process (see Scheme 3), while primarily employed for the reduction of tetrachlorosilane ($SiCl_4$) to monosilane using alkali metal hydrides regenerated *in situ* by molten-salt electrolysis, has also been investigated for related hydride-mediated silicon transformations. The process enables continuous, high-yield production of ultra-pure monosilane and was demonstrated at pilot scale with strong industrial relevance for low-cost, high-purity silicon production for semiconductors.[30]

Hengge *et al.* reported the synthesis of the cyclic hydrosilanes, cyclopentasilane (*cy*-Si_5H_{10}) and cyclohexasilane (*cy*-Si_6H_{12}) *via* the hydrogenation of their respective cyclic chlorosilanes using $LiAlH_4$, achieving excellent yields (see Scheme 4).[31]

In 2013, Kroke and co-workers reported the successful crystallization of cyclopentasilane, enabling its structural characterization by X-ray diffraction (see Fig. 2).[32]

An alternative approach involves the reduction of $[Si_6Cl_{14}]^{2-}$ complexes, which are generated from $HSiCl_3$ through a redistribution reaction, facilitated by alkylated amines such as tetraethylenediamine (TEEDA) or pentaethyldiethylenetriamine (PEDETA) and the presence of a base like ethyldiisopropylamine (EDIPA). The resulting hexacoordinate species can then be hydrogenated with $LiAlH_4$, yielding *cy*-Si_6H_{12} (see Scheme 5).[33] Wagner and co-workers have further explored the rich amine-mediated chemistry of chlorosilanes and related silicon cluster species; a comprehensive overview of this chemistry can be found in their review.[34]

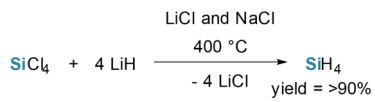

Scheme 3 Simplified Litz–Ring process.

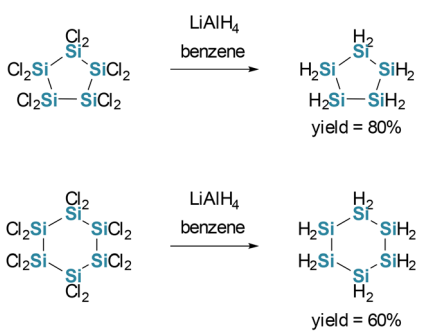

Scheme 4 Hydrogenation of cyclic chlorosilanes.

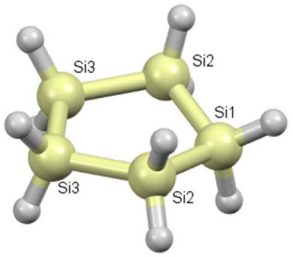

Fig. 2 Crystal structure of Si_5H_{10} adapted from original literature by Kroke and co-workers.

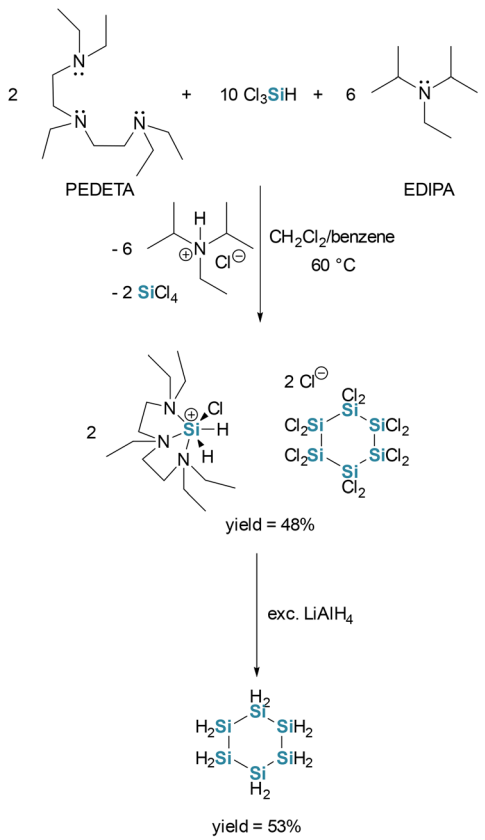

Scheme 5 Synthesis of cyclohexasilane *via* the reduction of the $[Si_6Cl_{14}]^{2-}$ complexes.

The first synthesis of an unsubstituted bicyclic halosilane, bi(cylclopentasilanyl), was reported by Stueger, Lassacher and Hengge in 1995.[35] The key intermediate bis(nonachlorocyclopentasilanyl) is obtained either by Hg-mediated coupling of nonachlorocyclopentasilane using $(t\text{-Bu})_2Hg$ in *n*-heptane or by catalytic phenyl abstraction from the perphenylated bicyclic compound with $HCl/AlCl_3$, both routes affording $Si_{10}Cl_{18}$ in good yields. Subsequent hydride reduction with $LiAlH_4$ at −40 °C selectively converts the Si–Cl functionalities into Si–H bonds, yielding the unsubstituted bicylic $Si_{10}H_{18}$ (see

This journal is © the Partner Organisations 2026

Open Access Article. Published on 24 April 2026. Downloaded on 5/15/2026 8:48:04 PM.
This article is licensed under a Creative Commons Attribution 3.0 Unported Licence.

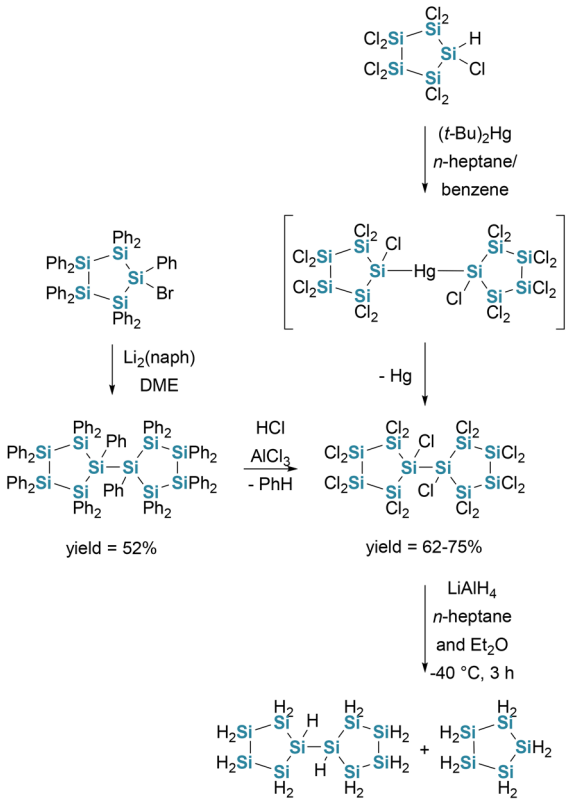

Scheme 6 Synthesis of bicyclic hydrosilane. Yields of the final product not reported since it could not be separated from the side-product (*cy*-Si_5H_{10}).

Scheme 6). This reduction is accompanied by the partial cleavage of the central Si–Si bond, leading to approximately 15% cyclopentasilane (*cy*-Si_5H_{10}) as a side product.

Disproportionation of chlorosilanes

The disproportionation is the main large-scale method used nowadays for the production of monosilane (SiH_4). Trichlorosilane ($HSiCl_3$) undergoes disproportionation in the presence of a catalyst (*e.g.* $AlCl_3$, $ZnCl_2$, BCl_3, $FeCl_3$). The reaction leads to the formation of SiH_4 in high purity alongside $SiCl_4$. The process is continuous and operates in a closed-loop system, allowing recycling of $SiCl_4$ (see Scheme 7).[36]

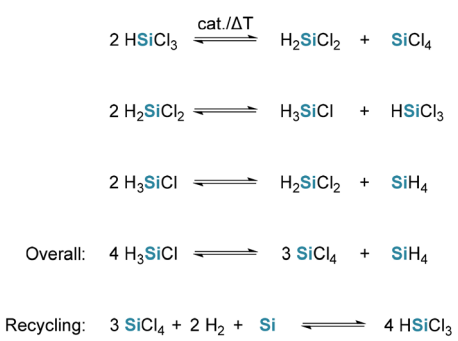

Scheme 7 Large-scale production of SiH_4.

Direct synthesis of Si and H_2

It is also possible to synthesize monosilane and also higher hydrosilanes from silicon powder and hydrogen in the presence of catalytic amounts of H_2S or various sulfides (see Scheme 8). The product distribution is controlled by the H_2 pressure. However, this method requires high temperatures and pressures, making it less practical compared to other methodologies.[37]

Catalytic dehydrogenative coupling

The formation of Si–Si bonds from monosilane (SiH_4) can be achieved through dehydrogenative coupling reactions, in which primary and secondary organomonosilanes undergo hydrogen abstraction in the presence of a catalyst (see Scheme 9). Such reactions typically require transition metal complexes from group 4 to 10 which work as catalysts.[38]

Harrod was the first to report the catalytic formation of higher hydrosilanes from SiH_4 in 1988.[39] Building on this work, Okumura *et al.* demonstrated the synthesis of disilane (Si_2H_6) and trisilane (Si_3H_8) *via* catalytic condensation of SiH_4 using platinum, rhodium and ruthenium-based complexes.[40] Moreover, *n*-tetrasilane was afforded *via* catalytic conversion of SiH_4, Si_2H_6 and Si_3H_8.[41] However, a significant challenge associated with these approaches is the concurrent formation of insoluble polymeric byproducts, which can negatively impact selectivity and complicate product isolation.

Wurtz-type coupling

A Wurtz-type approach to hydrosilane synthesis was introduced by Craig *et al.* in 1962, involving the reaction of iodosilane (H_3SiI) with a liquid sodium/mercury amalgam at room temperature (see Scheme 10).[42]

This method resulted in the formation of disilane with a reported yield of 67%.[42] However, the broader application of this method remains limited, as alkali metals tend to also react with Si–H bonds.

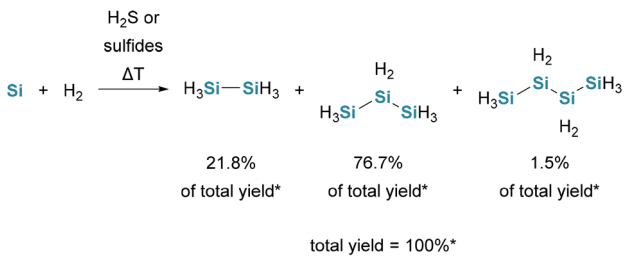

Scheme 8 Reaction of Si-powder and hydrogen at high temperatures. *Product distribution and total yield when CuS is used as the catalyst.

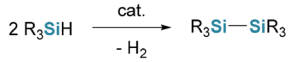

Scheme 9 Schematic equation for dehydrogenative coupling of silanes.

Open Access Article. Published on 24 April 2026. Downloaded on 5/15/2026 8:48:04 PM.
This article is licensed under a Creative Commons Attribution 3.0 Unported Licence.

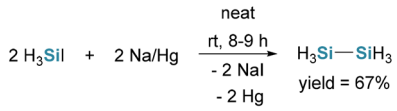

Scheme 10 Synthesis of disilane (Si_2H_6) *via* Wurtz-type coupling.

An alternative route to higher hydrosilanes involves the nucleophilic substitution of halosilanes with silanide anions at low temperatures (see Scheme 11).[43,44] A detailed discussion on the synthesis of silanides follows in Functionalization with group 1 (synthesis of silanides).

This method not only enables the formation of linear oligomers but also the synthesis of branched silanes, such as neopentasilane (*neo*-Si_5H_{12}) and neohexasilane ($Si(SiH_3)_3(Si_2H_5)$) (see Scheme 12). These branched species can be obtained through the reaction of phenylchlorosilane with a mixture of different potassiumsilanides ($KSiH(SiH_3)_2$, $KSi(SiH_3)_3$ and $KSi(SiH_3)_2(Si_2H_5)$) followed by sequential bromination and reduction of the resulting phenyl-substituted oligosilanes using HBr and $LiAlH_4$, respectively. Nevertheless, the separation and isolation of the individual products was not reported.[45]

Building on Fehér's work on silanide synthesis (see Functionalization with group 1 (synthesis of silanides)), Sundermeyer and co-workers investigated the protonation of higher silanides (KSi_nH_{2n+1}) with phenylsulfonic acid ($PhSO_3H$) resulting in a mixture of various branched hydrosilanes with the general formula $(SiH_{4-n}(SiH_3)_n)$.[46,47]

However, they noted that a selective synthesis of higher silanides could not be achieved under the investigated conditions, consequently the reactions were leading to mixtures or less well-defined products.

Stueger *et al.* demonstrated that $LiSi(SiH_3)_3$ (prepared from isolated neopentasilane) reacts selectively with $SiCl_2Ph_2$ to form the branched nonasilane $(SiH_3)_3SiSiPh_2Si(SiH_3)_3$. Subsequent dephenylation using triflic acid, followed by hydrogenation with i-Bu_2AlH, resulted in the formation of 2,2,4,4-tetrasilylpentasilane in good overall yield (see Scheme 13).[48,49]

In addition, an alternative synthesis of 2,2,4,4-tetrasilylpentasilane was achieved independently by two groups. While Dow Corning employed borosilicate glass surfaces to promote the conversion of neopentasilane,[50] the groups led by Stueger and Haas, as well as Evonik, demonstrated that 2,2,4,4-tetrasilylpentasilane also forms in the presence of a Lewis acid (see Scheme 14).[51]

In addition, Haas *et al.* turned to an alternative method inspired by earlier work of Gilman and Harrell.[52] In this approach, 0.5 equiv. of dibromoethane ($BrCH_2CH_2Br$) were added to $LiSi(SiH_3)_3$ at −80 °C, leading the formation of 2,2,3,3-tetrasilyltetrasilane (a branched octasilane) shown in Scheme 15 accompanied by minor amounts of 2,2,3,3,4,4-hexasilylpentasilane (a branched undecasilane). This reaction is driven by an initial halogen–metal exchange, forming $BrSi(SiH_3)_3$ as key intermediate.[21]

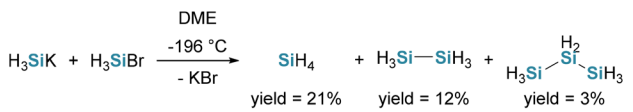

Scheme 11 Formation of mono-, di-, and trisilane *via* Wurtz-type coupling.

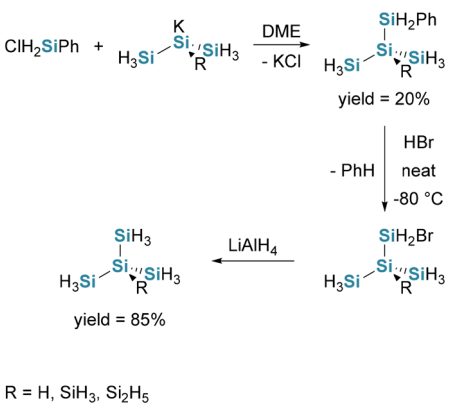

Scheme 12 Formation of branched silanes in a 3-step synthesis.

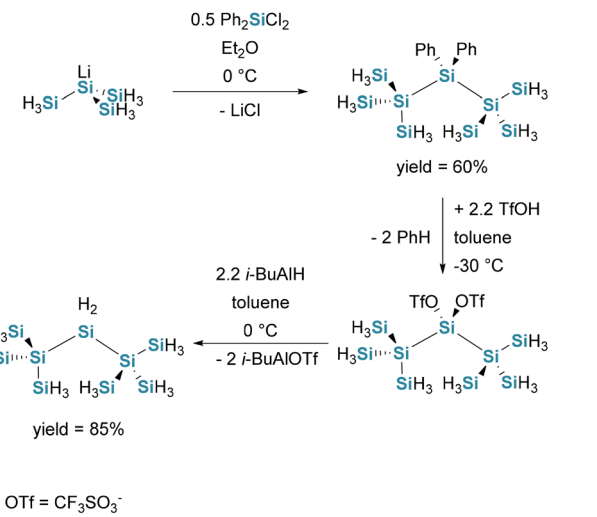

Scheme 13 Synthesis of $(SiH_3)_3SiSiPh_2Si(SiH_3)_3$ and subsequent treatment with TfOH and i-BuAlH.

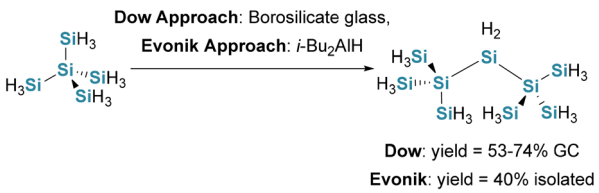

Scheme 14 Alternative synthesis of 2,2,4,4-tetrasilylpentasilane.

This journal is © the Partner Organisations 2026

Open Access Article. Published on 24 April 2026. Downloaded on 5/15/2026 8:48:04 PM.
This article is licensed under a Creative Commons Attribution 3.0 Unported Licence.

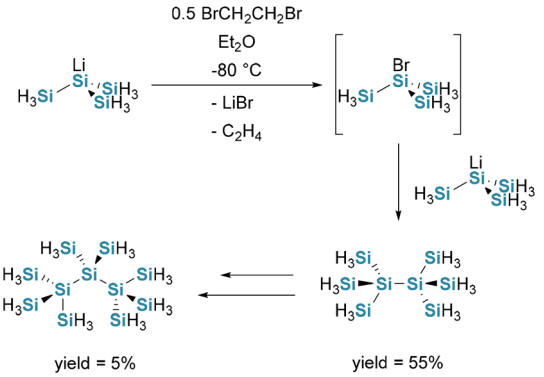

Scheme 15 Synthesis of branched octasilane with minor amounts of branched undecasilane.

Moreover, Stueger and co-workers successfully obtained crystals of the branched undecasilane appropriate for X-ray diffractometry (see Fig. 3).[21]

Impact of energy on SiH_4

An alternative route to higher hydrosilanes involves energy-induced transformation of monosilane, such as by pyrolysis, photolysis, or electrical discharge (see Scheme 16). These approaches rely on the homolytic cleavage of Si–H and Si–Si bonds, promoting the stepwise build-up of longer-chained silanes.

The most straightforward method employs thermal energy. As early as 1950, Fritz demonstrated that disilane could be synthesized through the pyrolysis of monosilane. Continued pyrolysis of disilane leads to the formation of trisilane, while further thermal treatment of trisilane results in the generation of tetrasilane, indicating that this process enables chain elongation through successive decomposition and recombination steps.[53,54]

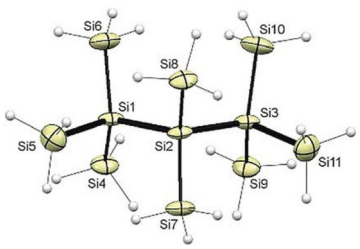

Fig. 3 Crystal structure from 2,2,3,3,4,4-hexasilylpentasilane (a branched undecasilane). Reproduced from Haas *et al.*[21] with permission from Angewandte Chemie International Edition, © 2017.

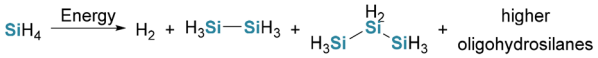

Scheme 16 Impact of energy on SiH_4. Total yield and product distribution depends on the energy source and reaction conditions.

In addition to thermal activation, monosilane can also be exposed to silent electrical discharge within an ozonizer. This method yields a mixture of disilane, trisilane, and smaller amounts of higher homologues.[2,55] A further photochemical approach involves the irradiation of SiH_4 with ultraviolet light. When mercury is employed as a photosensitizer, a distribution of di-, tri-, and higher silanes can be generated.[56]

Silafullerenes

A major conceptual advance in silicon hydride chemistry was achieved with the realization of silafullerenes, more precisely endohedral silafullerenes (see Fig. 4), by Wagner and co-workers in 2015–2021.[20,57] Building on earlier theoretical predictions that halide ions could template silicon cages, they reported the synthesis of the dodecahedral silicon cluster $[Cl@Si_{20}H_{20}]^-$, the silicon analogue of the smallest fullerene $C_{20}H_{20}$ (see Scheme 17).

The synthesis proceeds *via* controlled stepwise reduction of perchlorinated precursor, ultimately converting all exohedral Si–Cl bonds into Si–H functionalities while preserving an encapsulated chloride ion at the centre of the cage. Although formally ionic compounds and therefore isolated as a salt with a counter-cation, the cluster is structurally and chemically dominated by twenty-terminal Si–H bonds. As such, these silafullerenes represent a unique class of molecular hydrosilanes, bridging classical neutral hydrosilanes and anionic silicon clusters, and they offer a hydrogen-terminated silicon surface that is amenable to further functionalization while being stabilized by the endohedral Cl^- template.

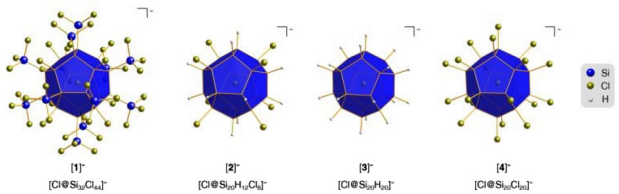

Fig. 4 Crystal structures from silafullerenes by Wagner *et al.* Reproduced from ref. 57 with permission from Journal of American Chemical Society, © 2021.

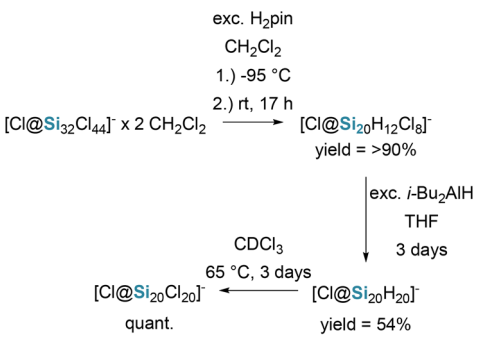

Scheme 17 Formation of silafullerenes by Wagner *et al.*

Open Access Article. Published on 24 April 2026. Downloaded on 5/15/2026 8:48:04 PM. This article is licensed under a Creative Commons Attribution 3.0 Unported Licence.

Silane derivatization

Functionalization with group 1 (synthesis of silanides). In recent years, alkali silanides $MSiH_3$ (M = Li, Na, K, Rb, Cs) have emerged as promising complex hydrides for solid-state hydrogen storage, showing reversible hydrogenation/dehydrogenation with their parent MSi phases and practical capacities near ambient conditions.[58] Recent studies have demonstrated favourable thermodynamics that enable hydrogen uptake and release under moderate operating windows, and catalytic approaches have further improved kinetics while maintaining reversibility.[59] Collectively, these advances position $MSiH_3$ as viable candidates that have been actively tested and refined for practical hydrogen storage applications.[60]

Furthermore, alkali metal silanides with the general formula MSi_xH_y (M = Li, Na, K, Rb, Cs) serve as versatile precursors for subsequent functionalization, enabling the incorporation of diverse heteroatoms while preserving the Si–H functionality. The scope and methodology of these transformations are discussed in detail in this review.

In 1961, Ring and Ritter reported the formation of potassium silanide ($KSiH_3$) by reducing monosilane with potassium metal in DME. Reaching 75–100% consumption of silane required about two months (see Scheme 18, path a). A Na/K alloy greatly accelerated the process, achieving 92% SiH_4 consumption in 14 days (see Scheme 18, path b). They also showed that KH reacts with disilane to give quantitative conversion within one day, whereas lithium hydride (LiH) affords only 12% conversion after 48 hours (see Scheme 18, path c). Although isolated yields were not determined directly, subsequent reactions of $KSiH_3$ proceeded in essentially quantitative yield.[15]

Hagenmuller and Pouchard prepared sodium silanide ($NaSiH_3$) by introducing SiH_4 into a finely dispersed suspension of Na in DME. Under these conditions, both reactants partially (approx. 20%) dissolve within 6 hours in equimolar proportions, affording a yellowish solution. However, the resulting $NaSiH_3$ solution is unstable and undergoes decomposition under the synthesis conditions.[61]

In 1966 Kennedy *et al.* reported a significant improvement in the preparation of potassium silanide by reacting disilane with potassium sand at −78 °C, achieving complete conversion to $KSiH_3$ within 24–48 h.[43]

Subsequent studies by Amberger and Römer demonstrated that using a K/Na alloy (5 : 1 w/w) in DME or diglyme affords full conversion to $KSiH_3$ at room temperature within 3 days. In contrast, THF and 2,2-dimethyl-1,3-dioxolane give slower reactions. While triglyme accelerates the conversion further, the resulting $KSiH_3$ solutions are less stable than those obtained in DME or diglyme. Notably, the addition of diethyl ether (Et_2O) to solutions of $KSiH_3$ induces precipitation of a white, crystalline solid that retains its reactivity under N_2 or vacuum and can be fully redissolved thereafter.[62]

Cradock, Gibbon, and van Dyke later showed that hexamethylphosphoramide (HMPA) enables complete conversion to $NaSiH_3$ and $KSiH_3$ at 10 °C within just 15 minutes. However, isolation of the free silanides from HMPA proved unsuccessful due to the high boiling point of the solvent and the high solubility of the products, which prevented precipitation upon addition of nonpolar solvents (see Scheme 19).[63]

Amberger, Römer, and Layer undertook a detailed study of alkali-metal reactivity in DME and diglyme, establishing a clear increase in rate down group 1 (Na < K < Rb < Cs). Relative to sodium, caesium reduced the time required to reach full conversion by up to 92%. Under otherwise comparable conditions, diglyme generally afforded faster conversions than DME (see Scheme 20, path a and b). Mixed-metal systems offered additional benefits: an Rb/Na alloy shortened reaction times relative to rubidium alone (see Scheme 20, path c). By contrast, an Na/Hg amalgam was distinctly sluggish, reaching only 17% conversion after 23 days (see Scheme 20, path d). Isolation of discrete $MSiH_3$ (M = Na, K, Rb, Cs) was not attempted; instead, the reactive solutions were directly subjected to subsequent functionalization.[64]

Bürger and Eujen were the first in 1974 to study the generation of higher silanides in more detail. They used K or $KSiH_3$ and reacted it with varying equivalents of silanes with the formula Si_nH_{2n+1} (n = 1–3) and were able to prove *via* nuclear magnetic resonance (NMR) spectroscopy the existence of $KSiH_n(SiH_3)_{3-n}$ (n = 1–3). When reacting $KSiH_3$ with an excess of SiH_4 they observe next to $KSiH_3$ the formation of KSi_2H_5 (see Scheme 21, path a). On the other hand, upon the reaction of K with di- or trisilane, or $KSiH_3$ with trisilane they report the formation of the higher silanides $KSiH_n(SiH_3)_{3-n}$ (n = 1–3) (see Scheme 21, path b). Furthermore, they note that when an excess of trisilane is used the main product is $KSi(SiH_3)_3$ (see Scheme 21, path c), and an excess of K leads to cleavage of Si–Si-bonds. Finally, when they reacted the formed silanides with HCl, they always observe SiH_4 and Si_2H_6 next to small amounts of the expected silanes Si_nH_{2n+2}.[65]

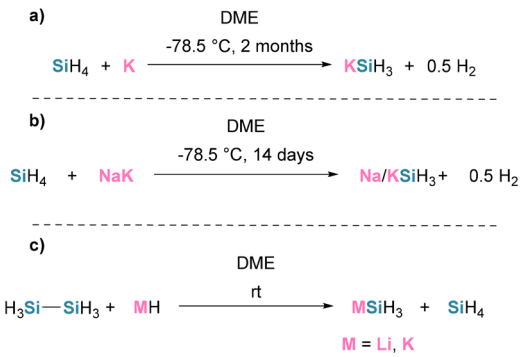

Scheme 18 Synthesis of $MSiH_3$ *via* reduction (path a–c). No yields were reported.

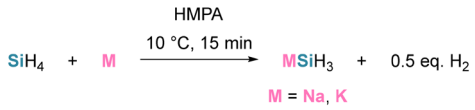

Scheme 19 Synthesis of $MSiH_3$ in HMPA. Isolation of the silanide failed.

This journal is © the Partner Organisations 2026

Open Access Article. Published on 24 April 2026. Downloaded on 5/15/2026 8:48:04 PM.
This article is licensed under a Creative Commons Attribution 3.0 Unported Licence.

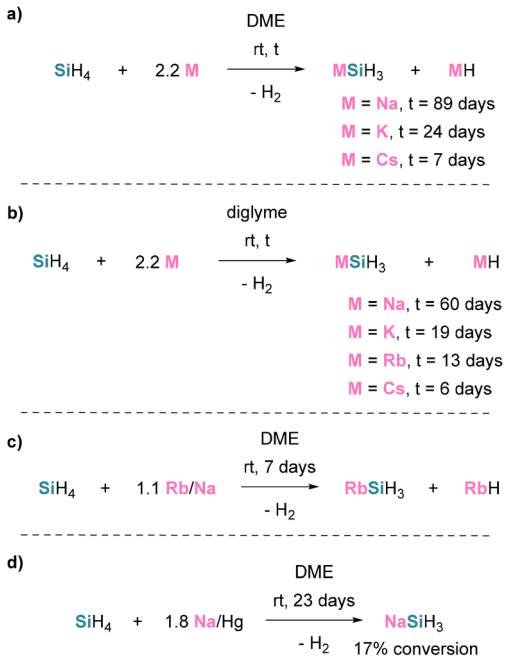

Scheme 20 Synthesis of $MSiH_3$ by Amberger, Römer, and Layer (path a–d). No yields were reported.

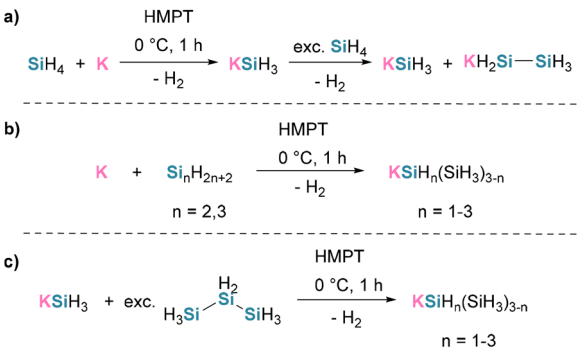

Scheme 21 Synthesis of higher silanides, isolated yields no reported (path a–c).

In the same year Fehér and Freund extended the generation of higher alkali-metal silanides using DME as solvent. Reaction of $KSiH_3$ with disilane furnished KSi_2H_5 cleanly. With equimolar trisilane, NMR spectroscopy revealed a product ensemble comprising $KSiH_3$, KSi_2H_5, $KSiH(SiH_3)_2$ and $KSi(SiH_3)_3$, with $KSiH(SiH_3)_2$ as the major species. In line with the observations of Bürger and Eujen, employing 3–4 equivalents of trisilane yielded exclusively $KSi(SiH_3)_3$ (see Scheme 22).[65,66] Isolation of the individual silanides for yield determination was not attempted; instead, the *in situ* solutions were directly subjected to electrophilic functionalization (see Scheme 51).[66]

Fehér, Betzen, and Krancher (1981) achieved the first isolation of solvent-free potassium silanide $KSiH_3$. Concentration of freshly prepared $KSiH_3$ solutions (generated using a Na/K alloy, 1 : 3 w/w) led to crystallization; subsequent high-vacuum

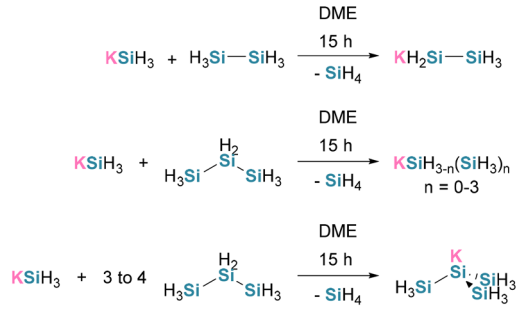

Scheme 22 Synthesis of higher silanides by Fehér and Freund, yields were not determined.

drying afforded analytically pure $KSiH_3$ in 63.5% isolated yield. They further quantified the solvent dependence of $KSiH_3$ solubility, finding a clear increase with donor atom count (triglyme > diglyme > DME), consistent with enhanced cation coordination. In benzene, addition of 18-crown-6 (18-c-6) increased solubility linearly with crown concentration. A temperature-dependent study in DME (10–51 °C) revealed an inverse temperature dependence, with the highest solubility at 10 °C.[67]

In a subsequent report, Fehér and Krancher showed that replacing the Na/K with an ultrasonically prepared K dispersion reduced the reaction time by up to 9 h. Moreover, adding 17% (v/v) benzene to 0.8–0.9 M DME solutions of $KSiH_3$ accelerated recrystallization to the solvent-free $KSiH_3$. The isolated yields were essentially unchanged: 64.4% using the Na/K dispersion and 64.9% with the K dispersion.[68]

Fehér and Krancher (1983)[69] then examined the formation of higher silanides from various hydrosilane precursors, targeting the homologous series $KSiH_n(SiH_3)_{3-n}$ (n = 1–3) over a range of silane stoichiometries (see Tables 1–3). "Reaction time" was defined as the point at which the analyzed composition became invariant; longer times were generally required at higher silane loadings. Transient higher silanides – namely KSi_5H_{11} and KSi_6H_{13} – were detected at early stages but disappeared upon extended reaction, while increasing the silane-to-metal ratio favored formation of higher silanides overall. Product ratios were established by quenching with a fivefold excess of benzyl chloride followed by GC analysis of the resulting products. No H_2 evolution during the build-up reaction was observed; rather, SiH_4 was the only gaseous byproduct. In addition to the targeted silanides and SiH_4, the reactions produced KH and a potassium-containing silicon hydride

Table 1 Results of the reactions between $KSiH_3$ + xSi_2H_6 with the composition of the reaction solution at the respective time in mol%

Molar ratio x	1	2	3	4	5
Reaction time [h]	0.25	0.5	6	24	72
KH	Trace	Trace	4.8	3.9	1.5
$KSiH_3$	33.3	Trace	Trace	—	—
KSi_2H_5	63.9	6.5	Trace	—	—
$KSiH(SiH_3)_2$	2.8	93.5	68.8	22.2	5.0
$KSi(SiH_3)_3$	—	Trace	26.4	73.9	93.5

Open Access Article. Published on 24 April 2026. Downloaded on 5/15/2026 8:48:04 PM.
This article is licensed under a Creative Commons Attribution 3.0 Unported Licence.

Table 2 Results of the reactions between $KSiH_3$ + xSi_3H_8 with the composition of the reaction solution at the respective time in mol%

Molar ratio x	0.5	1.0	1.5	2.0	2.5	3.0
Reaction time [h]	0.25	0.33	24	48	72	72
KH	—	—	2.7	3.9	2.0	—
$KSiH_3$	42.6	2.5	—	—	—	—
KSi_2H_5	50.8	61.5	Trace	Trace	—	—
$KSiH(SiH_3)_2$	6.6	34.5	91.0	22.3	2.5	2.2
$KSi(SiH_3)_3$	—	1.5	6.3	73.8	95.5	97.8

Table 3 Results of the reactions between $KSiH_3$ and the respective silane (A = iso-Si_4H_{10}, B = *n*-Si_4H_{10}, C = Si_5H_{12}) with their compositions at the respective time in mol%

Reaction	$KSiH_3$ + 2A		$KSiH_3$ + 2B		$KSiH_3$ + 2C	
Reaction time [h]	1	72	1	72	24	48
KH	2.2	3.6	1.8	4.2	7.1	1.8
$KSiH_3$	Trace	—	Trace	—	—	—
KSi_2H_5	Trace	—	Trace	—	—	—
$KSiH(SiH_3)_2$	82.6	1.5	85.9	1.7	66.9	3.4
$KSi(SiH_3)_3$	15.2	94.9	12.3	94.1	26.0	94.8

polymer, $(K_{0.09}SiH_{1.19})_n$. On the basis of these observations, a mechanism (see Scheme 23) was proposed in which stepwise nucleophilic substitutions at silicon generate KH and higher silanes as intermediates; these silanes undergo competing silylation and metalation. Because the intermediate silanes (other than SiH_4) re-enter the reaction network, the sequence converges to mixtures of $KSiH_n(SiH_3)_{3-n}$, SiH_4, and the potassium containing polymeric silicon hydride.[69]

Fieselmann and Dickson showed that adding 18-c-6 to the reaction of SiH_4 with potassium in glyme markedly accelerates formation of [K(18-c-6)SiH_3], reducing the reaction time to hours (see Scheme 24). Under these conditions the silanide precipitates as a white solid; after 3 h, monitoring of hydrogen evolution indicated that 87% of the SiH_4 had been consumed. The resulting silanide was subsequently subjected to electrophilic functionalization (see Scheme 48).[70]

F. Fehér, Krancher, and M. Fehér (1991) revisited the Na/SiH_4 system and established that reactions of SiH_4 with sodium in ether solvents invariably yield mixtures of sodium silanides $NaSiH_{3-n}(SiH_3)_n$ (n = 0–3), rather than exclusively $NaSiH_3$ (see Scheme 25, path a). Product distributions determined by benzyl chloride trapping followed by GC analysis, together with direct NMR characterization of the silanide solutions, contradict earlier claims by Hagenmuller and Pouchard of sole $NaSiH_3$ formation.[61,71] The sodium silanides proved markedly more stable in solution than previously suggested, showing no detectable degradation over weeks at room temperature. In DME, the steady-state composition contained approximately twice as much $NaSiH_3$ as $NaSi_2H_5$; in diglyme, the ratio increased to about 4.5 : 1. Minor $NaSiH(SiH_3)_2$ was consistently observed, with only trace amounts of $NaSi(SiH_3)_3$. Substantial NaH formation was detected only at −30 °C, and the overall conversion of SiH_4 to sodium silanides at room temperature was 54–60%. Further investigations examined the effects of used sodium, reaction vessel size, solvent volume, reaction time, and temperature; full details are provided in the original publication. Attempts to isolate discrete sodium silanides by concentrating the solutions promoted redistribution toward higher silanides (see Table 4), whereas evaporation to dryness gave only NaH and polysilanes, indicating complete silanide decomposition (see Scheme 25, path b). The related reaction of $KSiH_3$ with excess of SiH_4 in DME exhibited a pronounced concentration dependence: dilute solutions favored the distribution KSi_2H_5 > $KSiH_3$ > $KSiH(SiH_3)_2$, whereas more concentrated mixtures reacted approximately twice as fast but

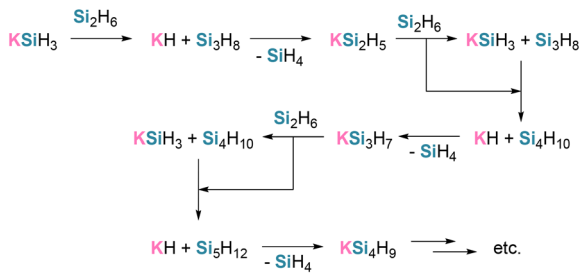

Scheme 23 Proposed mechanism by Fehér and Krancher towards the formation of higher silanides.

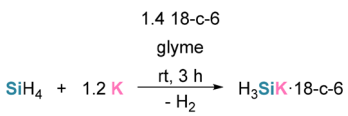

Scheme 24 Formation of $KSiH_3$ complexed with 18-c-6, no yields reported.

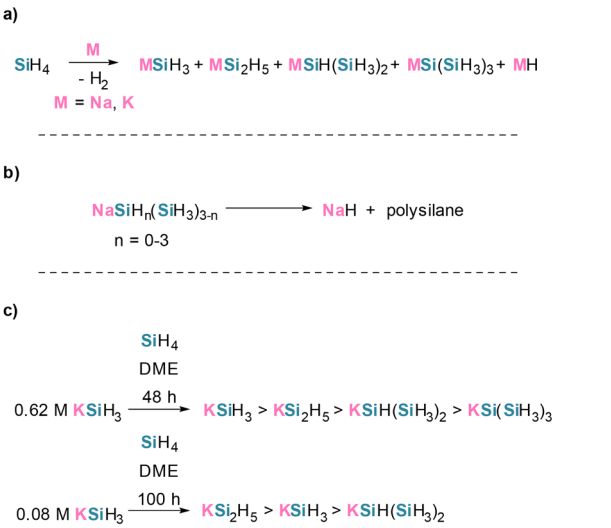

Scheme 25 a) Monosilane reacting with Na or K forming different silanides $MSiH_n(SiH_3)_{3-n}$ (n = 0–3). (b) Attempted isolation of formed silanides leading to degradation. (c) Concentration dependency of formed silanides.

This journal is © the Partner Organisations 2026

Open Access Article. Published on 24 April 2026. Downloaded on 5/15/2026 8:48:04 PM. This article is licensed under a Creative Commons Attribution 3.0 Unported Licence.

Table 4 Results of the silanide solution composition before and after concentrating the solution

Silanide	Composition of the starting solution [mol%]	Composition of the solution after concentrating it [mol%]
$NaSiH_3$	65	25.7
$NaSi_2H_5$	30.4	16.1
$NaH(SiH_3)_2$	4.6	30.3
$NaSi(SiH_3)_3$	Trace	27.9

afforded $KSiH_3$ > KSi_2H_5 > $KSiH(SiH_3)_2$ > $KSi(SiH_3)_3$ (see Scheme 25, path c).[71]

Lobreyer, Oeler, and Sundermeyer (1991) designed a purpose-built reactor (design details in Fig. 5) that enabled complete consumption of 15 g of potassium to form $KSiH_3$ at 65 °C in only 105 minutes in diglyme and 150 minutes in DME. The yield of $KSiH_3$ was quantitative with respect to potassium.[46,72] This represented a substantial acceleration over the fastest previously reported procedure, which required 11–12 hours to consume 15 g of potassium.[68]

In a follow-up study, Lobreyer *et al.* attempted to prepare $NaSiH_3$ in diglyme using the same reactor. Instead, they consistently obtained mixtures of sodium silanides $NaSiH_n(SiH_3)_{3-n}$ (n = 0–3). Spectroscopic analysis after functionalization with *p*-toluenesulfonic acid (PTSA) indicated approximately 50% conversion to $NaSi(SiH_3)_3$. Analogously, direct reaction of potassium metal with SiH_4 in the specialized reactor furnished higher potassium silanides $KSiH_{3-n}(SiH_3)_n$ (n = 0–3) in approx. 90% yield relative to the potassium input, as determined by titration. For both K and Na, extended reaction times at 100 °C afford greater quantities of K/$NaSiH_n(SiH_3)_{3-n}$ (n = 0, 1); concentrating the solution by solvent removal likewise promotes formation of higher silanides. Using K at 70 °C yields exclusively $KSiH_3$ with no evidence of the build-up reaction. The resulting solutions were subsequently engaged in follow-up transformations with C-, P-, and Sn-based electrophiles (see Schemes 53, 129 and 73).[47]

Stueger *et al.* accessed iso-tetrasilanides by the reaction of methyllithium (MeLi) with neopentasilane.[73] Later Lainer *et al.* succeeded in the isolation of iso-tetrasilanide through the addition of tetramethylethylenediamine (TMEDA) (see Scheme 26, path a). Full removal of solvent leads to decomposition, but the isotetrasilanide precipitates from the reaction solution, enabling isolation.

Analogously, neopentasilane with M*O*t*B*u (M = Li, Na, K, Rb, Cs) in THF, and with $LiN(iPr)_2$ in Et_2O (see Scheme 26, path b and c) also led to the isotetrasilanides.[48,74] For M = K, identical outcomes were obtained in Et_2O and DME as in THF.[48] Attempts at isolation or recrystallization led to yellow, insoluble polymers; however, ethereal solutions were stable for several hours and could be employed for downstream functionalization (see Scheme 55). Formation of iso-tetrasilanides was quantitative as determined *via* NMR-spectroscopy.[48]

In 2015, Leich, Spaniol, and Okuda introduced a concise, high-yield route to the α-polymorphs of potassium silanide, α-$KSiH_3$ and α-$KSiD_3$, *via* hydrogenolysis/deuterolysis of the tri-

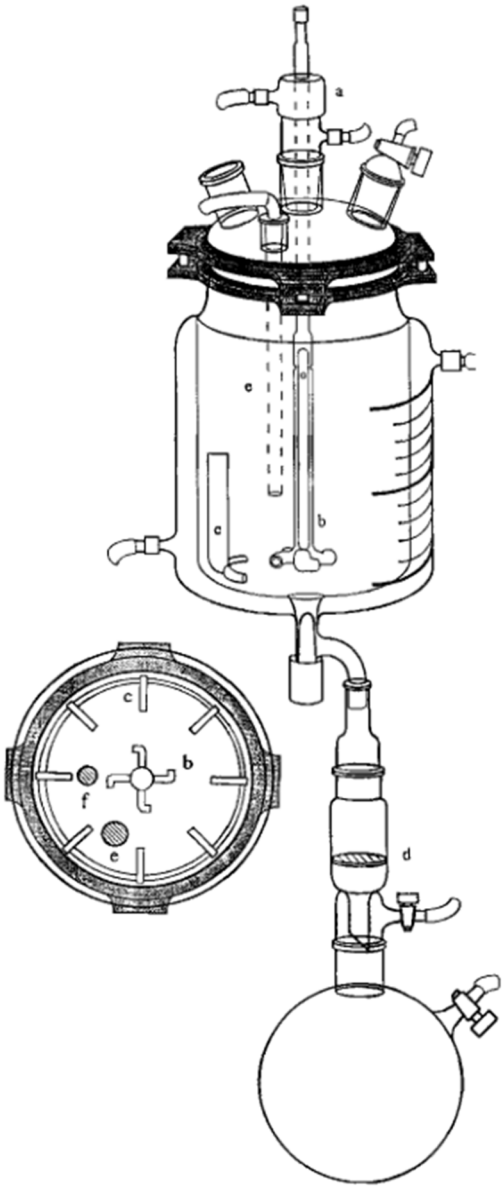

Fig. 5 Reactor design developed by Lobreyer, Oeler, and Sundermeyer. (a) Stirrer bearing, (b) gas-sparging (hollow) stirrer, (c) vortex breaker, (d) G4 frit, (e) gas inlet, (f) temperature probe. Reproduced from ref. 46 with permission from European Chemical Society. © 1991.

phenylsilyl complex $[K(Me_6TREN)SiPh_3]$ (Me_6TREN = tris[2-(dimethylamino)ethyl]amine), affording isolated yields of up to 98% (see Scheme 27).[75]

Schuhknecht *et al.* broadened the hydrogenolysis strategy by using the chelating ligand 1,4,7,10-tetramethyl-1,4,7,10-tetraaminocyclododecane (Me_4TACD). The triphenylsilyl precursors $[(L)MSiPh_3]_n$ (M = Li, Na, K, Rb, Cs; L = Me_4TACD) underwent hydrogenolysis with H_2 (Scheme 28, path a) to give the corresponding hydridosilanide complexes $[(L)MSiH_3]_m$ in yields up to 93% for M = Na, K, and Rb. In the lithium system, only small amounts (<10%) of $[(L)LiSiH_3]_m$ could be isolated; extensive ligand decomposition was observed alongside

Open Access Article. Published on 24 April 2026. Downloaded on 5/15/2026 8:48:04 PM.
This article is licensed under a Creative Commons Attribution 3.0 Unported Licence.

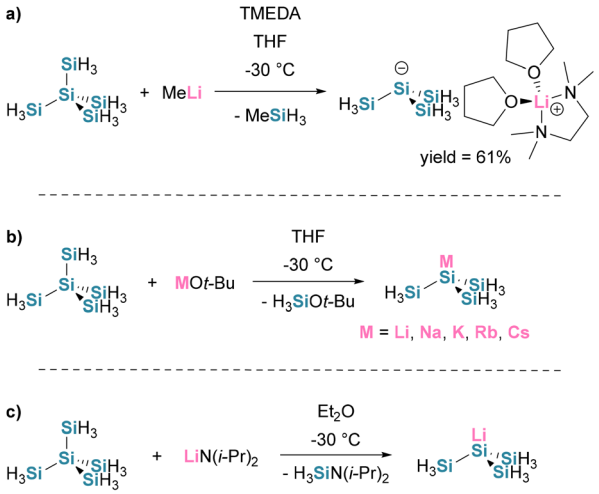

Scheme 26 Synthesis of isotetrasilanides *via* different routes (path a–c). Yields according to NMR-spectroscopy are quantitative.

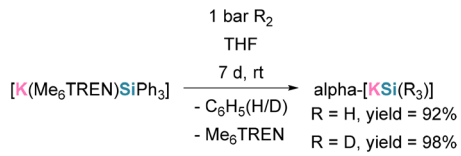

Scheme 27 Generation of silanide through hydrogenolysis/deuterolysis.

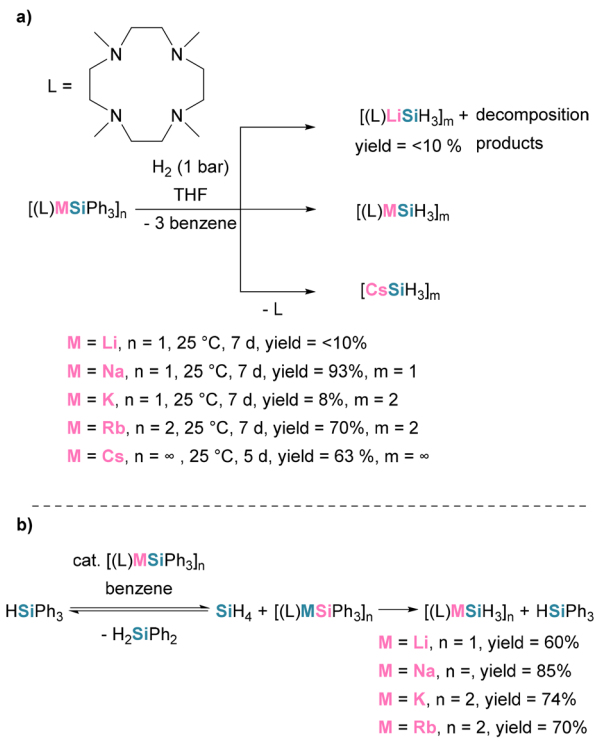

Scheme 28 Generation of silanides through a hydrogenolysis reaction (path a) and a redistribution route (path b).

neutral silanes $H_{n+1}SiPh_{3-n}$ (n = 0–3). For cesium, hydrogenolysis afforded the ligand-free, polymeric trihydridosilanide $[CsSiH_3]_\infty$.

Alternatively, $[(L)MSiH_3]_m$ (M = Li, Na, K, Rb) can be prepared *via* a redistribution route (Scheme 28, path b): catalytic amounts of $[(L)MSiPh_3]_n$ promote scrambling of $HSiPh_3$ in solution to generate H_2SiPh_2 and SiH_4 *in situ*; subsequent reaction of SiH_4 furnishes the hydridosilanide complexes. This indirect route is particularly advantageous for M = Li, substantially improving the final yield relative to direct hydrogenolysis.[76]

Functionalization with group 2 (synthesis of silanides). The field of silanide chemistry has been dominated by studies of alkali metal derivatives, whereas alkaline earth metal analogues have been almost entirely overlooked. It was only in very recent work that these compounds were shown to be stable and isolable.

Lainer *et al.* prepared the magnesium silanide $Mg[Si(SiH_3)_3]_2$ in low yield by salt metathesis of the isotetrasilanide $LiSi(SiH_3)_3$ with $MgBr_2$ (see Scheme 29, path a); however, the product is unstable and decomposes over several days at room temperature. In contrast, reaction of $LiSi(SiH_3)_3$ with $[(^{Aryl}NacNac)MgI(OEt_2)]$ afforded the corresponding ligand-supported magnesium silanide $[(^{Aryl}NacNac)MgSi(SiH_3)_3]$ (Aryl = 2,6-diisopropylphenyl (Dipp), 2,4,6-trimethylphenyl (Mes)) in good yields (see Scheme 29, path b). This complex remains stable after solvent removal, when stored at low temperature. Single-crystal X-ray diffraction of $[(^{Dipp}NacNac)MgSi(SiH_3)_3]\cdot Et_2O$ (see Fig. 6) provided the first crystallographic characterization of a higher silanides.[74]

Functionalization with group 3 (synthesis of silyltetrels)

Silylboranes. In silicon device manufacturing, p-type films are typically deposited by co-flowing diborane with silane in chemical vapor deposition (CVD), with the B_2H_6/SiH_4 ratio, temperature, and plasma conditions governing boron incorporation into polycrystalline, amorphous, or epitaxial silicon.[77,78] In contrast, molecules that already contain Si–B

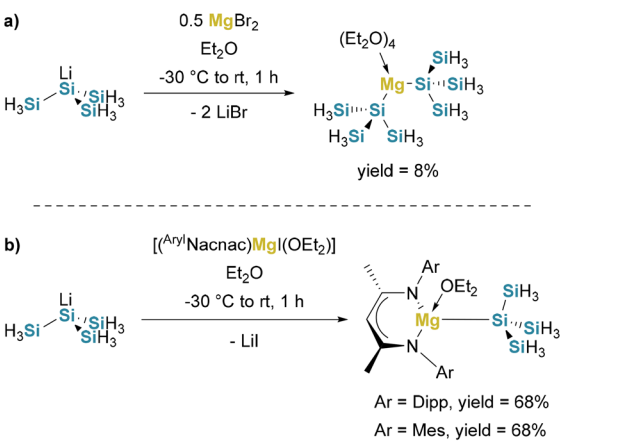

Scheme 29 Synthesis of magnesium isotetrasilanides by Lainer *et al* (path a and b).

This journal is © the Partner Organisations 2026

Open Access Article. Published on 24 April 2026. Downloaded on 5/15/2026 8:48:04 PM.
This article is licensed under a Creative Commons Attribution 3.0 Unported Licence.

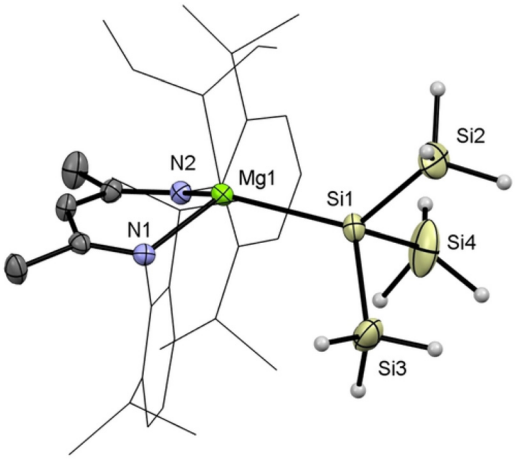

Fig. 6 Crystal structure of the magnesium isotetrasilanide [(^{Dipp}NacNac)MgSi(SiH_3)$_3$]·Et_2O from ref. 74 published by wiley under CC-BY 4.0. © 2022.

bonds while retaining Si–H provide cleaner, single-source feedstocks that co-deliver silicon and boron and, ideally, evolve only hydrogen as a byproduct, thereby minimizing carbon/halogen contamination and facilitating precise control of dopant concentration.[79]

Amberger and Römer employed $KSiH_3$ to access a range of silyl boranes *via* salt metathesis with chloroboranes. While several new SiH_3–BR_2 derivatives were obtained (see Scheme 30, path a–c), reactions with $ClB(n\text{-}Bu)_2$, Cl_2BNMe_2, BCl_3, and $HBCl_2$ did not yield isolable target compounds (see Scheme 30, path d). From these results they concluded that isolable silyl boranes require compensation of the electron

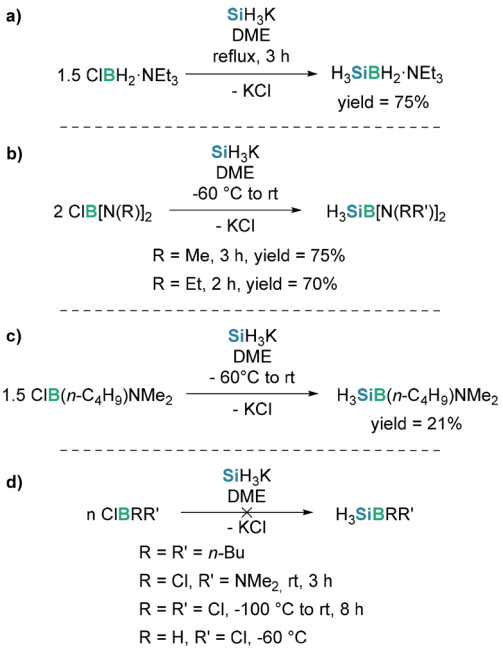

Scheme 30 Synthesis of silylboranes using SiH_3K (path a–d).

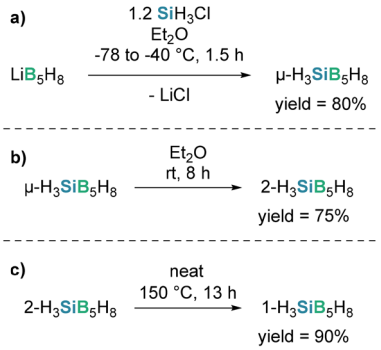

Scheme 31 Generation of μ-silylpentaborane and its isomerization reactions (path a–c).

deficiency at boron by neighbouring donor substituents capable of pi donation (*e.g.*, amino groups), whereas purely inductive electron release from alkyl substituents is insufficient; consistent with this, $H_3SiB(n\text{-}Bu)_2$ could not be isolated.[62]

Gaines and Iorns prepared the silylborane μ-$H_3SiB_5H_8$ in 80% isolated yield by reacting LiB_5H_8 with H_3SiCl, representing the first fully hydrogenated silicon–borane compound (see Scheme 31, path a). Stirring μ-$H_3SiB_5H_8$ with diethyl ether at ambient temperature for 8 h afforded 2-$H_3SiB_5H_8$ (see Scheme 31, path b).[80] In a subsequent study, heating of 2-$H_3SiB_5H_8$ to 150 °C for 13 h gave 1-$H_3SiB_5H_8$, identified as the most stable isomer (see Scheme 31, path c).[80,81] Geisler and Norman selectively halogenated the silyl substituent in silyl-substituted pentaboranes using BCl_3, BBr_3, and HBr (see Scheme 32, path a–c). Under otherwise comparable conditions, BCl_3-mediated chlorination of μ-$H_3SiB_5H_8$ required longer reaction times than chlorination of 2-$H_3SiB_5H_8$ (Scheme 32, path a and c).[82]

Geisler, Soice, and Norman investigated BCl_3-mediated halogenation of the silyl substituent in silylpentaboranes (see Scheme 33, path a).[83] For 1-$H_3SiB_5H_8$, the halogenation rate was indistinguishable from that of 2-$H_3SiB_5H_8$, whereas the μ isomer required higher temperatures and longer reaction

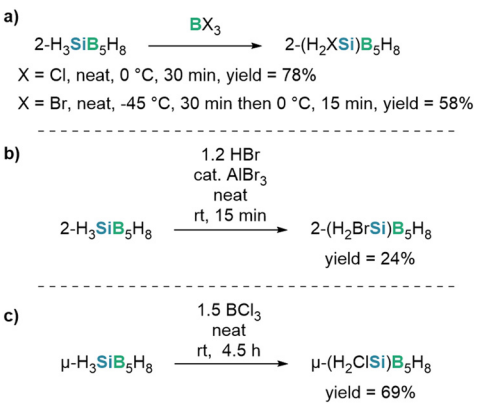

Scheme 32 Halogenation reactions of 2- and μ-silylpentaborane (path a–c).

Open Access Article. Published on 24 April 2026. Downloaded on 5/15/2026 8:48:04 PM.
This article is licensed under a Creative Commons Attribution 3.0 Unported Licence.

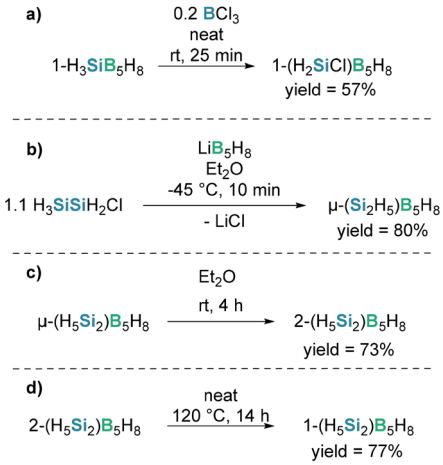

Scheme 33 Halogenation of 1-silylpentaborane and generation of disilylpentaborane and its isomers (path a–d).

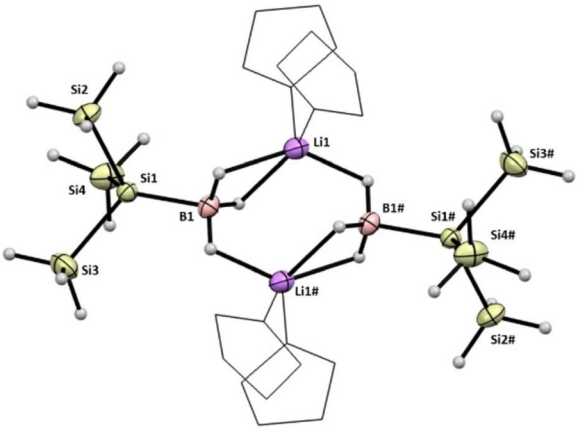

Fig. 7 Crystal structure of hypersilyl borate $[(H_3Si)_3SiBH_3]Li$ from ref. 84 published by Wiley under CC-BY 4.0. © 2024.

times to reach full conversion (see Scheme 33, path c and d).[82,83] They also synthesized μ-disilylpentaborane by treating LiB_5H_8 with Si_2H_5Cl (see Scheme 33, path b). The μ isomer rearranged to the 2 isomer upon stirring in Et_2O at room temperature for 4 h, and to the 1 isomer only under more forcing conditions (120 °C, 14 h) (see Scheme 33, path c and d). This behaviour parallels that of the corresponding monosilylpentaboranes; in both series, the thermodynamic stability follows $\mu \ll 2 < 1$.[80,81,83]

Lainer *et al.* synthesized the lithium hypersilyl borate $[(H_3Si)_3SiBH_3]Li$ in a single step by treating the isotetrasilanide $LiSi(SiH_3)_3$ with $Me_2S{\cdot}BH_3$. The obtained salt is notably robust, remaining unchanged for extended periods as a solid or in solution at ambient temperature (see Scheme 34). Attempts to access cationic or neutral derivatives by hydride abstraction with $B(C_6F_5)_3$ or with $Me_3N{\cdot}HCl$ were unsuccessful; in both cases, uncharacterized polysilanes formed. The structure of the new hypersilyl borate was confirmed by single-crystal X-ray diffraction (see Fig. 7).[84]

Silylalane. Hagenmuller and Pouchard (1964) reported the synthesis of $Al(SiH_3)_3$ by salt metathesis of $NaSiH_3$ with $AlCl_3{\cdot}DME$; however, the product is highly labile and decomposes at 0 °C or upon exposure to a stream of H_2 (see Scheme 35, path a).[61] In related work, Semenenko and Taisumov obtained H_2AlSiH_3 by reacting $KSiH_3$ with $AlH_2Cl{\cdot}Et_2O$ (see Scheme 35, path b).[85] Amberger and Römer synthesized the silylalane $H_3SiAl(n\text{-}Bu)_2$ by salt metathesis of $KSiH_3$ with $ClAl(n\text{-}Bu)_2$ (see Scheme 36). After solvent removal, the material was obtained as the contact adduct $H_3SiAl(n\text{-}Bu)_2{\cdot}KCl$. Separation of KCl required heating to 220 °C, affording pure $H_3SiAl(n\text{-}Bu)_2$.[86] Notably, $H_3SiAl(n\text{-}Bu)_2$ exhibits high thermal stability; in contrast, related silylboranes already undergo slow decomposition at ambient temperature.[62,86]

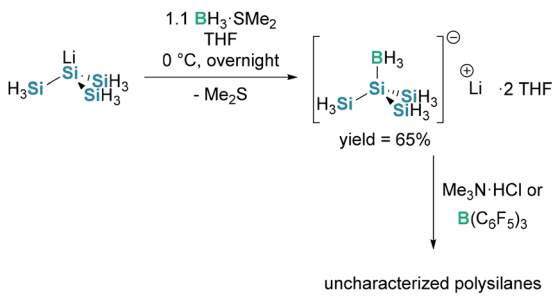

Scheme 34 Synthesis of lithium hypersilyl borate and attempted hydride abstraction reactions.

Functionalization with group 4 (synthesis of silyltetres)

Organosilanes. Organosilanes and related derivatives, such as silicon carbide coatings are increasingly important across semiconductor, aerospace, aircraft engines, and mechanical

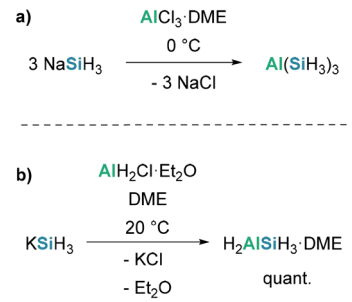

Scheme 35 Generation of trisilylalane by Hagenmuller and Pouchard (path a) and monosilylalane by Semenenko and Taisumov (path b). For path (a) no yields were reported.

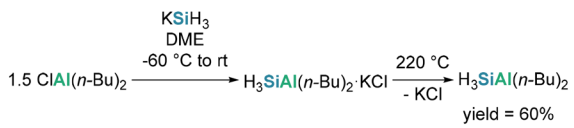

Scheme 36 Synthesis of silylalane by Amberger and Römer.

This journal is © the Partner Organisations 2026

Open Access Article. Published on 24 April 2026. Downloaded on 5/15/2026 8:48:04 PM.
This article is licensed under a Creative Commons Attribution 3.0 Unported Licence.

engineering. In semiconductor fabrication, alkylsilanes act as precursors for surface passivation, enable area-selective deposition, and improve device stability,[87] they also strengthen dielectric layers through siloxane networks[88] and promote adhesion between photoresists and SiO_2 or other substrates.[89] Furthermore high-purity alkylsilanes are critical for high-quality coatings and can function as anti-reflective layers to suppress reflections and enhance photolithography efficiency.[90]

For the synthesis of organosilanes two prevalent methods are used in the literature, either the reduction of silyl halides or *via* transformations of inorganic silanes.

Reduction of silyl halides is the most commonly used approach for the synthesis of alkylsilylhydrides. Most frequently $LiAlH_4$ is used for the reduction, though other common reductants like lithium hydride, sodium hydride, triethyl aluminium ($AlEt_3$) and diisobutylaluminium hydride can be employed as well (see Scheme 37).[28,91]

Consequently using di- to tetrabromosilylmethane with $LiAlH_4$ allows for the synthesis of the respective silylmethane.[92–94] When bromosilylmethanes were treated in standard solvents such, as *n*-Bu_2O, the yields were very poor, however, using tetraline in combination with benzyltriethylammoniumchloride (TEBAC), excellent yields were achieved (see Scheme 38, path b).[93]

Schmidbaur and co-workers were the first to report tetrasilylmethane ($C(SiH_3)_4$). The usual choice of a polar solvent was replaced with a two-phase system with phase transfer catalyst, in order to supress the cleavage of Si–C bonds, but the sideproduct trisilylmethane ($HC(SiH_3)_3$) was still observed (see Scheme 38, path a).[94,95] Furthermore they were able to obtain 2,2-disilylpropane from 2,2-dibromosilylpropane $Me_2C(SiH_2Br)_2$.[96]

While commonly Et_2O is used as the solvent of choice for the synthesis of lower boiling silanes, Kozhevnikov and co-workers were able to obtain methylsilane ($MeSiH_3$) in excellent yield, using *n*-Bu_2O as solvent (see Scheme 39, path a).[97] Bellama and co-workers prepared disilylmethane ($H_2C(SiH_3)_2$), *via* reduction of bistrichlorosilylmethane ($H_2C(SiCl_3)_2$), in 50% yield (see Scheme 39, path b).[98]

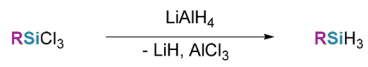

R = Me,1.1 $LiAlH_4$, dioxane, reflux, 30 min, yield = 80-90%
R = Vinyl,1.1 $LiAlH_4$, dioxane, reflux, 30 min, yield = 80-90%
R = Et,1.1 $LiAlH_4$, dioxane, reflux, 30 min, yield = 88%
R = Pr, Et_2O, reflux, 1 h
R = *n*-Bu,1.1 $LiAlH_4$, dioxane, reflux, 30 min, yield = 80-90%
R = *i*-Bu,1.1 $LiAlH_4$, dioxane, reflux, 30 min, yield = 80-90%
R = Ph, THF, reflux, 12 h, yield = 23%
R = Ph, excess $LiAlH_4$, Et_2O, reflux, 1 h yield = 86%

Scheme 37 Synthesis of organosilanes *via* reduction with $LiAlH_4$. The yields for R = Me, vinyl, *n*-Bu and i-Bu were only given as range of 80 to 90% by Tannenbaum *et al.* For R = Pr, no detailed yield was given.

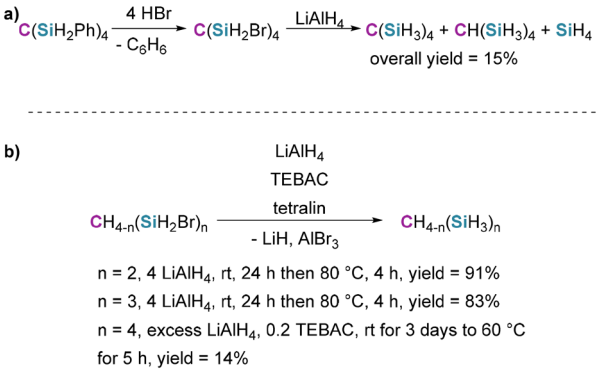

n = 2, 4 $LiAlH_4$, rt, 24 h then 80 °C, 4 h, yield = 91%
n = 3, 4 $LiAlH_4$, rt, 24 h then 80 °C, 4 h, yield = 83%
n = 4, excess $LiAlH_4$, 0.2 TEBAC, rt for 3 days to 60 °C for 5 h, yield = 14%

Scheme 38 Synthesis of $C(SiH_3)_4$ starting from $C(SiH_2Ph)_4$ (path a) and synthesis of $CH_{4-n}(SiH_3)_n$ (path b).

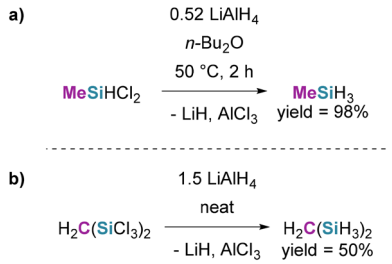

Scheme 39 Synthesis of $MeSiH_3$ (path a) and $H_2C(SiH_3)_2$ (path b) *via* reduction with $LiAlH_4$.

A representative example of metal-hydride reduction of alkylsilyl halides is the conversion of 1,1,3,3-tetrachloro-1,3-disilabutane to 1,3-disilabutane. The tetrachloro precursor is prepared in 41% yield by reacting HCl with elemental Si and $MeSiCl_2CH_2Cl$ using Cu based catalysts,[99] followed by reduction with $LiAlH_4$ to afford 1,3-disilabutane (see Scheme 40).[100]

Fritz and co-workers showed that treatment of chlorinated C-spiro-linked 2,4-disilacyclobutanes with $LiAlH_4$ results in the cleavage of the four membered rings (see Schemes 41 and 42, path b). In contrast, when they employed i-Bu_2AlH no cleavage was observed, and the hydrogenated C-spiro-linked 2,4-disilacyclobutanes were obtained (see Schemes 41 and 42, path a).[101]

Pyrolysis of the methylchlorosilanes methyltrichlorosilane ($MeSiCl_3$), dichlorodimethylsilane (Me_2SiCl_2) and chlorotrimethylsilane (Me_3SiCl) at 700 °C afford mixtures of linear and cyclic alkylchlorosilanes, for example, 1,3-disilapropane. The chlorine containing pyrolysis products were then reduced with $LiAlH_4$, though isolation of pure compounds is problematic.[102] Furthermore, pyrolysis of a mixture of SiH_4 and ethylene leads to formation of mixtures of the alkylsilanes ethylsilane ($EtSiH_3$), diethylsilane (Et_2SiH_2), triethylsilane (Et_3SiH),

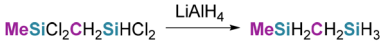

Scheme 40 Synthesis of 1,3-disilabutane by reduction with $LiAlH_4$. No yield and experimental details were reported for the $LiAlH_4$ reduction.

Open Access Article. Published on 24 April 2026. Downloaded on 5/15/2026 8:48:04 PM.
This article is licensed under a Creative Commons Attribution 3.0 Unported Licence.

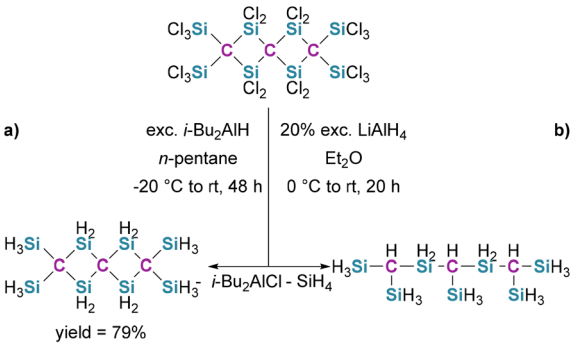

Scheme 41 Example of the hydration of a C-spiro linked 2,4-disilacyclobutane with $LiAlH_4$ (path b) and i-Bu_2AlH (path a). No yield for the $LiAlH_4$ reaction was reported.

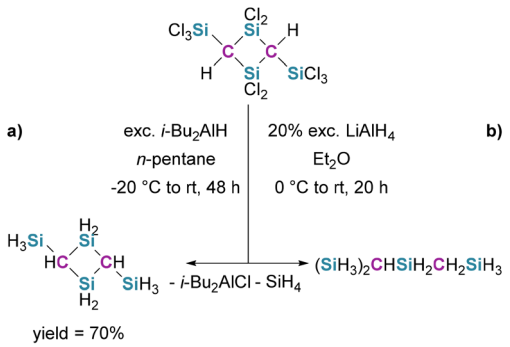

Scheme 42 Hydration of a C-spiro linked 2,4-disilacyclobutane with $LiAlH_4$ (path b) and i-Bu_2AlH (path a). No yield for the $LiAlH_4$ reaction was reported.

though no yields were reported.[103] The copyrolysis of disilane with methylsilane ($MeSiH_3$) afforded methyldisilane (MeH_2SiSiH_3), with dimethylsilane (Me_2SiH_2) it led to formation of 1,1-dimethyldisilane ($Me_2SiHSiH_3$) and with trimethylsilane (Me_3SiH) it resulted in the formation of 1,1,1-trimethyldisilane (Me_3SiSiH_3), though again no isolation was performed.[104]

Furthermore, freshly prepared bis- and tristrifluoromethanesulfonatosilylmethanes are effective precursors for di- and trisilylmethanes. Although the formation of these intermediates proceeds in essentially quantitative yield, they undergo decomposition and isomerization at ambient temperature; therefore, immediate reduction is required to achieve optimal yields (see Scheme 43).[105]

Westermark *et al.* employed $LiAlH_4$ in combination with aluminium chloride ($AlCl_3$) to reduce alkyltriethoxysilanes to the respective alkylsilanes in good yields (see Scheme 44).[106]

Trialkylstannanes can be used together with Lewis-base catalysts for the partial and full reduction of alkylsilylhalides to alkylhydrosilanes. Usually a distribution of products is obtained, depending on the catalyst used, the stannane used and the molar ratio of stannane to silane.[107–109] When using tributyltin hydride (Bu_3SnH) and catalytic amounts of triphenylphosphine (PPh_3), methylchlorodisilanes show signifi-

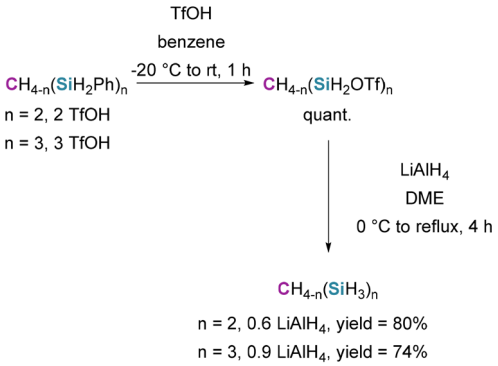

Scheme 43 Synthesis of di- and trisilylmethane *via* reduction.[105]

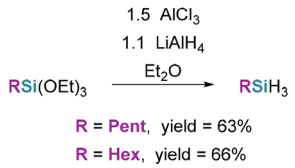

Scheme 44 Reduction of alkyltriethoxysilanes to afford alkylsilanes.

cant Si–Si bond cleavage; in contrast, no cleavage is observed when the analogous methylbromodisilanes are used (see Scheme 45).[107]

One of the first reported synthesis of monoalkylsilanes is the synthesis of $MeSiH_3$ from H_3SiCl, by Stock and Somieski in 1919. But no information about the purity of the obtained $MeSiH_3$ is given (see Scheme 46).[10]

Another approach is the direct hydrosilylation of unsaturated substrates, though early work demonstrated that direct addition of SiH_4 to alkenes or alkynes generally affords product mixtures with low yields under both thermal and photochemical conditions.[110] The use of catalysts, for example alkali metal aluminates[111] and $LiAlH_4$ [112] promotes more selec-

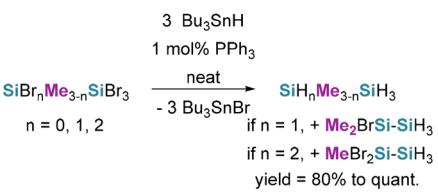

Scheme 45 Reduction of methylbromodisilanes with Bu_3SnH and PPh_3. No specific yields were reported for the individual compounds, but yields were given as 80% to quantitative yields for the reductions.

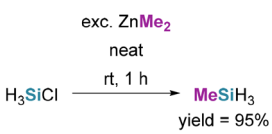

Scheme 46 Synthesis of $MeSiH_3$ *via* reaction of H_3SiCl with $ZnMe_2$.

This journal is © the Partner Organisations 2026

Open Access Article. Published on 24 April 2026. Downloaded on 5/15/2026 8:48:04 PM.
This article is licensed under a Creative Commons Attribution 3.0 Unported Licence.

tive addition of SiH_4 to alkenes, significantly improving the selectivity. The best results were achieved by employing Pt $(PPh_3)_4$ as catalyst (see Scheme 47).[113]

SiH_4 was also employed as feedstock for nucleophilic substitution *via* silyl anions. Conversion of SiH_4 into $KSiH_3$ allows for subsequent reaction with organic halides, for example $MeSiH_3$ was obtained by reaction of methyliodide (MeI) with $KSiH_3$ (see Scheme 48, path a).[114] Ritter and Ring obtained $MeSiH_3$ in excellent yields by treating $KSiH_3$ with excess methyl chloride (MeCl) (see Scheme 48, path b).[15] Fieselmann and Dickson improved the yields by using potassium(18-crown-6) silanide ($[K(18\text{-c-}6)]SiH_3$) and demonstrated the synthesis of $H_2C(SiH_3)_2$ (see Scheme 48, path c).[70] Similar to Na- and $KSiH_3$, $RbSiH_3$ and $CsSiH_3$ are suitable for the reaction with MeI as well.[64]

Nucleophilic substitution between $KSiH_3$ and bromomethylsilane ($MeSiH_2Br$) only leads to formation of methyldisilane in poor yields of 5%, a more suitable approach is the reaction between a monohalodisilane with methyllithium (MeLi) (see Scheme 49, path a and b).[92]

Alkali metal silanides derived from SiH_4 can be converted to alkylsilanes in hexamethylphosphoramide upon treatment with the corresponding alkyl halides, typically in good yields (see Scheme 50).[63]

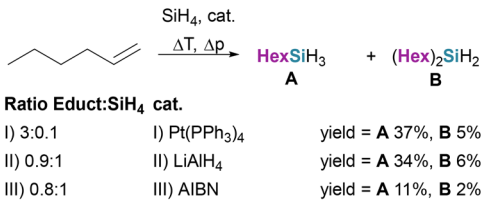

Scheme 47 Synthesis of alkylsilanes *via* addition of SiH_4 to an alkene.

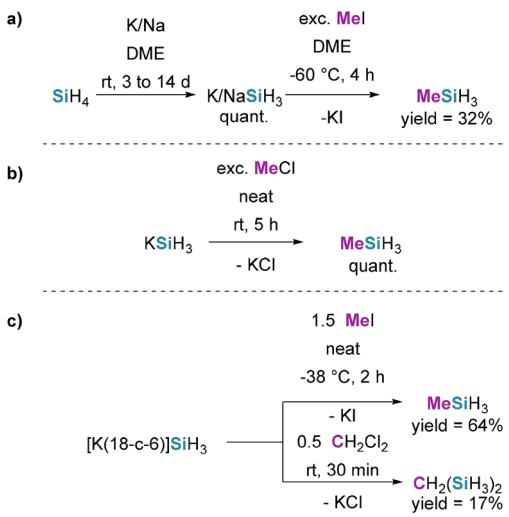

Scheme 48 Synthesis of alkylsilanes by reaction of $KSiH_3$ with MeX (X = Cl, I) (path a–c).

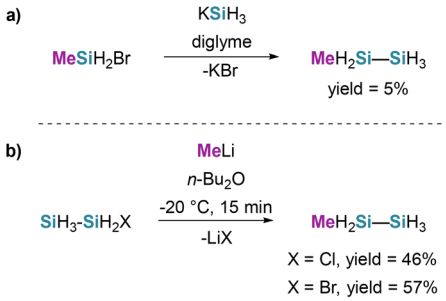

Scheme 49 Synthesis of methyldisilane (path a and b).

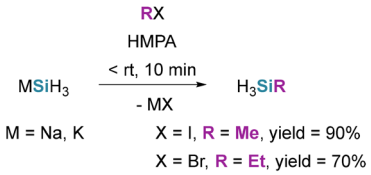

Scheme 50 Synthesis of methyl- and ethylsilane from K- or $NaSiH_3$. No detailed procedures with exact amounts of reagents were given for R = Me, Et.

Treatment of mixtures of potassium silanides with ethyl chloride (EtCl) afforded the corresponding ethylsilanes in approximately 25% overall yield, notably individual product yields were not reported (see Scheme 51).[66]

Furthermore, treatment of mixtures of higher potassium silanides with phenyl chlorosilane (PhH_2SiCl) afforded the corresponding phenylsilanes in approximately 20% overall yield, notably no specific yield was given for the individual products (see Scheme 52).[45]

Sundermeyer and co-workers accessed the methyl-substituted silanes $MeSiH_3$, methyldisilane ($MeSiH_2SiH_3$), 2-methyltrisilane ($SiH_3SiHMeSiH_3$) and $MeSi(SiH_3)_3$ *via* the buildup reaction between SiH_4 and K in diglyme, and subsequent alkylation with methyl *p*-toluenesulfonate (*p*-TosMe) (see Scheme 53).[47,115]

Stueger and co-workers employed lithium and potassium isotetrasilanides to access methylisotetrasilane ($MeSi(SiH_3)_3$) and a range of alkyl- and phenyl-substituted neopentasilanes. Treatment of solutions of lithium isotetrasilanide ($LiSi(SiH_3)_3$)

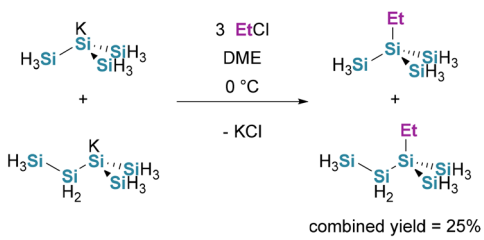

Scheme 51 Synthesis of ethyl substituted silanes from potassium silanides with ethylchloride. No specific yield for the individual compounds was given.

Open Access Article. Published on 24 April 2026. Downloaded on 5/15/2026 8:48:04 PM.
This article is licensed under a Creative Commons Attribution 3.0 Unported Licence.

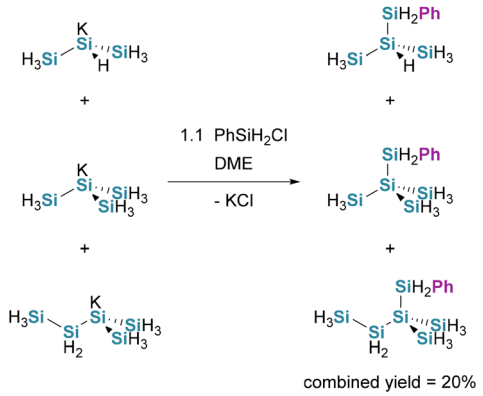

Scheme 52 Synthesis of phenylisotetra-, phenylneopenta-, and phenylneohexasilane from the respective potassium silanide and phenylchlorosilane. No specific yield for the individual compounds was assigned.

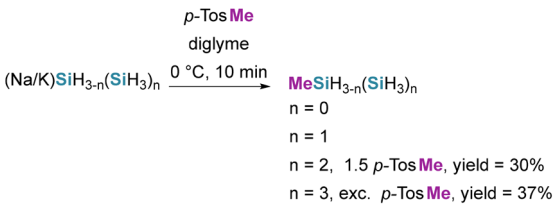

Scheme 53 Synthesis of methylsilanes from silanide mixtures. While products are formed with n = 0–3, the isolated yield was only given for n = 2 and n = 3.

with methyl *p*-toluenesulfonate afforded methylisotetrasilane in 36% yield, while using triphenylchlorosilane ($ClSiPh_3$) as the electrophile furnished triphenylsilylneopentasilane ($SiPh_3Si(SiH_3)_3$) in 50% yield (see Scheme 54, path a and b). When dimethylphenylchlorosilane ($ClSiMe_2Ph$) or phenylchlorosilane ($ClSiH_2Ph$) were employed, both the corresponding monosubstituted neopentasilanes and the disubstituted derivatives were obtained (see Scheme 55, path a and b). To suppress disubstitution, the authors avoided an

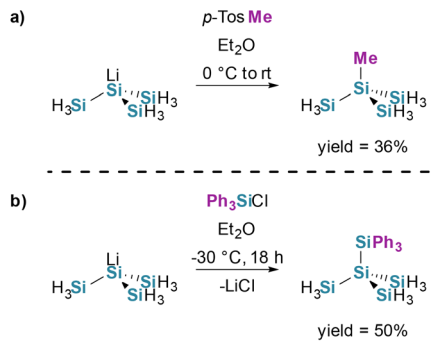

Scheme 54 Synthesis of methylisotetrasilane (path a) and triphenylsilylneopentasilane (path b) from lithiumisotetrasilanide.

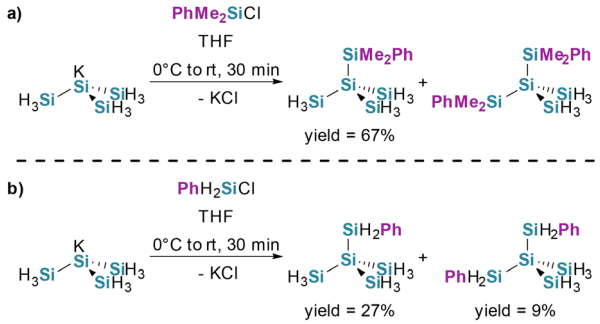

Scheme 55 Synthesis of dimethylphenyl- and phenylneopentasilane from potassiumisotetrasilanide, with concomitant formation of the respective disubstituted product (path a and b). The yield for disubstituted bisdimethylphenylneopentasilane was not reported.

excess of potassium silanide by adding the silanide slowly to the electrophile.[48]

Stueger, Haas and co-workers obtained several phenyl-substituted organosilanes in good yields by treating lithium isotetrasilanide with phenylchlorosilanes as electrophiles. When dichlorophenylsilane (Cl_2HSiPh) and 1,2-dichloro-1,2-tetrakisphenyl-disilane were employed as electrophiles, the corresponding branched nonasilane and branched decasilane were isolated as pure compounds, however, the silane byproducts were not identified (see Scheme 56, path a and b). A crystal X-ray structure was determined for $(SiH_3)_3Si(SiPh_2)_2Si(SiH_3)_3$ (see Fig. 8).[49]

In contrast, when dichlorodiphenylsilane (Cl_2SiPh_2) was used as electrophile the corresponding diphenylnonasilane, and two cyclic phenylsilane byproducts were obtained in low yields (see Scheme 57). A crystal structure from $(SiH_3)_3SiPh_2(SiH_3)_3$ was obtained (see Fig. 9).[49]

Moreover, treatment of $(H_3Si)_3Si(SiPh_2)_2Si(SiH_3)_3$ with triflic acid gave the partially hydrogenated derivative $(H_3Si)_3Si(SiPhH)_2Si(SiH_3)_3$, this compound was not isolated but was

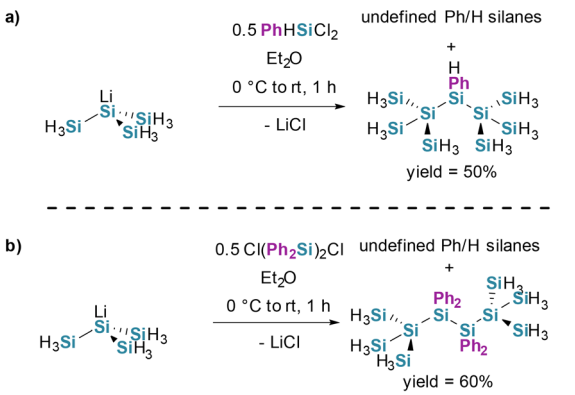

Scheme 56 Synthesis of phenylsubstituted nona- and decasilanes from lithium isotetrasilanide (path a and b). Both compounds were isolated as pure compounds, but during the reaction undefined silanes emerged as byproducts.

This journal is © the Partner Organisations 2026

Open Access Article. Published on 24 April 2026. Downloaded on 5/15/2026 8:48:04 PM.
This article is licensed under a Creative Commons Attribution 3.0 Unported Licence.

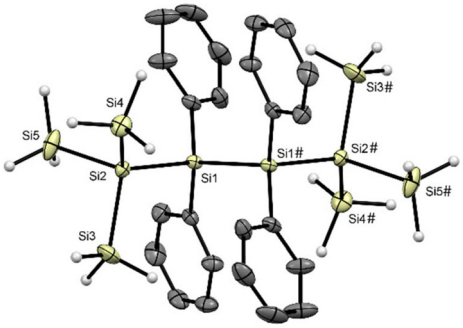

Fig. 8 Crystal structure of $(SiH_3)_3Si(SiPh_2)_2Si(SiH_3)_3$, adapted from Stueger and Haas *et al.*[49] with permission from American Chemical Society © 2019.

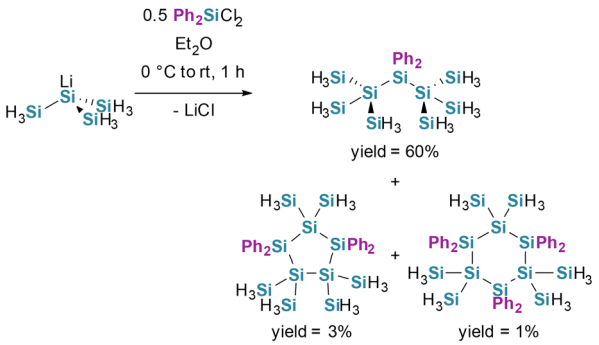

Scheme 57 Synthesis of phenylsubstituted organosilanes with dichlorodiphenylsilane.

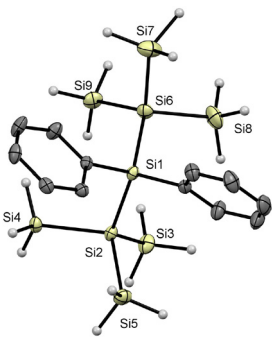

Fig. 9 Crystal structure of $(SiH_3)_3SiPh_2(SiH_3)_3$, adapted from Stueger and Haas *et al.*[49] with permission from American Chemical Society © 2019.

used *in situ* to prepare the fully hydrogenated product $(H_3Si)_3Si(SiH_2)_2Si(SiH_3)_3$ (see Scheme 58).[49]

Haas and co-workers converted dodecamethoxyneopentasilane to the corresponding potassium silanide using potassium *t*-butoxide (KO*t*-Bu) (see Scheme 59, path a). The subsequent treatment of the silanide with electrophiles, such as MeI resulted in the formation of the corresponding nonamethoxyisotetrasilanes (see Scheme 59, path b). Reduction of these derivatives with a slight excess of i-Bu_2AlH afforded the corresponding organosilanes in good yields (see Scheme 59, path c).[22,116] Applying the same strategy to a potassium disilanide delivered the cyclic 1,1,4,4-tetrakis(silyl)octamethyl-cyclohexasilane (see Scheme 60). A crystal structure of this compound was also obtained (see Fig. 10).[22]

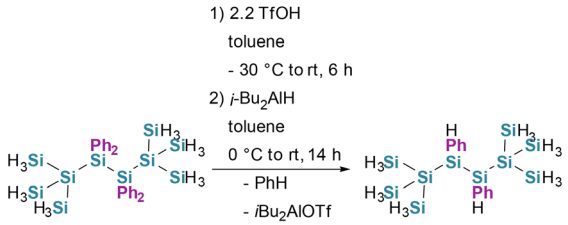

Scheme 58 Synthesis of $(H_3Si)_3Si(SiPhH)_2Si(SiH_3)_3$. The compound was not isolated and reacted further to $(H_3Si)_3Si(SiH_2)_2Si(SiH_3)_3$.

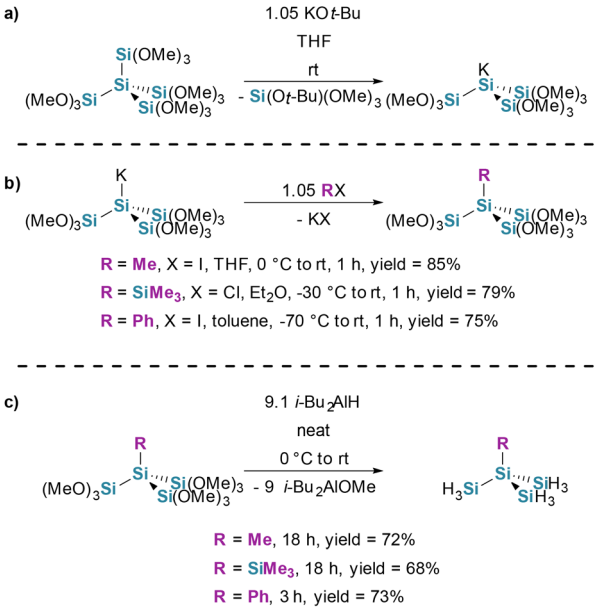

Scheme 59 Synthesis of organosilanes from potassium silanides *via* reaction with electrophiles and subsequent reduction with i-Bu_2AlH (path a–c).

Silyl halides are viable substrates for Grignard based synthesis of alkylsilanes, though only in moderate yields. As an example, H_3SiBr reacts with various Grignard reagents to afford the respective alkylsilane (see Scheme 61).[117]

Moreover, halomethylsilanes, such as, bromo- and chlorosilylmethane are suitable precursors to silylmethyl Grignard reagents ($XMgCH_2SiH_3$), which subsequently react with halosilanes to furnish silyl-substituted methanes, exemplified by $CH_2(SiH_3)_2$ (see Scheme 62). However, neither bromo- nor chloromethylsilane reacts with magnesium under standard conditions, the corresponding Grignard reagent is obtained only when activated magnesium is generated by reducing magnesium chloride ($MgCl_2$) with K in THF under reflux. They stated that they obtained 1,2-disilylethane ($H_3SiEtSiH_3$) in 26% yield from the preparation of H_3SiCH_2MgBr due to Wurtz-

Open Access Article. Published on 24 April 2026. Downloaded on 5/15/2026 8:48:04 PM.
This article is licensed under a Creative Commons Attribution 3.0 Unported Licence.

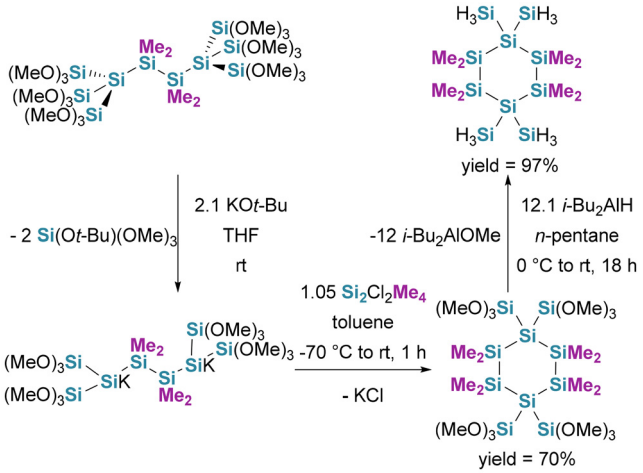

Scheme 60 Synthesis of organohexasilane compounds from a potassiumdisilanide.

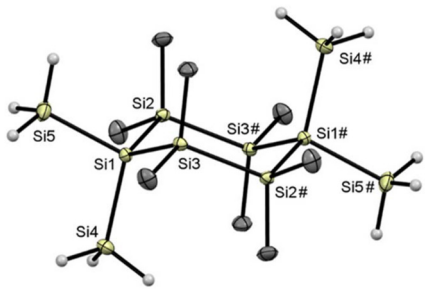

Fig. 10 Crystal structure of 1,1,4,4-tetrakis(silyl)octamethylcyclohexasilane. Adapted from Haas *et al.*[22] published by American Chemical Society under CC-BY 4.0.

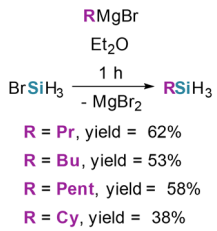

Scheme 61 Synthesis of alkylsilanes from silyl halides and Grignard reagents. No specific molar ratios or temperatures were given for the synthesis.

coupling. Further examples of this synthesis approach are given in Table 5.[118]

Dimethyltitanocene (Me_2TiCp_2) is able to catalyze redistribution reactions of diethoxymethylsilane ($(EtO)_2MeSiH$) affording triethoxymethylsilane ($(EtO)_3MeSi$) and methylsilane in excellent yields.[119] Other catalysts like sodium ethoxide are used for the redistribution as well (see Scheme 63).[120]

Ozonizer-type silent electrical discharge tubes were also employed in the synthesis of methyldisilane from a mixture of

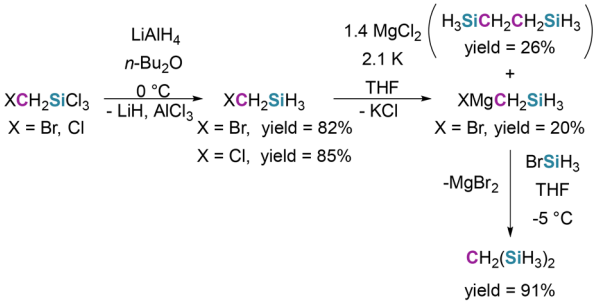

Scheme 62 Example synthesis of alkylsilanes from silylmethylgrignard compounds.

Table 5 Synthesis of silyl substituted methanes from halosilanes and grignard reagents

Grignard reagent	Halosilane	Product	Yield [%]
Me_3SiCH_2MgCl	H_3SiBr	$Me_3SiCH_2SiH_3$	86
Me_2SiHCH_2MgCl	H_3SiBr	$Me_2SiHCH_2SiH_3$	20–30*
$MeSiH_2CH_2MgCl$	H_3SiBr	$MeSiH_2CH_2SiH_3$	92
H_3SiCH_2MgBr	H_3SiBr	$CH_2(SiH_3)_2$	91
H_3SiCH_2MgBr	Me_2SiHCl	$H_3SiCH_2SiHMe_2$	30*
H_3SiCH_2MgBr	Me_3SiCl	$H_3SiCH_2SiMe_3$	85

Yields marked with asterisk are crude yields.

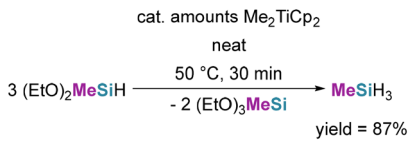

Scheme 63 Catalytic redistribution of $(EtO)_2MeSiH$.

Me_2O and SiH_4, though this approach is not synthetically useful due to the low yield of 4% and the poor selectivity.[121]

Treatment of silanes with organolithium reagents provides an alternative route to organosilanes. Bolduc and Ring reported that condensing disilane into a solution of ethyllithium (LiEt) in benzene (C_6H_6), furnishes ethyldisilane ($EtH_2Si–SiH_3$) in 37% yield by the following reaction at room temperature (see Scheme 64).[122]

This approach can be expanded to larger silanes such as tri-, *n*-tetra- and *n*-pentasilane as well. When solutions of the respective silanes in *n*-hexane are treated with *n*-butyllithium (*n*-BuLi) solutions, the respective *n*-butylsilane is afforded (see

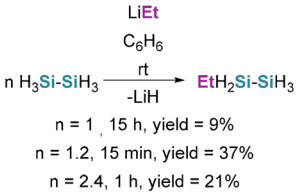

Scheme 64 Synthesis of ethyldisilane from disilane and ethyllithium.

This journal is © the Partner Organisations 2026

Open Access Article. Published on 24 April 2026. Downloaded on 5/15/2026 8:48:04 PM.
This article is licensed under a Creative Commons Attribution 3.0 Unported Licence.

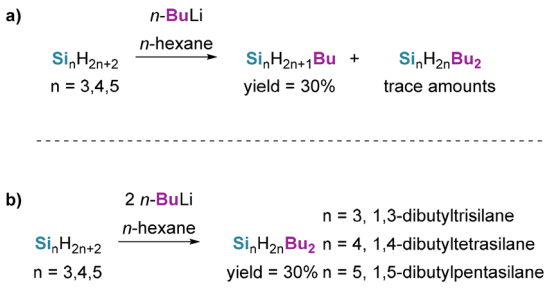

Scheme 65 Synthesis of butylsilanes from tri-, tetra- and pentasilane (path a and b). No specific yields for the disubstituted *n*-butylsilanes with 1 equivalent *n*-BuLi and no individual yields for the monosubstituted yields were given.

Scheme 65, path a and b). Disubstituted dibutylsilanes are observed as well and are the main product of the reaction when 2 equivalents of *n*-BuLi are used. Additionally, a solid polysilane is formed as well. While it was mentioned that SiH_4 and disilane are formed in the reaction with trisilane as well, it was not indicated if these silanes are observed with tetra- and pentasilane as well.[123]

Silylgermanes. Hydrosilanes with a direct silicon–germanium bond, commonly referred to as silylgermanes, have recently attracted increasing attention as single source precursors for the deposition of mixed Si–Ge materials. In conventional processes, SiGe thin films are typically obtained from mixtures of monogermane (GeH_4) and monosilane. However, the significantly different activation energies and surface reaction kinetics of these two hydrides often lead to non-uniform incorporation during growth. As a result, classical co-flow deposition can suffer from compositional inhomogeneities, gas-phase depletion effects, and segregation phenomena such as the formation of germanium-rich cluster or islands. Silylgermanes offer a promising strategy to circumvent these intrinsic limitations. The presence of a covalent Si–Ge bond within a single molecular precursor ensures that silicon and germanium are delivered to the substrate in a fixed stoichiometric relationship, potentially enabling more uniform incorporation at the surface. Moreover, many silylgermanes decompose readily under mild conditions, allowing high deposition rates even at comparatively low substrate temperatures. This combination of single-source stoichiometric control and enhanced low-temperature reactivity makes silylgermanes an appealing class of feedstocks for chemical vapor deposition, liquid phase deposition, and related techniques aimed at producing SiGe:H amorphous alloys, mixed semiconductors, and advanced thin-film architectures. Their potential enables both: fundamental material research and technologically relevant applications.[46,124]

The most basic member of the Si–Ge hydride family is monosilylgermane (H_3SiGeH_3). Its first targeted preparation was reported by Cox and Varma in 1964, who achieved the formation of H_3SiGeH_3 in approximately 20% yield *via* the nucleophilic substitution of chlorogermane with potassium silanide (see Scheme 66). This study represents the earliest

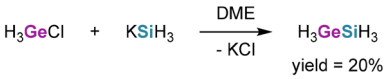

Scheme 66 Synthesis of silylgermane (H_3GeSiH_3).

attempt to generate a Si–Ge single-bonded hydride under controlled conditions.[125]

In the same year, Phillips and co-workers identified H_3SiGeH_3 as a minor product during silent electrical discharge experiments, although the hydride was obtained only in trace amounts (~2%).[126]

An alternative approach to the silylation of germyl anions employs silyltriflate (H_3Si-OTf) or silylnonaflate (H_3Si-ONf) as highly electrophilic silylating agents (see Scheme 67). This approach was demonstrated by Sundermeyer and co-workers (1994) and later expanded by Kouvetakis and co-workers (2005). Using these reagents, H_3SiGeH_3 can be obtained in moderate yields ranging from 22–35%, representing a significant improvement over earlier methods based on halide replacement.[46,127]

Sundermeyer and co-workers also demonstrated the synthesis of branched silylgermane with the general formula $(SiH_3)_nGeH_{4-n}$ (n = 2–4). In their studies, a mixture of branched silylsilanides $(SiH_3)_{3-n}SiNa$ (n = 0–2) was first generated by reacting sodium with monosilane in diglyme. Subsequent treatment of this anion mixture with monogermane induced a rearrangement in which the germanium atom migrated into the central position of the silyl framework, forming branched silylgermanides. Finally, silylation with H_3SiONf afforded the corresponding silylgermanes (see Scheme 68). However, the individual products could not be separated, and yields were therefore only estimated by gas chromatography, limiting the characterization of the mixture.[18]

With a similar procedure, Ritter *et al.* synthesized the different silylgermanes with the general formular $(H_3Ge)_nSiH_{4-n}$. They also employed silyltriflates $(H_nSi(OTf)_{4-n})$ and silylnonaflates $(H_nSi(ONf)_{4-n})$, enabling the selective synthesis and isolation of the individual products (Scheme 69).[127]

More recently, Stueger *et al.* introduced a complementary and highly selective approach to silyl-germanes based on nucleophilic substitution reactions of well-defined silanide reagents.[73] Using lithium tris(silyl)silanide, $LiSi(SiH_3)_3$, the previously unknown germaisotetrasilane $Ph_3GeSi(SiH_3)_3$ could be synthesized in high yield on a multigram scale by reaction with Ph_3GeCl (see Scheme 70). The resulting Ph_3Ge-substi-

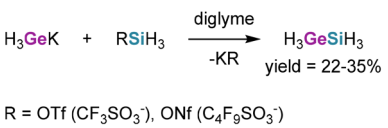

Scheme 67 Synthesis of silylgermane (H_3GeSiH_3) after treatment of $KGeH_3$ with SiH_3-OTf and SiH_3-ONf.

Open Access Article. Published on 24 April 2026. Downloaded on 5/15/2026 8:48:04 PM.
This article is licensed under a Creative Commons Attribution 3.0 Unported Licence.

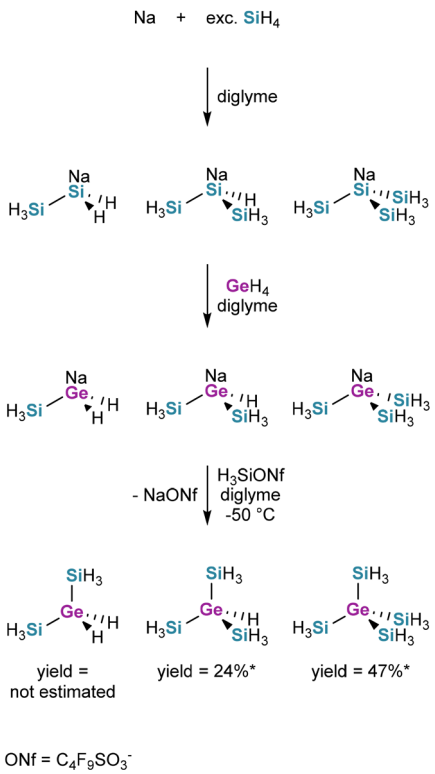

Scheme 68 3-Step-synthesis of silylgermanes. *No isolated yields; only determined *via* gaschromatography.

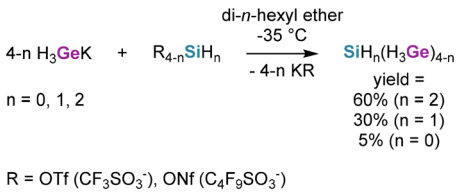

Scheme 69 Synthesis of germylsilanes.

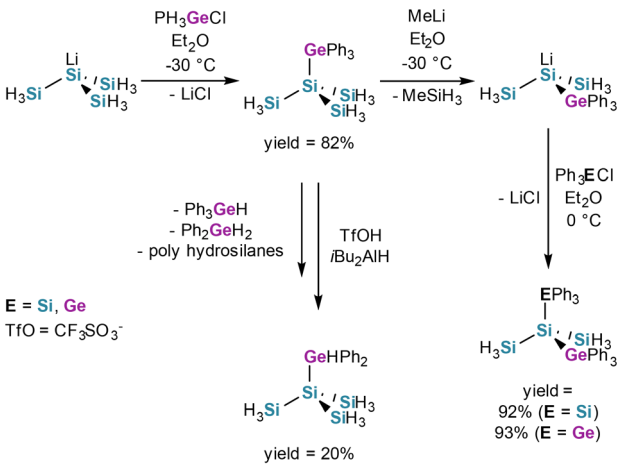

Scheme 70 Synthesis of different branched germasilicon hydrides.

tuted silyl-germanes serve as versatile intermediates for further derivatization. Selective treatment with methyllithium induces cleavage of a single Si–Si bond while preserving the Si–Ge linkage, generating lithium silanide species that can be reacted with other chlorosilanes or chlorogermanes. This strategy enables the efficient synthesis of higher substituted silylgermanes containing one or two Ph_3Ge groups in excellent yields. In contrast, attempts to access hydrogen rich silylgermanes *via* stepwise dephenylation at the germanium center using triflic acid followed by hydride reduction were significantly less selective.

It was also possible to obtain single crystals suitable for X-ray diffraction analysis (Fig. 11 and 12).

Mixed silylgermanes with preformed Si–Ge bonds were reported by Wagner and co-workers as part of a two-step synthesis strategy toward single-source precursors for Si–Ge materials.[128] In a first step, dichlorogermanes (R_2GeCl_2, R = Ph, *n*-Bu) were reacted with hexachlorodisilane in the presence of catalytic [*n*-Bu_4N]Cl, generating bis(trichlorosilyl)-germanes $Cl_3Si–GeR_2–SiCl_3$ in high yields. The reaction proceeds *via in situ* formation of the nucleophilic $[SiCl_3]^-$ species, enabling efficient Si–Ge bond formation under mild conditions. Subsequent hydride reduction of the $SiCl_3$ groups with $LiAlH_4$ afforded the corresponding hydrosilanes $H_3Si–GeR_3–SiH_3$ in good to excellent yields (see Scheme 71).

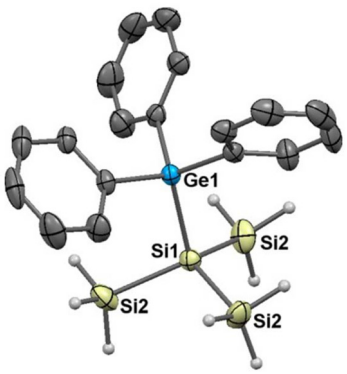

Fig. 11 Crystal structure of $Si(GePh_3)(SiH_3)_3$. Reproduced from ref. 73 with permission from American Chemical Society, © 2016.

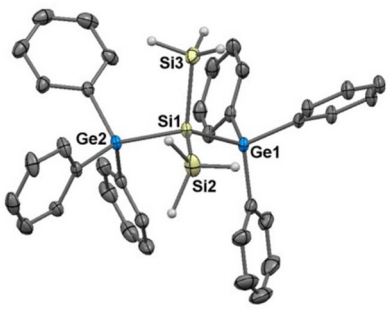

Fig. 12 Crystal structure of $Si(GePh_3)_2(SiH_3)_2$. Reproduced from Stueger *et al.*[73] with permission from American Chemical Society, ©2016.

This journal is © the Partner Organisations 2026

Open Access Article. Published on 24 April 2026. Downloaded on 5/15/2026 8:48:04 PM.
This article is licensed under a Creative Commons Attribution 3.0 Unported Licence.

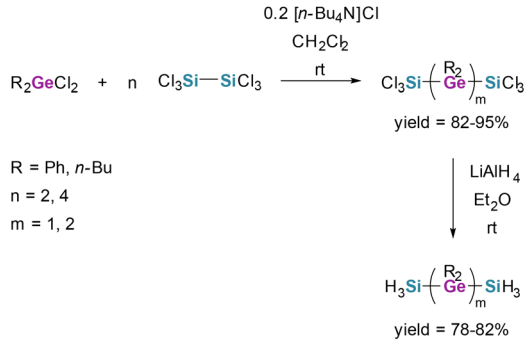

Scheme 71 Formation of germylsilanes with the general formula $H_3Si–(GR)_m–SiH_3$.

Moreover, Wagner and co-workers were successful in gaining crystals for X-ray diffractometry of intermediates and products (see Fig. 13). This modular approach provides convenient access to well-defined silylgermanes while avoiding preformed Si–Cl bonds and suppressing scrambling reactions typically encountered for fully hydride-substituted Si–Ge compounds.

Silylstannanes. Hydridic silylstannanes, defined by a direct Si–Sn bond, represent the heaviest mixed group-14 hydrides accessible to experimental investigation. In contrast to silylgermanes, whose synthesis, stability and application as single-source precursors have been explored in considerable detail, purely hydridic Si–Sn compounds remain rarely studied. The difference is mainly due to the high instability of Sn–H and Si–Sn bonds, which strongly limits the stability, isolation and handling of silylstannanes.

The simplest hydridic silylstannane, $H_3Si–SnH_3$, has been experimentally synthesized only under highly controlled conditions. The first targeted synthesis was reported by Wiberg and co-workers, who obtained the compound *via* low-temperature hydride reduction of prefunctionalized Si–Sn acetates or chlorides using $LiAlH_4$, generating ethereal solutions of the mixed hydride (see Scheme 72).[129]

However, even under these conditions, $H_3Si–SnH_3$ was found to be stable only in highly diluted solutions below −80 °C, while enrichment or warming led to rapid decomposition into silane, metallic tin and hydrogen. Complementary matrix-isolation IR studies later provided spectroscopic evidence for hydridic Si–Sn species formed by insertion of atomic tin into silane, yielding $HSnSiH_3$ complexes stabilized in inert argon matrices at cryogenic temperatures.[130] Together, these studies demonstrate while hydridic silylstannanes can be generated and spectroscopically characterized, their extreme thermal lability fundamentally limits their isolation and practical application. Sundermeyer and co-workers were successful in generating silyl stannides with the general formular $NaSn(SiH_3)_nH_{3-n}$ *via* the reaction of $NaSi(SiH_3)_nH_{3-n}$ and SnH_4 at −40 °C (see Scheme 73).[47] In contrast to the corresponding silylgermanides systems (see Scheme 68), no further follow-up chemistry or reactivity studies were reported.

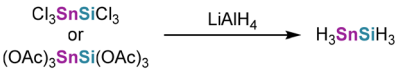

Scheme 72 Formation of silylstannane (H_3SnSiH_3) *via* the treatment of chloro-, or acetatesilylstannane with $LiAlH_4$. No yields reported.

Functionalization with group 5 (synthesis of silylpnictogens)

Silylamines. Silicon nitride SiN_x is a workhorse in metal–oxide–semiconductors and memory as spacers, liners, hard masks, barriers, and passivation layers, but continued scaling demands conformal, low-temperature films with minimal C/O impurities that can degrade fixed charge, trap density, and leakage.[77] This has sharpened interest in aminosilanes composed exclusively of H, Si, and N, most notably silylamine (H_3SiNH_2), disilylamine ($HN(SiH_3)_2$), trisilylamine ($N(SiH_3)_3$), and the preceramic polymer perhydropolysilazane (PHPS); $[SiH_2NH]_n$. These molecules deliver direct Si–N bonds and high hydrogen content, enabling clean decomposition to volatile byproducts for example H_2 and SiH_4 and facilitating low-impurity SiN_x *via* CVD and plasma-enhanced atomic layer deposition ALD at lower temperatures.[131–134] In particular, $N(SiH_3)_3$ and related small H–Si–N aminosilanes can function as single-source Si–N precursors or as nitrogen-rich co-reactants with silane, improving nucleation and conformality in high-aspect-ratio features while avoiding carbon bearing ligands.[131–133] At the polymeric scale, PHPS offers a purely H–Si–N spin-on route that converts at comparatively low tempera-

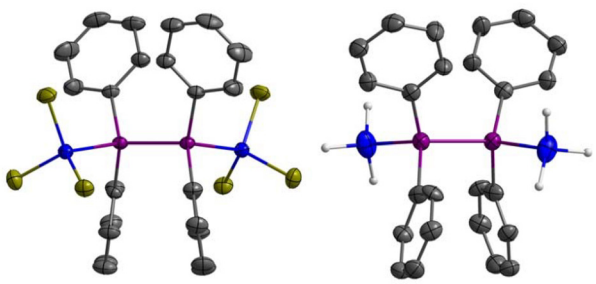

Fig. 13 Crystal structures of $Cl_3Si–(GePh_2)_2–SiCl_3$ and $H_3Si–(GePh_2)_2–SiH_3$. Reproduced from Wagner and co-workers[128] with permission from American Chemical Society, ©2022.

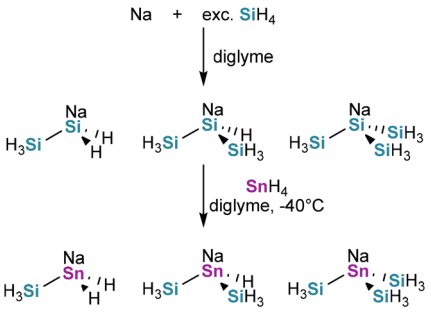

Scheme 73 Generation of silylstannides.

Open Access Article. Published on 24 April 2026. Downloaded on 5/15/2026 8:48:04 PM.
This article is licensed under a Creative Commons Attribution 3.0 Unported Licence.

tures to dense SiN_x, supporting gap-fill, barriers, and passivation without introducing heteroatom contaminants.[134] Collectively, these H–Si–N-only chemistries target key integration needs at ≤400 °C, with ongoing work focused on tuning precursor volatility and reactivity, controlling incorporated hydrogen, and optimizing plasma densification for device reliability.[131–133]

A widely used route to silylamines involves the reduction of silylamino halides. Although several hydride reagents are effective, $LiAlH_4$ is most commonly employed and usually Cl is the halide of choice. The employed silylamino halides are typically prepared by reacting silyl halides with the corresponding lithium amides,[135,136] or *via* reaction of the respective amine with the silylhalide,[137] followed by hydride reduction to afford the target silylamines. A general reaction is given in Scheme 74, path a, several examples can be found in Scheme 74, path b to g.[135–139]

Another widely used reductant for aminohalosilanes is diisobutylaluminium hydride. For example, reduction of diisopropylaminopentachlorodisilane with i-Bu_2AlH affords the partially halogenated diisopropylaminodichlorodisilane in 83% yield (see Scheme 75).[140]

An alternative, synthetically straightforward route exploits nucleophilic substitution at halogenated silanes by the corresponding amines, typically generating the ammonium halide of

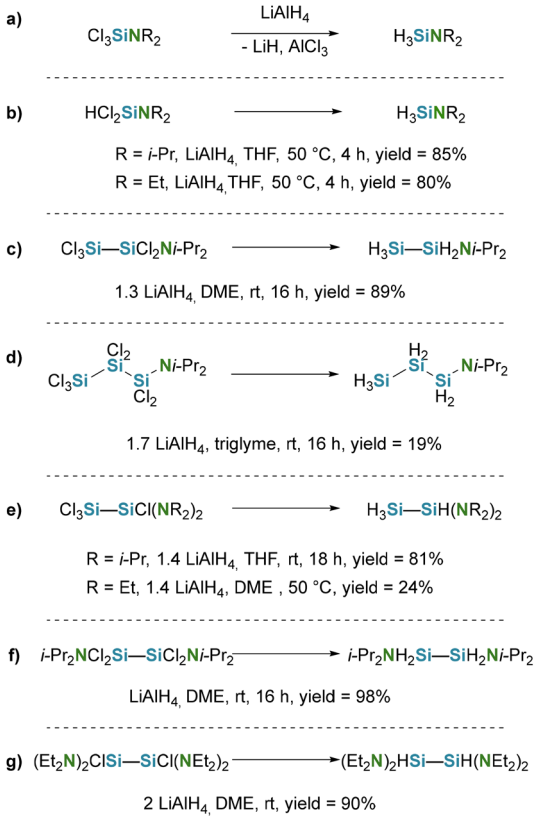

Scheme 74 General synthesis of silylamines from chlorosilanes and example synthesis (path a–g).

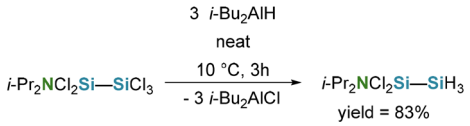

Scheme 75 Example synthesis of partially halogenated aminochlorosilanes using i-Bu_2AlH.

the amine as a byproduct.[141–143] Stock and Somieski were able to obtain trisilylamine from the reaction between ammonia (NH_3) and H_3SiCl, notably if an excess of NH_3 was used the reaction was unselective, while excess H_3SiCl leads to the selective formation of trisilylamine.[11,144,145] They reasoned that the reaction proceeds stepwise with silylamine and disilylamine ($HN(SiH_3)_2$) as intermediates, but could not isolate them and they observed the formation of a polymeric solid and SiH_4 (see Scheme 76).[144] Later Aylett and Hakim showed that disilylamine decomposes to trisilylamine and NH_3 and in the presence of NH_3 disilylamine decomposes to SiH_4 and a solid polymer.[146]

Burg and Kuljian adapted Stocks and Somieskis synthesis by slowly mixing gaseous ammonia, from below, into H_3SiCl, resulting in the formation of trisilylamine in 80% yield (see Scheme 77). Notably they mentioned that slow addition of ammonia is necessary to obtain high yields and good selectivity.[147] When ammonia and H_3SiCl were condensed into a flask the reaction afforded trisilylamine in low yields.[148]

Emeléus and Miller already employed this method in 1939 for the synthesis of dimethylsilylamine (Me_2NSiH_3), ethyldisylamine ($EtN(SiH_3)_2$) and methyldisilylamine ($MeNSiH_3$) (see Scheme 78, path a and b), though they only identified them and gave no yields.[141] For instance, monochlorodisilane (H_3SiSiH_2Cl) undergoes substitution with diisopropylamine (*i*-Pr_2NH) to furnish diisopropylaminodisilane ($H_3Si–SiH_2Ni–Pr_2$), concomitant with formation of diisopropylammonium chloride (*i*-Pr_2NH_2Cl) (see Scheme 78, path c).[143] Both iso-

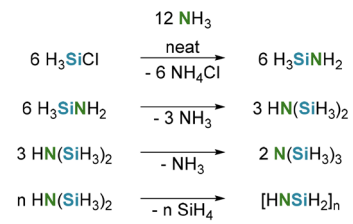

Scheme 76 Synthesis of trisilylamine from H_3SiCl and NH_3, according to Stock. No yield was reported.

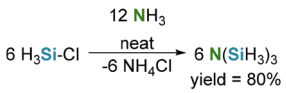

Scheme 77 Synthesis of trisilylamine with gaseous ammonia and H_3SiCl, according to Burg.

This journal is © the Partner Organisations 2026

Open Access Article. Published on 24 April 2026. Downloaded on 5/15/2026 8:48:04 PM.
This article is licensed under a Creative Commons Attribution 3.0 Unported Licence.

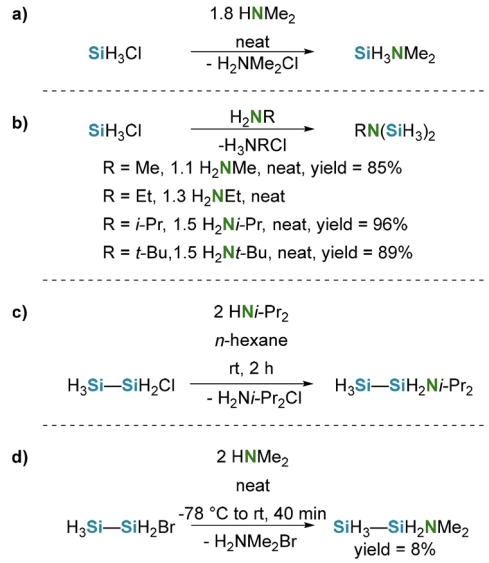

Scheme 78 Example synthesis of silylamines from halosilanes and amines (path a–d). When no yields are given for the product, no yield was reported.

propylamine (i-PrNH$_2$) and *t*-butylamine (*t*-BuNH$_2$) react with H$_3$SiCl to afford the corresponding disilylamines in good yields (see Scheme 78, path b),[142] while monochlorodisilane reacts with diisopropylamine to give diisopropylaminodisilane.[149] Burg and Kuljian prepared methyldisilylamine (MeN(SiH$_3$)$_2$) from methylamine (MeNH$_2$) and ammonia in 85% yield (see Scheme 78, path b).[147] Bromodisilane (H$_3$Si–SiH$_2$Br) reacts with dimethylamine (Me$_2$NH) to afford dimethylaminodisilane (H$_3$Si–SiH$_2$NMe$_2$) in 8% yield (see Scheme 78, path d).[150]

Furthermore, disilylamine reacts with H$_3$SiI to afford trisilylamine in 67% yield, when a slight excess of H$_3$SiI is used to afford trisilylamine the yield increases to 87%, though no experimental details were given (see Scheme 79, path a).[146,151] Similarly, anhydrous hydrazine reacts with H$_3$SiI to give tetrasilylhydrazine in 40% yield, which is a strong reducing agent, but explodes in contact with air (see Scheme 79, path b).[152]

Ward and MacDiarmid treated iododisilane with NH$_3$ to afford trisdisilylamine in 64% yield (see Scheme 80).[153]

Diaminosilylamines, such as *t*-BuN(SiH$_2$NMe$_2$)$_2$, can be obtained from dichlorosilane (H$_2$SiCl$_2$) in a two-step synthesis

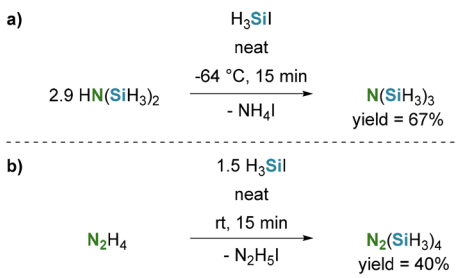

Scheme 79 Synthesis of trisilylamine (path a) and tetrasilylhydrazine (path b) using H$_3$SiI.

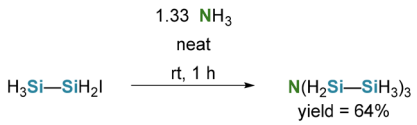

Scheme 80 Synthesis of tridislanylamine from monoiododisilane and NH$_3$.

in good yields. H$_2$SiCl$_2$ reacts with the respective primary amine, either in excess[154] or under use of a aiding base like trimethylamine (NMe$_3$),[155] for example *t*-BuNH$_2$ to obtain a dichlorosilylamine, which subsequently reacts with an amine to afford the respective diaminosilylamine (see Scheme 81).[154,155]

Wells and Schaeffer investigated the reaction of trisilylamine with ammonia by condensing both reagents into a flask and allowing them to react in the liquid phase. The reaction afforded *N*,*N*′,*N*″-trisilylcyclotrisilazane only in trace amounts, however, multiple runs provided sufficient material for characterization. They reasoned that ammonia catalyses the elimination of SiH$_4$ from trisilylamine (see Scheme 82).[148]

Various azapolysilanes can be prepared by reacting diisopropylaminodisilane with primary amines, such as *t*-BuNH$_2$. Alternatively by the reaction of chlorodisilane with primary amines in the presence of triethylamine as a base, or by the treatment of 1,2-dichlorodisilane (ClH$_2$Si–SiH$_2$Cl) with primary amines and triethylamine (NEt$_3$) (see Scheme 83).[156]

Furthermore, alkalimetal amides, such as sodium amide, are suitable reagents to form silylamines *via* reaction with silylhalides. After formation of the respective sodium amide a silylhalide is added affording the formation of silylamines, this approach allows for the synthesis of diisopropylaminosilane (i-Pr$_2$NSiH$_3$) (see Scheme 84).[157]

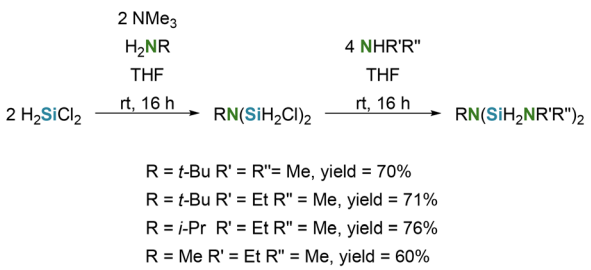

Scheme 81 Synthesis of diaminosilylamines from H$_2$SiCl$_2$ and the respective amines.

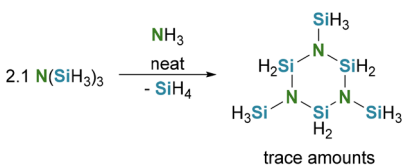

Scheme 82 Reaction between trisilylamine and ammonia.

Open Access Article. Published on 24 April 2026. Downloaded on 5/15/2026 8:48:04 PM.
This article is licensed under a Creative Commons Attribution 3.0 Unported Licence.

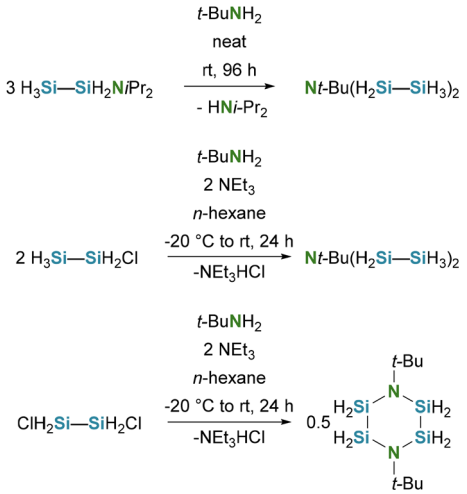

Scheme 83 Example synthesis of silylamines from diisopropylaminodisilane, monochlorodisilane and 1,2-chlorodisilane. No isolated yields were given.

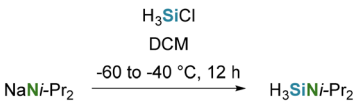

Scheme 84 Synthesis of silylamines from alkalimetal amides and silylhalides. No isolated yields were given.

Schmidbaur and co-workers accessed 1,1- and 1,2-diaminodisilanes from solutions of 1,2-disilanediylditriflate. The solution of 1,2-disilanediylditriflate is afforded from di-*p*-tolyldisilane and triflic acid and reacts with solutions of the respective amine and triethylamine to afford the 1,2-diaminodisilanes (see Scheme 85, path a and b). Notably, in the case of diethylamine ($HNEt_2$) the 1,1-substituted diethylaminodisilane is also formed (see Scheme 85, path a), whereas the 1,1-diisopropylaminodisilane is not observed (see Scheme 85, path b).[158]

When primary amines are employed, the reaction furnishes six-membered cyclic aminosilanes containing two disilyl units, rather than the 1,1- and 1,2-substituted linear diaminodisilanes obtained with secondary amines (see Scheme 86, path a). When 1,4-difunctional diamines are used instead, the reaction yields five-membered cyclic compounds bearing an exocyclic silyl substituent (see Scheme 86, path b).[158]

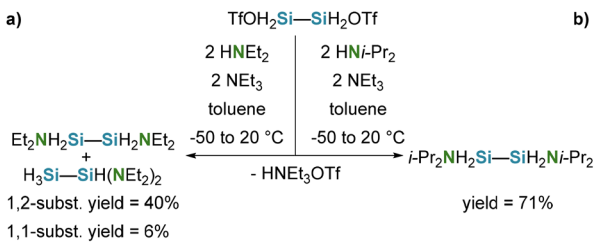

Scheme 85 Synthesis of diaminodisilanes from disilanediylditriflate using secondary amines (path a and b).

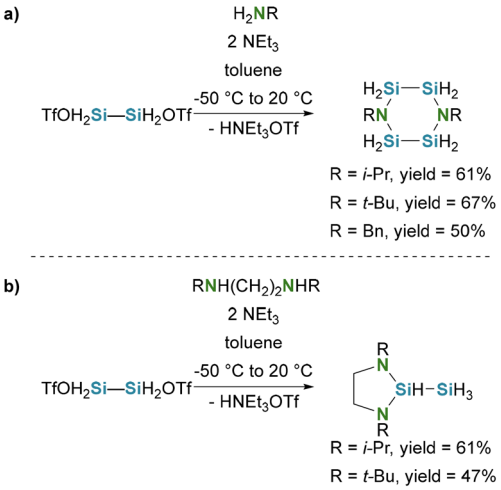

Scheme 86 Synthesis of cyclic silylamines from disilanediylditriflate. (path a and b)

Dehydrogenative coupling offers an attractive, atom-economical route to silylamines. A variety of catalysts promote the coupling of amines with hydrosilanes, including the Lewis acid trispentafluorophenylborane ($B(C_6F_5)_3$),[159] transition metal systems such as triruthenium dodecacarbonyl ($Ru_3(CO)_{12}$),[160] main-group reagents such as di-*n*-butylmagnesium (n-Bu_2Mg),[161] Mn based catalysts[162] and Zn based catalysts.[163] Sanchez *et al.* reported the dehydrogenative coupling of amino- and diaminosilanes derived from disilane and trisilane using ruthenium on carbon (Ru/C) as the catalyst, although only non-isolated yields were provided (see Scheme 87, path a and b).[164]

SiH_4 can be dehydrogenatively coupled with diisopropylamine using di-*n*-butylmagnesium n-Bu_2Mg as catalyst, as shown by Maddock *et al.* (see Scheme 88).[159,161]

Moreover, Rekken employed Zn-based catalysis to achieve dehydrogenative coupling, affording diisopropylaminodisilane and bisdiisopropylaminodisilane. They further demonstrated that Zn-based catalysis is applicable to SiH_4, albeit with low conversions. No isolated yields were reported, the product compositions were determined by GC-FID, and diisopropylamine was used in large excess (see Scheme 89).[163]

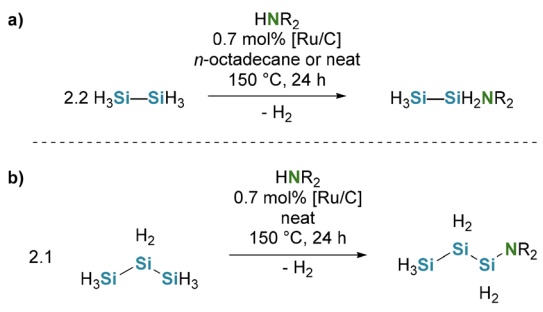

Scheme 87 Synthesis of aminodisilane (path a) and aminotrisilane (path b) using Ru/C as catalyst. Only non-isolated yields were reported. Several R groups can be employed.

This journal is © the Partner Organisations 2026

Open Access Article. Published on 24 April 2026. Downloaded on 5/15/2026 8:48:04 PM.
This article is licensed under a Creative Commons Attribution 3.0 Unported Licence.

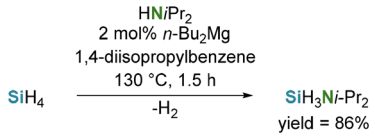

Scheme 88 Dehydrogenative coupling of SiH_4 and diisopropylamine, using *n*-Bu_2Mg.

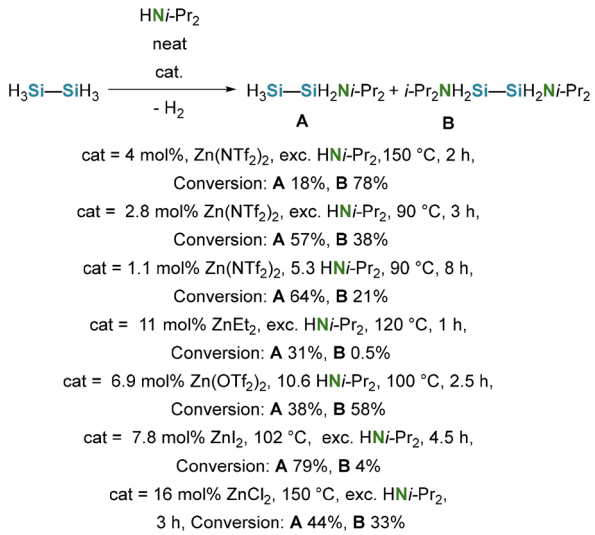

Scheme 89 Dehydrogenative coupling of disilane with diisopropylamine, using Zn based catalysts. Only conversions were reported.

Using $Zn(NTf_2)_2$ as a catalyst enabled the dehydrogenative coupling to afford diisopropylaminoneopentasilane, however, only crude product conversions determined by GC-FID were reported (see Scheme 90).[163]

In 2022, Trovitch and co-workers demonstrated that the dehydrogenative coupling of SiH_4 with primary and secondary amines proceeds using the manganese-based catalyst $[(^{2,6\text{-iPr}_2\text{Ph}}\text{BDI})\text{Mn}(\mu\text{-H})]_2$.[162] With primary or secondary amines, di- and trisubstituted aminosilanes are obtained, and the steric demand of the amine strongly influences the reaction time. Diamines and triamines furnish polycarbosilazanes, whereas ammonia affords perhydropolysilazane (see Scheme 91).[162]

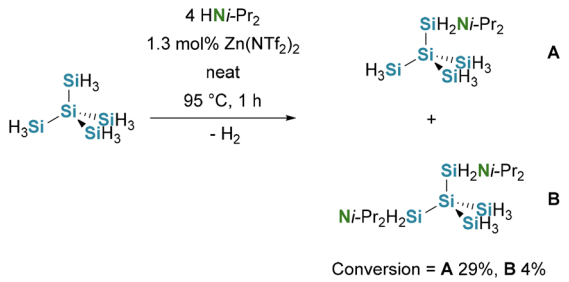

Scheme 90 Dehydrogenative coupling of neopentasilane with Zn $(NTf_2)_2$ and diisopropylamine. Only conversions were reported.

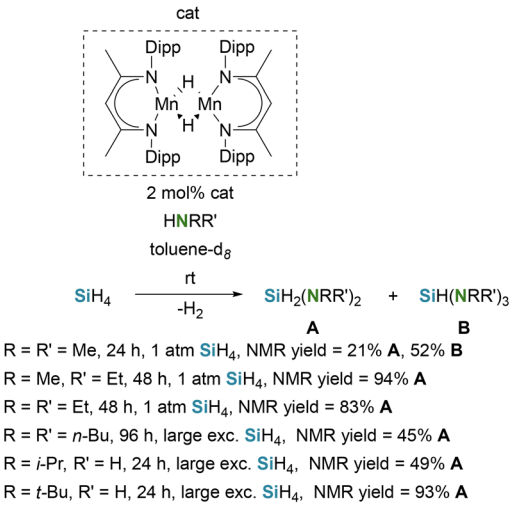

Scheme 91 Synthesis of aminosilanes from SiH_4 *via* Mn based catalysis.

A different approach to obtain aminosilanes is the amine exchange pathway. Various aminosilanes are accessible *via* transamination with amines at room temperature or elevated temperature. The educts of choice for transaminations in the literature are diisopropylaminosilanes. For example, diisopropylaminosilane forms disilylamine with NH_3 and subsequently forms trisilylamine (see Scheme 92).[159]

Aylett and Hakim reported the synthesis of disilylamine in 75% yield by treating diphenylaminosilane (Ph_2NSiH_3) in toluene at low temperature with ammonia (see Scheme 93).[151]

Transamination of diisopropylaminosilane proceeds with a broad range of secondary amines; with primary amines, the corresponding disilylamines are obtained, while polyfunctional amines undergo silylation at multiple amino groups (see Scheme 94, path a to c).[143]

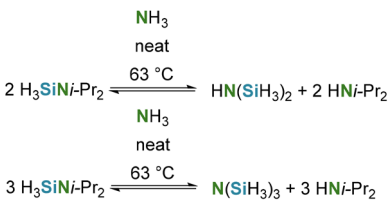

Scheme 92 Synthesis of di- and trisilylamine, *via* transamination of diisopropylamine. No detailed ratios of the reagents were given; therefore, the overall equation is given.

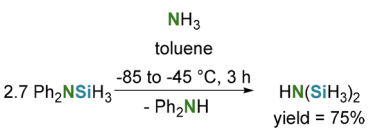

Scheme 93 Synthesis of disilylamine *via* transamination of Ph_2NSiH_3 with NH_3.

Open Access Article. Published on 24 April 2026. Downloaded on 5/15/2026 8:48:04 PM.
This article is licensed under a Creative Commons Attribution 3.0 Unported Licence.

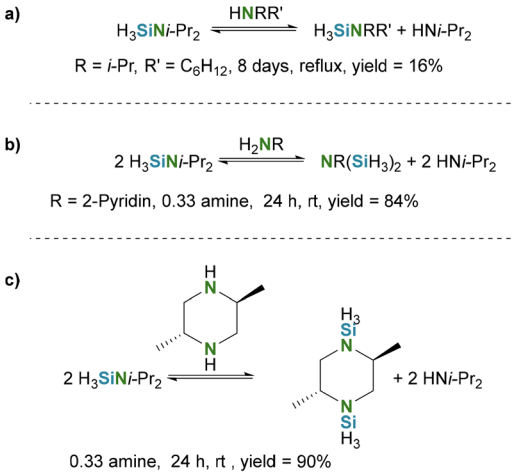

Scheme 94 Example transaminations of diisopropylaminosilane (path a–c).

This methodology extends to larger aminosilane frameworks, for example, Zhou *et al.* employed diisopropylaminodisilane in transamination reactions to access a range of monosubstituted as well as bissubstituted (disilanyl)amines, although only GC-MS conversions were reported and no isolated yields (see Scheme 95 and Table 6).[165]

Using an NH_3 : diisopropylaminodisilane ratio of 1 : 3 gives 99% conversion to bisdisilanylamine; with an additional equivalent of diisopropylaminodisilane, trisdisilanylamine is obtained.[165] Furthermore, Rekken *et al.* obtained trisdisilanylamine by thermal degradation of bisdisilanylamine at 110 °C (see Scheme 96, path a to c).[166]

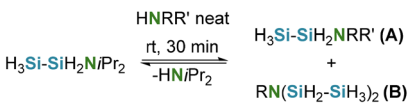

Scheme 95 Transamination of diisopropylaminosilane. For conversions see Table 6. R = organic rest, R′ = H or organic rest, see Table 6.

Table 6 Conversions of transamination reactions

	GC conversion [%]	
Amine (2 eq.)	A	B
Diethyl	38	—
Methyl	69	22
Ethyl	73	23
Propyl	62	21
Butyl	71	25
2-Aminobutane	96	1
Pentylamine	51	13
2-Aminopentane	95	1
1,2-Dimethylpropyl	98	—
t-Pentyl	83	—
Cyclopentyl	84	12
Cyclohexyl	92	5
Aniline	74	—
o-Toluidine	38	—

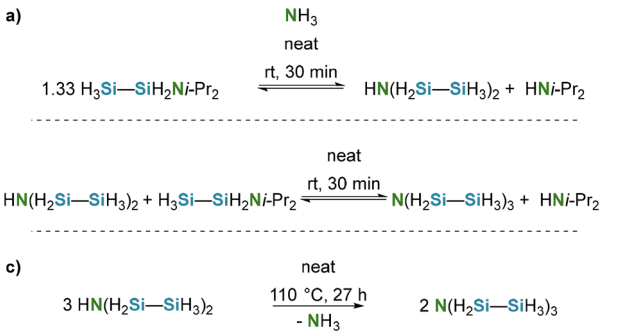

Scheme 96 Transamination of diisopropylaminosilane affording bis- and trisdisilanylamine and thermal degradation of bisdisilanylamine (path a–c). No isolated yields were reported. For the thermal redistribution of bisdisilanylamine only the general equation is given.

Silyl iso-cyanide (H_3SiNC) was previously prepared but wrongfully assigned as silyl cyanide (H_3SiCN) and no detailed analysis of its properties was carried out.[167] MacDiarmid was able to obtain and analyze both silyl iso-cyanide and silyl iso-thiocyanate (H_3SiNCS). The treatment of silver cyanide (AgNC) with H_3SiI at room temperature afforded silyl iso-cyanide in 90% yield and by reaction with mercuric cyanide at elevated temperatures, though no yield was reported (see Scheme 97, path a). Silyl iso-thiocyanate was afforded *via* the reaction between H_3SiI and silver thiocyanate (AgNCS) in 66% yield (see Scheme 97, path b).[168] Furthermore, the reaction between trisilylamine and cyanic acid (HOCN) affords silyl iso-cyanate (H_3SiNCO) in 95% yield, and with thiocyanic acid (HSCN), it leads to the formation of silyl iso-thiocyanate in 58% yield (see Scheme 97, path c and d).[169]

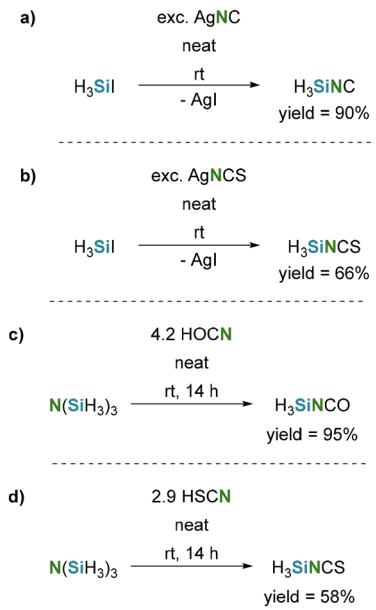

Scheme 97 Synthesis of silyl iso-cyanide, silyl iso-cyanate and silyl iso-thiocyanate from H_3SiI (path a and b) and trisilylamine (path c and d).

This journal is © the Partner Organisations 2026

Open Access Article. Published on 24 April 2026. Downloaded on 5/15/2026 8:48:04 PM.
This article is licensed under a Creative Commons Attribution 3.0 Unported Licence.

Gaseous silylphosphane (H_3SiPH_2) reacts readily with cyanic acid as well as thiocyanic acid affording silyl iso-cyanate or silyl iso-thiocyanate in yields greater than 80% (see Scheme 98, path a and b).[170]

Disilylsulfide ($S(SiH_3)_2$) is a viable feedstock for the synthesis of silyl i-thiocyanate. In combination with silver thiocyanate (AgNCS), it afforded H_3SiNCS in 86% yield (see Scheme 99). When instead cyanogen chloride was employed, the reaction led to a mixture of disilylsulfide, silyl cyanide, sulfur, and silyl i-thiocyanate, but the mixture proved to be inseparable.[171]

Ebsworth and Mays reported the synthesis of silyl i-cyanate *via* treatment of silvercyanate (AgOCN) and powdered glass with iodosilane vapor with an overall yield of 20% (see Scheme 100).[172]

Silylamines such as $N(SiH_3)_3$ and $N(H_2Si–SiH_3)_3$ serve as precursors to silylaminoboranes. Trisilylamine reacts quantitatively at low temperature with boron trihalides BX_3 (X = Cl, F) to afford the corresponding disilylaminohaloboranes.[147,173] Witz and Sujishi showed that boron trifluoride (BF_3) forms adducts with trisilylamine, methyldisilylamine, and dimethylsilylamine, these adducts decompose at room temperature to give silyl fluoride and the corresponding silylaminoborane (see Scheme 101, path a and b).[173]

Furthermore, trisilylamine reacts readily with bromodiborane (B_2H_5Br) at low temperature to afford disilylaminoborane

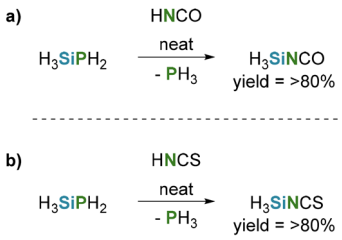

Scheme 98 Synthesis of silyl iso-cyanate (path a) and silyl iso-thiocyanate (path b). No amounts of the used reagents were given.

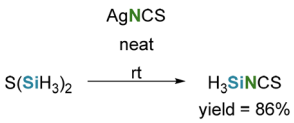

Scheme 99 Synthesis of silyl i-thiocyanate from disilylsulfide. The amount of AgNCS used was not reported.

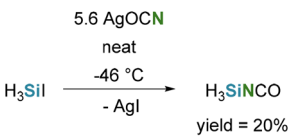

Scheme 100 Synthesis of silyl i-cyanate from iodosilane and silvercyanate.

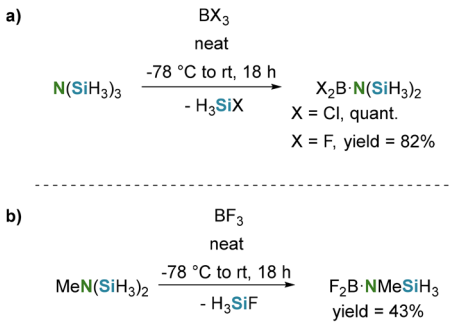

Scheme 101 Synthesis of bissilylaminodichloro- and bissilylaminodifluoroborane (path a and b).

in quantitative yield; subsequent treatment with diborane furnishes bissilylaminodiborane in 80% yield (see Scheme 102, path a and b).[147] The same methodology extends to methyldisilylamine, but instead of the desired methylsilylaminoborane it yields methylsilylaminodiborane in 20% yield, accompanied by formation of H_3SiBr, SiH_4 and B_2H_6 (see Scheme 102, path c). The yield was improved to 44% by adding 1.3 equivalents of diborane, an effect attributed to reduced disproportionation of the intermediate methylsilylaminoborane (see Scheme 102, path c).[147]

MacDiarmid and Abedini formed the corresponding adduct of trisdisilanylamine with BF_3 at low temperature; upon heating, the adduct decomposed to afford bisdisilanylaminofluoroborane and fluorodisilane, although only the isolated yield of the fluorodisilane was reported (see Scheme 103).[150]

Norman and Scantlin reported that boranes catalyze the condensation of trisilylamine and methyldisilylamine to give

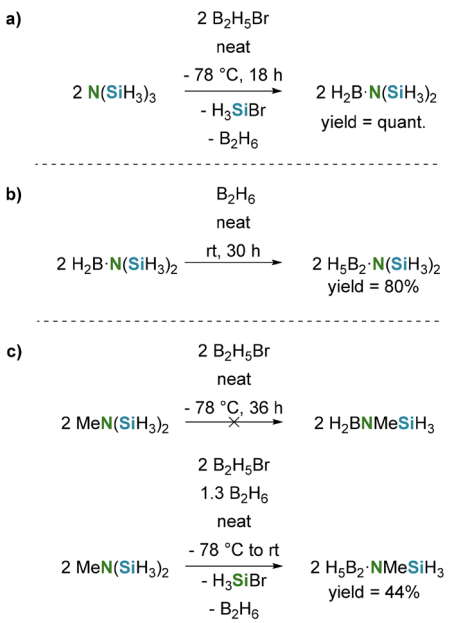

Scheme 102 Reactions between trisilylamine (path a and b) and methyldisilylamine (path c and d) with bromodiborane and subsequent reaction of the formed silylamnioboranes with diborane.

Open Access Article. Published on 24 April 2026. Downloaded on 5/15/2026 8:48:04 PM.
This article is licensed under a Creative Commons Attribution 3.0 Unported Licence.

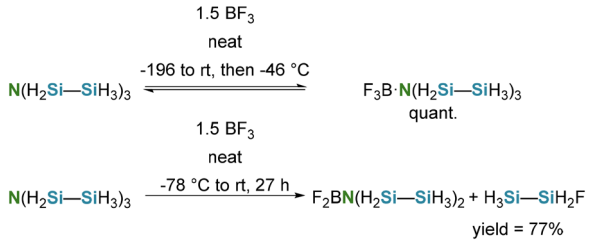

Scheme 103 Synthesis of $F_2BN(SiH_2SiH_3)_2$. In the second reaction only the yield for fluorodisilane was reported.

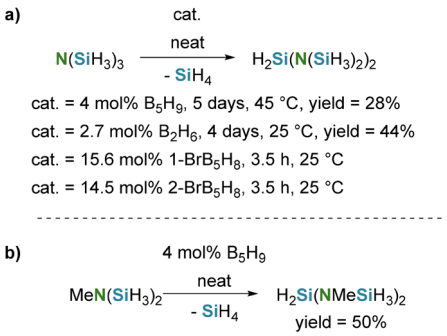

Scheme 104 Borane catalyzed condensation of trisilylamine (path a) and methyldisilylamine (path b). Path (a) no isolation was performed under catalysis by 1- and 2-BrB_5H_8.

the corresponding silazanes with simultaneous liberation of SiH_4, in good yields (see Scheme 104, path a and b). When B_2H_6 or B_5H_9 is used, the reaction affords $H_2Si(N(SiH_3)_2)_2$ with only minor formation of higher condensation products $Si_7N_3H_{16}$. In contrast 1- and 2-BrB_5H_8 catalyze much faster reactions that are more difficult to control, leading to increased formation of $Si_7N_3H_{16}$.[174]

Silyl azide (H_3SiN_3) can be prepared by reacting trisilylamine with hydrazoic acid (HN_3) in *n*-Bu_2O, however, it is unstable at room temperature and slowly decomposes with evolution of SiH_4 (see Scheme 105, path a).[175] Alternatively,

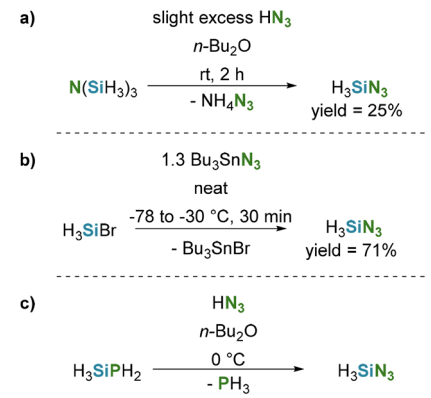

Scheme 105 Synthesis of silylazide (path a–c). No yield or experimental details were reported for the reaction of H_3SiPH_2 with hydrazoic acid.

treatment of H_3SiBr with tributyltinazide (Bu_3SnN_3) affords silylazide in 71% yield (see Scheme 105, path b).[176] A further route involves treating H_3SiPH_2 with a dilute solution of hydrazoic acid, though no yield was reported (see Scheme 105, path c).[170]

Fritz and Berkenhoff investigated the reaction between silylphosphane and NH_3 and concluded that at −80 °C silylamine forms and subsequently converts to polymeric solids of the type $[SiH_2NH]_x$. To support this interpretation, they also examined the reaction of H_3SiCl and NH_3, which led to the same solids, although the proposed intermediates could not be directly observed (see Scheme 106).[177]

Norman and Jolly further investigated the H_3SiPH_2 and NH_3 system. They found that depending on reaction time, temperature, and ratio of H_3SiPH_2 to NH_3, a complex product mixture is formed. At −78 °C to −63 °C and a ratio above 6 : 1 $H_3SiPH_2 : NH_3$ mainly PH_3 and $HN(SiH_3)_2$ are formed in a 2 : 1 ratio, with small amounts of $N(SiH_3)_3$ and SiH_4 from subsequent reactions.[178] When the reaction was carried out with a ratio of $H_3SiPH_2 : NH_3$ below 6 : 1 or at higher temperatures, only a complex product mixture was observed, notably small amounts of the silazanes $SiH_2(NHSiH_3)_2$ and $(SiH_3)_2NSiH_2NHSiH_3$ were formed. They also could not find direct evidence for the formation of H_3SiNH_2.[178]

Glidewell further examined the reactions between H_3SiPH_2 and amines and imines. In the gas phase, methylamine and diethylamine react with PH_3 to give the corresponding silylamines in quantitative yield. In contrast, methylamine does not react with gaseous H_3SiPH_2 and with condensed H_3SiPH_2 only a white polymeric solid is obtained (see Scheme 107).[170]

Treatment of cyanamide (CH_2N_2) with H_3SiPH_2 or with disilylsulfide affords disilylcarbodiimide ($C(NSiH_3)_2$) in excellent yields (see Scheme 108, path a and b). However, the yield of the $S(SiH_3)_2$ reaction was not explicitly reported. In contrast,

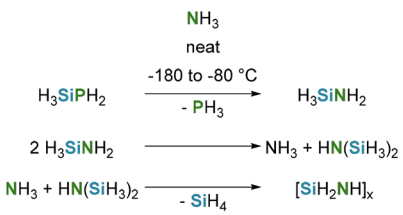

Scheme 106 Ammonolysis of H_3SiPH_2 according to Fritz. No details about the amounts of H_3SiPH_2 and NH_3 as well as reaction time were given. For the following reaction of the formed H_3SiNH_2 only the general formula is given.

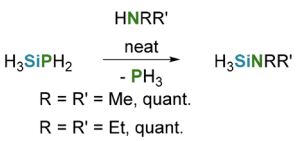

Scheme 107 Synthesis of silylamines from H_3SiPH_2 with amines. The amounts of reagents used were not given.

This journal is © the Partner Organisations 2026

Open Access Article. Published on 24 April 2026. Downloaded on 5/15/2026 8:48:04 PM.
This article is licensed under a Creative Commons Attribution 3.0 Unported Licence.

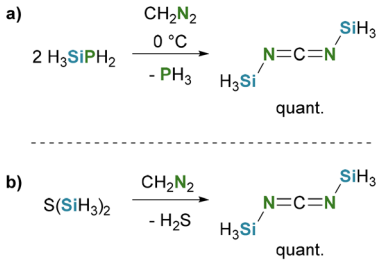

Scheme 108 Synthesis of disilylcarbodiimide (path a and b). No experimental details were given, therefore only the general formula is given.

trisilylphosphane ($P(SiH_3)_3$) gives the carbodiimide only in poor yield with concomitant decomposition of $P(SiH_3)_3$, and SiH_3PMe_2 undergoes complete decomposition under the reaction conditions.[170]

Passing H_3SiI vapor over powdered glass wool and silver cyanamide (Ag_2CN_2) led to the formation of disilylcarbodiimide in 20% yield, with SiH_4, and HCN as side products. Neither using $PbCN_2$, or H_3SiBr with Ag_2CN_2 improves the yields and results in 10–20% yield of disilylcarbodiimide. Notably, H_3SiI and undiluted Ag_2CN_2 led to an explosion.[179] When H_3SiI vapor is diluted with N_2, the yield of the reaction is increased to up to 60%.[180] While it was first unclear if disilylcyanamide $NCN(SiH_3)_2$ or disilylcarbodiimide was formed during the reaction, later IR spectra studies[180] and gas phase electron diffraction[181] showed that disilylcarbodiimide is formed (see Scheme 109).

Schmidbaur and Schuh employed NaH and $NaNH_2$ in the presence of 18-c-6 as a phase-transfer catalyst to convert 1,4-disilabutane and *n*-tetrasilane into their corresponding aminosilanes (see Scheme 110, path a and b). While 1,4-disilabutane reacts with diethylamine using the $NaNH_2$/18-c-6 system in pentane to afford the aminosilanes with evolution of H_2, *n*-tetrasilane undergoes cleavage, giving mixtures of smaller aminosilanes and higher silanes. They found that NaH alone does not catalyze these reactions. When pyrrole was used with *n*-tetrasilane instead of diethylamine, the main product was $Si(NC_4H_4)_4$, accompanied by formation of trisilane.[182]

Perhydropolysilazanes such as bisdisilylaminosilane are obtainable from trisilylamine with a suitable catalyst, such as $B(C_6F_5)_3$ or $PdCl_2$ (for more examples see Scheme 111 and Table 7). Though it is not stated if the product obtained is pure and no number average molecular weight M_n for the products was given. When the reaction is carried out with

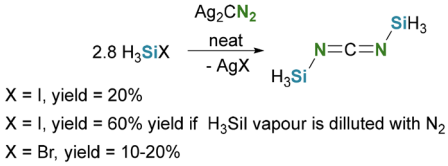

Scheme 109 Synthesis of disilylcarbodiimide from halosilanes and Ag_2CN_2.

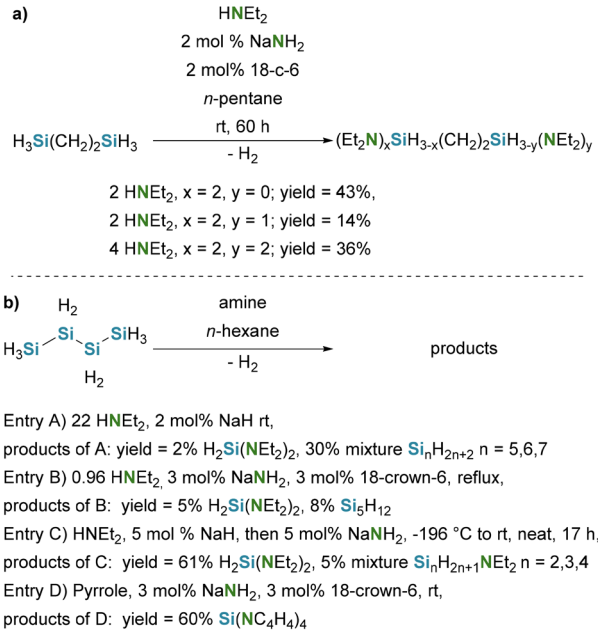

Scheme 110 Reactions of 1,4-disilabutane (path a) and *n*-tetrasilane (path b) with amines under $NaNH_2$ catalysis.

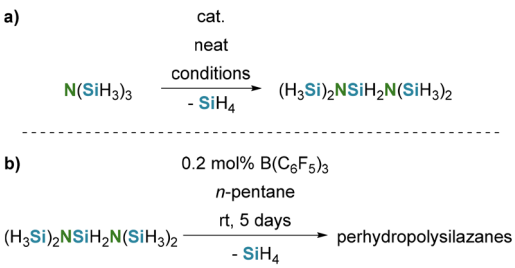

Scheme 111 Synthesis of bis(disilylamino)silane and perhydropolysilazanes. Yields for path a are given in Table 7. No yields or molecular weight distributions were given for path b.

Table 7 Synthesis of bis(disilylamino)silane

Catalyst	Catalyst loading [mol%]	Cocatalyst [mol%]	*T* [°C]	*t* [h]	Yield [%]
Pt/C	5	NEt_3 31%	100	18	48
Pt/C	5	NMe_2Et 25%	100	4	36
Pt/C	5	NMe_2Et 25%	100	22	46
Pt/C	0.4	NMe_2Et 25%	100	4	31
Pt/C	0.4	NMe_2Et 25%	105	25	39
$[RuCl_2((AMPY)(DPPB))]$	0.4	—	100	18	10
$[RuCl_2((AMPY)(DPPB))]$	0.4	NEt_3 30%	100	18	83
$[RhCl(PPh_3)_3]$	0.4	NMe_2Et 25%	100	1	86
[(*R*,*R*)-teth-TsDpenRuCl]	0.6	NMe_2Et 25%	100	1.5	83
$Ru_3(CO)_{12}$	1.1	NMe_2Et 25%	80	1	80

increased catalyst loading, M_n increases and the ratio of SiH_2 : SiH_3 of the products increases as well.[183]

Silylphosphanes. For further information about silylphosphanes containing partially hydrated and fully non hydrated

Open Access Article. Published on 24 April 2026. Downloaded on 5/15/2026 8:48:04 PM.
This article is licensed under a Creative Commons Attribution 3.0 Unported Licence.

silyl groups Fritz and Scheer wrote an excellent review, which is beyond the scope of fully hydrated silylphosphanes of this review.[184]

The composition of silylphosphane precursors is especially relevant for semiconductor applications. Silylphosphanes consisting only of P, Si, and H are attractive for semiconductor processing because they are carbon- and halogen-free and decompose to benign H_2, reducing impurity incorporation that degrades carrier lifetimes and interface quality.[185,186] Their preformed Si–P bonds make them single-source reagents that deliver Si and P together, enabling *in situ* n-type doping of Si/Ge and the growth of Si–P materials with improved dopant incorporation efficiency and spatial uniformity compared with separate feeds.[186,187]

The first reported silylphosphane H_3SiPH_2 was prepared by Fritz, in 1952, *via* thermal decomposition of equimolar amounts of SiH_4 and PH_3, proceeding through a radical mechanism.[12,53,188] Furthermore, under the reaction conditions, less volatile species such as $H_2Si(PH_2)_2$ and SiP_2 are generated.[189,190] This pathway enabled the first investigations into the properties of silylphosphanes but was problematic for the synthesis of H_3SiPH_2 in a preparative scale, due to the further decomposition of H_3SiPH_2 towards SiP_2 during the reaction (see Scheme 112).[190]

Sabherwal and Burg adapted the thermal decomposition conditions to a decreased temperature of 300 °C in the presence of trace amounts of I_2, leading to a significantly increased yield of 61% for H_3SiPH_2.[191] The enhanced yield was attributed to a lower degree of product degradation, due to the lower temperature and to the formation of H_3SiI, which reacts with PH_3 to give H_3SiPH_2 and HI. The formed HI then reacts with SiH_4 to regenerate H_3SI.[191] Another early report of silylphosphanes was made by Aylett *et al.* in 1955, who demonstrated that H_3SiI reacts with white phosphorous to afford PI_2SiH_3 with various side products, most notably $P(SiH_3)_3$, which they could not characterize fully. They further showed that H_3SiPH_2 can be formed *via* reaction of NMe_3SiH_3I with PH_3.[13]

In addition to the thermal route photochemistry was also investigated to yield silylphosphanes. Blazejowski obtained small quantities of H_3SiPH_2 by IR irradiation of a PH_3/SiH_4 mixture, photosensitized by SiF_4,[192] later by irradiation of a PH_3/SiH_4 mixture,[193] and by photolysis of PH_3/SiH_4 mixtures at 147 nm.[194] The formation of H_3SiPH_2 and hydrosilanes such as disilane and trisilane is rationalized by the generation of silylene groups that insert into Si–H and P–H bonds.[192,193] Another alternative approach towards silylphosphanes such as H_3SiPH_2 employed electrical discharge methods. Mixtures of SiH_4 and PH_3 form silylphosphanes in an ozonizer-type silent electrical discharge tube.[195,196] Using this setup Jolly and Gokhale obtained $HP(SiH_3)_2$ from a mixture of H_3SiPH_2 and SiH_4.[196,197] Furthermore ozonizer-type silent electrical discharge tubes have also facilitated the preparation of $H_3SiSiH_2PH_2$ from disilane and PH_3. However the silent electrical discharge approach has proven to be unsuitable for larger scales, due to the low yields and poor selectivity (see Scheme 113, path a and b).[196,197]

Halide mediated exchange reactions between silylphosphane and halodisilanes were also investigated in order to obtain silylphosphanes. Drake *et al.* obtained disilanylphosphane ($H_3SiSiH_2PH_2$) *via* exchange reaction between H_3SiPH_2 and disilylhalides (see Scheme 114).[198,199]

They further employed SiH_2Cl_2 and $SiHCl_2SiH_2Cl$ with H_3SiPH_2 to synthesize the chlorinated silylphosphanes SiH_2ClPH_2 and $SiHCl_2SiH_2PH_2$ (see Scheme 115, path a and b). Whereas 1,1-dichlorodisilane does not react with H_3SiPH_2, 1,2-dichlordisilane undergoes facile conversion to 1,2-diphosphinodisilane *via* the intermediate $SiH_2ClSiH_2PH_2$ (see Scheme 115, path c). Furthermore 1,1,2-trichlorodisilane affords 1,1-dichloro-2-phosphinodisilane.[199]

Silylphosphane synthesis can also be achieved through nucleophilic substitution of silyl halides by alkali metal phosphides. Amberger and Boeters demonstrated that the direct reaction of bromosilane with potassium dihydrophosphide (KPH_2) does not afford H_2PSiH_3, but instead leads to the synthesis of $P(SiH_3)_3$ (see Scheme 116).[200]

A sequence of transmetalation steps results in the formation of $P(SiH_3)_3$ steps involving mono- and disilylated intermediates (see Scheme 117).[16,200–202]

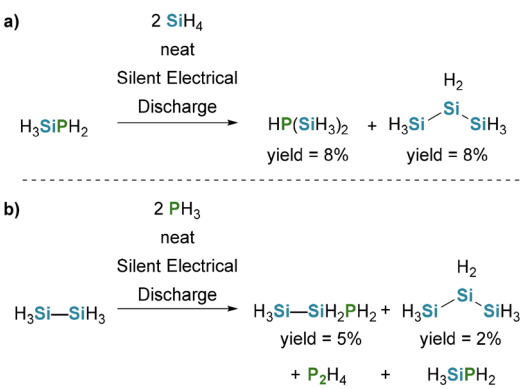

Scheme 113 Synthesis of $HP(SiH_3)_2$ (path a) and $Si_2H_5PH_2$ (path b) *via* silent electrical discharge. No yields for P_2H_4 and H_3SiPH_2 were given in the reaction of disilane.

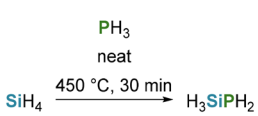

Scheme 112 Synthesis of H_3SiPH_2 *via* pyrolysis of SiH_4/PH_3 mixtures. No yields were reported.

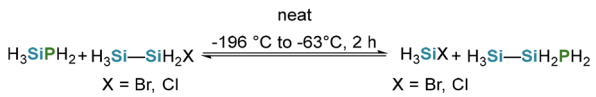

Scheme 114 Synthesis of $H_3SiSiH_2PH_2$ from H_3SiPH_2 and H_3SiSiH_2X. They noted that all compounds are present in equimolar amounts at the equilibrium.

This journal is © the Partner Organisations 2026

Open Access Article. Published on 24 April 2026. Downloaded on 5/15/2026 8:48:04 PM.
This article is licensed under a Creative Commons Attribution 3.0 Unported Licence.

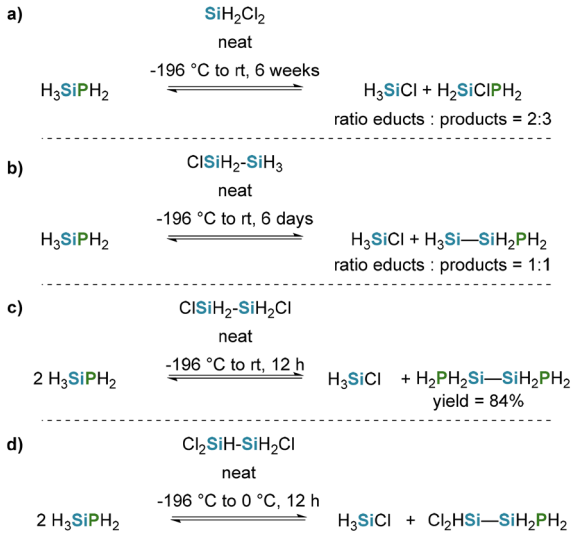

Scheme 115 Synthesis of silylphosphanes and chlorosilylphosphanes from H_3SiPH_2 with chlorosilanes (path a–d). No yields were given for the reaction of H_3SiPH_2 with 1,1,2-trichlorodisilane.

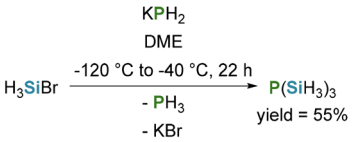

Scheme 116 Synthesis of $P(SiH_3)_3$ from KPH_2 and H_3SiBr.

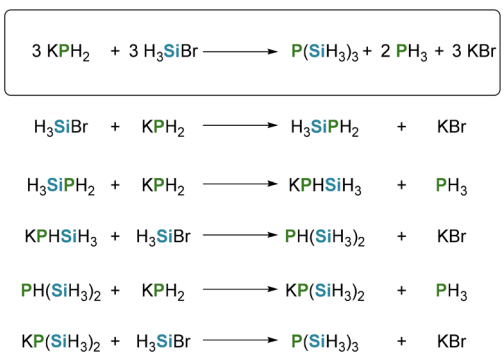

Scheme 117 Formation of $P(SiH_3)_3$ from H_3SiBr through the intermediates H_2PSiH_3 and $HP(SiH_3)_3$.

Glidewell and Sheldrick demonstrated that the intermediate mono- and disilylsubstituted silylphosphanes can be obtained as well, when using an excess of potassium dihydrophosphide with H_3SiBr, followed by acidification of the non-volatile products with hydrogen sulfide.[202]

Lewis acid driven redistribution reactions also lead to the formation silylphosphanes. MacDiarmid and Russ demonstrated that H_3SiPH_2 forms a Lewis adduct with BF_3, which subsequently decomposes at low temperatures to a mixture of

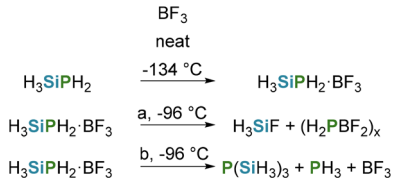

Scheme 118 Decomposition pathways of $H_3SiPH_2{\cdot}BF_3$. Both reactions a and b occur equally.

compounds containing $P(SiH_3)_3$. Both pathways (a and b) proceed to comparable extents (see Scheme 118).[203]

Further investigations showed that boranes promote the redistribution of silylphosphanes and their mixtures into trisilylphosphanes.[203–206] In the first step of these redistribution reactions the silylphosphanes form Lewis acid–base complexes (see Scheme 119, path a) and, depending on the used borane, then undergo redistribution into trisilylphosphanes (see Scheme 119, path b).[204] The best yields are obtained when using an excess of BF_3 with 83% formation of $P(SiH_3)_3$ and small amounts of $HP(SiH_3)_2$ and 90% for $P(SiH_2SiH_3)_3$ with small amounts of $HP(SiH_3)_2$ as side product.[204,206] BCl_3 induces only limited redistribution, while BBr_3 predominantly led to the formation of H_3SiBr and BH_3 complexes only redistributed in trace amounts.[204] Mixed trisilylphosphanes are obtained when mixtures of H_3SiPH_2 and $H_3SiH_2SiPH_2$ are subjected to these conditions.[204]

When disilanylphosphane is converted to borane adducts and subsequently heated, redistribution to trisilylphosphanes is not observed, instead SiH_4 and a polymeric substance is formed (see Scheme 120, path a). Only when 9 equivalents of disilanylphosphane were employed could trisdisilanylphosphane be detected, though no yields were given (see Scheme 120, path b).[205]

In 2010 Tice *et al.* reported a solvent free approach in which $P(SnMe_3)_3$ reacts with H_3SiBr to afford $P(SiH_3)_3$ in 98% yield (see Scheme 121).[207]

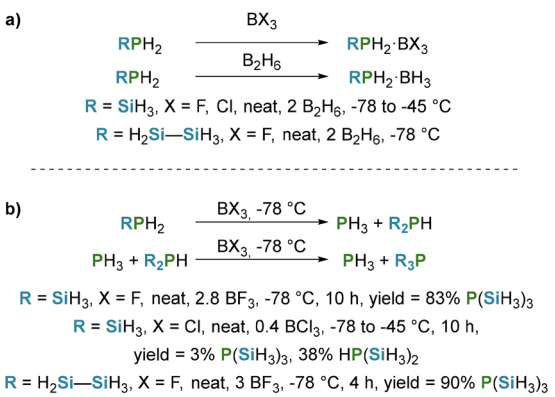

Scheme 119 Formation of Lewis acid–base complexes of boranes and silylphosphanes and subsequent BF_3 promoted redistribution reaction, forming trisilylphosphanes (path a and b). No yields were given for the BX_3 and diborane adducts.

Open Access Article. Published on 24 April 2026. Downloaded on 5/15/2026 8:48:04 PM.
This article is licensed under a Creative Commons Attribution 3.0 Unported Licence.

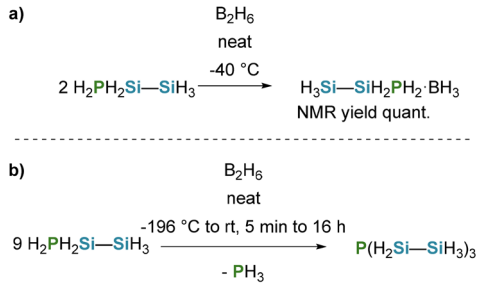

Scheme 120 Formation of the borane adduct of $H_2PSiH_2SiH_3$ (path a) and thermal degradation into trisdisilanylphosphane (path b). No isolated yields were given.

Scheme 121 Synthesis of $P(SiH_3)_3$ from $P(SnMe_3)_3$.

Recently Li *et al.* employed exchange reactions between $P(SiMe_3)_3$ and an excess of monochlorosilanes to generate the corresponding trisilylphosphanes (see Scheme 122).[208]

The direct reaction between metalated phosphanes and silylhalides was also thoroughly investigated. Lithium tetrakisdihydrogenphosphidoaluminate was prepared by Finholt *et al.* in 1963,[209] which proved as a useful reagent for phosphanylation. In contrast to reactions of silylhalides with KPH_2 [16,200–202] the transmetalation sequence leading to the formation of $P(SiH_3)_3$ is not observed when metal tetrakisdihydrogenphosphidoaluminates are employed, giving access to H_3SiPH_2 (see Scheme 123, path a and b).[210,211]

Use of $LiAl(PH_2)_4$ as phosphanylation agent enables the synthesis of diverse silylphosphanes from silylhalides, notably they were able to use SiH_2Br_2 to obtain $SiH_2(PH_2)_2$ and $SiHBr_3$ for $SiH(PH_2)_3$ respectively.[210,212,213] Norman and co-workers showed that analogous methodology employing sodium tetrakisdi-hydrogenphosphidoaluminate ($NaAl(PH_2)_4$) enables access to several silylphosphanes, as well as germylphosphanes.[210,212] The reaction of $NaAl(PH_2)_4$ with H_3SiBr has proven to be a viable synthetic approach for the phosphanylation of silicon halides, allowing the synthesis of silylphosphanes such as H_2PSiH_3.[211] In 1994 Becker *et al.* successfully employed silyltriflate ($CF_3SO_2OSiH_3$) as silylation

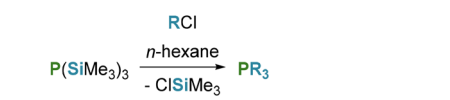

R = SiH_3, 4.6 RCl, 90°C, 48 h, yield = 85%
R = H_2Si—SiH_3, 1.1 RCl 60 °C, 24 h, yield = 22%
R = H_2Si—SiH_2—SiH_3, 11 RCl, 68 °C, 24 h, yield = 93%

Scheme 122 Synthesis of trisilylphosphanes *via* exchange reaction of $P(SiMe_3)_3$ with monochlorosilanes.

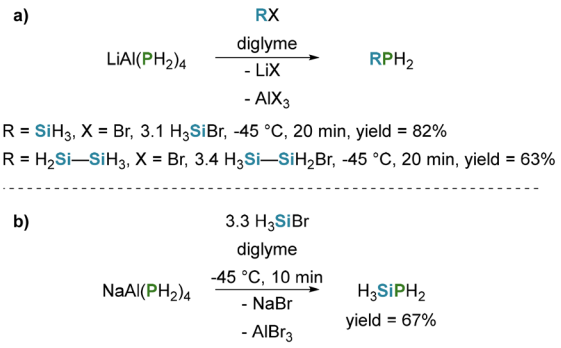

Scheme 123 Synthesis of silylphosphanes from metal tetrakis(dihydrogenphosphido)aluminates (path a and b).

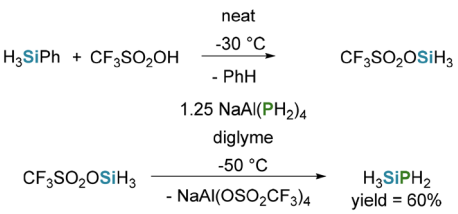

Scheme 124 Synthesis of H_3SiPH_2 from $CF_3SO_2OSiH_3$. No yield for silyltriflate was given, as it is freshly prepared and used immediately without isolation.

agent for $NaAl(PH_2)_4$ to obtain H_3SiPH_2 in 60% yield (see Scheme 124).[214]

Lithium dialkylphosphides are useful for preparing metalated silylphosphanes *via* reaction with H_3SiPH_2 (see Scheme 125, path a and b). Solutions of the monometalated silylphosphanes with concentrations above 0.1 mol l^{-1} undergo disproportionation at room temperature in apolar solvents, establishing an equilibrium between $H_3SiPHLi$ and $LiP(SiH_3)_2$ (see Scheme 125, path b).[215] This behavior prevents the direct synthesis of disilylphosphanes from monometalated $H_3SiPHLi$ by subsequent reaction with silylhalides, as trisilylphosphanes will be formed as well.[215] Precipitation of $LiPH_2$ after removing most of the solvent and adding benzene drives

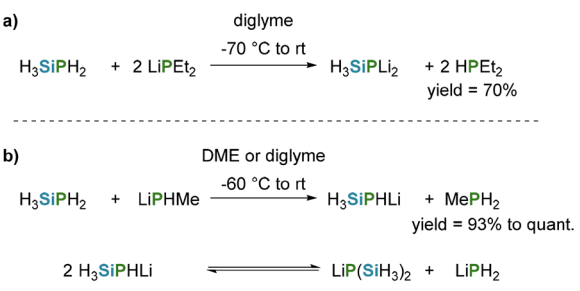

Scheme 125 Synthesis of metalated silylphosphanes from H_3SiPH_2 (path a and b) and disproportionation equilibrium of $H_3SiPHLi$. No isolated yield was given for the metalated silylphosphanes but for the associated byproducts.

This journal is © the Partner Organisations 2026

Open Access Article. Published on 24 April 2026. Downloaded on 5/15/2026 8:48:04 PM.
This article is licensed under a Creative Commons Attribution 3.0 Unported Licence.

the equilibrium towards $LiP(SiH_3)_2$ and allows for recrystallization in Et_2O.[215]

The monometalated $H_3SiPHLi$ can be treated with $AlCl_3$ in diglyme to form $LiAl(PHSiH_3)_4$, which reacts with H_3SiBr to afford $HP(SiH_3)_2$. Owing to the disproportionation of $H_3SiPHLi$ into $LiP(SiH_3)_2$ and $LiPH_2$, the initially formed $LiAl(PHSiH_3)_4$ also contains $LiAlP(SiH_3)_2$ and $LiAlPH_2$, which in turn yield H_3SiPH_2 and $P(SiH_3)_3$ upon reaction with H_3SiBr. Additionally, $HP(SiH_3)_2$ undergoes dismutation to monosilyl- and trisilylphosphane, leading to the approximately equimolar formation of mono-, di-, and trisilylphosphanes. By quickly separating the disilylphosphanes the dismutation can be circumvented. The dismutation is only observed with PH containing silylphosphides (see Scheme 126).[215]

Drake and Anderson converted $P(SiH_3)_3$ with $LiAlH_4$ to the disilylphosphinoaluminate ion $LiAlH[P(SiH_3)_2]_3$, which further reacts with halides, such as, monobromodisilane H_3SiSiH_2Br to give $P(SiH_3)_2SiH_2SiH_3$ (see Scheme 127, path a).[216] H_3SiPEt_2 derived from H_3SiBr undergoes H/Li exchange with $LiPEt_2$ to form $H_2Si(PEt_2)_2$ and LiH. Subsequent reactions of $H_2Si(PEt_2)_2$ with 2 equivalents of $LiPEt_2$ provides $HSi(PEt_2)_3$ (see Scheme 127, path b).[217]

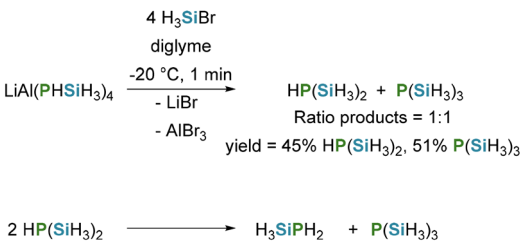

Scheme 126 Synthesis $HP(SiH_3)_2$ from $LiAl(PHSiH_3)_4$ and subsequent disproportionation into H_3SiPH_2 and $P(SiH_3)_3$.

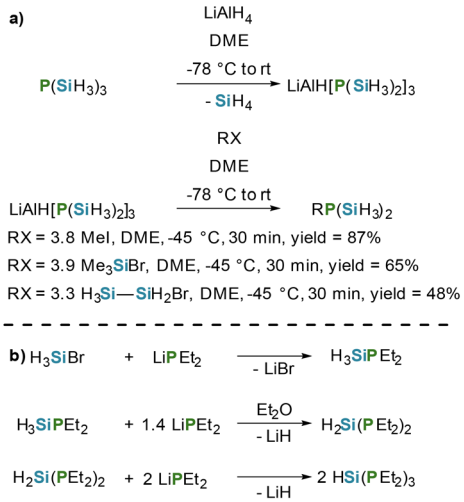

Scheme 127 Path (a) synthesis of disilylphosphinoaluminate and subsequent reactions with halides. Path (b) synthesis of $H_3SiP(Et)_2$, $H_2Si(P(Et)_2)_2$ and $HSi(P(Et)_2)_3$ from H_3SiBr. No isolated yields were given.

$HSi(PEt_2)_3$ is interesting in the context of silylphosphanes, as it reacts with $LiPEt_2$ to give $LiSi(PEt_2)_3$, which reacts with H_3SiBr, resulting in the formation of $H_3SiSiH(PEt_2)_2$, but was only isolated with sideproducts (see Scheme 128).[217] Metalation of silylphosphanes using *n*-BuLi leads to cleavage of the Si–P bond.[215,217]

Silylphosphides as interesting reagents for further functionalization were obtained either *via* metalation of silylphosphanes,[218,219] or by employing build up reactions of silanes.[115] In 1973, Cradock *et al.* obtained $LiP(SiH_3)_2$ from $P(SiH_3)_3$ in 90% yield by metalation with MeLi (see Scheme 129, path a).[218,219] In 1994 Sundermeyer and coworkers accessed $KPHSiH_3$ and $KP(SiH_3)_2$ *via* the buildup reaction between SiH_4 and K in diglyme and subsequent reaction with PH_3 (see Scheme 129, path b).[47] $LiP(SiH_3)_2$ can be syn-

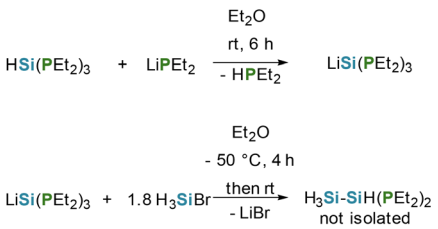

Scheme 128 Synthesis $H_3SiSiH(PEt_2)_2$ from $LiSi(PEt_2)_3$. The formation of $H_3SiSiH(PEt_2)_3$ was confirmed but isolation as not possible due to degradation during distillation.

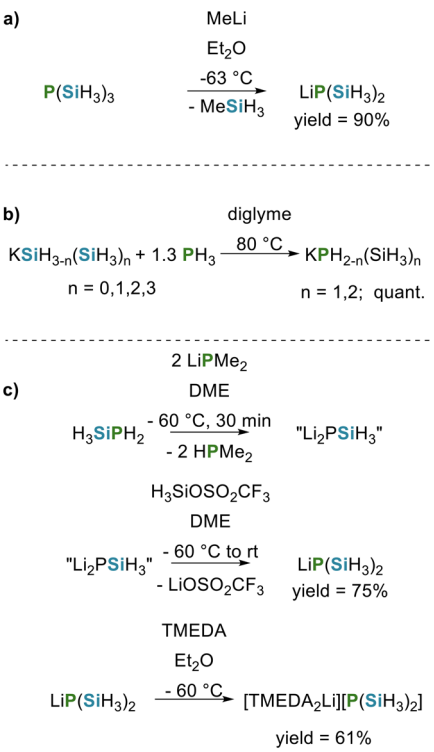

Scheme 129 Synthesis of $LiP(SiH_3)_2$ (path a), $KPHSiH_3$, $KP(SiH_3)_2$ (path b) and $[Tmeda_2Li][P(SiH_3)_2]$ (path c).

Open Access Article. Published on 24 April 2026. Downloaded on 5/15/2026 8:48:04 PM. This article is licensed under a Creative Commons Attribution 3.0 Unported Licence.

thesized through the dismutation of H_3SiPH_2 and $LiPHCH_3$ (see Scheme 125, path b), and isolated as $[(TMEDA)_2Li][P(SiH_3)_2]$ (see Scheme 129, path c). A crystal structure is shown in Fig. 14.[214]

Silylarsanes. Silylarsanes containing only As, Si, and H, are promising precursors for semiconductor fabrication because they are carbon- and halogen-free, which helps minimize contamination during CVD/PECVD/ALD and supports cleaner, low-temperature decomposition to volatile byproducts, mainly H_2.[186,220] Arsenic is a shallow donor in group-IV semiconductors, so silylarsanes can serve as single-source, *in situ* n-type dopant feeds for Si, Ge, and Si-rich alloys, leveraging the high activation of As and notably low diffusivity in Si to form ultra-shallow, abrupt junctions that are advantageous for modern complementary metal–oxide–semiconductors source/drain engineering.[185]

The smallest member of the silylarsane family is silylarsane (H_3SiAsH_2) and was prepared by Jolly and Drake in 1962. Similar to the synthesis of H_3SiPH_2, using an equimolar mixture of SiH_4 and arsine (AsH_3) in ozonizer-type silent electrical discharge tube yields H_3SiAsH_2, as well as disilanylarsane ($H_3SiH_2SiAsH_2$) (see Scheme 130).[195] Notably disilane as well as trisilane are formed as sideproducts.[221]

When H_3SiAsH_2 and B_2H_6 are condensed into a vessel they react upon warming to 0 °C by forming a solid as well as disilylarsane ($HAs(SiH_3)_2$) and trisilylarsane ($As(SiH_3)_3$) (see Scheme 131).[221] Reactions between H_3SiAsH_2 and bromodiborane (B_2H_5Br) only afford the formation of bromosilane and a arsine containing polymer.[221] H_3SiAsH_2 forms the 1 : 1 adduct with BX_3 (X = Cl, Br), but $H_3SiAsH_2BX_3$ decomposes at low temperatures forming H_3SiX.[221]

Aylett *et al.* showed in 1955, that monoiodosilane reacts with arsenic to afford diiodosilylarsane (AsI_2SiH_3) with various side products, most notably trisilylarsane, additionally they showed that trimethylarsane ($AsMe_3$) undergoes reaction with iodosilane, giving access to trisilylarsane.[13]

Arsenides show similar reactivity towards silyl halides as phosphides. Trisilylarsane can be accessed through nucleophilic substitution of silyl halides by alkali metal arsenides. Amberger and Boeters used bromosilane with potassium dihydroarsenide ($KAsH_2$) to afford $As(SiH_3)_3$ (see Scheme 132).[200] The same reported method of Glidewell and Sheldrick, in which H_3SiPH_2 and $HP(SiH_3)_2$ can be obtained from the reaction of KPH_2 with H_3SiBr *via* acidification with H_2S also works for potassium arsenide $KAsH_2$, but leads mostly to silylarsine in 54% yield.[202] The formation of $As(SiH_3)_3$ from $KAsH_2$ proceeds *via* a series of transmetalation steps, similar to the respective synthesis of trisilylphosphane $P(SiH_3)_3$ (see Scheme 117).[202]

Metalated silylarsanes can react with silyl halides to form the respective silylarsanes. Lithium tetrakisdihydrogenarsidoaluminate ($LiAl(AsH_2)_4$) reacts with silylhalides H_3SiX (X = Br, I) to afford silylarsine, though monochlorosilane only led to formation of H_3SiAsH_2 in trace amounts (see Scheme 133).[222,223]

Anderson and Drake were able to obtain disilylarsane $HAs(SiH_3)_2$ by treating $LiAl(AsH_2)_4$ with bromosilane. After removal of the volatiles the remaining solid was treated with dihydrogen selenide (H_2Se), resulting in the formation of HAs

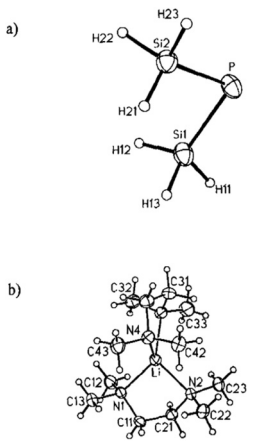

Fig. 14 Crystal structure of the anion (a) and cation (b) of $[(TMEDA)_2Li][P(SiH_3)_2]$. For better visibility the anion and cation are not shown in the same scale. Adapted from G. Becker, B. Eschbach, D. Käshammer, *et al.*[214] with permission from John Wiley and Sons © 1994.

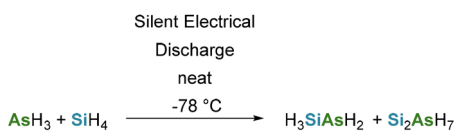

Scheme 130 Synthesis of H_3SiAsH_2 and Si_2AsH_7 from a SiH_4/AsH_3 mixture. No experimental details were given.

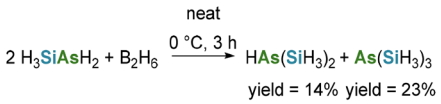

Scheme 131 Synthesis of $HAs(SiH_3)_2$ and $As(SiH_3)_3$ from H_3SiAsH_2 and B_2H_6.

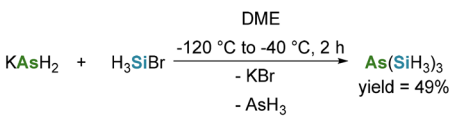

Scheme 132 Synthesis of $As(SiH_3)_3$ from $KAsH_2$ and H_3SiBr.[200]

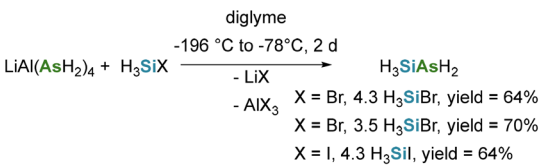

Scheme 133 Synthesis of H_3SiAsH_2 from $LiAl(AsH_2)_4$ and silylhalides.

This journal is © the Partner Organisations 2026

Open Access Article. Published on 24 April 2026. Downloaded on 5/15/2026 8:48:04 PM.
This article is licensed under a Creative Commons Attribution 3.0 Unported Licence.

$(SiH_3)_2$.[202] Furthermore the treatment of lithium tetrasilylarsenide ($LiAs(SiH_3)_4$) with bromodisilane led to the formation of disilanylarsane ($H_3SiH_2SiAsH_2$) in 59% yield (see Scheme 134).[223]

Disilanylarsane can also be obtained from the exchange reaction with monohalodisilanes H_3SiH_2SiX (X = Cl, Br) at low temperatures. The yields for $H_3SiH_2SiAsH_2$ can be brought to 30%, by stepwise removal of the formed silyl halide H_3SiX (see Scheme 135).[198]

Lithium disilylarsenide ($LiAs(SiH_3)_2$) can be obtained from trisilylarsane in 90% yield by metalation with MeLi, as shown by Cradock *et al.* in 1973.[218,219]

Similar to trisilylphosphanes, trisilylarsanes are also available through an exchange reaction between tristrimethylsilylarsane ($As(SiMe_3)_3$) and monohalosilanes, though only the reaction with chlorotrisilane is reported (see Scheme 136).[208]

Silylstibanes. Antimony can act similar to other group V elements as n-type dopant.[185] Antimony has a significantly larger atomic size compared to phosphorous and arsenic, leading to slower diffusion and therefore more precise control of dopant profiles, which is especially useful for specialized applications, such as, power electronics and high-temperature devices.[224] Compared to phosphorous and arsenic there are only few investigations into the synthesis of silylstibanes.

The nucleophilic substitution of phosphides and arsenides with silyl halides gave access to their respective trisilyl compound, but similar reactions with antimonides and stibanes did not lead to the desired trisilylstibane ($Sb(SiH_3)_3$).[200,225] Amberger and Boeters instead accessed $Sb(SiH_3)_3$ *via* the salt methathesis reaction of lithium antimonide (Li_3Sb) with H_3SiBr (see Scheme 137).[200,225]

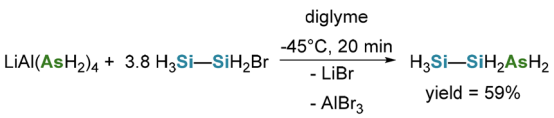

Scheme 134 Synthesis of $H_3SiH_2SiAsH_2$ from $LiAl(AsH_2)_4$ and H_3SiSiH_2Br.

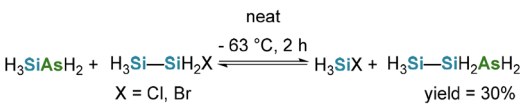

Scheme 135 Synthesis of $H_3SiSiH_2AsH_2$ *via* exchange reaction from H_3SiSiH_2X (X = Cl, Br) and H_3SiAsH_2.

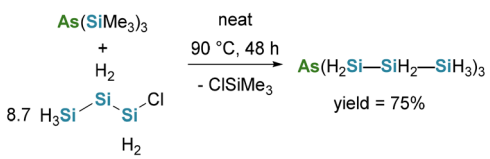

Scheme 136 Synthesis of $As(SiH_2SiH_2SiH_3)_3$ *via* exchange reaction from $H_3SiH_2SiH_2SiCl$ and $As(SiMe_3)_3$.

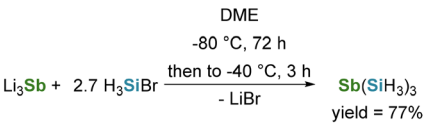

Scheme 137 Synthesis of $Sb(SiH_3)_3$ *via* salt metathesis reaction of Li_3Sb and H_3SiBr.

Functionalization with group 6 (synthesis of silylchalcogenes)

Siloxanes. Single-source Si–O feedstocks deliver silicon and oxygen in a fixed stoichiometric ratio, simplifying process control compared with separate silane and oxidant flows, and reducing parasitic gas-phase reactions.[226] When designed to be carbon- and halogen-free, they can evolve only hydrogen or water as byproducts, lowering contamination.[227]

In 1917, Stock, Somieski, and Wintgen reported the first isolation of $O(SiH_3)_2$. Their method involved shaking H_3SiBr with degassed H_2O, allowing the mixture to stand, and then purifying the product by fractional distillation (see Scheme 138). They proposed that hydrolysis generates H_3SiOH as intermediate, which rapidly self-condenses to give $O(SiH_3)_2$ with loss of water.[228]

In a follow-up study Stock and Somieski isolated $O(Si_2H_5)_2$ by reacting Si_2H_5Br (which was contaminated with $Si_2H_nBr_{6-n}$, n = 0–6) with degassed H_2O, and then extracting it with benzene (see Scheme 139). They failed in isolating the pure compound and always had some H_2O next to $O(Si_2H_5)_2$. The higher silyl bromides present in the educt as contaminations did not interfere with the reaction, since their resulting siloxanes polymerized and then precipitated as a white solid.[145]

Emeléus, MacDiarmid, and Maddock attempted the reduction of $O(SiCl_3)_2$ with $LiAlH_4$, but were unable to prepare $O(SiH_3)_2$ *via* this route. Instead, they obtained $O(SiH_3)_2$ in 37% yield by passing H_2 through boiling $O(SiCl_3)_2$, then directing the saturated gas stream over aluminium foil at 500 °C (see Scheme 140, path a). They also generated $O(SiH_3)_2$ *via* hydrolysis of SiH_3I, $S(SiH_3)_2$, and $Se(SiH_3)_2$ (see Scheme 140, path b

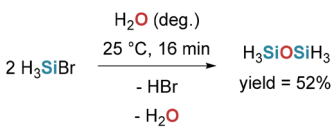

Scheme 138 Synthesis of $O(SiH_3)_2$ *via* hydrolysis of SiH_3Br.

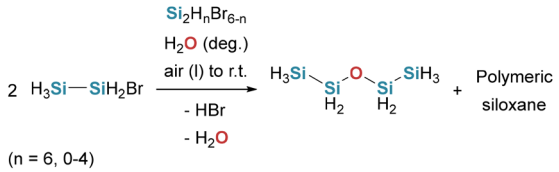

Scheme 139 Hydrolysis of Si_2H_5Br, contaminated with higher bromosilanes, leading to $O(Si_2H_5)_2$ and polymeric siloxanes. Yields of the siloxane were not determined.

Open Access Article. Published on 24 April 2026. Downloaded on 5/15/2026 8:48:04 PM. This article is licensed under a Creative Commons Attribution 3.0 Unported Licence.

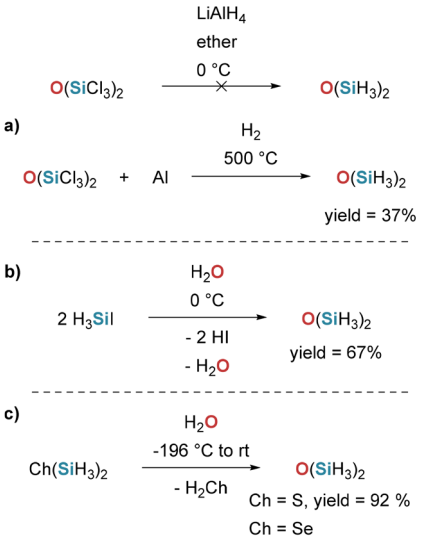

Scheme 140 Synthesis of $O(SiH_3)_2$ from $O(SiCl_3)_2$ (path a), SiH_3I (path b), $S(SiH_3)_2$ and $Se(SiH_3)_2$ (path c). Yields of $Se(SiH_3)_2$ hydrolysis reaction not determined.

and c). For the $Se(SiH_3)_2$ route, the yield could not be determined because H_2Se could not be separated from the silylether.[229]

Kriner, MacDiarmid, and Evers investigated reactions of $O(SiH_3)_2$ with aluminum halides. Treatment with $Me_4Al_2Br_2$ afforded $Me_4Al_2(OSiH_3)_2$ (see Scheme 141), which is stable at −78 °C but decomposes at room temperature to give SiH_4 and a non-volatile viscous residue. In contrast, reactions of $O(SiH_3)_2$ with Al_2X_6 (X = Cl, Br, I) yielded only the corresponding halosilanes; no aluminum-containing products could be isolated.[230]

Ward and MacDiarmid isolated pure $O(Si_2H_5)_2$ by hydrolysing purified Si_2H_5I. Purification of $O(Si_2H_5)_2$ required an extensive protocol: multiple fractional distillations, drying over P_2O_5 (noting that prolonged contact causes degradation of the silylether and formation of PH_3), followed by repeated distillations. The final product was obtained in 96% yield (see Scheme 142).[231]

Sternbach and MacDiarmid (1961) investigated routes to H_3SiOCH_3. Reacting SiH_4 with methanol (MeOH) at room temperature gave only unreacted SiH_4, H_2, and a complex mixture of methoxysilanes. With copper powder as a promoter, low yields of $H_2Si(OCH_3)_2$ and $HSi(OCH_3)_3$ were isolated (see Scheme 143, path a). Direct reaction of SiH_3I with methanol was highly vigorous, leading mainly to polymeric material; only traces of H_3SiOCH_3 were detected in the volatile fraction (see Scheme 143, path b). In contrast, treating the amine adduct $SiH_3I{\cdot}N(Me)_3$ with methanol furnished $MeOSiH_3$ in 28% yield (see Scheme 143, path c). They further showed that $MeOSiH_3$ reacts with BF_3 to give SiH_3F and $MeOBF_2$ (see Scheme 143, path d).[232]

Onyszchuk found that $O(SiH_3)_2$ reacts with BF_3 and BCl_3 to give H_3SiOBX_2 (X = F, Cl), but both products are highly unstable. The fluorinated derivative decomposed during isolation, even at low temperature, and could not be isolated. The chloro analogue decomposes more slowly and was successfully isolated at −64 °C; several subsequent distillations at −112 °C were used to remove H_3SiCl formed in the process (see Scheme 144).[233]

Van Dyke and MacDiarmid prepared the unsymmetrical silylether $H_3SiOSi_2H_5$ by two routes: path (a) hydrolysis of a mixture containing SiH_3I and Si_2H_5Br; path (b) equilibration between $O(SiH_3)_2$ and $O(Si_2H_5)_2$ (see Scheme 145).[234]

Van Dyke examined the reactions of $O(SiH_3)_2$ with phosphorus halides PX_3 (X = F, Cl, Br). No reaction was observed

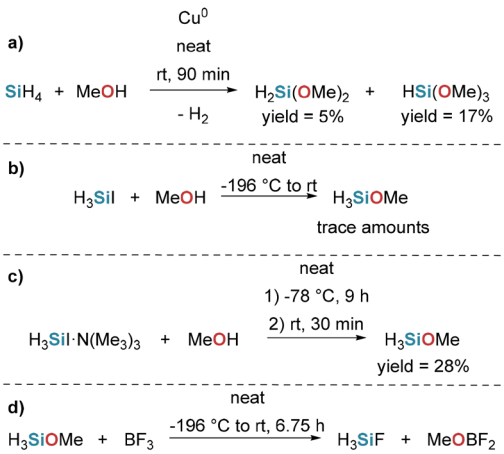

Scheme 143 Synthesis of alkoxysilanes (path a–c) and reaction of H_3SiOMe with BF_3 (path d).

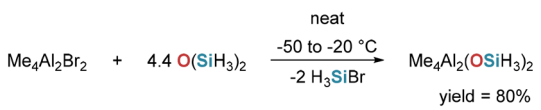

Scheme 141 Synthesis of $Me_4Al_2(OSiH_3)_2$ from $Me_4Al_2Br_2$ and $O(SiH_3)_2$.

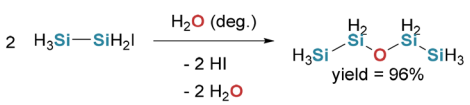

Scheme 142 Hydrolysis of $O(Si_2H_5)_2$ from Si_2H_5I.

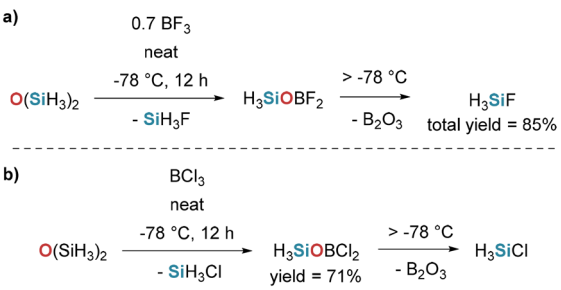

Scheme 144 Reactions of $O(SiH_3)_2$ with BF_3 (path a) and BCl_3 (path b).

This journal is © the Partner Organisations 2026

Open Access Article. Published on 24 April 2026. Downloaded on 5/15/2026 8:48:04 PM.
This article is licensed under a Creative Commons Attribution 3.0 Unported Licence.

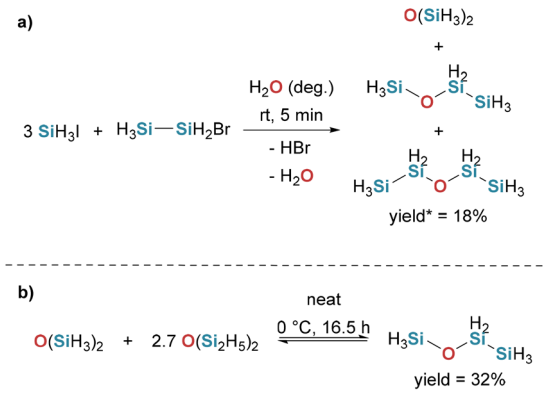

Scheme 145 Synthesis of the unsymmetrical silylether $H_3SiOSi_2H_5$ *via* hydrolysis (path a) and equilibration reactivity of silylethers (path b). *Yield of product mixture.

with PF_3 or PCl_3. In contrast, PBr_3 caused H_2 evolution and formation of a yellow solid; the product mixture contained, in addition to unreacted starting materials, SiH_3Br and $(H_3SiO)_nSiH_{4-n}$ (n = 2, 3) (see Scheme 146, path a). These products were inseparable, so no yields were reported. The absence of SiH_4 formation and the appearance of a yellow, presumably polymeric phosphorus hydride $(PH)_x$ led Van Dyke to propose the transformation shown in (Scheme 146, path b).[235]

Glidewell and Rankin prepared the aryl silylether $PhOSiH_3$ in nearly quantitative yield by reacting $S(SiH_3)_2$ with phenol (PhOH) (see Scheme 147).[236]

Ebsworth and Thompson prepared silyl esters RCO_2SiH_3 (R = CF_3, H, Me) by protonolysis of trisilylamine ($N(SiH_3)_3$) with the corresponding carboxylic acids (see Scheme 148, path a). Side products depended on R: with R = CF_3 they observed traces of monosilane; with R = H they detected SiH_4, $H_3SiOSiH_3$, and traces of CO_2. They next examined the reaction of silver trifluoroacetate ($F_3CC(O)OAg$) with silyl halides H_3SiX

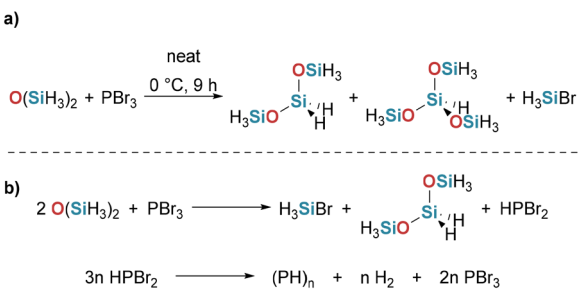

Scheme 146 a) Reaction of $O(SiH_3)_2$ with PBr_3 and (b) the proposed reaction mechanism, no yields were reported.

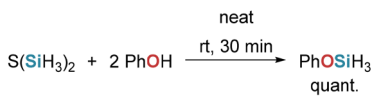

Scheme 147 Synthesis of $PhOSiH_3$ using $S(SiH_3)_2$.

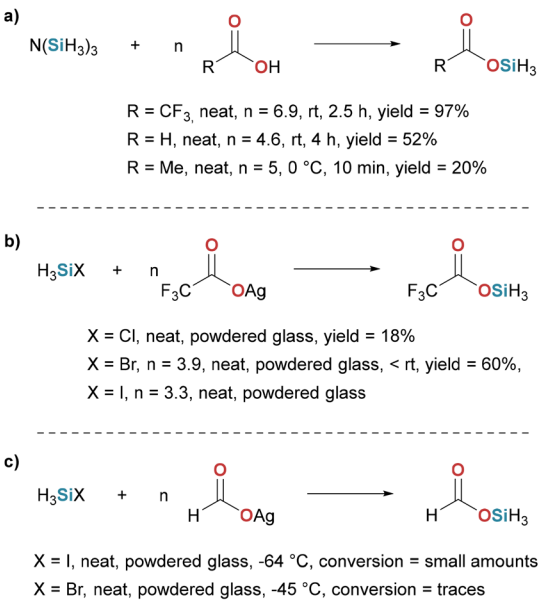

Scheme 148 Synthesis towards silyl esters using $N(SiH_3)_3$ (path a) and SiH_3X (X = Cl, Br, I) (path b and c). Yield of reaction between H_3SiI and silver trifluoroacetate not reported.

(X = Cl, Br, I) (see Scheme 148, path b). SiH_3Cl gave the trifluoroacetate silyl ester in low yield, SiH_3Br improved the yield to about 60%, and with SiH_3I isolation of the ester failed. Finally, they attempted the analogous synthesis with silver formate (HC(O)OAg). With SiH_3I, substantial iodine was liberated along with non-condensable gases; the mixture contained disiloxane, formic acid, and SiH_3I bearing only small amounts of silyl formate ($HC(O)OSiH_3$). With H_3SiBr only traces of silyl formate were obtained, and warming the reaction tube to 0 °C caused it to explode (see Scheme 148, path c).[169]

Cradock *et al.* reported that treatment of $O(SiH_3)_2$ with MeLi liberates $MeSiH_3$ in approximately 85% of the theoretical amount, forming $Li(OSiH_3)$ (see Scheme 149). They then attempted to react solutions containing $Li(OSiH_3)$ with different electrophiles, but never observed the expected product.[219]

Drake, Henderson, and Hemmings synthesized the silyl esters $H_3SiOC(O)CX_3$ (X = F, Cl) by adapting the Ebsworth–Thompson protocol, replacing $N(SiH_3)_3$ with a bis(silyl) carbodiimide [$C(NSiH_3)_2$] as the silylating agent (see Scheme 150).[169,237] This provided a complementary route to the trihaloacetate esters.

Glidewell prepared mixed silyl ethers $ROSiH_3$ (R = Me, Et, i-Pr, *t*-Bu) by reacting the corresponding lithium tetraalumi-

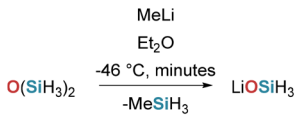

Scheme 149 Synthesis of $Li(OSiH_3)$, no reaction details reported and yields were not determined.

Open Access Article. Published on 24 April 2026. Downloaded on 5/15/2026 8:48:04 PM.
This article is licensed under a Creative Commons Attribution 3.0 Unported Licence.

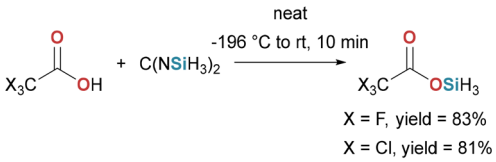

Scheme 150 Synthesis of silyl esters using $C(NSiH_3)_2$.

nates with SiH_3Br (see Scheme 151, path a). The phenyl silyl ether $PhOSiH_3$ was obtained from PhONa using either SiH_3Br or silyl trifluoroacetate (Scheme 151, path b). He further showed that silylphosphine can serve as an SiH_3-transfer reagent: 2,2,2-trifluoroethanol was smoothly converted to $CF_3CH_2OSiH_3$ (a transformation that failed under the tetraaluminate/SiH_3Br conditions), and benzyl alcohol gave $BnOSiH_3$ selectively (Scheme 151, path b and c).[238]

Fehér, Fischer, and Skrodzki found that UV irradiation (medium-pressure Hg lamp) of trisilane in the presence of acetone affords a mixture of alkoxysilanes (silylethers) (see Scheme 152, path a). They note that the substitution pattern can be tuned by conditions: short irradiation times with an excess of silane favour predominantly monosubstituted alkoxysilanes, whereas excess ketone and prolonged irradiation shift the distribution toward highly alkoxylated silanes. They further showed that the formed isopropoxysilanes undergo acid-promoted hydrolysis with dilute, non-oxidizing acids to give the corresponding bis-silyl ethers (disiloxanes), in high yields (see Scheme 152, path b).[239]

Lobreyer, Oeler, and Sundermeyer (1991) reported two routes towards silyl nonaflate. Reaction of silver nonaflate with SiH_3Cl afforded low yields (see Scheme 153, path a), whereas an alternative approach employing phenylsilane with perfluorobutanesulfonic acid gave significantly improved isolated yields (see Scheme 153, path b). The resulting silyl nonaflate was then used in further functionalization reactions (Scheme 67).[46]

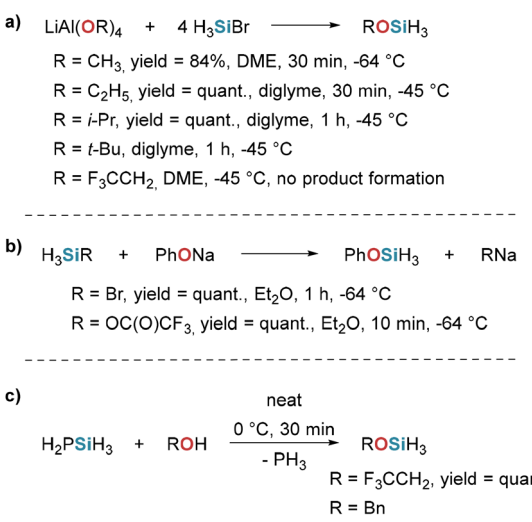

Scheme 151 Synthesis towards mixed silyl ethers using SiH_3Br and tetraaluminates, SiH_3R (R = Br, $OC(O)CF_3$) and PhONa, and H_2PSiH_3 with ROH (R = F_3CCH_2, Bn). Treatment of mixed silylethers $ROSiH_3$ (R = Et, i-Pr, *t*-Bu, F_3CCH_2) with HI (path a–c). Yield of the reactions between lithium aluminate and H_3SiBr, and silylphosphine and BnOH were not determined.

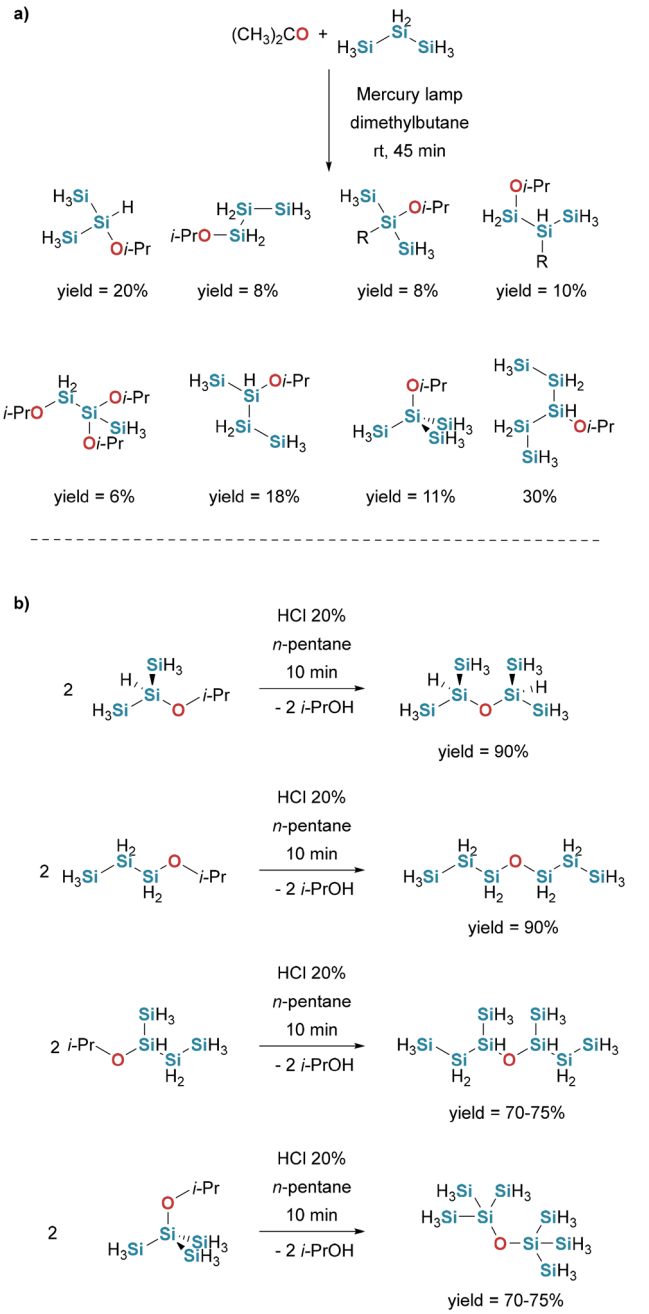

Scheme 152 UV irradiation of trisilane in the presence of acetone leading to different mixed silylethers (path a) and the hydrolysis of formed silylethers with aqueous HCl (path b).

Silylthiones. Single-source Si–S feedstocks deliver silicon and sulfur simultaneously in a fixed stoichiometric ratio, sim-

This journal is © the Partner Organisations 2026

Open Access Article. Published on 24 April 2026. Downloaded on 5/15/2026 8:48:04 PM.
This article is licensed under a Creative Commons Attribution 3.0 Unported Licence.

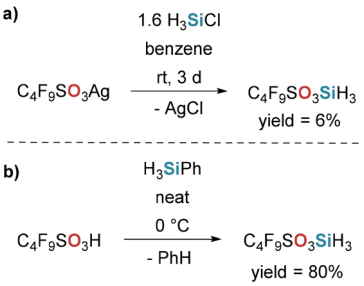

Scheme 153 Formation of silyl nonaflate using silver nonaflate with SiH_3Cl (path a) and perbutanesulfonic acid with phenylsilane ($PhSiH_3$) (path b).

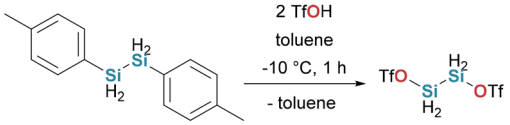

Scheme 154 Synthesis towards disilyl di(triflate) using (p-tolyl-SiH_2)$_2$ and triflic acid. Isolated yields not reported.

plifying process control. They also suppress gas-phase parasitic reactions and reactor memory effects compared with separate silane/H_2S or organosulfide co-flows.[134] Because Si and S are pre-bonded, these precursors can enable lower-temperature deposition; used examples like bis(trimethylsilyl)sulfide demonstrate processability.[240] By contrast, a carbon-free analogue such as disilyl sulfide ($S(SiH_3)_2$) would, in principle, evolve only hydrogen or hydrogen sulfide as volatiles and minimize residual carbon.

Emeléus, MacDiarmid, and Maddock prepared disilyl sulfide $S(SiH_3)_2$ by passing SiH_3I vapour three times through a tube packed with HgS. Subsequent reaction of $S(SiH_3)_2$ with H_2S at room temperature for 31 days furnished SiH_3SH (see Scheme 155).[229]

Downs and Ebsworth prepared F_3CSSiH_3 by passing H_3SiI vapor over $Hg(SCF_3)_2$ deposited on glass wool. The initially obtained material partially decomposed to give SiH_3F and CSF_2; repeated fractional distillation removed these volatile by products and furnished pure F_3CSSiH_3 (see Scheme 156).[241]

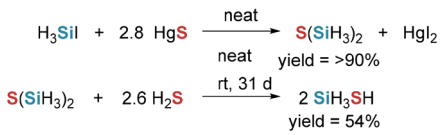

Scheme 155 Synthesis of $S(SiH_3)_2$ using SiH_3I and HgS, reaction of $S(SiH_3)_2$ with H_2S forming SiH_3SH.

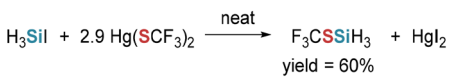

Scheme 156 Reaction between SiH_3I and $Hg(SCF_3)_2$ forming F_3CSSiH_3.

Sternbach and MacDiarmid synthesized $MeSSiH_3$ by reacting $SiH_3I{\cdot}NMe_3$ with MeSH at 0 °C (see Scheme 157).[242]

Ward and MacDiarmid prepared $S(Si_2H_5)_2$ by passing Si_2H_5I vapor over excess HgS at room temperature (see Scheme 158).[153]

Schmeißer and Frouzanfar attempted to prepare monosubstituted thiosilanes $(RS)SiH_3$ by $LiAlH_4$ reduction of RS-$SiCl_3$, but instead obtained di-, tri-, and tetrasubstituted products. They attributed this outcome to $AlCl_3$ formed *in situ*, which promotes disproportionation of thiolato groups. The product distribution depends on the substituent R: with *n*-alkyl groups, $(RS)_3SiH$ formed together with SiH_4 (see Scheme 159, path a);

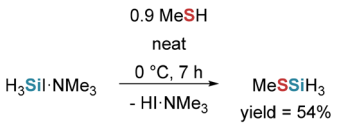

Scheme 157 Formation of $MeSSiH_3$ by reacting $SiH_3I{\cdot}NMe_3$ with MeSH.

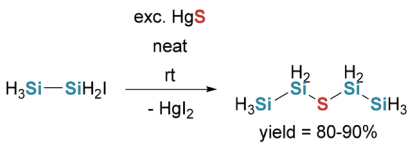

Scheme 158 Synthesis of $S(Si_2H_5)_2$ by the reaction of Si_2H_5I with HgS.

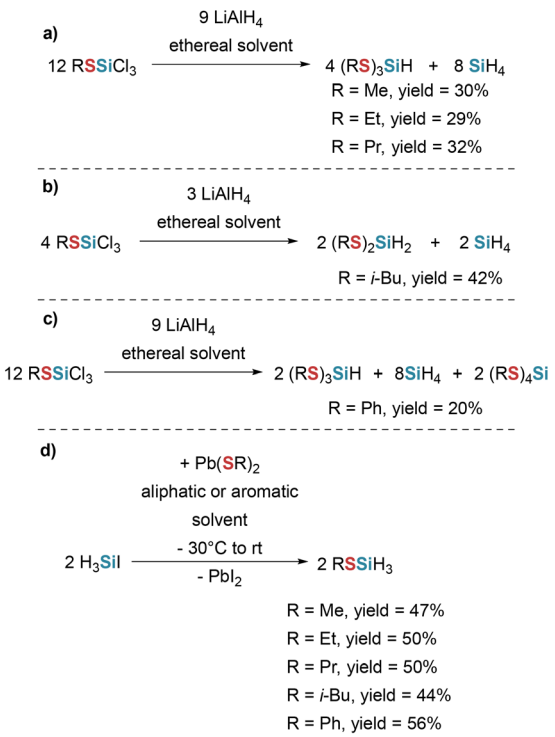

Scheme 159 Synthesis of mono-, di-, tri- and tetrasubstituted thiosilanes starting either from trichlorosilanes and $LiAlH_4$ (path a–c), or from SiH_3I and lead mercaptides (path d).

Open Access Article. Published on 24 April 2026. Downloaded on 5/15/2026 8:48:04 PM.
This article is licensed under a Creative Commons Attribution 3.0 Unported Licence.

with a branched alkyl group (i-Bu), $(RS)_2SiH_2$ and SiH_4 were obtained (see Scheme 159, path b); and with phenyl, a mixture of tri- and tetrasubstituted thiosilanes accompanied by SiH_4 (Scheme 159, path c). Monosubstituted thiosilanes were obtained only when employing lead mercaptides in aliphatic or aromatic solvents, which furnished isolable $(RS)SiH_3$ (Scheme 159, path d).[243]

Glidewell and Rankin prepared $PhSSiH_3$ by salt metathesis of PhSK with SiH_3Br. They also examined the reactivity of PhSK toward boron halides: no reaction was observed with BF_3, whereas BCl_3 afforded a white 1 : 1 adduct at low temperature that dissociated on warming to ambient temperature (see Scheme 160).[236]

Glidewell later obtained disilyl sulfide $S(SiH_3)_2$ in excellent yields by salt metathesis of Li_2S with SiH_3Br (see Scheme 161). Alternatively, treatment of SiH_3Br with $Me_3N{\cdot}H_2S$ also furnished $S(SiH_3)_2$.[171]

Ebsworth, Glidewell, and Sheldrick monitored the reaction of trisilylphosphine $P(SiH_3)_3$ with elemental sulfur in CS_2 in an NMR tube over an extended period. After 3 weeks, NMR spectroscopy indicated 16% formation of $S(SiH_3)_2$; after 2 months, conversion to $S(SiH_3)_2$ was essentially complete. In contrast, $P(SiH_3)_3$ showed no detectable reaction with H_2S under analogous conditions (see Scheme 162).[244]

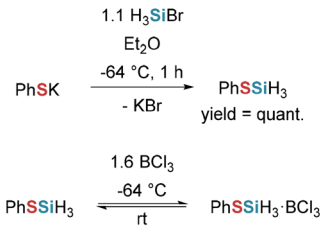

Scheme 160 Formation of $PhSSiH_3$ and reaction of $PhSSiH_3$ with BCl_3.

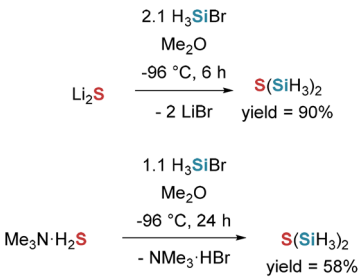

Scheme 161 Synthesis of disilylsulfide by Glidewell.

Scheme 162 Synthesis of disilylsulfide by reacting trissilylphosphane with sulfur.

Drake and Riddle subjected gas mixtures to silent electrical discharge and observed broad product formation. For an equimolar SiH_4/H_2S mixture, in addition to higher silanes, $S(SiH_3)_2$ and H_3SiSH were detected. Using SiH_4/MeSH, the products included $S(SiH_3)_2$, H_3SiSMe, Me_2S and Me_2S_2, along with higher silanes. Finally, a $SiH_4/GeH_4/H_2S$ mixture afforded $H_3SiSGeH_3$, H_3SiSH, H_3GeSH, $S(SiH_3)_2$, $S(GeH_3)_2$, higher silanes and germanes, as well as mixed silylgermanes (see Scheme 163).[245]

Glidewell obtained $MeSSiH_3$ by reacting $LiAl(SMe)_4$ with H_3SiBr (see Scheme 164). Treatment of Li_2S with H_3SiBr furnished the expected $S(SiH_3)_2$, but it could not be isolated, contrary to his previous work were isolation was successful (Scheme 161).[171,238]

Anderson and Drake prepared a range of thiosilanes by using the thiolato-aluminate $LiAl(SMe)_4$ as nucleophilic RS-source. Treatment of $LiAl(SMe)_4$ with H_3SiBr or H_5Si_2Br furnished the corresponding $MeSSiH_3$ and $MeSSi_2H_5$, respectively (see Scheme 165), providing a convenient route to both silyl- and disilanyl-substituted thiosilanes.[246]

Cradock, Ebsworth, and Jessep obtained $S(SiH_3)_2$ in quantitative yield by treating $N(SiH_3)_3$ with H_2S, also forming the ammonium salt $NH_3{\cdot}HSSiH_3$. The same ammonium salt was also obtained quantitatively by combining $HSSiH_3$ with NH_3 (see Scheme 166, path a). Using partially substituted amines

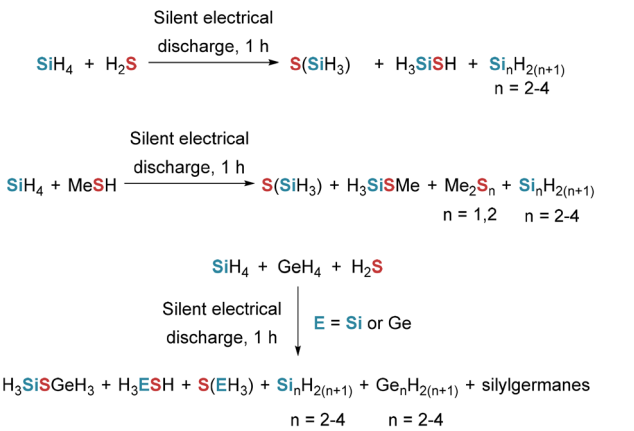

Scheme 163 Silent electrical discharge reactions of different SiH_4 mixtures. Yields of individual products were not reported.

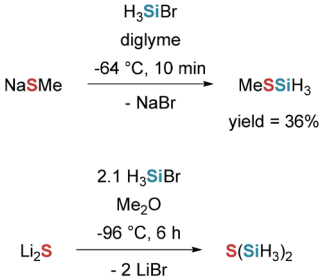

Scheme 164 Synthesis of silylsulfides starting from alkali sulfides. No yields for $S(SiH_3)_2$ reported.

This journal is © the Partner Organisations 2026

Open Access Article. Published on 24 April 2026. Downloaded on 5/15/2026 8:48:04 PM.
This article is licensed under a Creative Commons Attribution 3.0 Unported Licence.

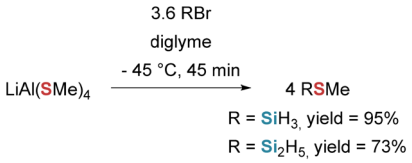

Scheme 165 Synthesis of silylsulfides using the thiolato-aluminate $LiAl(SMe)_4$.

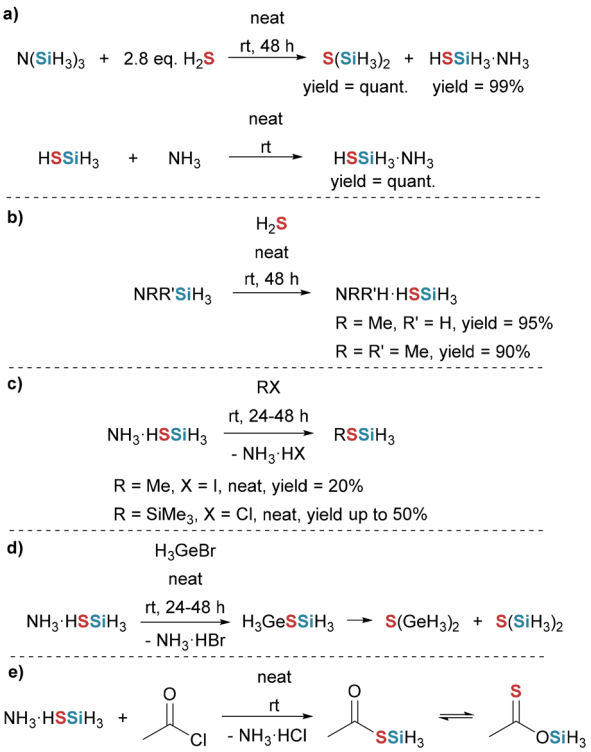

Scheme 166 Generation of disilylsulfide and the ammonium salt $HSSiH_3{\cdot}NH_3$ and reactivity studies of the ammonium salt (path a–e). Yields of the reactions between the ammonium salt and H_3GeBr and acetylchloride not reported.

derived from $N(SiH_3)_3$, they similarly prepared $NMe_2H{\cdot}HSSiH_3$ and $NMeH_2{\cdot}HSSiH_3$ (see Scheme 166, path b). They then explored the electrophile scope of $NH_3{\cdot}HSSiH_3$. MeI afforded $MeSSiH_3$, and Me_3SiCl gave $Me_3SiSSiH_3$, as expected (see Scheme 166, path c). Reaction with H_3GeBr produced $H_3GeSSiH_3$ together with the follow-up products $S(GeH_3)_2$ and $S(SiH_3)_2$ (see Scheme 166, path d). With acetyl chloride, using an excess led predominantly to SiH_3Cl, whereas sub-equimolar MeC(O)Cl furnished $MeC(O)SSiH_3$, which isomerized in solution to $MeC(S)OSiH_3$ with an isomer ratio of at least 7 : 1 in favor of $MeC(S)OSiH_3$ (see Scheme 166, path e).[247]

Cradock *et al.* reported that treatment of $S(SiH_3)_2$ with MeLi liberates $MeSiH_3$ in approximately 90% of the theoretical amount, forming $Li(SSiH_3)$ (see Scheme 167). A solution of $Li(SSiH_3)$ can then be quenched with Me_3SiCl to give the expected $(Me_3Si)S(SiH_3)$.[248]

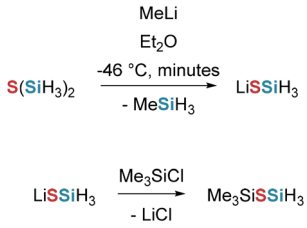

Scheme 167 Generation of $Li(SSiH_3)$ and its reactivity with Me_3SiCl. No yields were reported.

Finch and Van Dyke generated $H_3GeSSiH_3$ by treating $S(SiH_3)_2$ with H_3GeCl, but the product disproportionates to $S(GeH_3)_2$ and $S(SiH_3)_2$, preventing isolation of pure $H_3GeSSiH_3$ (see Scheme 168). $S(GeH_3)_2$ can be removed readily, but $H_3GeSSiH_3$ and $S(SiH_3)_2$ have very similar volatilities and could not be separated by distillation.[249] This behaviour mirrors the disproportionation reaction observed by Cradock, Ebsworth, and Jessep when $NH_3{\cdot}HSSiH_3$ was reacted with GeH_3Br, which likewise furnished $H_3GeSSiH_3$ together with $S(GeH_3)_2$ and $S(SiH_3)_2$ (see Scheme 166, path d).[247]

Cradock *et al.* published follow-up chemistry on $Li(SSiH_3)$, reacting it with Me_3SiCl yields $Me_3SiSSiH_3$ (see Scheme 169, path a). Reaction with MeI results in the expected $MeSSiH_3$ formation; acetylchloride giving the thioester $MeC(O)SSiH_3$ and with Me_2SiCl_2 the corresponding $Me_2Si(SSiH_3)_2$ (see Scheme 169, path b and c). They also reported several unsuccessful attempts that did not deliver the targeted S-substituted products (see Scheme 169, path d). Reactions with $MeSiCl_3$, $SiCl_4$, $PBrF_2$, PF_3, $HgCl_2$, $SnCl_2$, and BCl_3 mainly produced $S(SiH_3)_2$, SiH_3F, or SiH_4. Finally, chalcogen exchange experiments showed that reacting $Li(SSiH_3)$ with $Se(SiH_3)_2$, or alternatively $Li(SeSiH_3)$ with $S(SiH_3)_2$, converged in both cases to $Li(SeSiH_3)$ and $S(SiH_3)_2$ (see Scheme 169, path e).[219]

Haas and Vongher isolated the cyclic trimer $(SSiH_2)_3$ in 1978. Their route began with diiodosilane (SiH_2I_2) and HgS at elevated temperature, followed by filtration and solvent removal to give an oligomeric mixture. After leaving the oligomeric mixture exposed to light for about one week, this mixture converted into a gummy-like, polymeric solid. Vacuum depolymerization at 210 °C for 2 h furnished $(SSiH_2)_3$ (see Scheme 170), which is stable at −80 °C but slowly polymerizes at 20 °C over several days. Thermolysis in the presence of Al_2S_3 showed no change up to 170 °C; above this temperature the trimer decomposes to give mainly H_3SiSH and $S(SiH_3)_2$, with traces of H_2S.[250]

Haas and Hitze reported new routes to cyclotrisilathiane $(SSiH_2)_3$ in 1984. When $Li(SSiH_3)$ was combined with SiH_2Cl_2,

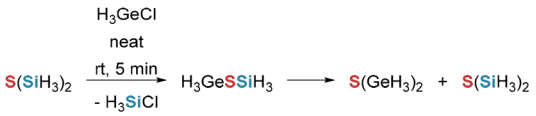

Scheme 168 Synthesis of $H_3GeSSiH_3$ and its disproportionation towards digermyl- and disilylsulfide, no yields were reported.

Open Access Article. Published on 24 April 2026. Downloaded on 5/15/2026 8:48:04 PM.
This article is licensed under a Creative Commons Attribution 3.0 Unported Licence.

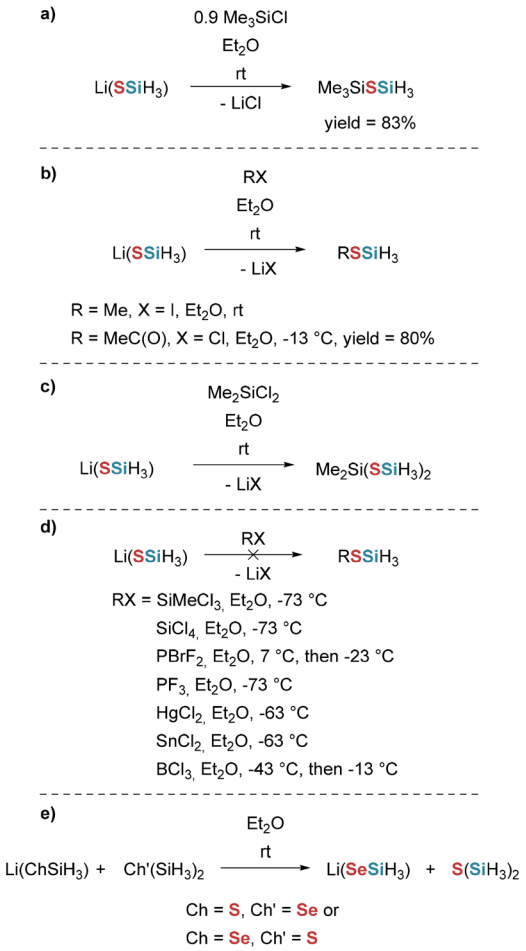

Scheme 169 Reactivity of $Li(SSiH_3)$ with different electrophiles (path a–e). Yields of $MeC(O)SSiH_3$ and $Me_2Si(SSiH_3)_2$ were not reported.

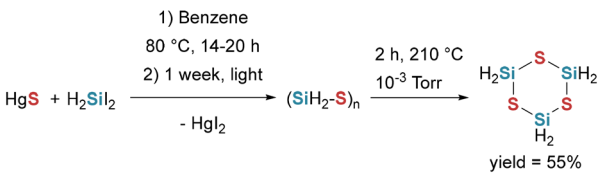

Scheme 170 Synthesis of the cyclic $(SSiH_2)_3$ by reacting HgS with SiH_2I_2.

the expected $H_2Si(SSiH_3)_2$ was not obtained; instead, its decomposition products $S(SiH_3)_2$ and $(SSiH_2)_3$ were formed (see Scheme 171, path a). The analogous reaction with SiH_2I_2 gave similar outcomes. Notably, $(SSiH_2)_3$ prepared from SiH_2Cl_2 was more stable than material obtained from SiH_2I_2, which the authors attributed to iodide catalyzing polymerization. Alternatively, reacting $S(SiH_3)_2$ directly with SiH_2Cl_2 furnished cyclotrisilathiane and, in parallel, $H_2Si(SSiH_3)_2$, which they succeeded in isolating (see Scheme 171, path b). Using the purified $H_2Si(SSiH_3)_2$, they conducted a thermal stability study and determined its degradation pathway leading to cyclotrisilathiane (see Scheme 171, path c).[251]

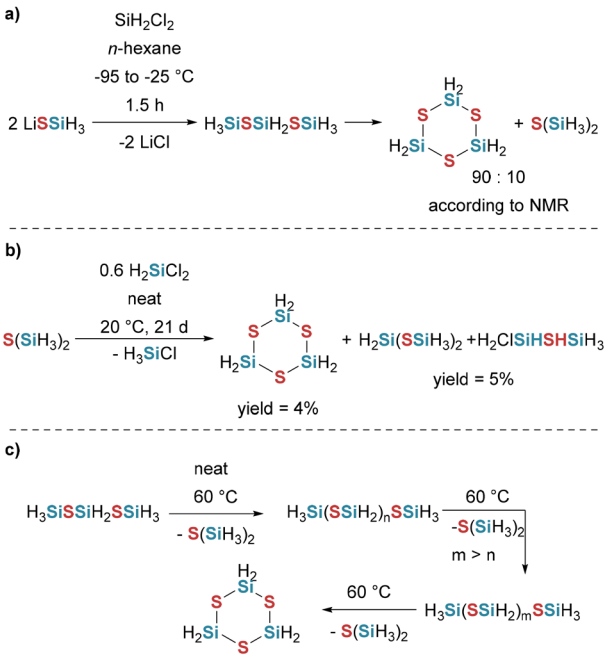

Scheme 171 Synthesis of the cyclotrisilathiane *via* different routes (path a–c). Yields for $H_2ClSiSSiH_3$ were not reported.

Haas, Süllentrup, and Krüger generated the new six-membered cyclic disilathiane $(SSi_2H_4)_2$ by two routes. By combining $(H_2SiCl)_2$ with $S(SiH_3)_2$ (see Scheme 172, path a), or by reacting $Li(SSiH_3)$ with one equivalent of $(ClSiH_2)_2$, wherein two molecules of the intermediate $(ClH_5Si_2)S(SiH_3)$ undergo self-condensation with elimination of SiH_3Cl to close the ring (see Scheme 172, path b).[252]

A thermolysis study at 90 °C for 1 h showed that, alongside the recovered ring, $S(Si_2H_5)_2$ is the principal degradation product (Scheme 173, path a). They also accessed linear disilathianes of the type $(H_3Si)_nS(Si_2H_5)_{2-n}$ (n = 0, 1) by treating $S(SiH_3)_2$ with two or one equivalent(s) of Si_2H_5Cl, respectively (Scheme 173, path b and c).[252]

Silylselenides. Relative to oxygen and sulfur, selenium has a larger covalent radius, higher electronic polarizability, and greater metallic character, yielding softer Si–Se bonds, greater

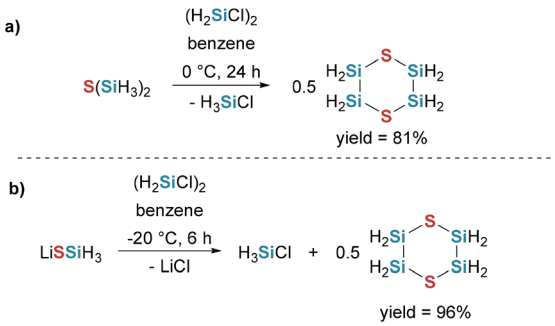

Scheme 172 Two pathways towards the cyclic disilathiane $(SSi_2H_4)_2$ by Haas, Süllentrup and Krüger (path a and b).

This journal is © the Partner Organisations 2026

Open Access Article. Published on 24 April 2026. Downloaded on 5/15/2026 8:48:04 PM.
This article is licensed under a Creative Commons Attribution 3.0 Unported Licence.

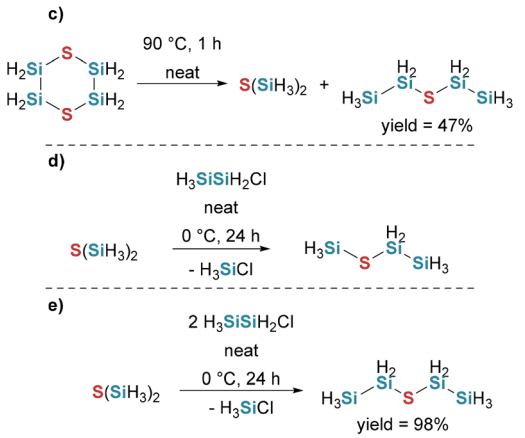

Scheme 173 Thermolysis of disilathiane $(SSi_2H_4)_2$ (path a) and generation of the unsymmetrical silylsulfide (path b) and disilylsulfide (path c). No yields reported for $H_3SiS(Si_2H_5)$.

structural compliance, and stronger dielectric screening in Si-based semiconductors. Consequently, Se enables tunable band gaps and defect energetics, higher carrier mobilities with reduced interface-state densities in passivation layers, and superior electronic conductivity for conductive interlayers. Its higher atomic mass also enhances spin–orbit coupling, providing an additional lever for band-structure engineering.[253]

In 1955, Emeléus, MacDiarmid, and Maddock attempted to synthesize $Se(SiH_3)_2$ by reacting SiH_3I with either Se or HgSe over extended periods, but both approaches failed. By contrast, using Ag_2Se led to rapid formation of $Se(SiH_3)_2$ within about 30 minutes (see Scheme 174).[229]

Ebsworth, Emeléus, and Welcman prepared perfluoroalkyl silyl selenides $RSeSiH_3$ ($R = CF_3$, C_3F_7) by reacting H_3SiI with $Hg(SeR)_2$ (see Scheme 175).[254]

Contrary to the H_2S case, Ebsworth, Glidewell, and Sheldrick reported that $P(SiH_3)_3$ reacts with H_2Se to furnish the expected $Se(SiH_3)_2$ (see Scheme 176).[244]

Cradock and Ebsworth obtained $Se(SiH_3)_2$ in quantitative yield by reacting Li_2Se with H_3SiBr (see Scheme 177), providing a straightforward halide/selenide metathesis.[255]

Drake and Riddle applied silent electrical discharge to equimolar SiH_4/H_2Se and observed, in addition to higher silanes,

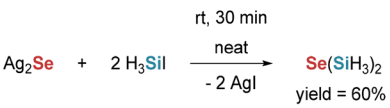

Scheme 174 Synthesis of disilylselenide using Ag_2Se and SiH_3I.

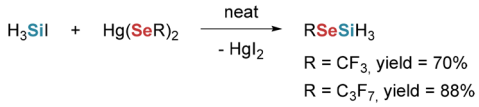

Scheme 175 Synthesis of mixed silylselenides.

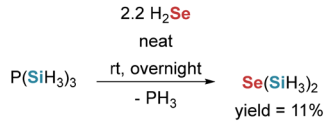

Scheme 176 Generation of disilylselenide through the reaction of trisilylphosphide and H_2Se.

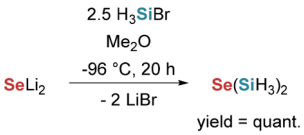

Scheme 177 Synthesis of disilylselenide using lithiumselenide and SiH_3Br.

the formation of $Se(SiH_3)_2$ and H_3SiSeH (see Scheme 178). With ternary $SiH_4/GeH_4/H_2Se$ mixtures, the product spectrum expanded to include $H_3SiSeGeH_3$, H_3ESeH and $Se(EH_3)_2$ (E = Si, Ge), along with higher silanes, higher germanes, and silylgermanes.[245]

Anderson and Drake synthesized $MeSeSiH_3$ by combining H_3SiBr with $LiAl(SeMe)_4$ (see Scheme 179), directly analogous to the sulfur congener prepared from $LiAl(SMe)_4$ (Scheme 165).[246]

Cradock, Ebsworth, and Jessep showed that $N(SiH_3)_3$ reacts with H_2Se to give $Se(SiH_3)_2$ together with the ammonium selenosilane $NH_3{\cdot}HSeSiH_3$ (see Scheme 180, path a). Replacing NH_3 with partially substituted amines such as $HNMeSiH_3$ or Me_2NSiH_3 resulted in the formation of the corresponding salts $HNRR'{\cdot}HSeSiH_3$ (R, R′ = H, Me) (see Scheme 180, path b). The $NH_3{\cdot}HSeSiH_3$ adduct was examined in detail: methylation with MeI delivered $MeSeSiH_3$; treatment with Me_3SiCl afforded

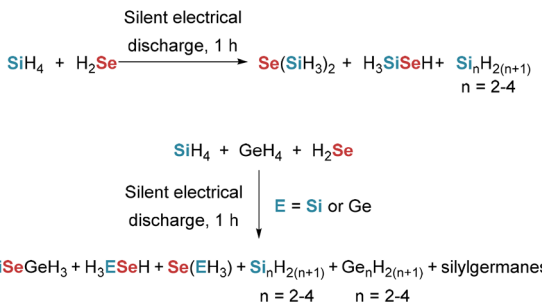

Scheme 178 Silent electrical of SiH_4/H_2Se and $SiH_4/GeH_4/H_2Se$ mixtures. Yields of individual products were not reported.

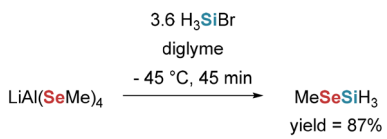

Scheme 179 Synthesis of the mixed $MeSeSiH_3$ selenide using $LiAl(SeMe)_4$ and SiH_3Br.

Open Access Article. Published on 24 April 2026. Downloaded on 5/15/2026 8:48:04 PM.
This article is licensed under a Creative Commons Attribution 3.0 Unported Licence.

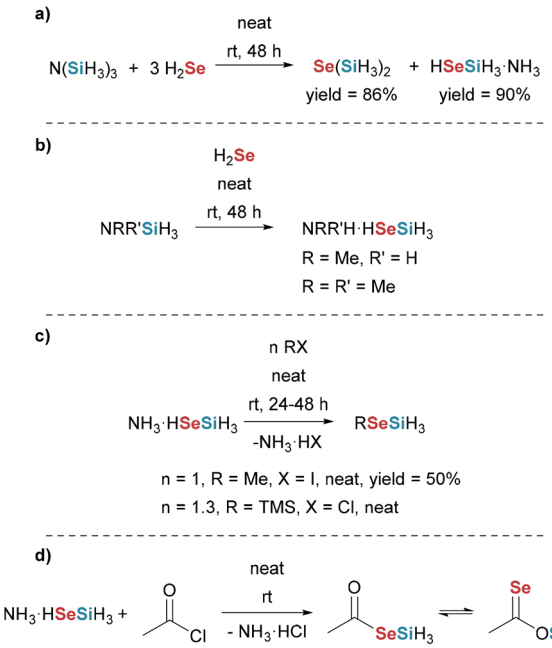

Scheme 180 Generation of disilylselenide and the ammonium salt $HSeSiH_3{\cdot}NH_3$ and reactivity studies of the ammonium salt (path a–d). Yields of the reaction between the ammonium salt and Me_3SiCl and acetylchloride not reported.

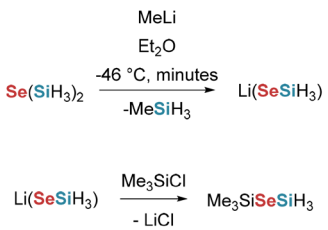

Scheme 181 Generation of $Li(SeSiH_3)$ by the reaction of disilylselenide and MeLi and its reaction with Me_3SiCl. Yields of products were not determined.

$Me_3SiSeSiH_3$, which slowly disproportionated at room temperature to $(Me_3Si)_2Se$ and $Se(SiH_3)_2$ (see Scheme 180, path c); and exposure to PF_2Br produced a complex mixture containing PF_3, SiH_3F, unreacted PF_2Br, H_2Se, $Se(SiH_3)_2$, and $SiH_3{\cdot}NH{\cdot}PF_2$. Finally, reaction with acetyl chloride yielded a mixture of $Se(SiH_3)_2$, diacetyl selenide ($Se[(O)CMe]_2$), and the desired silylselenoacetate $MeC(O)SeSiH_3$, which could not be isolated; nonetheless, the isomer ratio at room temperature was determined to be approximately 2.5 : 1, with $MeC(O)SeSiH_3$ as the major isomer (see Scheme 180, path d).[247]

Cradock *et al.* reported that treating $Se(SiH_3)_2$ with MeLi evolves methylsilane ($MeSiH_3$) in approximately 90% of the theoretical amount and forms $Li(SeSiH_3)$. The resulting solution of $Li(SeSiH_3)$ can then be quenched with Me_3SiCl to afford the expected $Me_3SiSeSiH_3$ (see Scheme 181).[248]

Barker, Drake, and Hemmings showed that $LiAl(SeMe)_4$ reacts with H_3SiBr to give $H_3SiSeMe$ and with H_2SiBr_2 to give

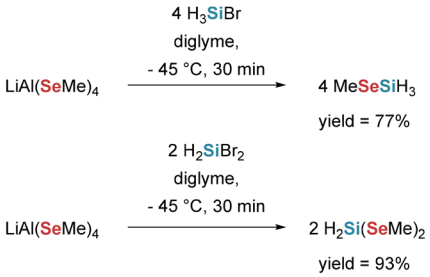

Scheme 182 Generation of mixed silylselenides using $LiAl(SeMe)_4$.

$H_2Si(SeMe)_2$; both products were successfully isolated, and in each case only traces of SiH_4 were detected as a byproduct (see Scheme 182).[256]

Cradock *et al.* showed that $Li(SeSiH_3)$ reacts cleanly with Me_3SiCl to furnish $Me_3SiSeSiH_3$ (see Scheme 183, path a). If NMe_3 is present prior to quenching, the Lewis adduct $Me_3SiSeSiH_3{\cdot}NMe_3$ is formed, subsequent treatment with BF_3 releases the free selenide (with formation of $NMe_3{\cdot}BF_3$) (see Scheme 183, path b). Acylation with acetyl chloride affords $MeC(O)SeSiH_3$, which isomerizes in solution and exists in equilibrium with $MeC(Se)OSiH_3$ (see Scheme 183, path c). Extending this electrophile scope gave divergent outcomes. With $MeC(O)_2O$ or $MeCO_2H$, the main product is again the acetyl silyl selenide $MeC(O)SeSiH_3$. In contrast, CF_3CO_2H reacts mainly to the silyl trifluoroacetate $CF_3C(O)OSiH_3$, while

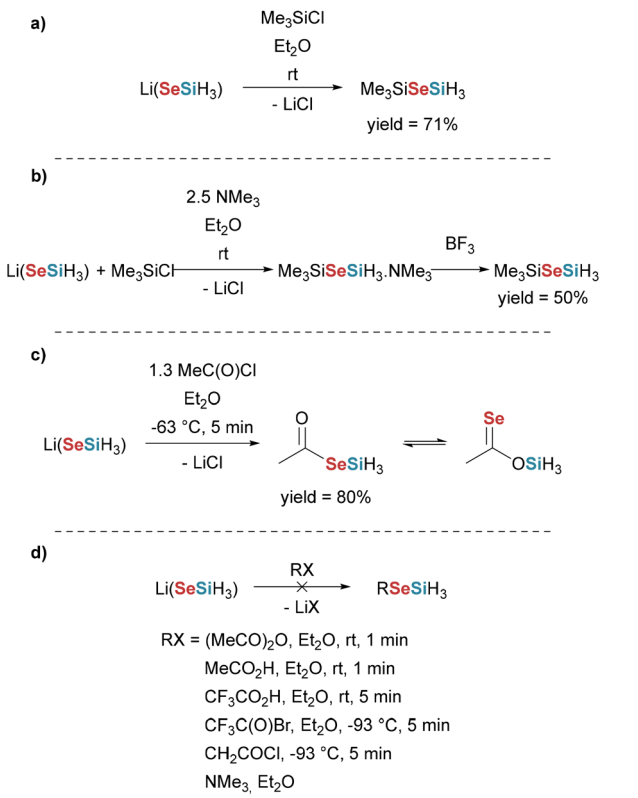

Scheme 183 Reactivity scope of $Li(SeSiH_3)$ (path a–d).

This journal is © the Partner Organisations 2026

Open Access Article. Published on 24 April 2026. Downloaded on 5/15/2026 8:48:04 PM.
This article is licensed under a Creative Commons Attribution 3.0 Unported Licence.

the acyl halides $CF_3C(O)Br$ and $CClH_2C(O)Cl$ lead predominantly to $Se(SiH_3)_2$. No reaction is observed with NMe_3 alone under the same conditions (see Scheme 183, path d).[219]

Drake and Hemmings synthesized phenylselenosilanes by two complementary routes: reaction of Li(SePh) with H_3SiBr to give $PhSeSiH_3$, and reaction of the selenoaluminate $LiAl(SePh)_4$ with H_2SiBr_2 to furnish $H_2Si(SePh)_2$ (see Scheme 184).[257]

Drake, Glavinčevski, and Hemmings prepared $Se(SiH_3)_2$ by reacting H_3SiI with the selenoaluminate $LiAl(SeH)_4$, which serves as an efficient selenide-transfer reagent (see Scheme 185).[258]

Haas and Hitze were the first to obtain the cyclic selenosilane $(SeSiH_2)_3$ by heating HgSe with H_2SiI_2 to 120 °C. The initial reaction produced oligomeric mixtures, which upon depolymerization under vacuum at 140 °C, followed by recrystallization in benzene furnished crystalline $(SeSiH_2)_3$ (see Scheme 186, path a). The crystals are unstable at 20 °C and revert to an oligomeric mixture within 1–2 hours. Attempts to reach the same product *via* Na_2Se and H_2SiI_2 in benzene at 20 °C led to decomposition into iodine and selenium; performing the reaction in ether gave the same outcome, with decomposition occurring above −40 °C. Reactions between SiH_2I_2 and $K_6[HgSe_4]$ behaved similarly (see Scheme 186, path b). When Ag_2Se was combined with H_2SiI_2, no reaction was observed at 20 °C, and upon refluxing the mixture, SiH_3I and $Se(SiH_3)_2$ were obtained instead of $(SeSiH_2)_3$ (see Scheme 186, path c).[259]

Haas, Süllentrup, and Krüger generated the new cyclic compound $(SeSi_2H_4)_2$ by reacting $(SiH_2Cl)_2$ with $Se(SiH_3)_2$, with elimination of H_3SiCl (see Scheme 187, path a). Thermolysis of this ring at 90 °C for 1 h gave $Se(Si_2H_5)_2$ as the principal degradation product together with Si_2H_6 (see Scheme 187, path b). They also obtained the new linear disilaselenides $(H_3Si)_nSe(Si_2H_5)_{2-n}$ (n = 0, 1) by reacting $Se(SiH_3)_2$ with one or two equivalents of Si_2H_5Cl (see Scheme 187, path c and d).[252]

Silyltelluride. Relative to O, S, and Se, tellurium has the largest covalent radius, highest electronic polarizability, and greatest metallic character in group 16, yielding the softest Si–Te bonds and enhanced lattice compliance in Si-based semiconductors. These attributes enable deeper band-structure modulation, tuning band gaps or sub-bandgap states into the near-IR, and can produce higher electronic conductivity in Te-rich chalcogenide passivation or interlayer stacks.[260]

Bürger and Goetze were the first in 1967 to synthesize $Te(SiH_3)_2$ by reacting Li_2Te with SiH_3I in tetralin and heating the mixture at 70 °C for 3 days (see Scheme 188).[261]

Two years later, Cradock, Ebsworth, and Rankin obtained $Te(SiH_3)_2$ by reacting SiH_3Br with Li_2Te in Me_2O at low temperature (see Scheme 189).[255]

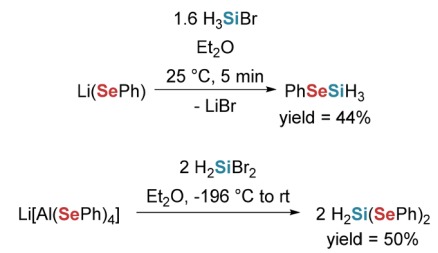

Scheme 184 Generation of phenylselenosilanes.

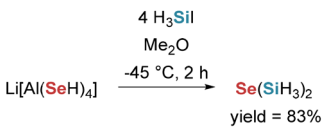

Scheme 185 Synthesis of disilylselenide using selenoaluminate and SiH_3I.

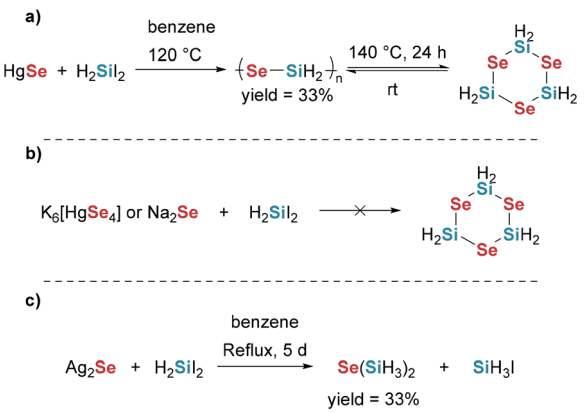

Scheme 186 Attempted reactions towards the cyclic selenosilane $(SeSiH_2)_3$ and its successful generation using HgSe and SiH_2I_2 (path a–c).

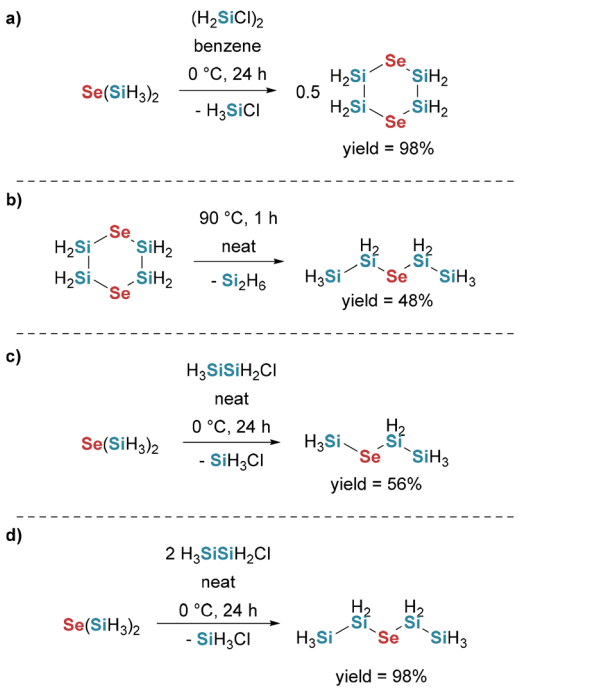

Scheme 187 Synthesis of the cyclic disilylselenide $(SeSi_2H_4)_2$ *via* different pathways (path a) and generation of mixed and symmetrical disilylselenides (path b–d).

Open Access Article. Published on 24 April 2026. Downloaded on 5/15/2026 8:48:04 PM.
This article is licensed under a Creative Commons Attribution 3.0 Unported Licence.

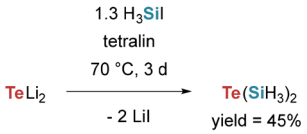

Scheme 188 Synthesis of $Te(SiH_3)_2$ using $TeLi_2$ and SiH_3I in tetralin.

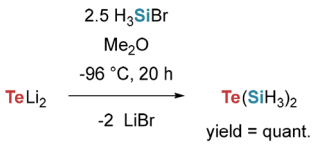

Scheme 189 Synthesis of $Te(SiH_3)_2$ using $TeLi_2$ and SiH_3Br.

Anderson and Drake prepared $MeTeSiH_3$ by reacting the telluroaluminate $LiAl(TeMe)_4$ with SiH_3Br, but the product was obtained only in low yield (see Scheme 190).[246]

Drake and Hemmings attempted to prepare $RTeSiH_3$ (R = Me, Ph) by reacting LiTeR with SiH_3Br, but they were unable to isolate the desired products; instead, they observed $Te(SiH_3)_2$ and traces of silane among the volatile species alongside intractable polymeric material. In contrast, an exchange route employing $RTeMe_3Si$ (R = Me, Ph) with SiH_3Br or SiH_3I, eliminating Me_3SiBr or Me_3SiI, results in a successful $RTeSiH_3$ formation (see Scheme 191, path a). They also found that $MeTeSiH_3$ decomposes after prolonged storage or upon laser excitation to give $H_2Si(TeMe)_2$ and SiH_4 (see Scheme 191, path b).[262]

Drake, Glavinčevski, and Hemmings later synthesized $Te(SiH_3)_2$ by reacting SiH_3I with an excess of Li_2Te at low temperatures in Me_2O (see Scheme 192).[258]

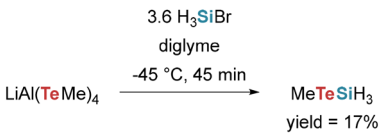

Scheme 190 Synthesis of the mixed $MeTeSiH_3$ using $LiAl(TeMe)_4$ and SiH_3Br.

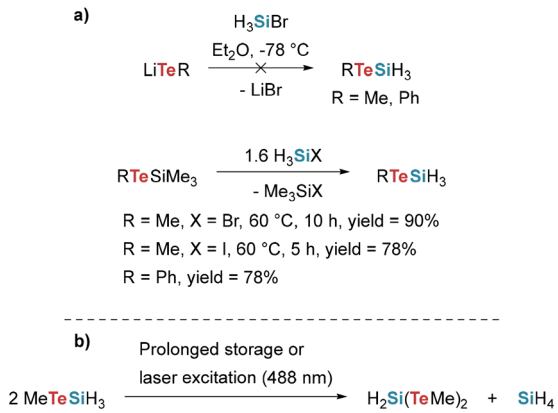

Scheme 191 Attempted and successful reaction towards $RTeSiH_3$ (path a) and decomposition products of $MeTeSiH_3$ (path b).

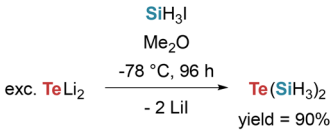

Scheme 192 Generation of disilyltelluride using SiH_3I and $TeLi_2$ in ether.

Functionalization with group 7 (synthesis of silylhalogenes)

Halohydrosilanes represent a central class of silicon compounds in which Si–X bonds (X = F, Cl, Br, I) replace one or more Si–H or Si–Si functionalities. The strong polarity and thermodynamic stability of Si–halogen bonds significantly influence their chemical behaviour: halohydrosilanes are highly sensitive to hydrolysis, readily undergo redistribution reactions, and frequently serve as activated intermediates in silicon bond construction. From a synthetic perspective, they occupy a strategic position between elemental silicon and hydrosilanes, acting both as precursors to reduce silicon species and electrophilic building blocks for tailored silicon frameworks.

Industrial and technological interest in halohydrosilanes is driven largely by thin-film deposition processes. In chemical vapor deposition and liquid phase deposition or solution-based routes, halohydrosilanes provide a controlled silicon delivery, variable reactivity, and favourable volatility. Chlorinated and fluorinated silanes, in particular, are widely exploited for semiconductor fabrication, surface passivation, and the formation of silicon-containing coatings. Their decomposition pathways allow precise regulation of film growth kinetics, impurity profiles, and microstructure – critical parameters for semiconductor devices, photovoltaics, and protective layers. Furthermore, halohydrosilanes serve as key intermediates in the preparation of higher hydrosilanes and functional silicon oligomers, linking fundamental synthesis with applied materials chemistry.[263]

Synthetic access to halohydrosilanes generally follows several recurring strategies (see Scheme 193).

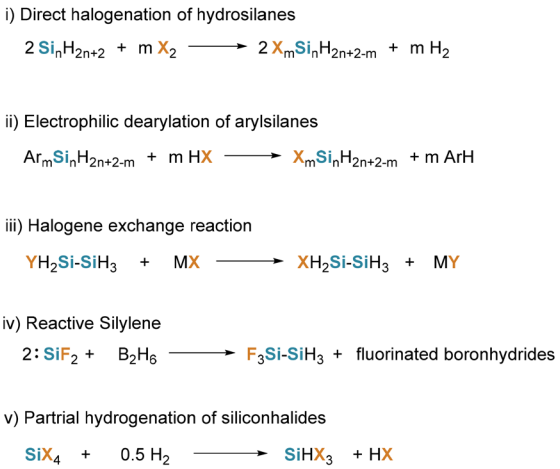

Scheme 193 Method (i)–(v) for the formation of different halohydrosilanes.

This journal is © the Partner Organisations 2026

Open Access Article. Published on 24 April 2026. Downloaded on 5/15/2026 8:48:04 PM.
This article is licensed under a Creative Commons Attribution 3.0 Unported Licence.

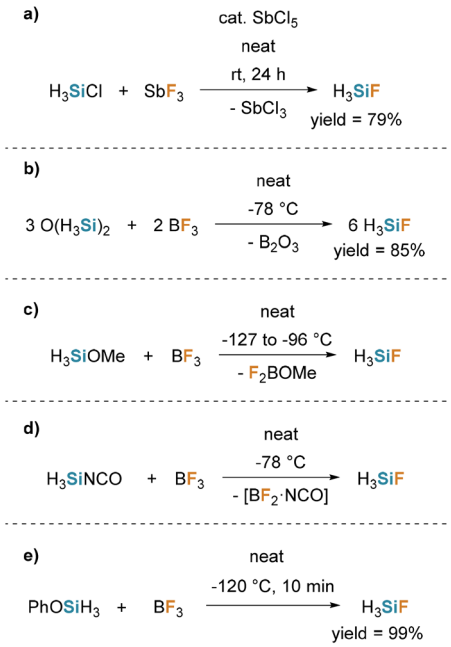

Scheme 194 Methods for the synthesis of monofluorosilane (path a–e). For the reactions of $H_3SiOMe + BF_3$ (path c) and $SiH_3{\cdot}NCO + BF_3$ (path d) no yields reported.

Structurally, halohydrosilanes can be devided into acyclic perhalogenated, cyclic compounds and mixed derivatives. The following sections summarize the principal compound classes and their synthetic approaches, organized according to the halogen substituent – beginning with fluorohydrosilanes and proceeding through chlorosilanes and bromohydrosilanes to iodohydrosilanes – reflecting their sequence in the periodic table.

Fluorohydrosilanes. Intensive investigations towards the synthesis, properties and reactivity of fluorohydrosilanes began in the early 1970s. Particular attention has been devoted to disilane derivatives because of their relevance to semiconductor processing, whereas comparatively fewer studies have addressed the preparation of higher fluorinated silanes.[264]

Monofluorosilane (H_3SiF) has been prepared primarily through electrophilic fluorination or Lewis-acid-induced Si–X bond cleavage reactions. Early work by Emeléus and Maddock demonstrated that H_3SiF can be obtained in approximately 79% yield by fluorination of chlorosilane with antimony trifluoride at room temperature (see Scheme 194, path a), although competing oxidative fluorination and disproportionation limited product stability and purity.[265] A significant cleaner and higher-yielding approach was later introduced by Onyszchuk, who showed that boron trifluoride induces efficient Si–O bond cleavage in disiloxane, affording H_3SiF in up to 85% isolated yield under solvent-free conditions (see Scheme 194, path b).[233] Related studies by Sternbach and MacDiarmid further established that boron trifluoride readily converts alkoxysilanes into H_3SiF, confirming the general applicability of BF_3-mediated fluorination pathways, although this route was not optimized for preparative yields (see Scheme 194, path c).[232] In addition, Ebsworth and Mays reported the formation of H_3SiF from the reaction of silyl isocyanate with boron trifluoride at −78 °C, an observation made in the course of probing the reactivity of silylisocyanate rather than as dedicated synthetic approach to H_3SiF (see Scheme 194, path d).[172] Treatment of $PhOSiH_3$ with HF affords H_3SiF in excellent yields (see Scheme 194, path e).[236] The most common method for the synthesis of fluorohydrooligosilanes is the co-condensation of SiF_2 with B_2H_6 at a cool copper surface (method iv). The reactive SiF_2 intermediate is generated *in situ* by passing SiF_4 over elemental silicon at high temperatures. Under these conditions, a mixture of $F_3Si–SiH_3$, $F_3Si–SiF_2H$ and $H_2Si–(SiF_3)_2$ is formed (see Scheme 195). Although isolated yields were not determined, spectroscopic analyses indicated that $H_2Si–(SiF_3)_2$ is formed in relatively higher amounts, while $F_3Si–SiH_3$ and $F_3Si–SiF_2H$ are produced in comparable portions. This species were separated by high vacuum, low temperature fractional condensation.[266]

$F_3Si–SiH_3$ is also formed as a byproduct during the synthesis of SiF_2HPH_2 and SiF_3PH_2 *via* the condensation of SiF_2 with PH_3 (method iv) (see Scheme 196).[267]

Reactions of SiF_2 with protic reagents (such as HBr) typically generate initially formed fluorinated bromodisilanes that are thermally unstable and undergo rapid secondary transformation. Scheme 197 shows that the reaction with HBr first produces 1-bromo-1,1,2,2-tetrafluorodisilane, which decomposes quickly to a mixture of different mixed halohydrosilanes. Subsequent treatment of the resulting mixture with excess SbF_3 converts it efficiently into $F_3Si–SiF_2H$.[268]

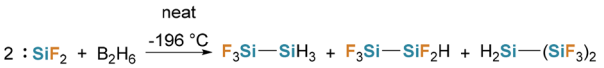

Scheme 195 Formation of different fluorohydrosilanes from Si_2F with B_2H_6; no yields reported.

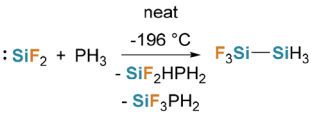

Scheme 196 Formation of $F_3Si–SiH_3$ as a byproduct during the condensation of SiF_2 and PH_3; no yields reported.

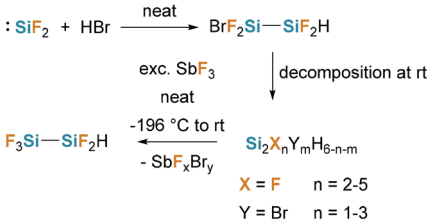

Scheme 197 Treatment of SiF_2 with HBr yielding in the unstable $BrF_2Si–SiF_2H$. Subsequent treatment of decomposition products with SbF_3 affording $F_3Si–SiF_2H$. No yields reported.

Open Access Article. Published on 24 April 2026. Downloaded on 5/15/2026 8:48:04 PM.
This article is licensed under a Creative Commons Attribution 3.0 Unported Licence.

A similar pattern is observed with H_2S: the initially formed silanethiol $F_2HSi–SiF_2SH$ decomposes within minutes, again yielding $F_3Si–SiF_2H$ (see Scheme 198).[269]

Direct fluorination routes of hydrosilanes (method i) have not been reported, but indirect access is possible through selective hydrogenation of mixed halodisilanes (method v). In compounds containing both, fluorine and chlorine or bromine substituents, the heavier halides can be selectively reduced with Me_3SnH without cleaving Si–F bonds. Using this strategy, $F_3Si–SiH_3$ can be obtained in high yields from the corresponding mixed halo precursors (see Scheme 199).[270]

In contrast, partially fluorinated bromodisilanes do not undergo clean hydrogenation. Instead, F/Br redistribution occurs prior to reduction, producing mixtures of fluorinated disilanes. Stronger hydride reagent led to even less selective outcomes, promoting Si–Si bond cleavage and partial reduction of Si–F bonds. Together, these observations highlight the delicate balance between halogen redistribution, bond stability and reductive pathways in fluorinated disilane chemistry.[270]

$FH_2Si–SiH_3$ was obtained by fluorination of dichlorodisilanes or dichlorotrisilane with SbF_3 (method iii) (see Scheme 200).[271,272]

Scheme 198 Reaction of SiF_2 with H_2S. Decomposition at room temperature affords $F_3Si–SiF_2H$. No yields reported.

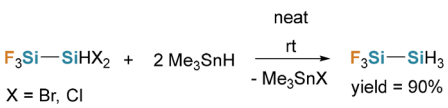

Scheme 199 Hydrogenation of mixed halodisilane yielding in $F_3Si–SiH_3$.

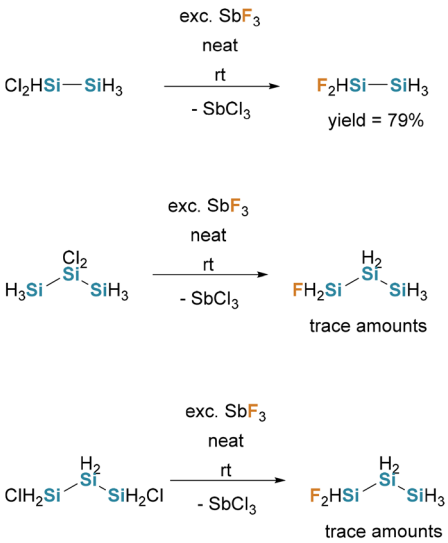

Scheme 200 Fluorination of oligohydrosilanes with SbF_3.

ZnF_2 is another well-established fluorinating agent and has been used to prepare $F_2HSi–SiHF_2$ and $FH_2Si–(SiH_2)_2–SiH_2F$ from their corresponding chlorinated or brominated precursors (method iii) (see Scheme 201).[273,274]

In addition, cleavage of Si–N bonds in $N(Si_2H_5)_3$ by BF_3 provides another pathway to $FH_2Si–SiH_3$ (see Scheme 202).[150]

Moreover, it is possible to fluorinate different methoxyoligosilanes to the corresponding branched fluorohydrosilanes with BF_3 (see Scheme 203).[275]

Finally, fluorohydrosilanes can be accessed *via* an electrical discharge approach. In this method, various monofluorosilanes were converted into $F_2HSi–SiH_3$, $FH_2Si–SiH_2F$, $F_2HSi–SiHF_2$, $F_3Si–SiF_2H$, $F_2HSi–Si_2H_5$ and $F_3Si–Si_2H_5$. However, the

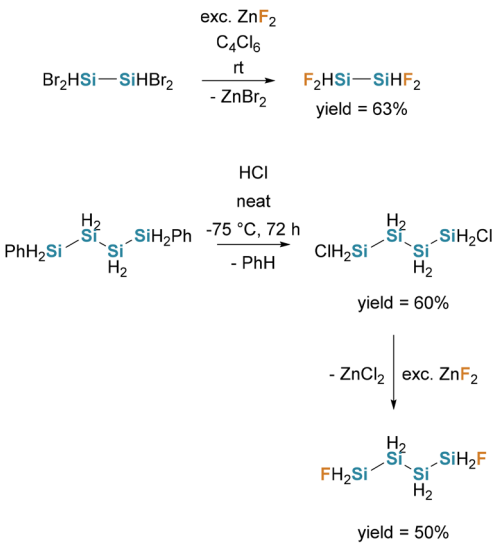

Scheme 201 Fluorination of chloro-, and bromooligohydrosilanes with ZnF_2.

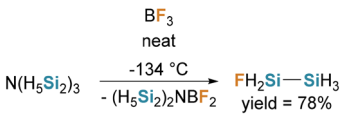

Scheme 202 Formation of $FH_2Si–SiH_3$ *via* the reaction of $N(H_5Si_2)_3$ and BF_3.

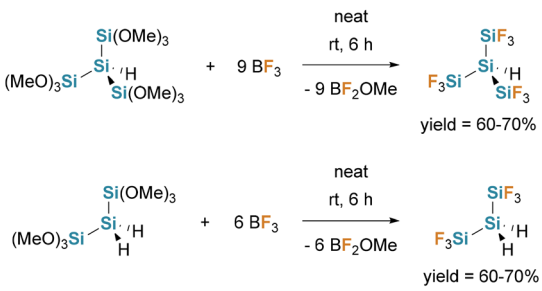

Scheme 203 Fluorination of branched methoxysilanes with BF_3.

This journal is © the Partner Organisations 2026

Open Access Article. Published on 24 April 2026. Downloaded on 5/15/2026 8:48:04 PM.
This article is licensed under a Creative Commons Attribution 3.0 Unported Licence.

resulting product mixtures proved difficult to impossible to separate.[271,276]

Chlorohydrosilanes. Chlorosilanes, particularly chlorohydrosilanes, serve as key precursors in the production of high-purity polycrystalline silicon. Driven by the rapid expansion of photovoltaic technologies, global polysilicon production capacity reached approximately 1.6 million metric tons in 2023.[277] The overwhelming majority of this material is manufactured *via* chemical vapour deposition (CVD) using trichlorosilane as primary feedstock.[278]

Already in 1919 Stock and Somieski reported the synthesis of monochlorosilane (H_3SiCl).[10] They treated monosilane with hydrogen chloride and catalytic amounts of $AlCl_3$ (method i) (see Scheme 204). Heating this mixture to 100 °C for 30 hours afforded $ClSiH_3$ in 50–55% yield, with dichlorosilane as byproduct (ratio $ClSiH_3 : Cl_2SiH_2 = 4:1$). More recent studies showed, that the yields of $ClSiH_3$ can be increased to 76% when a zeolite catalysator (Na-ZSM-5) is used.[279]

Hollandsworth *et al.* showed, that monosilane can also be chlorinated with silver chloride to afford monochlorosilane (see Scheme 204).[280] When phenylsilane ($PhSiH_3$) is used as starting material, H_3SiCl could be obtained in yields of 78% (method ii) (see Scheme 204, path c).[281] In addition, Glidewell and Rankin showed, that treatment of $PhOSiH_3$ with HCl affords H_3SiCl (see Scheme 204, path d).[236]

Starting in the 1960s, synthetic efforts towards chlorooligohydrosilanes increasingly focused on the chlorination (method i) of smaller hydrosilanes such as disilane, trisilane and tetrasilane.

Early studies by Drake *et al.* and van Dyke *et al.* established boron trichloride as an efficient chlorination reagent for these substrates (see Scheme 205, path a).[271,276,282,283] In analogy to observations made of monosilane, hydrogen chloride[284] and silverchloride[285,286] were subsequently shown to be suitable chlorinations agents for disilane as well (see Scheme 205, path b and c). Beyond these systems, tetrachlorostannane was demonstrated to chlorinate di-, tri-, and tetrasilane efficiently, thereby broadening the scope of applicable chlorination reagents (see Scheme 205, path d).[287] Finally, direct halogenation using molecular chlorine was reported by Fehér and coworkers, providing a more straightforward, albeit harsher, approach to the chlorination of disilane (see Scheme 205, path e).[288]

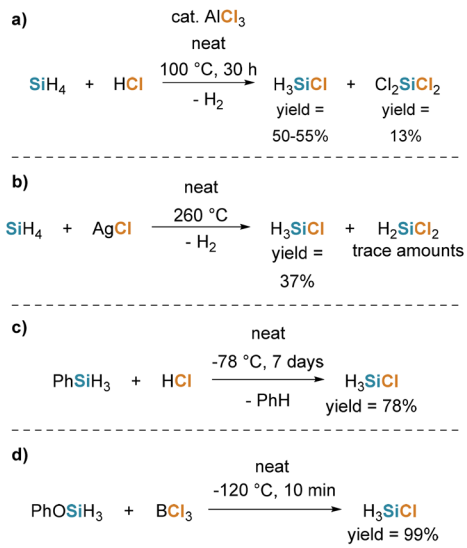

Scheme 204 Methods for the synthesis of monochlorosilane (path a–d).

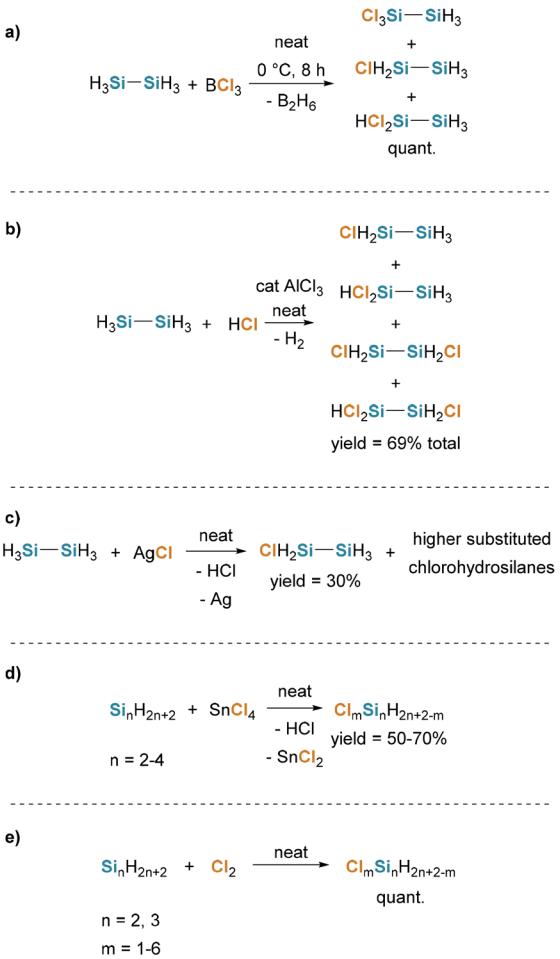

Scheme 205 Chlorination of oligohydrosilanes using different chlorination agents (path a–e).

However, all of the mentioned methods for direct halogenation of oligohydrosilanes yield complex product mixtures that often require time consuming separation or further derivatization before reliable analysis is possible.[271,276,284,286–289] Another challenge is the tendency of higher silanes to undergo isomerization.[283]

Van Dyke, and MacDiarmid prepared the silylethers $H_3SiOSi_2H_5$ and $H_3SiOSi_2H_5$ (see Scheme 145). In subsequent reactions, both $O(Si_2H_5)_2$ and $H_3SiOSi_2H_5$ reacted with BCl_3 to give Si_2H_5Cl as the main product (see Scheme 206).[234]

In 2012 Stueger *et al.* demonstrated the selective chlorination of neopentasilane with 3.5 equivalents $SnCl_4$ to afford tetra(chlorosilyl)silane (see Scheme 207 and Fig. 15).[290]

Open Access Article. Published on 24 April 2026. Downloaded on 5/15/2026 8:48:04 PM.
This article is licensed under a Creative Commons Attribution 3.0 Unported Licence.

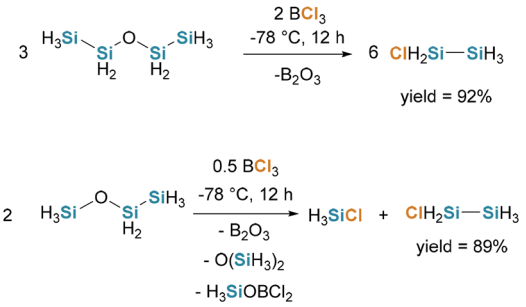

Scheme 206 Reaction of silylethers with BCl_3.

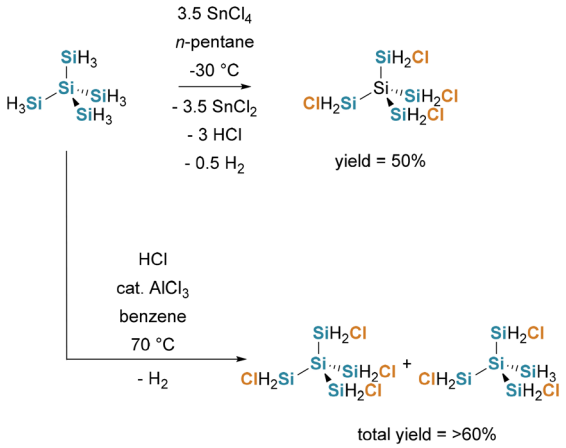

Scheme 207 Synthesis of branched chlorooligohydrosilanes.

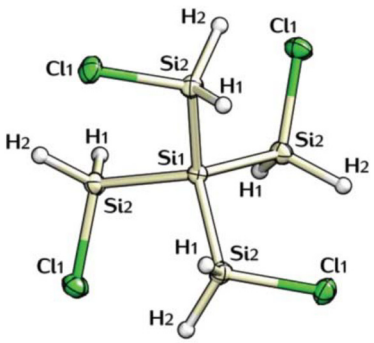

Fig. 15 Crystal structure of $Si(SiH_2Cl)_4$ reproduced from Stueger *et al.*[48] with permission from American Chemical Society, © 2012.

However, a significant drawback of employing $SnCl_4$ as halogenating reagent is the formation of large quantities of $SnCl_2$, which are difficult to remove completely, particularly on a preparative scale. To address limitation, the authors also examined an alternative protocol based on gaseous HCl in presence of catalytic $AlCl_3$ and obtained the selective formation of tetra (chlorosilyl)silane (85%), accompanied only by minor amounts of 1,2,3-trichloroneopentasilane as byproduct (15%) in a total yield of more than 60%.[291]

An additional example for the synthesis of branched chlorohydrosilanes, is the preparation of $HSi(SiCl_3)_3$. Höfler *et al.* reported two efficient synthetic approaches to this compound. The first involves the reaction of dodecachloroneopentasilane ($Si(SiCl_3)_4$) with HCl, eliminating $SiCl_4$, affording the target product in 70% yield (see Scheme 208). The second approach is based on the chlorination of $HSi[Si(OMe)_3]_3$ with nine equivalents of BCl_3, providing $HSi(SiCl_3)_3$.[292]

The synthesis of an even higher branched chlorooligohydrosilane was demonstrated by Christopoulos *et al.* First, they generated phenylnonasilane *via* the reaction of the trissilyllithium anion and 0.5 equivalents dichlorophenylsilane. Subsequent treatment with triflic acid affords the triflate substited nonasilane, which can be chlorinated with an excess of lithiumchloride and the chlorononasilane can be obtained in yields of 81% (see Scheme 209).[49]

An alternative method for the synthesis of chlorohydrosilanes is the partial hydration of perchlorooligosilanes using hydrating reagents, such as $LiAlH_4$ or Bu_3SnH (method v). But also these approach were found to yield in unselective product mixtures.[107,109]

A more attractive strategy involves the controlled partial hydrogenation (method v) with substoichiometric amounts of $i\text{-}Bu_2AlH$ (see Scheme 210). This methodology enables access

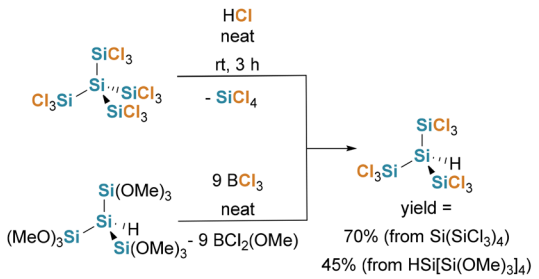

Scheme 208 Two methods for the synthesis of hexachlorotrisilane.

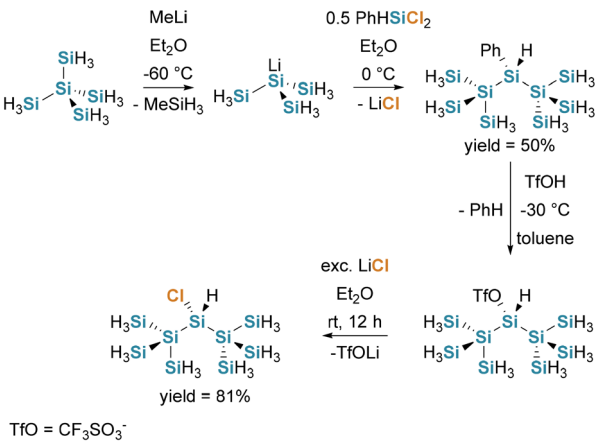

Scheme 209 Synthesis of chlorononasilane starting from neopentasilane.

This journal is © the Partner Organisations 2026

Open Access Article. Published on 24 April 2026. Downloaded on 5/15/2026 8:48:04 PM.
This article is licensed under a Creative Commons Attribution 3.0 Unported Licence.

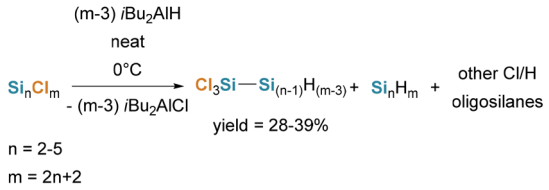

Scheme 210 Synthesis of chlorooligosilanes *via* partial hydrogenation.

to broader range of chlorohydrooligosilanes under comparatively mild conditions. i-Bu_2AlH promotes selective Si–Cl hydrogenation in both linear and branched chlorooligosilanes without inducing Si–Si bond cleavage.[291]

An additional method to prevent the complete hydrogenation of oligochlorosilanes with $LiAlH_4$ is the implementation of $N(SiMe_3)_2$ or $N(SiMe_2Ph)_2$ substituents as protecting groups into the molecule (see Scheme 211). After the hydrogenation, these groups can easily be cleaved off with HCl.[139]

In contrast to hydrosilanes, aryl-substituted silanes ($Ar_mSi_nH_{2n+2-m}$) are excellent starting materials for the selective synthesis of chlorohydrosilanes ($Cl_mSi_nH_{2n+2-m}$, n = 2–7, m = 1–9) (Scheme 212). The aryl substituents can be cleanly replaced by chlorine upon treatment with liquefied hydrogen chloride or with HCl solutions in benzene, enabling controlled halogen incorporation with good selectivity (method ii).[252,273,274,293,294]

To suppress equilibrium of the chlorinated products,[295] Uhlig *et al.* proposed a stepwise dephenylation strategy in which triflic acid is first used to remove the organic substituents, followed by either hydride reduction with $LiAlH_4$ or chlorination with Et_3NHCl (see Scheme 213). Using $Ph_3Si–SiH_3$ as precursor, this route enables the selective formation of $HCl_2Si–SiH_3$ and $Cl_3Si–SiH_3$, respectively.[296]

An analogous electrical discharge strategy for the formation of fluorohydrosilanes, has also been applied for chlorohydrosilanes. Under comparable conditions, monochlorosilane undergoes coupling reactions to give mixtures of chloro-substituted di- and oligosilanes. Similar to the fluorinated systems, these discharge processes produce complex product distributions, and separation of the individual components is challenging.[276]

Bromohydrosilanes. Also bromohydrosilanes have attracted high interest as alternative silicon precursors for vapor-phase deposition processes, particularly in efforts to move beyond the well-established chlorosilane chemistry used in large-scale silicon production.[297]

Monobromosilane can be synthesized by reacting monosilane with various bromination agents, including HBr[117] (see Scheme 214, path a), $SnBr_4$[298] (see Scheme 214, path b), and AgBr[280] (see Scheme 214, path c) (method i). A more efficient approach involves the conversion of phenylsilane with hydrogen bromide and catalytic amounts of $AlBr_3$ (see Scheme 214, path d) (method ii).[281,299]

As already shown in the section Siloxanes, H_3SiBr is also formed at the reaction of $O(SiH_3)_2$ with PBr_3 (see Scheme 146, path a).

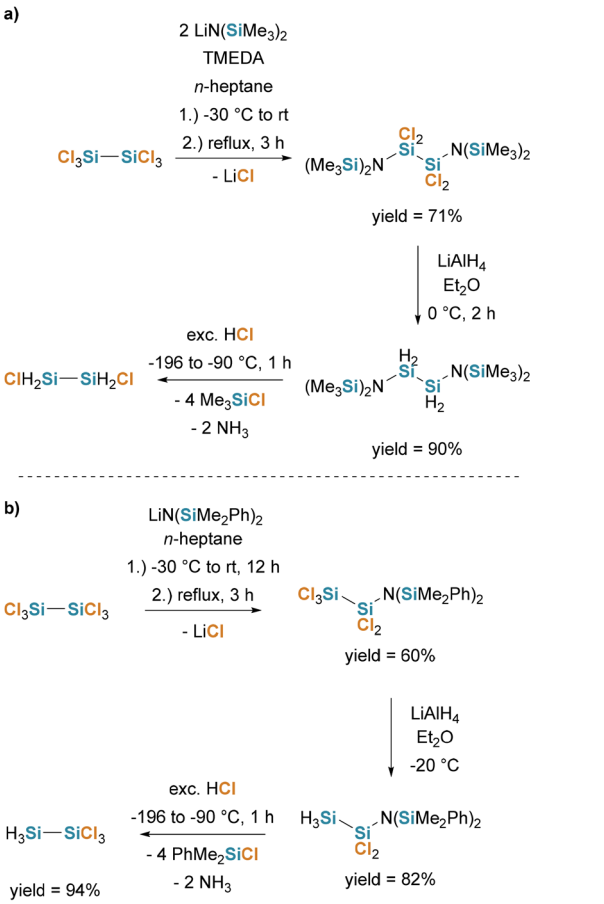

Scheme 211 Synthesis of chlorodisilanes using $N(SiMe_3)_2$ (path a) and $N(SiMe_2Ph)_2$ (path b) as protecting groups. No reported yields of $ClH_2Si–SiH_2Cl$.

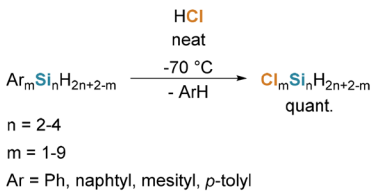

Scheme 212 Synthesis of chlorooligosilanes *via* dearylation.

Similar to the preparation of chlorooligohydrogermanes, different bromooligohydrosilanes can be generated through the bromination of oligohydrosilanes (method i) using reagents like BBr_3[271,272] (see Scheme 215, path a) HBr[117,286] (see Scheme 215, path b), $SnBr_4$[298] (see Scheme 215, path c), AgBr[280] and Br_2[288,300] (see Scheme 215, path d). These transformations typically proceed through non-selective halogen exchange leading to complex mixtures of mono- and oligobrominated silanes rather than single, well-defined products.

Also similar to the synthesis of chlorohydrosilanes, is the possibility of electrophilic cleavage of silicon–aryl bonds with HBr (method ii) (see Scheme 216).[274,294,301]

Open Access Article. Published on 24 April 2026. Downloaded on 5/15/2026 8:48:04 PM.
This article is licensed under a Creative Commons Attribution 3.0 Unported Licence.

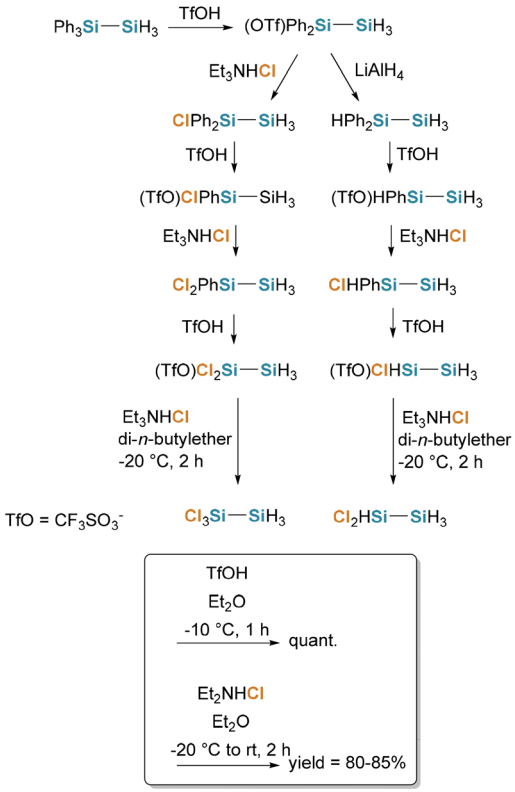

Scheme 213 Multi-step synthesis of chlorodisilanes by Uhlig *et al.*

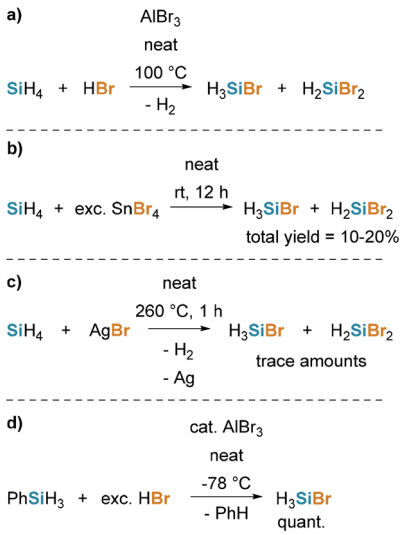

Scheme 214 Different methods for the synthesis of $BrSiH_3$ (path a–d). No reported yields for the bromination of SiH_4 with HBr (path a).

Iodohydrosilanes. Iodohydrosilanes have attracted increasing interest as highly reactive silicon precursors for CVD and LPD processes, owing to the weak Si–I bond, which enables low-temperature decomposition and efficient surface activation. Early synthetic and reactivity studies demonstrated that iodosilanes exhibit significantly higher reactivity than their

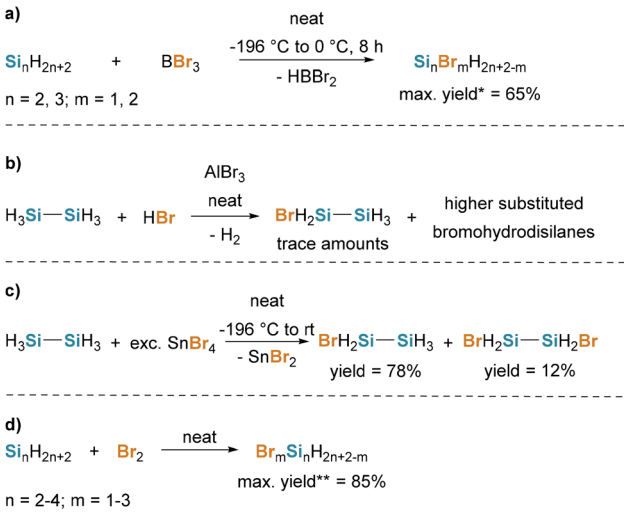

Scheme 215 Methods for the synthesis of bromooligosilanes (path a–d). *Yield was not isolated. **Yield of the product mixture.

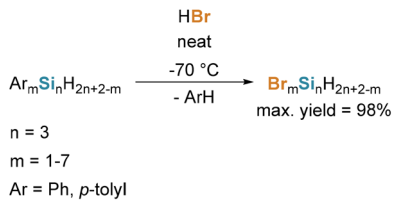

Scheme 216 Synthesis of bromooligosilanes *via* dearylation.

chloro- and bromo-analogues, making them particularly attractive for low-energy silicon deposition.[167] More recent work has highlighted their potential as single-source precursors, although their practical use remains limited by thermal instability and challenging handling properties.[302]

Maddock and co-workers first reported the preparation of monoiodosilane in 1939, describing its formation *via* the reaction of monosilane and hydrogen iodide in the presence of catalytic amounts of AlI_3 (method i) (Scheme 217, path a).[167,303] An alternative efficient method towards monoiodosilane employs phenylsilane as the starting material (method ii) (Scheme 217, path b).[281,304] Ward *et al.* further demonstrated that H_3SiI can be generated *via* the chlorination of phenylchlorosilane and subsequent hydration to form the chlorophenylsilane, which upon treatment with hydrogen iodide afforded monoiodosilane in yields of up to 65% (Scheme 217, path c).[299] Across a range of silyl ethers, treatment with HI afforded H_3SiI in quantitative yield and the corresponding alcohol (ROH) as byproduct (Scheme 217, path d).[238] It is also possible to convert $PhOSiH_3$ to H_3SiI by treatment with HI (Scheme 217, path e).[236]

In 1960, Ward and MacDiamid extended these studies to iodohydrooligosilanes.[231] In their work, disilane was reacted with hydrogen iodide in the presence of catalytic amounts alu-

This journal is © the Partner Organisations 2026

Open Access Article. Published on 24 April 2026. Downloaded on 5/15/2026 8:48:04 PM.
This article is licensed under a Creative Commons Attribution 3.0 Unported Licence.

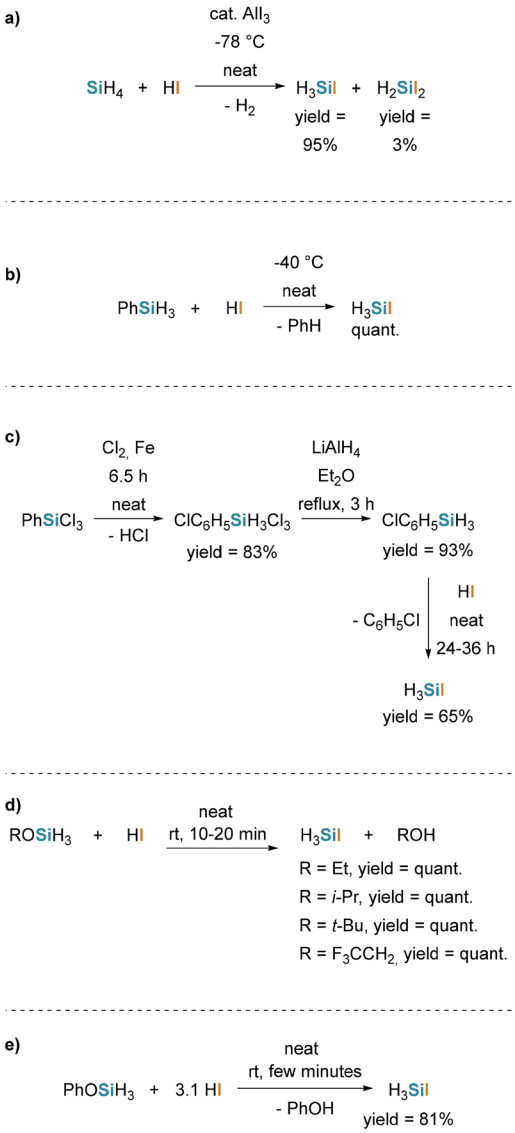

Scheme 217 Methods for the synthesis of $ISiH_3$ (path a–e).

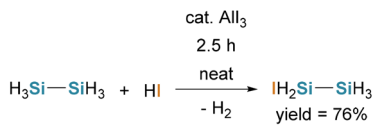

Scheme 218 Iodation of disilane with HI yielding in $IH_2Si–SiH_3$.

minium iodide, leading to the formation of iododisilane $IH_2Si–SiH_3$ (method i) (see Scheme 218).

Approximately a decade later Fehér *et al.* carried out intense studies to the synthesis of different iodooligohydrosilanes following an alternative approach applied to di-, tri- and tetrasilane, in which iodide serves as iodation reagent (see Scheme 219).[305,306] These reactions consistently produced mixtures of mono- and diiodinated silanes. Nevertheless, individual isomers of iodinated di-, tri-, and tetrasilanes could be separated and identified by gas chromatographic methods.

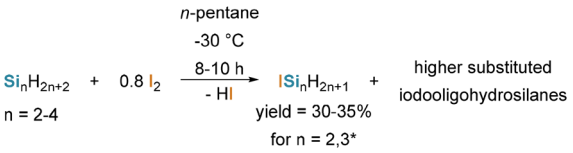

Scheme 219 Reaction of di-, tri- and *n*-tetrasilane with iodide. *Yield of the monoiodotetrasilane was not reported.

Nearly twenty years afterward, Hassler and co-workers reported significant progress in the synthesis of iodooligohydrosilanes. Analogous to strategies established for chloro- and bromohydrosilanes, their work demonstrated that electrophilic cleavage of silicon-aryl bonds with hydrogen iodine enables the selective introduction of iodine substituents (see Scheme 220). Using this approach, a broad range of iodohydrosilans was prepared in high efficiency.[294,307]

Cyclic halohydrosilanes

Nonahalocylcopentasilanes (HSi_5X_9) and octahalocyclo-pentasilanes ($1,3\text{-}H_2Si_5X_8$) (X = Cl, Br, I) can be prepared *via* dephenylation of the corresponding phenyl-substituted precursors HSi_5Ph_9 and H_2SiPh_8 (see Scheme 221).[35,308]

Partially chlorinated cyclopentasilanes were reported by Roewer and co-workers through the stepwise hydride reduction

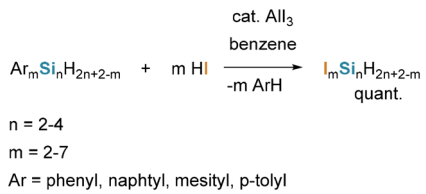

Scheme 220 Synthesis of iodooligosilanes *via* dearylation.

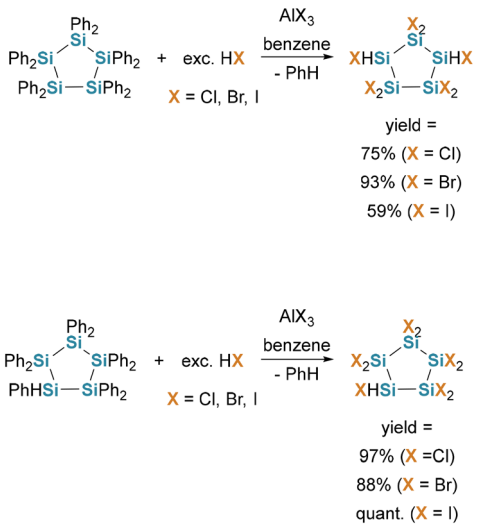

Scheme 221 Synthesis of cyclic halohydrosilanes.

Open Access Article. Published on 24 April 2026. Downloaded on 5/15/2026 8:48:04 PM.
This article is licensed under a Creative Commons Attribution 3.0 Unported Licence.

of decachlorocyclopentasilane using Me_3SnH (see Scheme 222). The reaction proceeds without detectable formation of SiHCl moieties. The major product observed was assigned to 1,1,3,3,-tetrachlorocyclopentasilane, while 1,1-dihydrooctachlorocyclopentasilane was not detected. Structural assignments were based on ^{29}Si NMR spectroscopic data; the intermediates were not isolated.[107]

Stueger *et al.* reported the partial hydrogenation of perchlorinated cyclopentasilane in 2012 in a three-step synthesis (see Scheme 223).[290] The final yield of the product (Si_5HCl_9) could not be determined since it could not be separated from cyclopentasilane which was formed as byproduct.

Mixed halohydrosilanes

The bromination of Si–H bonds using BBr_3 was employed to generate chlorobromohydrosilanes. Thus, $ClH_2Si–SiH_3$ and $Cl_2HSi–SiH_3$ were converted into $HBrClSi–SiH_3$ and $BrCl_2Si–SiH_3$, respectively (see Scheme 224). These products were detected by GC; however, no isolation was reported.[271]

Mixed halohydrosilanes of the general formula $Si_2X_mY_nH_{6-m-n}$ (X = F, Y = Br) are formed *via* co-condensation of SiF_2 with HBr. Upon warming the reaction mixture to room temperature, its composition changes, although the mixed halohydrosilanes $BrF_2Si–SiF_2H$, $F_3Si–SiFHBr$ and $F_3Si–SiHBr_2$ could be isolated but no yields were reported (see Scheme 225). The compounds $HBrFSi–SiF_2Br$ and $HBr_2Si–SiF_2Br$ were identified in the final reaction mixture by ^{19}F NMR spectroscopy, but were not isolated. Subsequent chlorination of $BrF_2Si–SiF_2H$ and $F_3Si–SiHBr_2$ with $SnCl_4$ afforded $F_3Si–SiHCl_2$ and $ClF_2Si–SiHF_2$. Yields of the isolated products have not been reported.[270,309]

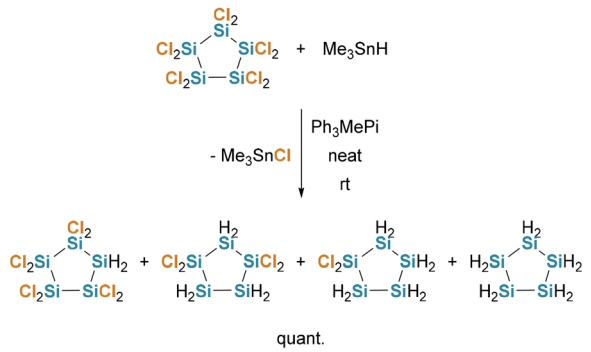

Scheme 222 Synthesis of cyclic chlorohydrosilanes.

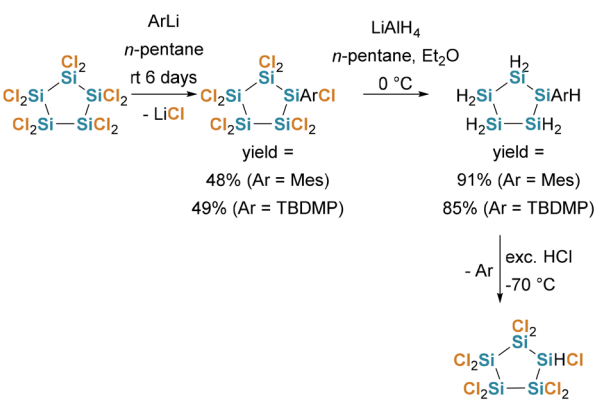

Scheme 223 Synthesis of nonachlorocyclopentasilane by Stueger *et al.* No yield of the final product reported.

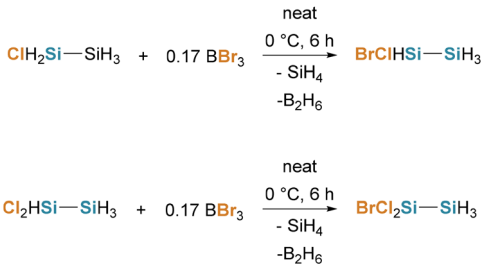

Scheme 224 Synthesis of mixed halodisilanes; no yields reported.

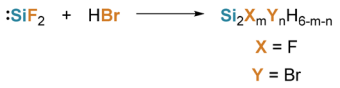

Scheme 225 Synthesis of mixed halodisilanes; no yields reported.

Key physical and chemical properties for the central hydrosilanes

In Table 8 the key physical and chemical properties for the central hydrosilanes are depicted.

Deposition methods

Silicon (Si) is the second most abundant element in the Earth's crust constituting approximately 28%.[310] As a semiconductor, silicon plays a crucial part in the electronics industry. Depending on deposition method and process conditions silicon thin films can exhibit monocrystalline, polycrystalline or amorphous structures, which significantly influence the electronic properties and application potential. Monocrystalline silicon (c-Si) possesses a long-range ordered crystal lattice and high charge carrier mobility, making it the preferred material for microelectronic devices. Polycrystalline silicon (poly-Si) consists of crystalline grains separated by grain boundaries, which reduce carrier mobility but allow deposition at lower temperatures, enabling its use in thin film transistors (TFTs) and photovoltaic devices. Amorphous silicon (a-Si) lacks long-range order and exhibits a high density of dangling bonds.[311–313] The structural motifs are summarized in Fig. 16.

Early on, a-Si attracted scientific interest as a semiconductor, however, it exhibited significant drawbacks with respect to electrical conductivity. At the beginning of the 1970s, new deposition methods were developed, that enabled

This journal is © the Partner Organisations 2026

Open Access Article. Published on 24 April 2026. Downloaded on 5/15/2026 8:48:04 PM.
This article is licensed under a Creative Commons Attribution 3.0 Unported Licence.

Table 8 Summary of key physical and chemical properties of central hydrosilanes

Silane	m.p. [°C]	b.p. [°C]	Physical/state	Solubility	Safety
SiH_4	−185	−112	Gas	Slightly in all organic and inorganic solvents	Pyrophoric
Si_2H_6	−133	−15	Gas	All organic and inorganic solvents	Pyrophoric
Si_3H_8	−115	53	Liquid	All organic and inorganic solvents	Pyrophoric
n-Si_4H_{10}	−89.9	108	Liquid	All organic and inorganic solvents	Pyrophoric
iso-Si_4H_{10}	−99.4	102	Liquid	All organic and inorganic solvents	Pyrophoric
n-Si_5H_{12}	−72.2	153	Liquid	All organic and inorganic solvents	Pyrophoric
neo-Si_5H_{12}	−57.8	134	Liquid	All organic and inorganic solvents	Pyrophoric
cyclo-Si_5H_{10}	−10.5	194	Liquid	All organic and inorganic solvents	Pyrophoric
n-Si_6H_{14}	−44.7	194	Liquid	All organic and inorganic solvents	Pyrophoric
cyclo-Si_6H_{12}	16.5	226	Liquid	All organic and inorganic solvents	Pyrophoric
n-Si_7H_{16}	−30.1	227	Liquid	All organic and inorganic solvents	Pyrophoric
Si_8H_{18}	28	*x*	Oil	All organic and inorganic solvents	Pyrophoric
$N(SiH_3)_3$	−106	52	Liquid	All organic and inorganic solvents	Pyrophoric
$N(SiH_2SiH_3)_3$	−97	176	Liquid	All organic and inorganic solvents	Pyrophoric
$Et_2NSiH_2SiH_2NEt_2$	*x*	23/0.05 Torr	Liquid	All organic and inorganic solvents	Pyrophoric
$SiH_3SiH(NEt_2)_2$	*x*	23/0.2 Torr	Liquid	All organic and inorganic solvents	Pyrophoric
$iPr_2NSiH_2SiH_2NiPr_2$	*x*	68/0.05 Torr	Liquid	All organic and inorganic solvents	Pyrophoric
H_3SiPH_2	<135	12.7	Gas	All organic and inorganic solvents	Pyrophori, toxic
$P(SiH_3)_3$	−73	114	Liquid	All organic and inorganic solvents	Pyrophori, toxic
$O(SiH_3)_2$	−144	−15.2	Gas	All organic and inorganic solvents	Not pyrophoric
$S(SiH_3)_2$	−70.0	58.8	Liquid	All organic and inorganic solvents	Pyrophori, toxic
$Se(SiH_3)_2$	−68.0	85.2	Liquid	All organic and inorganic solvents	Toxic
$Te(SiH_3)_2$	*x*	49/50 Torr	Liquid	All organic and inorganic solvents	Toxic

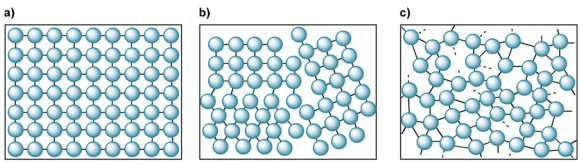

Fig. 16 Structural motifs of (a) monocrystalline silicon, (b) polycrystalline silicon and (c) amorphous silicon. Dangling bonds marked as dotted line.[314]

the preparation of amorphous silicon thin-films with improved electronic properties through the incorporating of hydrogen, resulting in hydrogenated amorphous silicon (a-Si:H).[315] As shown in Fig. 17, passivation of dangling bonds with hydrogen leads to a drastic reduction in defect density, thereby improving conductivity and carrier mobility. Furthermore, effective p- and n-type doping of a-Si:H can be achieved by incorporating appropriate dopant species, such as diborane or phosphine, during deposition, as dopant atoms are no longer compensated by dangling bond defects.[316]

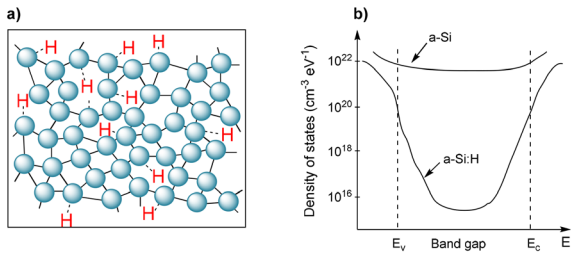

Fig. 17 (a) Schematic passivation of dangling bonds by hydrogen and (b) schematic illustration of density of states in a-Si and a-Si:H. Graphic adapted from Vora.[317]

Since then, several different deposition techniques have been employed to produce silicon thin films. These silicon thin films have a wide range of applications, including thin film transistors, flexible large area displays, and photovoltaics.[318,319]

Chemical vapor deposition

Chemical vapor deposition describes the deposition of a solid component on the surface of a substrate from the vapor phase by means of a chemical reaction. The term was first introduced by J. M. Blocher in 1960 to distinguish the process from other deposition methods, that do not involve chemical reactions such as sputtering.[320] During the CVD process, gaseous reactant species are supplied and transported into a reaction chamber, as schematically illustrated in Fig. 18. Upon entering the reactor, the reactant gases are conveyed toward the sub-

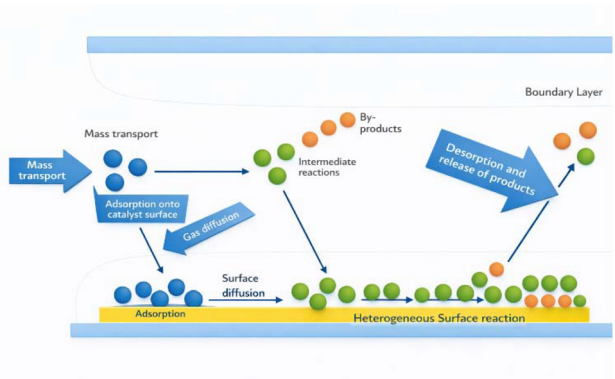

Fig. 18 Schematic illustration of the CVD process. Graphic adapted from Sun *et al.*[323] and Katsui *et al.*[322]

Open Access Article. Published on 24 April 2026. Downloaded on 5/15/2026 8:48:04 PM.
This article is licensed under a Creative Commons Attribution 3.0 Unported Licence.

strate by mass transport and may either diffuse directly through the boundary layer to adsorb onto the heated substrate surface or participate in gas-phase reactions, forming intermediate species and gaseous byproducts. These intermediates can subsequently reach the substrate by diffusion and adsorption. On the substrate surface, adsorbed species undergo surface diffusion and heterogeneous chemical reactions, ultimately leading to thin-film growth. Any unreacted gaseous precursors or byproducts are subsequently desorbed from the surface and removed from the chamber in the gas phase.[312,320–323]

A variety of CVD processes and techniques exist, including thermal CVD (TCVD), plasma-enhanced CVD (PECVD), photo-assisted CVD (PACVD), and hot-wire CVD (HWCVD). Depending on the deposition conditions such as temperature, pressure, and plasma environment, CVD can yield silicon films with different microstructures, including amorphous, microcrystalline, polycrystalline, or epitaxial silicon. The various CVD techniques therefore differ not only in deposition rate and defect concentration but also in the structural properties of the resulting films. A special form of CVD is atomic layer epitaxy (ALE), which enables the growth of monoatomic layers on a substrate surface. In the following section, these different methods are described in more detail.[315]

Thermal chemical vapor deposition

The most common sub-technique of CVD is the thermal CVD. In this process, thermal energy is used to activate the chemical reactions. The required energy can be supplied by several different methods, such as radio-frequency heating, thermal radiation or resistance heating. A typical reactor configuration for TCVD, including gas delivery, substrate heating, and exhaust, is schematically illustrated in Fig. 19.

The industrial implementation of silicon chemical vapor deposition emerged in the early 1960s at Bell Telephone Laboratories, where Theuerer demonstrated controlled epitaxial growth of single-crystalline silicon *via* hydrogen reduction of $SiCl_4$.[325] This chlorosilane-based approach enabled precise control over film thickness, doping, and conductivity type, establishing CVD as a technologically viable route for device-grade epitaxial layers. However, these processes required elevated substrate temperatures typically exceeding 1100 °C and involved kinetically demanding Si–Cl bond cleavage with concomitant HCl elimination. These limitations motivated the exploration of hydrosilanes as thermodynamically more labile alternatives for thermal silicon deposition. Lewis and co-workers demonstrated that monosilane undergoes efficient thermal decomposition to silicon and hydrogen, enabling high-purity silicon deposition at temperatures substantially lower than those required for chlorosilane reduction.[326] Subsequent kinetic studies by Joyce and Bradley revealed two distinct growth regimes during silane-based epitaxy: a transport-limited regime above ~1100 °C and a reaction-controlled regime at lower temperatures. Together, these studies established silane as a kinetically tuneable and technologically viable precursor for thermal silicon CVD. Further experimental and kinetic studies have demonstrated that the initial step of silane pyrolysis is most likely the formation of highly reactive silylene species ($:SiH_2$), accompanied by the release of molecular hydrogen as illustrated in Scheme 226. These intermediates readily insert into Si–H bonds of silanes, leading to the formation of higher polysilanes and initiating silicon hydride cluster growth. Subsequent dehydrogenation and rearrangement reactions generate unsaturated intermediates, including silenes and additional silylenes, which further propagate the reaction network. With increasing cluster size, intramolecular reactions can promote ring formation, yielding cyclic silicon hydrides that represent important intermediates in the early stages of silicon cluster and particle formation during silane pyrolysis. Depending on the reaction conditions, particularly temperature, pressure, and residence time, these species either contribute to heterogeneous film growth on heated surfaces or undergo homogeneous reactions leading to particle and powder formation in the gas phase. While the general mechanistic framework of silane pyrolysis is well established, the detailed reaction network remains highly complex and

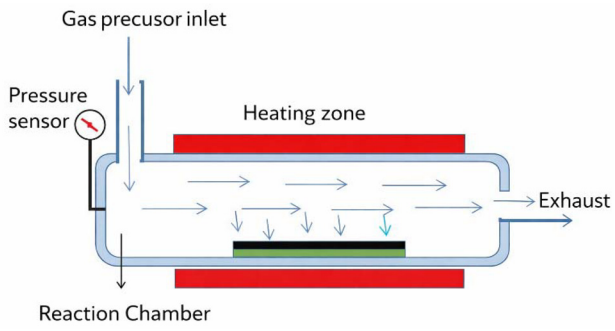

Fig. 19 Scheme of a typical reactor configuration for TCVD. Graphic adapted from Nnadozie *et al.*[324]

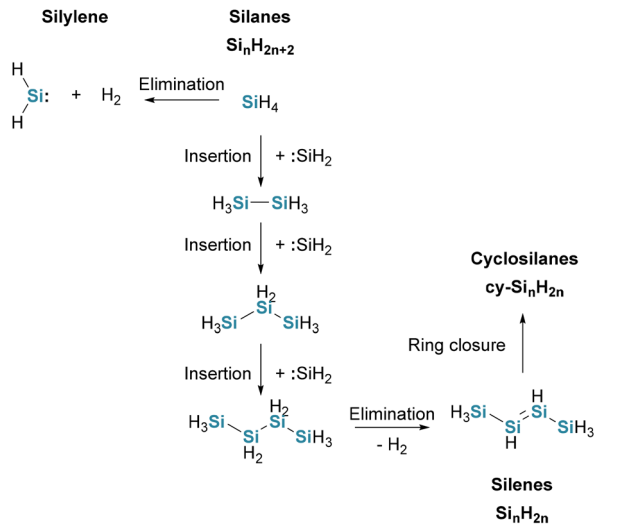

Scheme 226 Simplified mechanism of silane pyrolysis illustrating the formation of higher silanes and cyclic silicon hydrides.[327,328]

This journal is © the Partner Organisations 2026

Open Access Article. Published on 24 April 2026. Downloaded on 5/15/2026 8:48:04 PM.
This article is licensed under a Creative Commons Attribution 3.0 Unported Licence.

continues to be investigated through experimental and theoretical studies.[327–329]

Based on the operating pressure, TCVD can be further subdivided into atmospheric pressure CVD (APCVD), low-pressure CVD (LPCVD) and ultrahigh vacuum CVD (UHVCVD). In 1997, Sturm *et al.* demonstrated low-temperature LPCVD growth of β-SiC on Si using methylsilane as a single-source precursor, yielding polycrystalline, device-compatible SiC films.[330] Two years later, Madaura *et al.* reported for the first time the APCVD of SiC films on a Si substrate using trimethylsilane as a single source precursor. Although trimethylsilane contains only a single Si–H bond and therefore falls outside the scope of classical hydrosilanes discussed in this review, this study is noteworthy as an early example of silicon deposition chemistry employing molecular silane precursors. The SEM microphotographs of the SiC/Si interface are shown in Fig. 20.[331]

Hazbun *et al.* investigated the use of tetrasilane (Si_4H_{10}) as a precursor for ultra-high-vacuum CVD of silicon epitaxial layers. They demonstrated that tetrasilane enables significantly higher growth rates than monosilane and allows crystalline silicon deposition at temperatures as low as 400 °C, making it suitable for low-temperature epitaxy.[332] Furthermore, Byeon *et al.* investigated the epitaxial growth of Si and SiGe using high-order silanes such as disilane, trisilane, and tetrasilane under UHVCVD and LPCVD conditions without a carrier gas. They showed that higher-order silanes enable silicon epitaxy at reduced temperatures, with trisilane and tetrasilane providing significantly higher growth rates, while disilane yielded the highest crystal quality of the deposited films.[333] Halogenated hydrosilanes were likewise employed as silicon precursors for both oxide and carbide thin films. In high-temperature thermal CVD, silicon tetrachloride in combination with propane enabled the growth of epitaxial SiC layers, where chlorine-containing species suppress gas-phase nucleation and improve stoichiometric control of Si : C ratios.[334] In a related context, Sneh *et al.* reported atomic-layer controlled growth of SiO_2 using a binary reaction sequence with $SiCl_4$ and H_2O.[335] Nitrogen-functionalized hydrosilanes subsequently emerged as important precursors for the deposition of silicon nitride (Si_3N_4) thin films. Gumpher *et al.* demonstrated LPCVD of Si_3N_4 from di(*t*-butylamino)silane (BTBAS) and NH_3 at 550–600 °C, producing high-quality nitride films suitable for microelectronic applications.[336] The incorporation of preformed Si–N bonds in these precursors enhances surface reactivity while avoiding corrosive halide byproducts, thereby improving film purity and conformality in advanced deposition schemes.[337]

Silylphosphanes and related phosphinosilanes were explored primarily in patent literature as single-source Si–P precursors for *in situ* phosphorus doping during silicon CVD. Although conceptually attractive as potential alternatives to PH_3, limited thermal robustness and the maturity of established PH_3-based processes curtailed their broader implementation.[338] Silylgermanes containing preformed Si–Ge bonds were systematically developed as molecular single-source precursors for SiGe thin-film growth. Kouvetakis and co-workers first established the complete hydride series $(H_3Ge)_xSiH_{4-x}$ (x = 1–4), including silylgermane H_3GeSiH_3 and tetrasilylgermane $Ge(SiH_3)_4$, and demonstrated their application in low-pressure deposition of epitaxial $Si_{1-x}Ge_x$ layers at 300–450 °C. Thermal activation proceeds *via* Si–H and Ge–H bond cleavage with H_2 elimination while preserving the intrinsic Si : Ge stoichiometry encoded in the precursor, enabling compositionally controlled alloy growth without separate silane and germane feeds. This molecular design strategy facilitates the preparation of a new class of Si-based semiconductors with Ge-rich stoichiometry. Fig. 21 shows a X-ray transmission electron microscopy (XTEM) image of a $SiGe_2$ layer on a Si substrate.[127]

More recently, Wagner and co-workers introduced mixed-substituted Si–Ge hydrides such as $H_3SiR_2GeSiH_3$ (R = Ph, *n*-Bu), synthesized *via* Si_2Cl_6-mediated coupling and subsequent hydride formation, and demonstrated their conversion by low-pressure CVD into predominantly amorphous $Si_{1-x}Ge_x$ coatings with predefined Si : Ge ratios and reduced pyrophoricity compared to purely hydridic systems.[128]

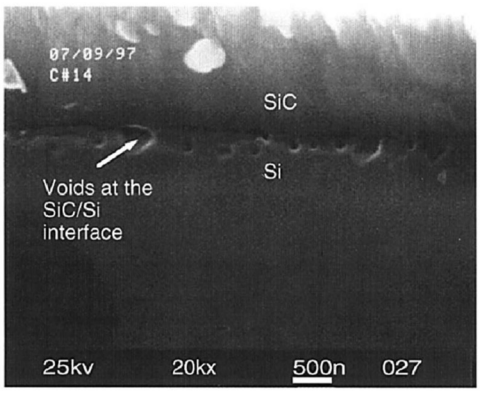

Fig. 20 Microphotographs of the SiC/Si interface as seen by cross-sectional SEM adapted from Madapura *et al.*[331] With permission from ECS – The Electrochemical Society, © 1999.

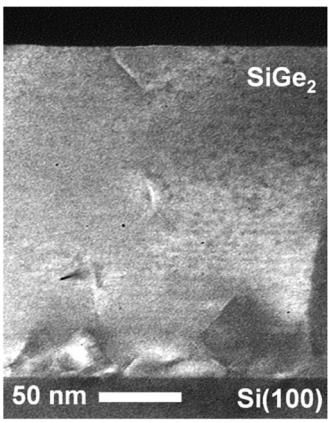

Fig. 21 XTEM micrograph of a $SiGe_2$ layer grown on Si(100) adapted from Kouvetaksi *et al.*[127] With permission from American Chemical Society, © 2005.

Open Access Article. Published on 24 April 2026. Downloaded on 5/15/2026 8:48:04 PM.
This article is licensed under a Creative Commons Attribution 3.0 Unported Licence.

While thermal processes are widely used in industry, primarily due to the technical ease of implementation, they also exhibit clear disadvantages. In particular, temperature-sensitive substrates may be damaged by the high process temperature. For this reason, alternative energy sources have been developed over the decades of research.[321,339,340]

Plasma-enhanced chemical vapor deposition

PECVD, also known as glow-discharge chemical vapor deposition is a variation of CVD in which electrical energy is used to activate the chemical reaction. By applying a high frequency voltage between two electrodes at reduced pressure a glow discharge is developed in which a non-thermal plasma consisting of electrons, ions and electronically excited species is formed. Through electron impact within the plasma, the precursor gases are ionized and dissociated, thereby generating chemically active ions and radicals. As a result, the electron temperature can reach values of 2000 K or higher, while the gas temperature, depending on process conditions, remains near room temperature. The activated species can take part in heterogeneous reactions on or near the substrate surface, leading to the deposition of a thin film. Since the reactive species are predominantly formed in the gas phase, only minimal thermal activation is required. This enables PECVD processes to be carried out at significantly lower temperatures than TCVD, in many cases at temperatures below 200 °C. Consequently, depositions on temperature-sensitive substrates such as glass and polymeric materials becomes possible.[321,339,341] The plasma-induced dissociation pathway of silane are summarized in the following Fig. 22.

In 1965, Sterling and Swann[342] were the first to report the deposition of an amorphous silicon layer from gaseous SiH_4 using plasma-assisted CVD. In the early 1970s, a research group at Havard University demonstrated the incorporation of hydrogen into a-Si leading to the development of hydrogenated amorphous silicon (a-Si:H) with a significantly reduced defect density and improved electronical properties.[343] Building on these findings, Spear and LeComber[344] first demonstrated the controlled n- and p-doping of a-Si:H by adding phosphine and diborane to SiH_4 in a reactor with a plasma at radio frequency voltages. This enabled precise control of the electrical conductivity over several orders of magnitude and paved the way for the realization of a-SiH-based devices, in particular thin-film solar cells and TFTs.[345] As a result of these advances, PECVD became the standard procedure for the deposition of silicon thin films in the 1980s. In 1983, Matsuda *et al.* deposited amorphous a-SiC:H films from SiH_4/CH_4 mixtures at substrate temperatures of 300–400 °C, producing films suitable for microelectronic and optical applications.[346] Pokhodnya *et al.* studied the intrinsic stress in a-Si:H films using cyclohexasilane (CHS) as a precursor.[347] Lee *et al.* reported the deposition of trisilylamine using PECVD forming highly conformal SiCN films. In Fig. 23 a transmission electron microscopy (TEM) cross-sectional view of the substrate with the deposited layer is shown.[348]

In the following decades, research efforts focused on optimizing the PECVD process with respect to material quality, increased deposition rates and long-term stability. New approaches such as very-high-frequency PECVD (VHF-PECVD),[349] microwave-assisted CVD (MW-CVD)[350] and "high power high pressure" regime RF-PECVD[351] were developed. Today RF-PECVD at a excitation frequency of 13.56 MHz remains the dominating deposition technique, notwithstanding its relatively low deposition rate of 1–2 Å s^{-1}.[352]

The following Fig. 24 shows a schematic illustration of a PECVD reactor.

Photo-assisted chemical vapor deposition

Photo-assisted chemical vapor deposition (PACVD), also known as photo-initiated CVD, is a variant of CVD in which photon energy, typically in the ultraviolet (UV) or vacuum-ultraviolet (VUV) range, is used to activate chemical reactions. Reaction initiation occurs *via* photolytic dissociation of the precursor molecules, leading to the formation of reactive radicals and electronically excited species, which subsequently participate in heterogeneous surface reactions resulting in thin film growth.[220,354] In 1983, Migitaka *et al.* and Takahashi *et al.* reported the preparation of a-Si:H films from monosilane[355] and disilane.[356] A schematic illustration of a PACVD reactor can be found in the article of Dorval Dion *et al.*[354]

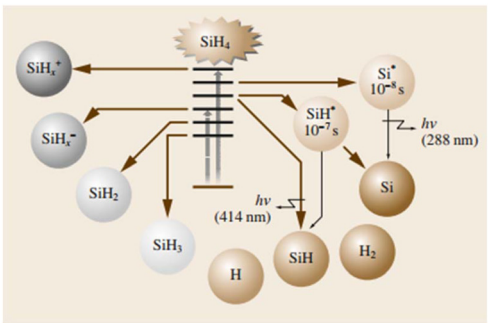

Fig. 22 Schematic dissociation pathway of SiH_4 and H_2 in the plasma adapted from Kasap *et al.*[313] With permission from Springer-Verlag US, © 2007.

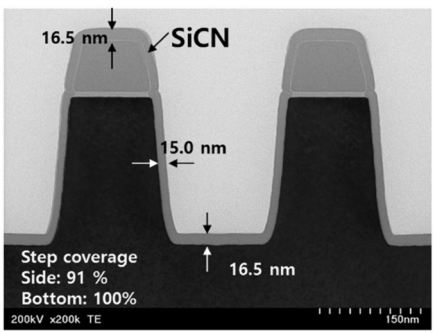

Fig. 23 TEM cross-sectional view of the substrate with the deposited SiCN layer adapted from Lee *et al.*[348] With permission from Elsevier B.V., © 2018.

Open Access Article. Published on 24 April 2026. Downloaded on 5/15/2026 8:48:04 PM.
This article is licensed under a Creative Commons Attribution 3.0 Unported Licence.

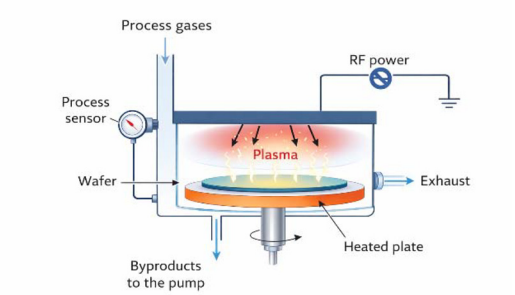

Fig. 24 Schematic illustration of a plasma-enhanced chemical vapor deposition (PECVD) reactor. Graphic adapted from Verma *et al.*[353] and altered with the help of AI. With permission from Springer Nature Singapore Pte Ltd., © 2023.

A key advantage of PACVD is the absence of plasma, which eliminates ion-induced damage to both the substrate and the growing film. Furthermore, in contrast to TCVD, which relies on pyrolytic mechanisms and requires high substrate temperatures, PACVD enables deposition at significantly lower temperatures, in some cases at room temperature. As a result, the choice of substrate material is not restricted by thermal stability. PACVD also has limitations, including the requirement that precursor molecules exhibit sufficient absorption within the emission spectrum of the light source, as well as relatively low deposition rates.[339,354]

PACVD is often discussed together with laser-assisted CVD (LACVD), also known as laser chemical CVD, and the two processes are not always strictly distinguished terminologically in literature, as both rely on photonic activation. The crucial difference, however, lies in the method of energy input. In contrast to PACVD, LACVD uses coherent, high-intensity laser radiation. LACVD can generate very high local energy densities and induce both photolytic and locally pyrolytic processes, for example, through targeted heating of the substrate surface. Laser-CVD is therefore particularly suitable for locally confined deposition or structuring processes.[220,339,357] A typical schematic of the LACVD process is shown in Fig. 25.

Hot-wire chemical vapor deposition

Hot-wire chemical vapor deposition (HWCVD), also known as catalytic CVD (Cat-CVD), is a plasma-free CVD process in which the decomposition of precursor gases occurs on a highly heated metal filament. Tungsten or tantalum are typically used as the filament material, which can be heated to temperatures of approximately 1400 to 2100 °C. At the surface of the hot wire, gaseous silane can be efficiently dissociated, with an almost complete separation into its atomic components. The reactive species generated subsequently undergo further reactions with SiH_4 in the gas phase, forming various secondary precursors that diffuse to the substrate surface and contribute to thin-film deposition.[359,360] The following Fig. 26 gives a schematic view of a HWCVD reactor.

A characteristic feature of HWCVD is the spatial separation of precursor decomposition and layer growth. Since the generation of reactive species occurs exclusively on the filament, the process is often referred to as a remote decomposition method. The temperatures of the filament and substrate can be adjusted independently, enabling deposition at comparatively low substrate temperatures while simultaneously achieving high deposition rates.

The basic principle of HWCVD was first published and patented in 1979 by Wiesmann *et al.* under the name thermal vapor deposition.[361] In the mid-1980s, Matsumura *et al.* first demonstrated the deposition of amorphous silicon using this method and introduced the term catalytic CVD.[362] Independently, Doyle *et al.* described a comparable concept under the name evaporative surface decomposition (ESD).[363]

A significant milestone was achieved in 1991 with the work of Mahan *et al.*, who demonstrated that amorphous silicon layers deposited using HWCVD can exhibit higher material quality than comparable films produced by PECVD.[364] The high quality of the deposited layers is attributed to the efficient decomposition of the precursor gases at filament temperatures above approximately 1500 °C. Typical deposition rates for amorphous silicon range from 10 to 50 Å s^{-1}, significantly exceeding those of conventional RF-PECVD processes.

Due to the absence of a plasma, ion-induced structural damage to the growing layer, that can be caused by ion bombardment or high-energy radiation, is largely avoided. The

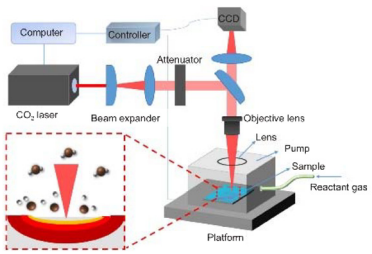

Fig. 25 Schematic illustration of a LACVD reactor. With permission from the Institute of Optics and Electronics, Chinese Academy of Science[358] © 2022.

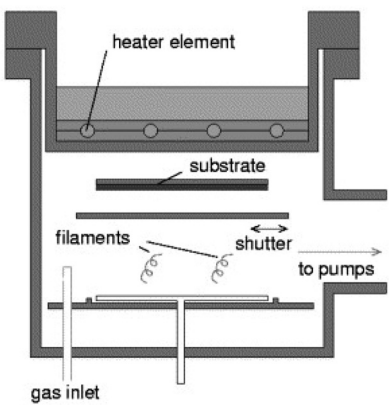

Fig. 26 Illustration of a schematic HWCVD reactor adapted from Schropp.[360] With permission from ECS – The Electrochemical Society, © 2009.

Open Access Article. Published on 24 April 2026. Downloaded on 5/15/2026 8:48:04 PM.
This article is licensed under a Creative Commons Attribution 3.0 Unported Licence.

term Cat-CVD refers to the catalytic effect of the hot wire in the dissociation of the precursor gases, although the filament is not an ideal catalyst in the strict chemical sense, as it undergoes aging and erosion during the process.[365] In the literature, the term HWCVD is predominantly used in physical and photovoltaic contexts, while Cat-CVD is particularly common in chemical research and Japanese literature. Current research is investigating, among other things, the application of HWCVD for the production of TFTs and thin-film solar cells.[360]

Atomic layer deposition

Atomic layer deposition is a thin film deposition technique, that can be classified as a special modification of CVD. In the literature, it is also referred to as atomic layer epitaxy or Atomic Layer Chemical Vapor Deposition (ALCVD). A key characteristic of ALD is the deposition of inorganic thin films with thicknesses down to a range of single monolayers, which is enabled by sequential, self-limiting surface reactions. As a result, highly homogeneous and conformal layers with excellent thickness control can be deposited.[131,366]

In ALD, gaseous precursors are introduced into the reactor in a strictly sequential manner. Each precursor reacts exclusively with the available reactive sites on the substrate surface until a saturated adsorption level is reached. The reactor is purged with inert gas between the individual precursor pulses to remove excess precursor molecules and volatile byproducts. This procedure effectively suppresses gas-phase reactions, such that the film growth is governed almost entirely by surface reactions.[133,367] The scheme of a sequential ALD cycle is shown in Fig. 27. Hirose *et al.* demonstrated the use of monosilane for room temperature ALD.[368] Matsunami *et al.* established epitaxial growth of β-SiC (3C-SiC) on Si substrates by reacting SiH_4 with hydrocarbons such as propane at temperatures above 1000 °C, enabling crystalline SiC layers for electronic applications and demonstrating *in situ* doping with nitrogen donors and aluminium or boron acceptors.[369] Halogenated hydrosilanes were also employed for SiC epitaxy:

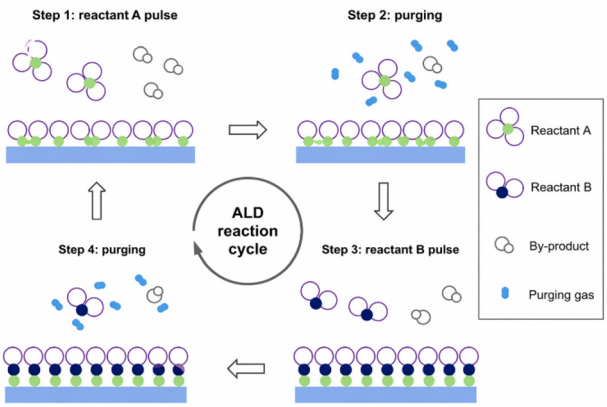

Fig. 27 Scheme of a sequential ALD cycle adapted from George.[131] With permission from American Chemical Society, © 2009.

Pedersen *et al.* employed methyltrichlorosilane in a hot-wall CVD reactor to obtain high-quality 4H-SiC layers.[370] Additional chlorinated silanes, including trichlorosilane, dichlorosilane, and hexachlorodisilane (Si_2Cl_6), have likewise been utilized for high-quality SiC epitaxial growth.[371]

Nitrogen-functionalized hydrosilanes became important precursors for the deposition of silicon dioxide (SiO_2) thin films. Bis(dimethylamino)silane (BDMAS) was introduced for atomic layer deposition of SiO_2 with H_2O[337] or O_3 [372] as oxidants, where ligand-exchange reactions with surface OH groups followed by ozone or oxygen plasma oxidation yield SiO_2.[372] Furthermore Faraz *et al.* reported the deposition of silicon nitride layer through plasma-enhanced atomic layer deposition of di(*sec*-butylamino)silane (DSBAS) on planar and on high aspect ratio 3D trench nanostructures. Fig. 28 shows a TEM image of the layer as-deposited and post wet-etch with dilute hydrofluoric acid.[373]

In contrast to hydrosilanes, oxygen-functionalized silicon precursors such as tetraethyl orthosilicate (TEOS, $Si(OEt)_4$) are widely used for the deposition of SiO_2 thin films in LPCVD, PECVD, and sub-atmospheric CVD processes.[374]

Liquid phase deposition

A viable alternative to established vapour-based deposition techniques is solution-based processing of silicon, commonly referred to as liquid phase deposition. In contrast to CVD methods, which require pyrophoric precursor gases, elaborate vacuum or plasma infrastructure, and often elevated deposition temperatures, LPD can generally be carried out at lower temperatures and under atmospheric pressure. This reduces equipment complexity as well as operating costs. Furthermore, LPD is compatible with flexible, large-area, and temperature-sensitive substrates and can enable higher throughput, particularly when combined with coating or printing techniques. Such approaches also facilitate direct patterning of materials and may reduce the number of required processing steps. Consequently, LPD is considered a promising route for applications in printable electronics, including large-area flexible displays, thin-film solar cells, TFTs and silicon-based anode

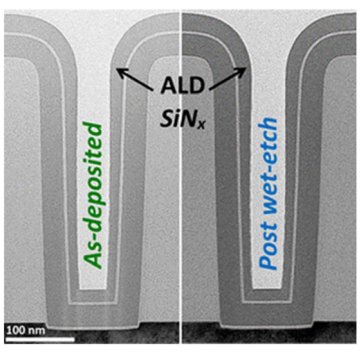

Fig. 28 TEM image of the silicon nitride layer as-deposited (left) and post wet-etch with dilute hydrofluoric acid (right) adapted from Faraz *et al.*[373] With permission from American Chemical Society, © 2017.

This journal is © the Partner Organisations 2026

Open Access Article. Published on 24 April 2026. Downloaded on 5/15/2026 8:48:04 PM.
This article is licensed under a Creative Commons Attribution 3.0 Unported Licence.

materials in lithium-ion batteries. The following section discusses the underlying chemical mechanisms of hydrosilane-based LPD and summarizes the key contributions in this field.[19,375,376]

The conceptual foundations of hydrosilane-based liquid processing date back to the late 1980s. West and Wolff[377] as well as Miller and Michl[378] demonstrated that organopolysilanes can be deposited as thin films and subsequently converted into silicon-rich amorphous networks by thermal or photochemical treatment, thereby establishing the processing and photochemistry toolkit for later hydrosilanes routes. However, true hydrosilanes themselves were only mentioned in passing in these studies, and a dedicated liquid-phase deposition strategy based explicitly on hydrosilane precursors had not been established. A decisive step toward practical implementation was achieved by Shimoda *et al.* in 2006,[19] who established *cy*-Si_5H_{10} as a molecular precursor for solution-processed silicon films. *Cy*-Si_5H_{10} was selected due to its favourable properties: it exhibits comparatively high stability and good availability making it suitable for handling and processing under inert conditions, and also exhibiting a high photoreactivity upon irradiation with ultraviolet light. In Shimodas LPD approach *cy*-Si_5H_{10} is first irradiated with UV light with a wavelength of 365 nm leading to a ring-opening polymerization and the formation of polydihydrosilane. The resulting polyhydrosilane can be dissolved in organic solvents to yield a processable liquid silicon material, often referred to as "silicon ink". The silicon ink is deposited by spin-coating on a substrate forming a uniform precursor. Subsequently thermal treatment induces the conversion of the polysilane network into a a-Si film. During initial heating, volatile components such as the solvent and *cy*-Si_5H_{10} evaporate. At a temperature below approximately 280 °C cleavage of Si–Si bonds begins, leading to a release of SiH_2 and SiH_3 species. Above a temperature of around 300 °C the Si–H bonds break resulting in the formation of the amorphous silicon film.[19,376,379–381] Fig. 29 illustrates the colour changes associated with variations in the chemical composition of the thin film at different annealing temperatures.

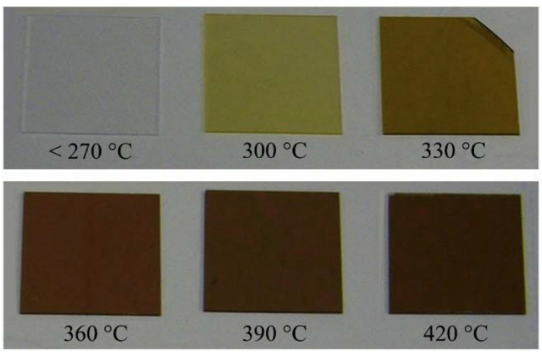

Fig. 29 Photographic image of the solution-processed polysilane films coated on quartz glass adapted from Trifunovic *et al.*[381] With permission from American Institute of Physics, © 2015.

The material can subsequently be further processed by additional thermal treatment or laser annealing to obtain polycrystalline silicon. Fig. 30 depicts a scheme for the solution-based formation of amorphous and polycrystalline silicon films.

In comparison to a-Si thin films formed through PECVD, the LPD produced films show a significantly lower mobility which is connected to a low concentration of hydrogen atoms. Films processed at temperatures below 300 °C exhibit charge carrier mobilities comparable to those obtained by PECVD. However, under these conditions the material can no longer be unambiguously classified as amorphous silicon and shows increased susceptibility to oxidation. Shimoda *et al.* therefore emphasizes the necessity of balancing low processing temperatures with sufficient structural stabilization and oxidation resistance in order to achieve device-relevant film quality.[380]

Beyond the preparation of intrinsic silicon inks, Shimoda and co-workers also developed n-type and p-type silicon inks by incorporating suitable dopant precursors, such as white phosphorus and decaborane, into the *cy*-Si_5H_{10}-derived system prior to film deposition. During subsequent thermal conversion, the dopant species are incorporated into the forming silicon network. These developments were later summarized under the term "liquid silicon family materials" (LSFMs), describing a materials platform in which *cy*-Si_5H_{10} acts as a common precursor for different silicon-based functional layers. In this concept, intrinsic, n-type, and p-type silicon films as well as device structures such as TFTs and solar cells can be fabricated using entirely liquid-based processing routes.

Subsequent studies expanded the precursor chemistry, the available activation strategies as well as the deposition

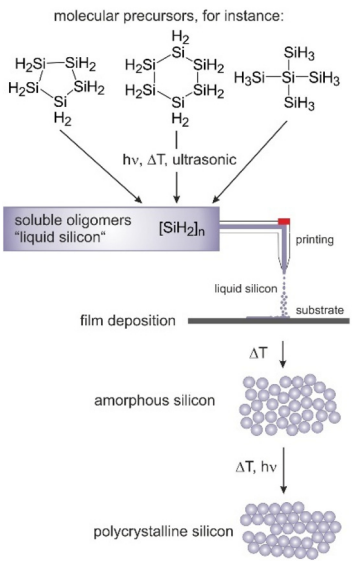

Fig. 30 Scheme for the solution-based formation of amorphous and polycrystalline silicon films adapted from Gerwig *et al.*[5] With permission from Chemistry – A European Journal published by Wiley-VCH GmbH, © 2024.

Open Access Article. Published on 24 April 2026. Downloaded on 5/15/2026 8:48:04 PM. This article is licensed under a Creative Commons Attribution 3.0 Unported Licence.

methods for hydrosilane-based LPD. Following Shimoda's initial work, *cy*-Si_5H_{10} remained the dominant hydrosilane precursor, and numerous studies focused on refining its processing and activation. In contrast to the spin-coated polysilane ink approach described by Shimoda, Frey *et al.* employed an aerosol-assisted spray deposition technique using neat *cy*-Si_5H_{10} as precursor. The *cy*-Si_5H_{10} was atomized and deposited onto heated substrates under inert atmosphere, while ultraviolet irradiation was applied within the deposition chamber to promote precursor activation. Film formation proceeded primarily *via* thermally assisted decomposition of the liquid precursor during and after deposition, followed by high-temperature annealing (700–950 °C) to obtain polycrystalline silicon.[382] Trifunovic *et al.* employed doctor-blade coating of *cy*-Si_5H_{10}, followed by ultraviolet curing at 365 nm and subsequent excimer laser at crystallization at 308 nm to obtain poly-Si at a maximum process temperature of 150 °C. In this approach, the solution-deposited precursor was directly transformed into crystalline silicon without requiring intermediate high-temperature annealing above 350 °C or a separate amorphous silicon conversion step. Therefore, this process is suitable for deposition on temperature-sensitive substrates like paper or polymer and facilitating low-cost electronics. Fig. 31 shows a poly Si film fabricated on paper.[381]

In parallel, alternative activation methods for *cy*-Si_5H_{10} were investigated. Cádiz Bedini *et al.* reported on ring-opening polymerisation induced by ultrasonic irradiation at a frequency of 26 kHz. The temperature was maintained below 75 °C, and it was confirmed, that no thermal activation of the precursor occurred under these conditions.

Masuda *et al.* demonstrated that *cy*-Si_5H_{10}-derived liquid silicon can be employed for solution-based silicon patterning using both inkjet printing and nanoimprinting strategies. In both approaches, *cy*-Si_5H_{10} was first photochemically polymerised at 365 nm to yield a processable polysilane precursor. In the inkjet printing approach, the polysilane solution was deposited in a digitally defined, maskless manner onto the substrate. Subsequent thermal conversion at approximately 380–400 °C yielded hydrogenated amorphous silicon, while additional annealing at 1000 °C enabled crystallisation to polycrystalline silicon. The method further allowed the incorporation of p- and n-type dopants directly into the printed structures. Fig. 32 shows a printed silicon pattern on a glass substrate.[383]

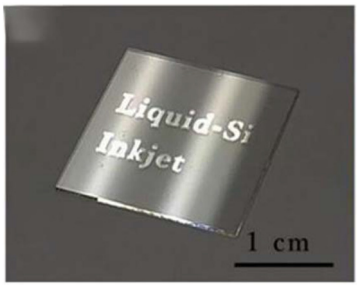

Fig. 32 Inkjet printed silicon pattern on a glass substrate adapted from Masuda *et al.*[383] With permission from Wiley-VCH GmbH, © 2020.

In contrast, the nanoimprinting approach consisted of spin-coating the *cy*-Si_5H_{10}-derived Liq-Si precursor onto the substrate. The deposited film was subsequently pre-cured at 140–220 °C, which initiated partial crosslinking of the polysilane network. Successful pattern replication was achieved only within this temperature window under an applied pressure of 10 MPa. At lower temperatures, insufficient crosslinking prevented stable feature transfer, whereas at higher temperatures the film lost its deformability. Crosslinking proceeds *via* thermally activated 1,2-hydrogen shift reactions, accompanied by the release of SiH_4 and H_2, leading to progressive solidification of the film. After imprinting and controlled cooling, post-annealing at approximately 380 °C completed the conversion to amorphous silicon. Despite significant volumetric shrinkage during polymer-to-silicon transformation, nanoscale patterns were retained. Fig. 33 shows a nanoimprinted pattern of a-Si.[384]

These studies demonstrate that *cy*-Si_5H_{10}-derived polysilanes are suitable precursors for lithography-free micro- and nanostructured silicon fabrication.

Gerwig *et al.* investigated the oligomerisation of *cy*-Si_5H_{10} using electron spin resonance (ESR), NMR, and Raman spectroscopy supported by DFT and molecular dynamics simulations. Their results showed that *cy*-Si_5H_{10} does not undergo a classical ring-opening polymerisation. Instead, short-lived silyl radicals are formed, which recombine to generate highly branched hydrooligosilanes. Silylene intermediates were found not to play a significant role. Competing decomposition and

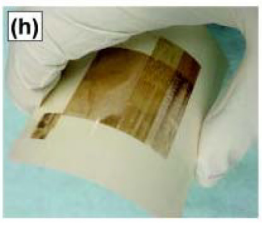

Fig. 31 Poly Si film fabricated on paper adapted from Trifunovic *et al.*[381] With permission from American Institute of Physics, © 2015.

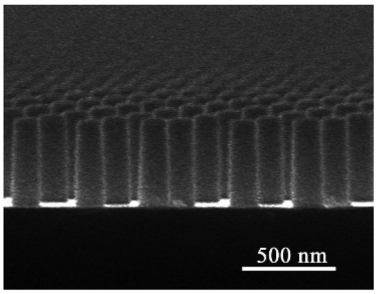

Fig. 33 Nanoimprinted pattern of a-Si adapted from Masuda *et al.*[384] With permission from American Chemical Society, © 2016.

This journal is © the Partner Organisations 2026

Open Access Article. Published on 24 April 2026. Downloaded on 5/15/2026 8:48:04 PM.
This article is licensed under a Creative Commons Attribution 3.0 Unported Licence.

disproportionation reactions produce volatile fragments, reducing hydrogen content and overall yield. ESR measurements confirmed the presence of tertiary silyl radicals as reactive intermediates.[5]

The influence of solvent and processing parameters on film formation was further examined. Optimised spin-coating and UV irradiation conditions yielded homogeneous silicon films, which were subsequently passivated by hydrogen plasma. The resulting thin films and TFT devices exhibited performance comparable to PECVD-processed materials.

Shen *et al.* introduced a liquid-source vapor deposition (LVD), where *cy*-Si_5H_{10} thermally decomposes between two parallel hot substrates at atmospheric pressure. In this configuration, a fraction of the precursor is directly converted into amorphous silicon on the substrate surface, while volatile silicon hydride radicals are simultaneously generated. These reactive intermediates diffuse within the confined deposition space and act as secondary growth species, thereby sustaining further film formation. This allows for the formation of denser amorphous silicon layers with reduced oxygen incorporation compared to conventional spin-coated films. The schematic set-up for LVD is shown in Fig. 34.[385]

However, the demanding synthesis and purification of *cy*-Si_5H_{10} highlight the need to consider alternative precursors such as cyclohexasilane (CHS) and NPS.[5,376] Iyer *et al.* investigated CHS as an alternative cyclic hydrosilane precursor. The CHS solution was spin-coated onto the substrate under simultaneous UV irradiation to induce ring-opening polymerisation and network formation. Subsequent thermal annealing and excimer laser treatment enabled the transformation of the amorphous intermediate into crystalline silicon. Furthermore, hydrogen plasma exposure was applied to passivate residual defect states and improve the structural and electronic quality of the films.[386] The following Fig. 35 shows SEM images of the surface of the thin film after different points in the formation process.

Cadiz Bedini *et al.* demonstrated the preparation of silicon ink from trisilane using ultrasonic irradiation. After subsequent UV irradiation, they used the resulting oligomeric mixture deposit a a-Si–H thin film *via* spin coating. Furthermore, the authors also reported on the deposition of Si nanoparticles from the sonicated silicon ink.[387]

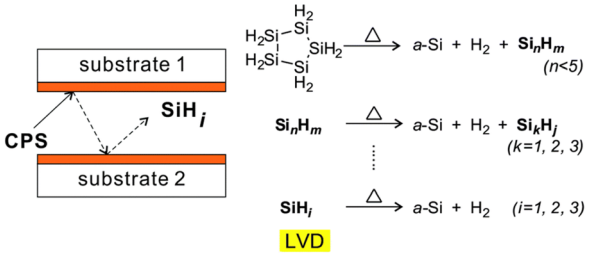

Fig. 34 Schematic set-up of the LVD process with *cy*-Si_5H_{10} as the precursor adapted from Shen *et al.*[385] Published by Royal Society of Chemistry under CC-BY 4.0, © 2015.

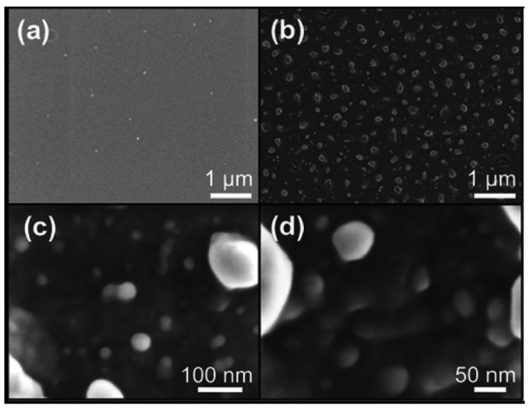

Fig. 35 SEM images of the thin film surface of (a) the amorphous silicon film, (b) the thermally treated silicon film, (c) the laser treated silicon film and (d) the laser treated silicon film at higher magnification adapted from Iyer *et al.*[386] With permission from American Chemical Society, © 2012.

Bronger *et al.* were the first to introduce neopentasilane in solution-based silicon processing. Using spin-coating and slot-die coating as deposition techniques, they showed that the branched molecular structure and increased Si–Si bond content of NPS significantly influence the thin film formation. Compared to *cy*-Si_5H_{10}, NPS exhibits improved solubility, which results in enhanced film homogeneity and uniformity. In addition, they reported an improved p-type doping efficiency for NPS-derived films relative to *cy*-Si_5H_{10}. The electronic performance approached that of comparable PECVD-deposited materials.[319] The working group of Haase executed further research to determine the usability of liquid silicon ink based on NPS for local n-and p-doping of solar cells.[388]

Further development explored hydrosilanes beyond simple cyclic or small branched molecules. Haas *et al.* introduced highly branched perhydrosilanes, namely 2,2,3,3-tetrasilyltetrasilane and 2,2,3,3,4,4-hexasilylpentasilane, which show a reduced pyrophoric character and a bathochromically shifted UV-absorption. After photolysis the obtained oligomeric polyhydrosilane mixture was spin-coated on glass substrates and thermally treated at 500 °C resulting in a homogeneous a-Si:H layer. Fig. 36 shows a photographic image and an optical micrograph of the solution processed a-Si:H film.[21]

In this context, Christopoulos *et al.* reported the synthesis and structural characterisation of highly branched hydrogen-

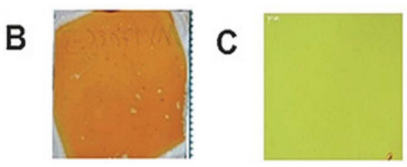

Fig. 36 Photographic image (B) and optical micrograph (C) of the solution processed a-Si: film adapted from Haas *et al.*[21] With permission from Wiley-VCH, © 2017.

Open Access Article. Published on 24 April 2026. Downloaded on 5/15/2026 8:48:04 PM.
This article is licensed under a Creative Commons Attribution 3.0 Unported Licence.

ated nonasilanes and decasilanes. Although no thin-film deposition experiments were performed, the study provided detailed information on molecular structure, bonding motifs, and stability of higher nuclearity hydrosilanes. Compared to smaller cyclic precursors, these compounds exhibit modified volatility and decomposition behaviour due to their increased silicon content and branching degree. The work therefore contributes to the understanding of structure–property relationships in hydrosilanes and identifies potential candidates for future liquid-phase silicon deposition studies.[49]

The increasing focus on precursor structure is also reflected in patent literature. Several patents disclose synthetic routes toward branched and doped hydridosilanes intended for thin-film deposition applications. These developments address precursor stability, controlled oligomerisation, and reduced pyrophoric character, highlighting the technological relevance of structure-tailored hydrosilanes for liquid-phase silicon processing.[389] More recently, precursor-engineered strategies have focused on single-source hydrosilane-based precursors that contain one or more heteroatoms covalently linked to silicon to enable controlled Si–C network formation. Matsuda and coworkers developed a polymeric polydihydrosilane precursor with pendant hexyl groups (PSH), which was deposited by solution-based methods and subsequently pyrolyzed to form an a-SiC coating. Fig. 37 shows a photographic image of PSH films coated on glass substrates and pyrolyzed at different temperatures.[390]

In a related molecular design approach, Haas and coworkers reported the systematic functionalization of higher silicon hydrides with carbon-containing substituents and demonstrated their application in LPD, where spin-coated precursor films were thermally converted into homogeneous Si/C thin films. Fig. 38 exemplary shows a picture and a light microscopy image of a thin layer formed from the precursor 1,1,1-trimethyl-2,2-disilyltrisilane.[22]

Structure–property–application relationships

Across CVD and LPD, recent work clarifies how structure–property–application relationships are essential to fully exploit the potential of hydrosilanes in modern materials science. The molecular structure of hydrosilanes governs their activation routes, processing windows, and ultimately film properties. In CVD, high volatility and clean gas-phase decomposition are structure-dependent parameters. Small, volatile hydrides such as SiH_4 or Si_2H_6 dissociate cleanly under plasma, hot-wire, or photon activation and remain advantageous for transport-limited growth formation of high-purity films. This includes hydrosilanes, where the incorporation of a Si–heteroatom bond can enhance surface reactivity, thereby improving the purity and conformality of a film. These attributes are particularly critical, as reduced impurity incorporation minimizes defect-mediated recombination, while improved conformality ensures uniform coverage and consistent electronic properties across complex device architectures. Consequently, both factors directly contribute to enhanced device performance and reliability in both microelectronics and thin-film solar cells.

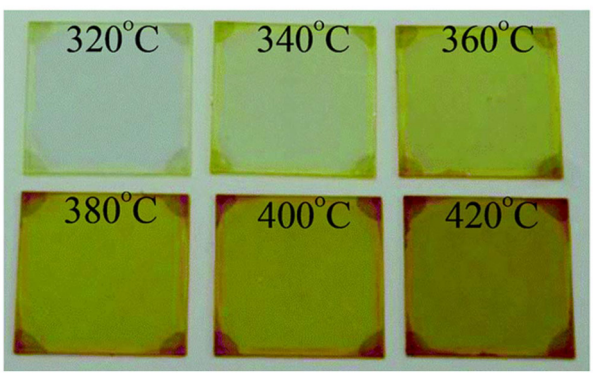

Fig. 37 Photographic image of PSH films coated on glass substrates and pyrolyzed at different temperatures adapted from Masuda *et al.*[390] With permission from Royal Society of Chemistry, © 2015.

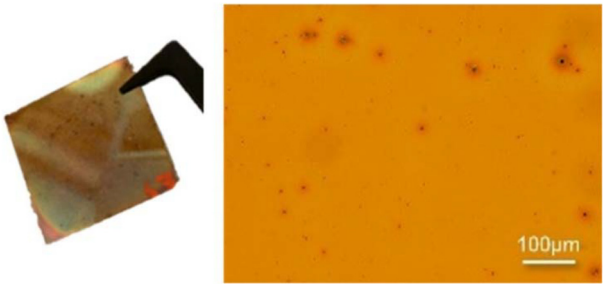

Fig. 38 A picture and a light microscopy image of a thin layer formed from the precursor 1,1,1-trimethyl-2,2-disilyltrisilane on glass adapted from Haas *et al.*[22] Published by American Chemical Society under CC-BY 4.0, © 2023.

In LPD, the balance shifts toward solubility, manageable reactivity, and photochemical responsiveness: higher and especially branched hydrosilanes exhibit superior solubility, reduced pyrophoricity, and bathochromically shifted UV absorption, enabling efficient photochemical activation and yielding homogeneous a-Si:H films. These features promote homogeneous film formation and improved control over hydrogen incorporation and network structure in a-Si:H materials. For example, branched hydrosilanes support more uniform coating behavior and facilitate dopant incorporation, while cyclic precursors follow distinct radical-mediated pathways that yield highly branched intermediates, influencing film densification and defect evolution. Thus, precursor structure directly governs the resulting microstructure and optoelectronic properties of the deposited films.

Across both deposition regimes, molecular functionalization (*e.g.*, preformed Si–N, Si–C, or Si–Ge bonds) provides a direct handle to encode composition and doping at the molecular level, linking precursor design directly to device-relevant properties. In the context of thin-film solar cells, such tailored precursors can influence key properties such as crystallinity, electronic structure, and impurity incorporation, thereby

Open Access Article. Published on 24 April 2026. Downloaded on 5/15/2026 8:48:04 PM.
This article is licensed under a Creative Commons Attribution 3.0 Unported Licence.

directly affecting device performance. These examples clearly demonstrate that the rational design of hydrosilane precursors-linking molecular structure to decomposition behavior and ultimately to material properties-represents a central strategy for advancing silicon-based technologies encoding film stoichiometry and network chemistry at the molecular level.

Conclusions

Over more than a century of research, the chemistry of hydrosilane has evolved from the early isolation of simple silanes to a sophisticated field spanning synthetic inorganic chemistry, materials science, and semiconductor technology. The development of reliable synthetic methodologies-from classical silicide hydrolysis to chlorosilane reduction, catalytic coupling reactions, and silanide-based strategies-has enabled access to a broad spectrum of linear, branched, cyclic, and cluster-type hydrosilanes. These advances have revealed the remarkable structural diversity of silicon hydrides and highlighted the different reactivity of Si–H and Si–Si bonds compared to their carbon analogues.

A central theme emerging from recent research is the pivotal role of silanide intermediates and Si–H bond activation processes in hydrosilane functionalization. Alkali-metal silanides and related species provide powerful synthetic entry points to a wide range of silicon-element bonds, enabling the preparation of silyl derivatives with elements across the periodic table. In parallel, dehydrogenative coupling reactions have emerged as a particularly powerful methodology for the controlled construction of Si–Si bonds, allowing the transformation of simple monosilanes into higher oligohydrosilanes and polysilane frameworks through catalytic hydrogen elimination. Together with advances in silicon cluster chemistry, including the synthesis of silafullerenes and higher branched hydrosilanes, these developments have significantly expanded the conceptual and structural landscape of molecular silicon hydride chemistry.

Beyond their fundamental chemical interest, hydrosilanes have become indispensable precursors for the preparation of silicon-containing materials and thin films. Chemical vapour deposition represents the most widely employed industrial technique for silicon film formation, where simple hydrosilanes such as monosilane and disilane serve as key feedstocks for the growth of polycrystalline, amorphous, or epitaxial silicon layers used in semiconductor devices and photovoltaic technologies. The controlled thermal or plasma-assisted decomposition of these molecules enables the deposition of high-purity silicon films with precisely tuneable properties. Building on this established technology, recent research has increasingly explored molecularly defined higher hydrosilanes and functionalized derivatives as advanced precursors. In particular, solution-based approaches such as liquid-phase deposition has emerged as attractive complementary strategy that offers advantages in terms of processability, scalability, and compatibility with emerging device architectures.

Outlook and challenges

The chemistry of hydrosilanes has evolved from a largely academic field into a key enabling technology for semiconductor processing and silicon-based materials. As highlighted throughout this review, hydrosilanes represent highly versatile molecular precursors that bridge fundamental silicon chemistry with industrially relevant applications such as chemical vapor deposition (CVD) and liquid phase deposition (LPD).

Building on this progress, future developments are expected to focus on improving synthetic accessibility, scalability, and the targeted functionalization of hydrosilane derivatives.

From an application perspective, hydrosilanes and especially higher oligomeric species offer significant potential as tailored single-source precursors for advanced materials. Their tunable reactivity and decomposition behavior enable precise control over film growth, composition, and doping in semiconductor fabrication. In particular, the development of functionalized hydrosilanes that incorporate heteroatoms directly into the molecular backbone represents a promising strategy toward cleaner and more efficient deposition processes, avoiding the need for co-feeding multiple gaseous precursors.

However, several key challenges currently limit the broader industrial implementation of these compounds. A major bottleneck is the economic feasibility, as the high cost of polysilanes has so far prevented their widespread use in large-scale applications such as solar cell manufacturing. Despite their attractive properties as solution-processable silicon precursors, their synthesis often involves multi-step procedures, low overall yields, and demanding purification protocols, all of which significantly increase production costs.

In addition, synthetic limitations remain a critical issue. For many technologically relevant doping elements, no scalable and robust synthetic routes to suitable hydrosilane-based precursors are currently available. While initial approaches toward Si–B, Si–P, or other heteroatom-functionalized systems have been reported, these methods often suffer from limited selectivity, stability issues, or poor scalability.

This lack of general and efficient synthetic strategies restricts the systematic exploration of doped silicon materials derived from hydrosilanes.

Another challenge lies in the control of reactivity and stability. The intrinsic reactivity of Si–H and Si–Si bonds, while advantageous for materials synthesis, can lead to undesired side reactions such as polymerization or decomposition, complicating handling and processing. This is particularly relevant for higher hydrosilanes, where competing reaction pathways often result in complex product mixtures and reduced selectivity.

Looking forward, addressing these challenges will require integrated efforts in synthesis, mechanistic understanding, and process development. Advances in catalytic methodologies, improved precursor design, and the development of scalable production routes will be essential to unlock the full potential of hydrosilanes in industrial applications. In this

Open Access Article. Published on 24 April 2026. Downloaded on 5/15/2026 8:48:04 PM. This article is licensed under a Creative Commons Attribution 3.0 Unported Licence.

context, the continued interplay between fundamental research and applied process engineering will be crucial for translating laboratory-scale discoveries into viable technologies.

Author contributions

D. G., M. Hx., M. P. and P. V.: were responsible for visualization, data presentation and writing original draft (lead). M. H. was in charge for methodology and conceptualization, review and editing of the manuscript (lead), project administration and funding acquisition.

Conflicts of interest

There are no conflicts to declare.

Data availability

This article is a review and does not report any original data. Therefore, no datasets were generated or analyzed during the current study.

Acknowledgements

The financial support by the Austrian Federal Ministry of Labour and Economy, the National Foundation for Research, Technology and Development and the Christian Doppler Research Association is gratefully acknowledged. The authors acknowledge the use of artificial intelligence tools (OpenAi (GPT 5)) for language polishing of the manuscript.

References

1 (*a*) E. Hengge, H. Keller-Rudek, D. Koschel, U. Krüerke and P. Merlet, *Gmelin Handbook of Inorganic Chemistry. Silicon, Supplement Vol. B1*, Springer, Berlin, Heidelberg, 1982; (*b*) J. H. Lorenz, *Survey of the preparation, purity, and availability of silanes*, Solar Energy Research Inst. (SERI), Golden, CO (United States) SERI/STR-211-2092, 1983.

2 M. Akhtar, Preparation of Ultra-High Purity Higher Silanes and Germanes, *Synth. React. Inorg. Met.-Org. Chem.*, 1986, **16**, 729.

3 *Encyclopedia of chemical technology. - 22: Silicon compounds to succinic acid and succinic anhydride: Silanes*, ed. R. E. Kirk, D. F. Othmer, J. I. Kroschwitz, M. Howe-Grant and B. Arkles, Wiley, New York, N.Y., 1997.

4 J. Baumgartner and C. Grogger, in *Comprehensive inorganic chemistry II. From elements to applications*, ed. J. Reedijk, Elsevier, Amsterdam, 2nd edn, 2013, pp. 51–82.

5 M. Gerwig, U. Böhme and M. Friebel, Challenges in the Synthesis and Processing of Hydrosilanes as Precursors for Silicon Deposition, *Chem. – Eur. J.*, 2024, **30**, e202400013.

6 T. Wiesner and M. Haas, in *Reference Module in Chemistry, Molecular Sciences and Chemical Engineering*, Elsevier, 2024.

7 E. Rivard, Group 14 inorganic hydrocarbon analogues, *Chem. Soc. Rev.*, 2016, **45**, 989.

8 H. Buff and F. Wöhler, Ueber neue Verbindungen des Siliciums, *Arch. Pharm.*, 1857, **142**, 284.

9 H. Moissan and S. Smiles, New Investigations of Liquid Silicon Hydride Si_2H_6, *C. R. Chim.*, 1902, 569.

10 A. Stock and C. Somieski, Siliciumwasserstoffe VI.: Chlorierung und Methylierung des Monosilans, *Ber. Dtsch. Chem. Ges. A/B*, 1919, **52**, 695.

11 A. Stock and K. Somieski, Siliciumwasserstoffe, X.: Stickstoffhaltige Verbindungen, *Ber. Dtsch. Chem. Ges. A/B*, 1921, **54**, 740.

12 G. Fritz, Notizen: Neue Wasserstoffverbindungen des Siliciums und des Phosphors. Das Silylphosphin SiH_3-PH_2, *Z. Naturforsch., B*, 1953, **8**, 776.

13 B. J. Aylett, H. J. Emeléus and A. G. Maddock, Phosphine and arsine derivatives of monosilane, *J. Inorg. Nucl. Chem.*, 1955, **1**, 187.

14 M. Baudler, Franz Fehér (1903–1991), *Eur. J. Inorg. Chem.*, 1998, **1998**, 2089.

15 M. A. Ring and D. M. Ritter, Preparation and Reactions of Potassium Silyl 1, *J. Am. Chem. Soc.*, 1961, **83**, 802.

16 E. Amberger and H. Boeters, The Preparation of Trisilylphosphine, *Angew. Chem., Int. Ed. Engl.*, 1962, **1**, 52.

17 E. Hengge and G. Bauer, Cyclopentasilane, the First Unsubstituted Cyclic Silicon Hydride, *Angew. Chem., Int. Ed. Engl.*, 1973, **12**, 316.

18 T. Lobreyer, H. Oberhammer and W. Sundermeyer, Synthesis and Structure of Tetrasilylgermane, $Ge(SiH_3)_4$ and Other Silylgermanes, *Angew. Chem., Int. Ed. Engl.*, 1993, **32**, 586.

19 T. Shimoda, Y. Matsuki, M. Furusawa, T. Aoki, I. Yudasaka, H. Tanaka, H. Iwasawa, D. Wang, M. Miyasaka and Y. Takeuchi, Solution-processed silicon films and transistors, *Nature*, 2006, **440**, 783.

20 J. Tillmann, J. H. Wender, U. Bahr, M. Bolte, H.-W. Lerner, M. C. Holthausen and M. Wagner, One-step synthesis of a 20silafullerane with an endohedral chloride ion, *Angew. Chem., Int. Ed.*, 2015, **54**, 5429.

21 M. Haas, V. Christopoulos, J. Radebner, M. Holthausen, T. Lainer, L. Schuh, H. Fitzek, G. Kothleitner, A. Torvisco, R. Fischer, O. Wunnicke and H. Stueger, Branched Hydrosilane Oligomers as Ideal Precursors for Liquid-Based Silicon-Film Deposition, *Angew. Chem., Int. Ed.*, 2017, **56**, 14071.

22 A. Sauermoser, T. Lainer, A. Knoechl, F. Goni, R. C. Fischer, H. Fitzek, M. Dienstleder, C. Prietl, A.-M. Kelterer, C. Bandl, G. Jakopic, G. Kothleitner and M. Haas, Fabrication of Amorphous Silicon-Carbon

 This journal is © the Partner Organisations 2026

Open Access Article. Published on 24 April 2026. Downloaded on 5/15/2026 8:48:04 PM.
This article is licensed under a Creative Commons Attribution 3.0 Unported Licence.

Hybrid Films Using Single-Source Precursors, *Inorg. Chem.*, 2023, **62**, 15490.

23 A. Stock and C. Somieski, Siliciumwasserstoffe. I. Die aus Magnesiumsilicid und Säuren entstehenden Siliciumwasserstoffe, *Ber. Dtsch. Chem. Ges.*, 1916, **49**, 111.

24 A. Stock, P. Stiebeler and F. Zeidler, Siliciumwasserstoffe, XVI.: Die höheren Siliciumhydride, *Ber. Dtsch. Chem. Ges. A/B*, 1923, **56**, 1695.

25 A. Stock, Siliciumwasserstoffe, *Z. Elektrochem. Angew. Phys. Chem.*, 1926, **32**, 341.

26 (*a*) F. Fehér, G. Kuhlbörsch and H. Luhleich, Beiträge zur Chemie des Siliciums und Germaniums. IV. Über die Drastellung des Rohsilas, *Z. Anorg. Allg. Chem.*, 1960, **303**, 283; (*b*) F. Fehér and H. Strack, Die gaschromatographische Trennung von Siliciumwasserstoffen an Squalan-Kieselgur-Trennsulen, *Naturwissenschaften*, 1963, **50**, 570; (*c*) F. Fehér, D. Schinkitz and J. Schaaf, Ein Verfahren zur Darstellung höherer Silane, *Z. Anorg. Allg. Chem.*, 1971, **383**, 303; (*d*) F. Fehér, H. Baier, B. Enders, M. Krancher, J. Laakmann, F. J. Ocklenburg and D. Skrodski, Beiträge zur Chemie des Siliciums und des Germaniums. XXXVII. Weitere Untersuchungen zur Darstellung eines Silangemisches, *Z. Anorg. Allg. Chem.*, 1985, **530**, 191; (*e*) F. Fehér, P. Hädicke and H. Frings, Beiträge zur chemie des siliciums und germaniums, XXIII (1) physikalisch-chemische eigenschaften der silane von trisilan bis heptasilan, *Inorg. Nucl. Chem. Lett.*, 1973, **9**, 931; (*f*) F. Fehér and D. Skrodzki, Beiträge zur chemie des siliciums und germaniums, XXVI (1) ramanspektren des trisilans, der tetra-, penta-, hexasilane und des n-heptasilans, *Inorg. Nucl. Chem. Lett.*, 1974, **10**, 577.

27 W. C. Johnson and S. Isenberg, Hydrogen Compounds of Silicon. I. The Preparation of Mono- and Disilane, *J. Am. Chem. Soc.*, 1935, **57**, 1349.

28 A. E. Finholt, A. C. Bond, K. E. Wilzbach and H. I. Schlesinger, The Preparation and Some Properties of Hydrides of Elements of the Fourth Group of the Periodic System and of their Organic Derivatives, *J. Am. Chem. Soc.*, 1947, **69**, 2692.

29 (*a*) F. Höfler and R. Jannach, Zur kenntnis des neopentasilans, *Inorg. Nucl. Chem. Lett.*, 1973, **9**, 723; (*b*) J. P. Cannady and X. Zhou, WO2008051328A1, 2008; (*c*) S. Wieber, M. Patz, M. Trocha, H. Rauleder, E. Müh, H. Stüger and C. Walkner, WO2011061088A1, 2011; (*d*) M.-Z. Oh, J. Haubrock, T. Schwärtzke, I. Moussallem and M. Trocha, WO2014095278A1, 2014.

30 (*a*) L. M. Litz and S. A. Ring, US3163590, 1964; (*b*) W. Sundermeyer and L. M. Litz, Die elektrochemische Darstellung von Hydriden in geschmolzenen Salzen, *Chem. Ing. Tech.*, 1965, **37**, 14.

31 (*a*) E. Hengge and G. Bauer, Cyclopentasilan, das erste unsubstituierte cyclische Siliciumhydrid, *Angew. Chem.*, 1973, **85**, 304; (*b*) E. Hengge and G. Bauer, Darstellung und Eigenschaften von Cyclopentasilan, *Monatsh. Chem.*, 1975, **106**, 503; (*c*) E. Hengge and D. Kovar, Darstellung von Cyclohexasilan, Si_6H_{12}, *Angew. Chem.*, 1977, **89**, 417.

32 D. Schmidt, U. Böhme, J. Seidel and E. Kroke, Cyclopentasilane Si_5H_{10}: First single crystal X-ray structure of an oligosilane SixHy and thermal analysis with TG/MS, *Inorg. Chem. Commun.*, 2013, **35**, 92.

33 (*a*) P. Boudjouk, S. D. Kloos, B.-K. Kim, M. Page and D. Thweatt, An unexpected redistribution of trichlorosilane. Synthesis, structure and bonding of (N,N,N′,N′-tetraethylethylenediamine)-dichlorosilane, *J. Chem. Soc., Dalton Trans.*, 1998, 877; (*b*) S. B. Choi, B. K. Kim, P. Boudjouk and D. G. Grier, Amine-promoted disproportionation and redistribution of trichlorosilane: formation of tetradecachlorocyclohexasilane dianion, *J. Am. Chem. Soc.*, 2001, **123**, 8117; (*c*) A. Elangovan, K. Anderson, P. Boudjouk and D. L. Schulz, US8975429B2, 2015.

34 J. Teichmann and M. Wagner, Silicon chemistry in zero to three dimensions: from dichlorosilylene to silafullerane, *Chem. Commun.*, 2018, **54**, 1397.

35 H. Stüger, P. Lassacher and E. Hengge, Anorganische Bi (cyclopentasilanyle): Synthese und spektroskopische Charakterisierung, *Z. Anorg. Allg. Chem.*, 1995, **621**, 1517.

36 (*a*) C. J. Bakay, US3968199A, 1976; (*b*) G. H. Wagner and C. E. Erickson, US2627451A, 1953.

37 (*a*) K. Tachiki, S. Katakura and Y. Yamahita, JP37008374, 1962; (*b*) K. Tachiki and Y. Yamahita, JP36021507, 1961.

38 J. Y. Corey, in *Advances in Organometallic Chemistry Volume 51*, ed. J. Y. Corey, Elsevier, 2004, vol. 51, pp. 1–52.

39 J. F. Harrod, in *Inorganic and Organometallic Polymers*, ed. M. Zeldin, K. J. Wynne and H. R. Allcock, American Chemical Society, Washington, DC, 1988, vol. 360, pp. 89–100.

40 (*a*) Y. Okumura, K. Takatsuna and J. Yagihashi, JP0218451, 1990; (*b*) H. Stüger, D. Wolf, B. Stützel, J. Sauer, Y. Onal, M. Trocha, G. Stochniol, A. Ebbers and N. Brausch, WO2010003729A1, 2010.

41 G. Nikiforov and G. Itov, WO2020077182A1, 2020.

42 A. D. Craig and A. G. MacDiarmid, Application of the Wurtz reaction to the synthesis of disilane and 1,2-dimethyldisilane, *J. Inorg. Nucl. Chem.*, 1962, **24**, 163.

43 R. C. Kennedy, L. P. Freeman, A. P. Fox and M. A. Ring, Formation and cleavage of the silicon-silicon bond in disilane, *J. Inorg. Nucl. Chem.*, 1966, **28**, 1373.

44 W. R. Bornhorst and M. A. Ring, Formation and cleavage of the germanium-germanium bond in digermane, *Inorg. Chem.*, 1968, **7**, 1009.

45 F. Fehér and R. Freund, Contributions to the chemistry of silicon and germanium, XXII (1) new silanes, bromosilanes and phenylsilanes, *Inorg. Nucl. Chem. Lett.*, 1973, **9**, 937.

46 T. Lobreyer, J. Oeler and W. Sundermeyer, Über die verbesserte Darstellung von Silyl– und Germylkalium sowie die Synthese von Silylgermanen, *Chem. Ber.*, 1991, **124**, 2405.

47 T. Lobreyer, W. Sundermeyer and H. Oberhammer, Über dehydrierende Aufbaureaktionen zu silylsubstituierten Alkalimetallgermaniden, –stanniden und –phosphiden; Molekülstruktur von Neopentasilan, *Chem. Ber.*, 1994, **127**, 2111.

Open Access Article. Published on 24 April 2026. Downloaded on 5/15/2026 8:48:04 PM. This article is licensed under a Creative Commons Attribution 3.0 Unported Licence.

48 H. Stueger, T. Mitterfellner, R. Fischer, C. Walkner, M. Patz and S. Wieber, Selective synthesis and derivatization of alkali metal silanides $MSi(SiH_3)_3$, *Chem. – Eur. J.*, 2012, **18**, 7662.
49 V. Christopoulos, M. Rotzinger, M. Gerwig, J. Seidel, E. Kroke, M. Holthausen, O. Wunnicke, A. Torvisco, R. Fischer, M. Haas and H. Stueger, Synthesis and Properties of Branched Hydrogenated Nonasilanes and Decasilanes, *Inorg. Chem.*, 2019, **58**, 8820.
50 X. Zhou, N. Chang, J. Young and X. Wang, Selective Synthesis of 2,2,4,4-Tetrasilylpentasilane, *Inorg. Chem.*, 2019, **58**, 12526.
51 H. Stüger, M. Haas, O. Wunnicke, M. D. Malsch and M. Holthausen, EP3590889A1, 2020.
52 H. Gilman and R. L. Harrell, Hexakis(trimethylsilyl)disilane: A highly branched and symmetrical organopolysilane, *J. Organomet. Chem.*, 1967, **9**, 67.
53 G. Fritz, Bildung siliciumorganischer Verbindungen III. Mitt.: Zum thermischen Zerfall von SiH_4, *Z. Naturforsch., B*, 1952, 507.
54 E. M. Tebben and M. A. Ring, Pyrolysis of disilane and trisilane, *Inorg. Chem.*, 1969, **8**, 1787.
55 (*a*) E. J. Spanier and A. G. MacDarmid, The Conversion of Silane to Higher Silanes in a Silent Electric Discharge, *Inorg. Chem.*, 1962, **1**, 432; (*b*) S. D. Gokhale, J. E. Drake and W. L. Jolly, Synthesis of the higher silanes and germanes, *J. Inorg. Nucl. Chem.*, 1965, **27**, 1911.
56 H. Niki and G. J. Mains, The ^{3}P1 Mercury-Photosensitized Decomposition of Monosilane, *J. Phys. Chem.*, 1964, **68**, 304.
57 M. Bamberg, M. Bursch, A. Hansen, M. Brandl, G. Sentis, L. Kunze, M. Bolte, H.-W. Lerner, S. Grimme and M. Wagner, $Cl@Si_{20}H_{20}$-: Parent Siladodecahedrane with Endohedral Chloride Ion, *J. Am. Chem. Soc.*, 2021, **143**, 10865.
58 (*a*) J. Zhang, S. Yan, H. Qu, X. F. Yu and P. Peng, Alkali metal silanides α-$MSiH_3$: A family of complex hydrides for solid-state hydrogen storage, *Int. J. Hydrogen Energy*, 2017, **42**, 12405; (*b*) A. Jain, H. Miyaoka, T. Ichikawa and Y. Kojima, Tailoring the absorption–desorption properties of $KSiH_3$ compound using nano-metals (Ni, Co, Nb) as catalyst, *J. Alloys Compd.*, 2015, **645**, S144–S147.
59 (*a*) R. Janot, W. S. Tang, D. Clémençon and J.-N. Chotard, Catalyzed $KSiH_3$ as a reversible hydrogen storage material, *J. Mater. Chem. A*, 2016, **4**, 19045; (*b*) S. Sharma, F. Guo, T. Ichikawa, Y. Kojima, S. Agarwal and A. Jain, Iron based catalyst for the improvement of the sorption properties of $KSiH_3$, *Int. J. Hydrogen Energy*, 2020, **45**, 33681.
60 W. S. Tang, J.-N. Chotard, P. Raybaud and R. Janot, Enthalpy–Entropy Compensation Effect in Hydrogen Storage Materials: Striking Example of Alkali Silanides $MSiH_3$ (M = K, Rb, Cs), *J. Phys. Chem. C*, 2014, **118**, 3409.
61 P. Hagenmuller and M. Pouchard, Some reactions of monosilane with sodium metal, *Bull. Soc. Chim. Fr.*, 1964, 1187.
62 E. Amberger and R. Römer, Reaktionen der Hydrylanionen. I. Reaktionen des Silylanions SiH mit substituierten Boranen, *Z. Anorg. Allg. Chem.*, 1966, **345**, 1.
63 S. Cradock, G. A. Gibbon and C. H. van Dyke, Germyl chemistry. V. Hexamethylphosphoramide as a solvent for the preparation and reaction of alkali metal derivatives of silane and germane, *Inorg. Chem.*, 1967, **6**, 1751.
64 E. Amberger, R. Römer and A. Layer, Reaktionen der hydrylanionen V. Darstellung von SiH_3Na, SiH_3K. SiH_3Rb, SiH_3Cs und SnH_3K und ihre Umsetzung mit CH_3I, *J. Organomet. Chem.*, 1968, **12**, 417.
65 H. Bürger, R. Eujen and H. C. Marsmann, ^{1}H- und ^{29}Si-kernresonanzspektroskopische Charakterisierung der Anionen $^{\ominus}SiH_{3(n}(SiH_3)_n$, *Z. Naturforsch., B*, 1974, **29**, 149.
66 F. Fehér and R. Freund, Beiträge zur chemie des siliciums und germaniums, XXIV (1) darstellung und kernresonanzspektroskopische untersuchung höherer silylanionen; Darstellung neuer phenyl- und alkylsilane, *Inorg. Nucl. Chem. Lett.*, 1974, **10**, 561.
67 F. Fehér, G. Betzen and M. Krancher, Beiträge zur Chemie des Siliciums und Germaniums. XXXIII [1]. Zur Darstellung von Kaliumsilyl, *Z. Anorg. Allg. Chem.*, 1981, **475**, 81.
68 F. Fehér and M. Krancher, Beiträge zur Chemie des Siliciums und Germaniums. XXXIV. Ein weiterer Beitrag zur Darstellung von Kaliumsilyl, *Z. Anorg. Allg. Chem.*, 1984, **509**, 95.
69 F. Fehér and M. Krancher, Contributions to the Chemistry of Silicon and Germanium, XXXVIII. Systematic Investigations on the Reaction of Higher Silanes with Potassium Silyl, *Z. Naturforsch., B*, 1985, **40**, 1010.
70 B. F. Fieselmann and C. R. Dickson, Improved synthetic route to potassium silyl using crown ethers, potassium, and silane and its use to prepare methylsilane and disilylmethane, *J. Organomet. Chem.*, 1989, **363**, 1.
71 F. Fehér, M. Krancher and M. Fehér, Beiträge zur Chemie des Siliciums und Germaniums. XL. Die Bildung von Alkalimetallsilanylen, MSi_nH_{2n+1} (M = Na, K), – eine neue Methode zur Knüpfung von Silicium–Silicium–Bindungen ausgehend von SiH_4 und Natrium oder Kalium, *Z. Anorg. Allg. Chem.*, 1991, **606**, 7.
72 W. Sundermeyer, T. Lobreyer and O. Johannes, DE4139113A1, 1993.
73 H. Stueger, V. Christopoulos, A. Temmel, M. Haas, R. Fischer, A. Torvisco, O. Wunnicke, S. Traut and S. Martens, Selective Synthesis and Derivatization of Germasilicon Hydrides, *Inorg. Chem.*, 2016, **55**, 4034.
74 T. Lainer, R. C. Fischer and M. Haas, The Synthesis of Tris (silyl)silanides Revisited. A Study of Reactivity and Stability, *Z. Anorg. Allg. Chem.*, 2022, **648**, e202200137.
75 V. Leich, T. P. Spaniol and J. Okuda, Formation of α-$KSiH_3$ by hydrogenolysis of potassium triphenylsilyl, *Chem. Commun.*, 2015, **51**, 14772.
76 D. Schuhknecht, V. Leich, T. P. Spaniol, I. Douair, L. Maron and J. Okuda, Alkali Metal Triphenyl- and Trihydridosilanides Stabilized by a Macrocyclic Polyamine Ligand, *Chem. – Eur. J.*, 2020, **26**, 2821.
77 S. M. Sze and K. K. Ng, *Physics of Semiconductor Devices*, Wiley, 2006.

 This journal is © the Partner Organisations 2026

Open Access Article. Published on 24 April 2026. Downloaded on 5/15/2026 8:48:04 PM. This article is licensed under a Creative Commons Attribution 3.0 Unported Licence.

78 S. Wolf and R. N. Tauber, *Silicon processing for the VLSI era*, Lattice Pr, Sunset Beach, Calif., 1986.

79 (*a*) A. J. Olivares, A. Zamchiy, V. S. Nguyen and P. Roca i Cabarrocas, Boron activation in silicon thin films grown by PECVD under epitaxial and microcrystalline conditions, *Appl. Surf. Sci. Adv.*, 2023, **18**, 100508; (*b*) Y. Kamochi, A. Motomiya, H. Habuka, Y. Ishida, S.-I. Ikeda and S. Hara, Boron-Silicon Thin Film Formation Using a Slim Vertical Chemical Vapor Deposition Reactor, *Adv. Chem. Eng. Sci.*, 2023, **13**, 7.

80 D. F. Gaines and T. V. Iorns, Group IV derivatives of pentaborane(9), *J. Am. Chem. Soc.*, 1968, **90**, 6617.

81 D. F. Gaines and T. V. Iorns, 1-Silyl derivatives of pentaborane(9), *Inorg. Chem.*, 1971, **10**, 1094.

82 T. C. Geisler and A. D. Norman, Preparation and properties of 2- and mu.-(halosilyl)pentaboranes(9), *Inorg. Chem.*, 1970, **9**, 2167.

83 T. C. Geisler, N. P. Soice and A. D. Norman, Relative stabilities of $XSiH_2B_5H_8$ (X = H, SiH_3, Cl) silylpentaborane(9)s: synthesis of chlorosilyl- and disilanyl-pentaboranes, *Phosphorus, Sulfur Silicon Relat. Elem.*, 1998, **132**, 123.

84 T. Lainer, C. Walkner, N. M. Tasch, R. C. Fischer, A. Torvisco, H. Stueger and M. Haas, Synthesis and Characterization of Alkali Metal Hypersilyl Borates, *Z. Anorg. Allg. Chem.*, 2024, **650**, e202400054.

85 K. N. Semenenko and K. A. Taisumov, Preparation of monosilylalane, *Russ. Chem. Bull.*, 1975, **24**, 1578.

86 E. Amberger and R. Römer, Notizen: Reaktionen der Hydrylanionen III. Synthese und Eigenschaften von Silyldibutylalan $(n\text{-}C_4H_9)_2AlSiH_3$, *Z. Naturforsch., B*, 1968, **23**, 559.

87 J. M. Castillo, M. Klos, K. Jacobs, M. Horsch and H. Hasse, Characterization of Alkylsilane Self-Assembled Monolayers by Molecular Simulation, *Langmuir*, 2015, **31**, 2630.

88 N. Aissaoui, L. Bergaoui, J. Landoulsi, J.-F. Lambert and S. Boujday, Silane layers on silicon surfaces: mechanism of interaction, stability, and influence on protein adsorption, *Langmuir*, 2012, **28**, 656.

89 X. Jiang and S. F. Bent, Area-Selective ALD with Soft Lithographic Methods: Using Self-Assembled Monolayers to Direct Film Deposition, *J. Phys. Chem. C*, 2009, **113**, 17613.

90 S. B. Khan, H. Wu, C. Pan and Z. Zhang, A Mini Review: Antireflective Coatings Processing Techniques, Applications and Future Perspective, *Res. Rev. J Mat. Sci.*, 2017, **05**, 36–54.

91 (*a*) S. Tannenbaum, S. Kaye and G. F. Lewenz, Synthesis and Properties of Some Alkylsilanes, *J. Am. Chem. Soc.*, 1953, **75**, 3753; (*b*) M. E. Freeburger, B. M. Hughes, G. R. Buell, T. O. Tiernan and L. Spialter, Physical organosilicon chemistry. II. Mass spectral cracking patterns of phenylsilane and ortho-, meta- and para-substituted benzyl- and phenyltrimethylsilanes, *J. Org. Chem.*, 1971, **36**, 933; (*c*) F. Mareš and V. Chvalovský, Organosilicon compounds XLV. Pyrolysis of trialkylsilanes, *J. Organomet. Chem.*, 1966, **6**, 327; (*d*) W. H. Nebergall, Some Reactions of Phenylsilane, *J. Am. Chem. Soc.*, 1950, **72**, 4702.

92 J. Zech and H. Schmidbaur, Synthetic pathways to disilylmethane, $H_3SiCH_2SiH_3$, and methyldisilane, $CH_3SiH_2SiH_3$, *Chem. Ber.*, 1990, **123**, 2087.

93 R. Hager, O. Steigelmann, G. Müller and H. Schmidbaur, A synthetic route to poly(silyl)methanes via poly(phenylsilyl)-methanes and poly(bromosily)methanes, *Chem. Ber.*, 1989, **122**, 2115.

94 R. Hager, O. Steigelmann, G. Müller, H. Schmidbaur, H. E. Robertson and D. W. H. Rankin, Tetrasilylmethane, $C(SiH_3)_4$, the Si/C-Inverse of Tetramethylsilane, $Si(CH_3)_4$, *Angew. Chem., Int. Ed. Engl.*, 1990, **29**, 201.

95 V. N. Gevorgyan, L. M. Ignatovich and E. Lukevics, Reduction of alkoxysilanes, halo-silanes and -Germanes with lithium aluminium hydride under phase-transfer conditions, *J. Organomet. Chem.*, 1985, **284**, C31–C32.

96 H. Schmidbaur and J. Zech, An Improved Synthetic Pathway to Tetrasilylmethane and the Synthesis of 2,2-Disilylpropane, *Eur. J. Solid State Inorg. Chem.*, 1992, **29**, 5–21.

97 D. V. Sidorov, P. A. Storozhenko, O. G. Shutova and B. E. Kozhevnikov, Synthesis of high-purity alkylsilanes, *Theor. Found. Chem. Eng.*, 2007, **41**, 668.

98 J. A. Morrison and J. M. Bellama, Synthesis and characterization of the (halosilyl)methylsilanes, *J. Organomet. Chem.*, 1975, **92**, 163.

99 I. N. Jung, S. H. Yeon and J. S. Han, Direct synthesis of bis(silyl)methanes containing silicon-hydrogen bonds, *Organometallics*, 1993, **12**, 2360.

100 J.-H. Boo, K.-S. Yu, Y. Kim, S. H. Yeon and I. N. Jung, Growth of Cubic SiC Films Using 1,3-Disilabutane, *Chem. Mater.*, 1995, **7**, 694.

101 G. Fritz, St. Lauble, M. Breining, A. G. Beetz, A. M. Galminas, E. Matern and H. Goesmann, Bildung siliciumorganischer Verbindungen. 111. Die Hydrierung Si–chlorierter, C–spiroverbrückter 2,4–Disilacyclobutane mit $LiAlH_4$ und i-Bu_2AlH. Der Zugang zum $Si_8C_3H_{20}$, *Z. Anorg. Allg. Chem.*, 1994, **620**, 127.

102 (*a*) G. Fritz and J. F. Willems, *Fortschritte Der Chemischen Forschung*, Springer-Verlag, Berlin/Heidelberg, 1964, p. 4/3; (*b*) G. Fritz, H. J. Buhl and D. Kummer, Bildung Siliciumorganischer Verbindungen. XXII. Untersuchungen an Pyrolyseprodukten der Methylchlorsilane (SiH–haltige Silicium–methylene), *Z. Anorg. Allg. Chem.*, 1964, **327**, 165.

103 G. Fritz, Bildung siliciumorganischer Verbindungen. IV. Das thermische Verhalten von $C_2H_5SiH_3$, $(C_2H_5)_2SiH_2$ und $(C_2H_5)_3SiH$, *Z. Anorg. Allg. Chem.*, 1953, **273**, 275.

104 M. Bowrey and J. H. Purnell, Insertion reactions of SiH_2 [silylene], *J. Am. Chem. Soc.*, 1970, **92**, 2594.

105 S. Bommers and H. Schmidbaur, Poly(trifluoromethanesulfonatosilyl)methanes - Precursors to Polysilylmethanes, *Z. Naturforsch., B*, 1994, **49**, 337.

106 H. Westermark, O. Theander and N. A. Sörensen, Preparation of Some Organic Silicon Hydrides, *Acta Chem. Scand.*, 1954, **8**, 1830.

Open Access Article. Published on 24 April 2026. Downloaded on 5/15/2026 8:48:04 PM. This article is licensed under a Creative Commons Attribution 3.0 Unported Licence.

107 U. Herzog and G. Roewer, Preparation of oligosilanes containing perhalogenated silyl groups and their hydrogenation by stannanes, *J. Organomet. Chem.*, 1997, **544**, 217.
108 (*a*) U. Herzog, E. Brendler and G. Roewer, Basekatalysierte hydrierung von methylchlortri- und -tetrasilanen mit trialkylstannanen zu methylchlorwasserstofftri- und -tetrasilanen, *J. Organomet. Chem.*, 1996, **511**, 85; (*b*) U. Herzog and G. Roewer, Base catalysed hydrogenation of methylbromooligosilanes with trialkylstannanesidentification of the first methylbromohydrogenoligosilanes, *J. Organomet. Chem.*, 1997, **527**, 117.
109 U. Herzog, G. Roewer and U. Pätzold, Katalytische hydrierung chlorhaltiger disilane mit tributylstannan, *J. Organomet. Chem.*, 1995, **494**, 143.
110 (*a*) D. G. White and E. G. Rochow, Reactions of Silane with Unsaturated Hydrocarbons, *J. Am. Chem. Soc.*, 1954, **76**, 3897; (*b*) R. N. Haszeldine, M. J. Newlands and J. B. Plumb, 375. Polyfluoroalkyl compounds of silicon. Part VI. Reaction of 3,3,3-trifluoropropene with silaneand the conversion of the products into silicones and polysiloxanes, *J. Chem. Soc.*, 1965, 2101.
111 A. J. Malcolm, C. R. Everly and G. E. Nelson, US4670574A, 1987.
112 M. Kobayashi and M. Itoh, Hydrosilylation of Olefins with Monosilane in the Presence of Lithium Aluminum Hydride, *Chem. Lett.*, 1996, **25**, 1013.
113 M. Itoh, K. Iwata and M. Kobayashi, Preparation of vinylsilane from monosilane and vinyl chloride, *J. Organomet. Chem.*, 1999, **590**, 36.
114 E. Amberger and E. Mühlhofer, Reaktionen der hydrylanionen II. Reaktionen des silylanions SiH_3 und germylanions GeH_3 mit monohalogenorganylverbindungen der 4. Hauptgruppe, *J. Organomet. Chem.*, 1968, **12**, 55.
115 T. Lobreyer, J. Oeler, W. Sundermeyer and H. Oberhammer, Über die–Synthese und Molekülstruktur von $CH_3M(SiH_3)_3$ (M=Si, Ge), *Chem. Ber.*, 1993, **126**, 665.
116 T. Lainer, M. Leypold, C. Kugler, R. C. Fischer and M. Haas, Dodecamethoxyneopentasilane as a New Building Block for Defined Silicon Frameworks, *Eur. J. Inorg. Chem.*, 2021, **2021**, 529.
117 H. E. Opitz, J. S. Peake and W. H. Nebergall, The Preparation of Monobromosilane and Organic Silyl Derivatives, *J. Am. Chem. Soc.*, 1956, **78**, 292.
118 H. Schmidbaur and J. Ebenhöch, Synthetic Pathways to Simple Di- and Trisilylmethanes: Potential Starting Materials for the CVD Deposition of Amorphous Silicon a-SiC :H, *Z. Naturforsch., B*, 1986, **41**, 1527.
119 S. Xin, C. Aitken, J. F. Harrod, Y. Mu and E. Samuel, Redistribution reactions of alkoxy- and siloxysilanes, catalyzed by dimethyltitanocene, *Can. J. Chem.*, 1990, **68**, 471.
120 E. Belov, G. Dubrovskaya, N. Efimov, S. Kleshcevnikova, E. Korobkov and E. Lebedev, in *Organosilicon Chemistry V: From Molecules to Materials*, 2003, pp. 518–521.
121 M. Abedini and A. G. MacDiarmid, Synthesis of Methyldisilane by the Silent Electric Discharge of a Mixture of Silane and Dimethyl Ether, *Inorg. Chem.*, 1966, **5**, 2040.
122 W. J. Bolduc and M. A. Ring, Preparation of ethyldisilane, *J. Organomet. Chem.*, 1966, **6**, 202.
123 F. Fehér and R. Freund, Beiträge zur chemie des siliciums und germaniums, XXV (1) reaktionen von trisilan, n-tetrasilan und n-pentasilan mit n-butyllithium in n-hexan, *Inorg. Nucl. Chem. Lett.*, 1974, **10**, 569.
124 (*a*) J. M. Hartmann, A. Abbadie, A. M. Papon, P. Holliger, G. Rolland, T. Billon, J. M. Fédéli, M. Rouvière, L. Vivien and S. Laval, Reduced pressure–chemical vapor deposition of Ge thick layers on Si(001) for 1.3–1.55-μm photodetection, *J. Appl. Phys.*, 2004, **95**, 5905; (*b*) J. Aubin, J. M. Hartmann, M. Bauer and S. Moffatt, Very low temperature epitaxy of Ge and Ge rich SiGe alloys with Ge_2H_6 in a Reduced Pressure – Chemical Vapour Deposition tool, *J. Cryst. Growth*, 2016, **445**, 65; (*c*) T. I. Kamins, E. C. Carr, R. S. Williams and S. J. Rosner, Deposition of three-dimensional Ge islands on Si(001) by chemical vapor deposition at atmospheric and reduced pressures, *J. Appl. Phys.*, 1997, **81**, 211; (*d*) M. Kummer, C. Rosenblad, A. Dommann, T. Hackbarth, G. Höck, M. Zeuner, E. Müller and H. von Känel, Low energy plasma enhanced chemical vapor deposition, *Mater. Sci. Eng., B*, 2002, **89**, 288; (*e*) M. D. Stephens, M. Pikulin and C. Ritter, The Utility of Novel Single-Source Germyl Silanes, *ECS Trans.*, 2006, **3**, 183; (*f*) J. C. Guillemin, L. Lassalle and T. Janati, Germane photochemistry. Photolysis of gas mixtures of planetary interest, *Planet. Space Sci.*, 1995, **43**, 75; (*g*) J. Kouvetakis, J. Tolle, R. Roucka, V. R. D'Costa, Y. Fang, A. V. Chizmeshya and J. Menendez, Nanosynthesis of Si-Ge-Sn Semiconductors and Devices via Purpose-built Hydride Compounds, *ECS Trans.*, 2008, **16**, 807; (*h*) J. Kouvetakis, J. Menendez and J. Tolle, Advanced Si-based Semiconductors for Energy and Photonic Applications, *Solid State Phenom.*, 2009, **156–158**, 77; (*i*) S.-M. Jang, K. Liao and R. Reif, Chemical Vapor Deposition of Epitaxial Silicon–Germanium from Silane and Germane: II In Situ Boron, Arsenic, and Phosphorus Doping, *J. Electrochem. Soc.*, 1995, **142**, 3520; (*j*) H. Oberhammer, T. Lobreyer and W. Sundermeyer, The Ge-Si bond in silylgermane. Discrepancy between experiment and theory, *J. Mol. Struct.*, 1994, **323**, 125.
125 R. Varma and A. P. Cox, Eine neue Synthese des Germylsilans, *Angew. Chem.*, 1964, **76**, 649.
126 P. L. Timms, C. C. Simpson and C. S. G. Phillips, 279. The silicon–germanium hydrides, *J. Chem. Soc.*, 1964, 1467.
127 J. Kouvetakis, C. J. Ritter, C. Hu, A. V. G. Chizmeshya, J. Tolle, D. Klewer and I. S. T. Tsong, Synthesis and fundamental studies of $(H_3Ge)_xSiH_{4(x}$ molecules: precursors to semiconductor hetero- and nanostructures on Si, *J. Am. Chem. Soc.*, 2005, **127**, 9855.
128 B. Köstler, F. Jungwirth, L. Achenbach, M. Sistani, M. Bolte, H.-W. Lerner, P. Albert, M. Wagner and S. Barth, Mixed-Substituted Single-Source Precursors for $Si_{1(x}Ge_x$ Thin Film Deposition, *Inorg. Chem.*, 2022, **61**, 17248.
129 E. Wiberg, E. Amberger and H. Cambensi, Zur Kenntnis der Äthan–homologen Mischhydride $H_3Si–SnH_3$ und

 This journal is © the Partner Organisations 2026

Open Access Article. Published on 24 April 2026. Downloaded on 5/15/2026 8:48:04 PM. This article is licensed under a Creative Commons Attribution 3.0 Unported Licence.

$H_3Ge–SnH_3$ sowie ihrer Phenyl–Acetato– und Chlorderivate, *Z. Anorg. Allg. Chem.*, 1967, **351**, 164.
130 B. Xu, L. Li, P. Shi, W. Yu, J. Zhao, X. Wang and L. Andrews, Matrix-Infrared Spectra and Structures of HM-SiH_3 (M = Ge, Sn, Pb, Sb, Bi, Te Atoms), *J. Phys. Chem. A*, 2018, **122**, 81.
131 S. M. George, Atomic layer deposition: an overview, *Chem. Rev.*, 2010, **110**, 111.
132 V. Miikkulainen, M. Leskelä, M. Ritala and R. L. Puurunen, Crystallinity of inorganic films grown by atomic layer deposition: Overview and general trends, *J. Appl. Phys.*, 2013, **113**, 21301.
133 R. L. Puurunen, Surface chemistry of atomic layer deposition: A case study for the trimethylaluminum/water process, *J. Appl. Phys.*, 2005, **97**, 121301–121352.
134 M. Leskelä and M. Ritala, Atomic layer deposition (ALD): from precursors to thin film structures, *Thin Solid Films*, 2002, **409**, 138.
135 B. D. Rekken and X. Zhou, WO2015184201A1, 2015.
136 J. W. Kim, S. J. Jang, H. G. Kim, J. H. Ju, Y. H. Cho, J. D. Kim and M. W. Kim, KR101040325B1, 2011.
137 H. Schuh, T. Schlosser, P. Bissinger and H. Schmidbaur, Disilanyl-amines—compounds comprising the structural unit Si-Si-N, as single-source precursors for plasma-enhanced chemical vapour deposition (PE-CVD) of silicon nitride, *Z. Anorg. Allg. Chem.*, 1993, **619**, 1347.
138 (*a*) W. Gollner, K. Renger and H. Stueger, Linear and Cyclic Polysilanes Containing the Bis(trimethylsilyl)amino Group: Synthesis, Reactions, and Spectroscopic Characterization, *Inorg. Chem.*, 2003, **42**, 4579; (*b*) J. F. Lehmann and H. P. Withers Jr., US2012277457A1, 2012.
139 H. Stüger, P. Lassacher and E. Hengge, Aminochlorodisilanes: Precursors to multifunctionalized disilane derivatives, *J. Organomet. Chem.*, 1997, **547**, 227.
140 N. Chang, B. K. Hwang, B. D. Rekken and X. Zhou, WO2017200908A1, 2017.
141 H. J. Emeléus and N. Miller, 175. Derivatives of monosilane. Part I. The reactions of chlorosilane with aliphatic amines, *J. Chem. Soc.*, 1939, 819.
142 D. G. Anderson and D. W. H. Rankin, Isopropyldisilylamine and disilyl-t-butylamine: preparation, spectroscopic properties, and molecular structure in the gas phase, determined by electron diffraction, *J. Chem. Soc., Dalton Trans.*, 1989, 779.
143 D. P. Spence, H. Chandra, B. Han, M. L. O'Neill, S. G. Mayorga and A. Mallikarjunan, EP2669248A1, 2013.
144 A. Stock, *Hydrides of Boron and Silicon*, Cornell University Press; Oxford University Press, Ithaca, NY, London, 1933.
145 A. Stock and K. Somieski, Siliciumwasserstoffe, VIII: Halogen–Abkömmlinge des Disilans, Si_2H_6 und ihre Hydrolyse, *Ber. Dtsch. Chem. Ges. A/B*, 1920, **53**, 759.
146 B. J. Aylett and M. J. Hakim, The Preparation and Some Properties of Disilylamine, *Inorg. Chem.*, 1966, **5**, 167.
147 A. B. Burg and E. S. Kuljian, Silyl-Amino Boron Compounds1, *J. Am. Chem. Soc.*, 1950, **72**, 3103.
148 R. L. Wells and R. Schaeffer, Studies of Silicon-Nitrogen Compounds. The Base-Catalyzed Elimination of Silane from Trisilylamine 1,2, *J. Am. Chem. Soc.*, 1966, **88**, 37.
149 M. Xiao, X. Lei, D. P. Spence, H. Chandra, B. Han, M. L. O'Neil, S. G. Mayorga and A. Mallikarjunan, US9337018B2, 2016.
150 M. Abedini and A. G. MacDiarmid, The Preparation and Properties of Some New Nitrogen and Fluorine Derivatives of Disilane, *Inorg. Chem.*, 1963, **2**, 608.
151 B. J. Aylett and M. J. Hakim, Silicon–nitrogen compounds. Part VI. The preparation and properties of disilazane, *J. Chem. Soc., A: Inorg. Phys. Theor.*, 1969, 639.
152 B. J. Aylett, The silyl group as an electron acceptor, *J. Inorg. Nucl. Chem.*, 1956, **2**, 325.
153 L. Ward and A. G. MacDiarmid, The preparation and properties of bis-disilanyl sulphide and tris-disilanylamine, *J. Inorg. Nucl. Chem.*, 1961, **21**, 287.
154 S. G. Kim, J. J. Park, S. J. Jang, B. Yang, S. Lee, S. D. Lee, S. I. Lee and M. W. Kim, WO2018182305A1, 2018.
155 S. W. Yoon, H. Y. Yang, H. N. Kim and G. H. Jo, US2023094481A1, 2023.
156 M. Xiao, X. Lei and D. P. Spence, EP2818474A1, 2014.
157 (*a*) Y. Jiang, X. Xu, W. Wang, Q. Liu and F. Tao, CN117510533A, 2024; (*b*) C. Tang, S. Zhu and J. Li, CN115677747A, 2023.
158 M. Söldner, A. Schier and H. Schmidbaur, 1,2-Disilanediyl Bis(triflate), $F_3CSO_3–SiH_2SiH_2–O_3SCF_3$, as the Key Intermediate for a Facile Preparation of Open-Chain and Cyclic 1,1- and 1,2-Diaminodisilanes, *Inorg. Chem.*, 1997, **36**, 1758.
159 B. M. Ketola, J. A. Maddock, B. D. Rekken, M. D. Telgenhoff and X. Zhou, WO2017106632A1, 2017.
160 M. Xiao, M. R. MacDonald, R. Ho and X. Lei, EP2913334A1, 2015.
161 A. Foss, J. Maddock, B. Rekken and M. Telgenhoff, WO2019226207A1, 2019.
162 T. T. Nguyen, T. K. Mukhopadhyay, S. N. MacMillan, M. T. Janicke and R. J. Trovitch, Synthesis of Aminosilane Chemical Vapor Deposition Precursors and Polycarbosilazanes through Manganese-Catalyzed Si–N Dehydrocoupling, *ACS Sustainable Chem. Eng.*, 2022, **10**, 4218.
163 B. D. Rekken, US2021130374A1, 2021.
164 A. Sanchez, G. Itov, P. Zhang and M. Stephens, WO2015048237A2, 2015.
165 X. Zhou, WO2017106615A1, 2017.
166 B. D. Rekken, X. Zhou, B. K. Hwang and B. Ketola, WO2017106587A1, 2017.
167 H. J. Emeléus, A. G. Maddock and C. Reid, 68. Derivatives of monosilane. Part II. The iodo-compounds, *J. Chem. Soc.*, 1941, 353.
168 A. G. MacDiarmid, Pseudo-halogen derivatives of monosilane, *J. Inorg. Nucl. Chem.*, 1956, **2**, 88.
169 E. A. V. Ebsworth and J. C. Thompson, The preparation and properties of some silyl esters, *J. Chem. Soc., A: Inorg. Phys. Theor.*, 1967, 69.

Open Access Article. Published on 24 April 2026. Downloaded on 5/15/2026 8:48:04 PM. This article is licensed under a Creative Commons Attribution 3.0 Unported Licence.

170 C. Glidewell, Reactions of silylphosphine with amines and imines, *Inorg. Nucl. Chem. Lett.*, 1974, **10**, 39.
171 C. Glidewell, Some reactions of disilyl sulphide, *J. Inorg. Nucl. Chem.*, 1969, **31**, 1303.
172 E. A. V. Ebsworth and M. J. Mays, 945. The preparation and properties of silyl isocyanate, *J. Chem. Soc.*, 1962, 4844.
173 S. Sujishi and S. Witz, The Reaction of Silylamines with Boron Trifluoride. Methyl- and Silylaminoboron Difluorides, *J. Am. Chem. Soc.*, 1957, **79**, 2447.
174 W. M. Scantlin and A. D. Norman, Borane-catalyzed condensation of trisilazane and N-methyldisilazane, *Inorg. Chem.*, 1972, **11**, 3082.
175 E. A. V. Ebsworth and M. J. Mays, 653. The preparation and properties of silyl azide, *J. Chem. Soc.*, 1964, 3450.
176 G. Maier, J. Glatthaar and H. P. Reisenauer, Hetero–π–Systeme, 17: Aminosilylen (Aminosilandiyl), *Chem. Ber.*, 1989, **122**, 2403.
177 G. Fritz and H. O. Berkenhoff, Hydrolyse, Alkoholyse und Ammonolyse des Silylphosphins, *Z. Anorg. Allg. Chem.*, 1957, **289**, 250.
178 A. D. Norman and W. L. Jolly, Reaction of silylphosphine with ammonia, *Inorg. Chem.*, 1979, **18**, 1594.
179 E. A. V. Ebsworth and M. J. Mays, 959. The preparation and properties of disilylcyanamide, *J. Chem. Soc.*, 1961, 4879.
180 E. Ebsworth and M. J. Mays, The vibrational spectra and structure of $(SiH_3)_2CN_2$, *Spectrochim. Acta*, 1963, **19**, 1127.
181 C. Glidewell and A. G. Robiette, Gas phase electron diffraction study of SiH_3N_3 and $(SiH_3)_2NCN$, *Chem. Phys. Lett.*, 1974, **28**, 290.
182 H. Schmidbaur and H. Schuh, Die unterschiedliche Reaktivität von 1,4-Disilabutan und n-Tetrasilan gegenüber sekundären Aminen/Differences in Reactivity of 1,4-Disilabutane and n-Tetrasilane towards Secondary Amines, *Z. Naturforsch., B*, 1990, **45**, 1679.
183 A. Sanchez, G. Itov, M. Khandelwal, C. Ritter, P. Zhang, J. M. Girard, Z. Wan, G. Kuchenbeiser, D. Orban, S. Kerrigan, R. Pesaresi, M. D. Stephens, Y. Wang and G. Husson, US2018072571A1, 2018.
184 G. Fritz and P. Scheer, Silylphosphanes: Developments in Phosphorus Chemistry, *Chem. Rev.*, 2000, **100**, 3341.
185 S. M. Sze, Y. Li and K. K. Ng, *Physics of semiconductor devices*, Wiley, Hoboken, NJ, Chichester, West Sussex, 2021.
186 *The Chemistry of Metal CVD*, ed. T. T. Kodas and M. J. HampdenSmith, Wiley, Weinheim, New York, 1994.
187 Z. Rappoport and Y. Apeloig, *The Chemistry of Organic Silicon Compounds*, Wiley, 2001, vol. 3.
188 G. Fritz, Bildung, Eigenschaften und Reaktionen des Silylphosphins, *Z. Anorg. Allg. Chem.*, 1955, **280**, 332.
189 G. Fritz, G. Becker, G. Poppenburg, M. Rocholl and G. Trenczeck, Compounds of Phosphorus with Silicon and Aluminum, *Angew. Chem., Int. Ed. Engl.*, 1966, **5**, 53.
190 G. Fritz and H. O. Berkenhoff, Über ein Siliciumphosphid Si2P, *Z. Anorg. Allg. Chem.*, 1959, **300**, 205.
191 I. H. Sabherwal and A. B. Burg, A convenient synthesis of silylphosphine, *Inorg. Nucl. Chem. Lett.*, 1972, **8**, 27.
192 J. Blazejowski and F. W. Lampe, The IR multiphoton decomposition of PH_3 SiH_4 mixtures sensitized by SiF_4, *J. Photochem.*, 1984, **24**, 235.
193 J. Blazejowski and F. W. Lampe, Monosilylphosphine formation by rapid silylene insertion in the IR photochemistry of SiH4-PH3 mixtures, *J. Photochem.*, 1982, **20**, 9.
194 J. Blazejowski and F. W. Lampe, The 147 nm photolysis of phosphine—silane mixtures, *J. Photochem.*, 1981, **16**, 105.
195 J. E. Drake and W. L. Jolly, Preparation of mixed hydrides of silicon, germanium, phosphorus, and arsenic, *Chem. Ind.*, 1962, 1470.
196 S. D. Gokhale and W. L. Jolly, The Synthesis of Disilanylphosphine and Disilylphosphine in a Silent Electric Discharge, *Inorg. Chem.*, 1965, **4**, 596.
197 S. D. Gokhale and W. L. Jolly, Disilanylphosphine and Disilylphosphine, *Inorg. Chem.*, 1964, **3**, 1141.
198 J. E. Drake, N. Goddard and J. Simpson, Some reactions of monohalogenated hydrides with monosilylphosphine and monosilylarsine, *Inorg. Nucl. Chem. Lett.*, 1968, **4**, 361.
199 J. E. Drake, N. Goddard and C. Riddle, Silicon–phosphorus hydrides. Part III. Exchange reactions of monosilylphosphine with chlorinated germanes and silanes, *J. Chem. Soc., A: Inorg. Phys. Theor.*, 1969, 2704.
200 E. Amberger and H. D. Boeters, Trisilylverbindungen, *Chem. Ber.*, 1964, **97**, 1999.
201 A. J. Blake, E. A. V. Ebsworth and S. G. D. Henderson, Structure of trisilylphosphine, $P(SiH_3)_3$, at 100 K, *Acta Crystallogr., Sect. C: Struct. Chem.*, 1991, **47**, 486.
202 C. Glidewell and G. M. Sheldrick, Preparation and properties of mono- and di-silylphosphine and mono-and disilyl-arsine, *J. Chem. Soc., A: Inorg. Phys. Theor.*, 1969, 350.
203 C. R. Russ and A. G. MacDiarmid, Cleavage and Addition Reactions of Silylphosphines and Silylarsines, *Angew. Chem., Int. Ed. Engl.*, 1966, **5**, 418.
204 D. E. Wingeleth and A. D. Norman, Redistribution of Primary Silyl- and Germylphosphines: Synthesis of Trisilyl- and Trigermylphosphines, *Phosphorus Sulfur Relat. Elem.*, 1988, **39**, 123.
205 J. E. Drake and N. Goddard, Silicon-phosphorus hydrides 2a comparative study by proton magnetic resonance spectroscopy of isomers disilanyl- and disilyl-phosphine, *J. Chem. Soc., A: Inorg. Phys. Theor.*, 1969, 662–665.
206 *Hydrides of Groups IV and V*, ed. W. L. Jolly, Interscience, New York, 1968, vol. 4.
207 J. B. Tice, A. V. G. Chizmeshya, J. Tolle, V. R. d' Costa, J. Menendez and J. Kouvetakis, Practical routes to $(SiH_3)_3P$: applications in group IV semiconductor activation and in group III-V molecular synthesis, *Dalton Trans.*, 2010, **39**, 4551.
208 F. Li, J. M. Girard and P. Zhang, WO2023121973A1, 2023.
209 A. E. Finholt, C. Helling, V. Imhof, L. Nielsen and E. Jacobson, Complex Aluminum Hydrides Containing Nitrogen, Phosphorus, and Arsenic, *Inorg. Chem.*, 1963, **2**, 504.

 This journal is © the Partner Organisations 2026

Open Access Article. Published on 24 April 2026. Downloaded on 5/15/2026 8:48:04 PM. This article is licensed under a Creative Commons Attribution 3.0 Unported Licence.

210 A. D. Norman, A new general method for the synthesis of unsubstituted phosphino-silanes and -germanes, *Chem. Commun.*, 1968, 812.
211 G. Fritz and H. Schäfer, Bildung von $NaAl(PH_2)_4$, $NaAl(HPCH_3)_4$ und die präparative Darstellung von $H_3Si\text{-}PH_2$ und seiner PH-haltigen Derivate, *Z. Anorg. Allg. Chem.*, 1971, **385**, 243.
212 A. D. Norman and D. C. Wingeleth, Lithium tetraphosphinoaluminate phosphination of halosilanes and -germanes, *Inorg. Chem.*, 1970, **9**, 98.
213 A. D. Norman, Bis(phosphino)silane and tris(phosphino) silane, *J. Am. Chem. Soc.*, 1968, **90**, 6556.
214 G. Becker, B. Eschbach, D. Käshammer and O. Mundt, Metallderivate von Molekülverbindungen. VII. Bis[1,2-bis (dimethylamino)ethan-N,N′]lithium-disilylphosphanid Synthese und Struktur, *Z. Anorg. Allg. Chem.*, 1994, **620**, 29.
215 G. Fritz, H. Schäfer and W. Hölderich, Zur Metallierung der PH_2–Gruppe in Silylphosphinen, *Z. Anorg. Allg. Chem.*, 1974, **407**, 266.
216 J. W. Anderson and J. E. Drake, Silicon–phosphorus hydrides. Part IV. The disilylphosphinoaluminate anion, *J. Chem. Soc., A: Inorg. Phys. Theor.*, 1971, 2246.
217 G. Fritz and G. Becker, Umsetzungen der Silylphosphine mit $LiP(C_2H_5)_2$ und $LiCH_3$, *Z. Anorg. Allg. Chem.*, 1970, **372**, 180.
218 S. Cradock, E. A. V. Ebsworth, H. Moretto, D. W. H. Rankin and W. J. Savage, Lithium-Derivate von Silanol und Verwandten Verbindungen, *Angew. Chem.*, 1973, **85**, 344.
219 S. Cradock, E. A. V. Ebsworth, D. W. H. Rankin and W. J. Savage, Preparation and spectroscopic studies of some reactions of lithium derivatives of silanol, disilylphosphine, and related compounds, *J. Chem. Soc., Dalton Trans.*, 1976, 1661.
220 H. O. Pierson, *Handbook of chemical vapor deposition (CVD). Principles, technology, and applications*, Noyes Publications, Park Ridge, N.J., U.S.A, 1992.
221 J. E. Drake and J. Simpson, Reactions of monosilylarsine with some boron Lewis acids and the reaction of monosilylphosphine with boron tribromide, *J. Chem. Soc., A: Inorg. Phys. Theor.*, 1968, 1039.
222 J. W. Anderson and J. E. Drake, Reactions of 'LiAl$(AsH_2)_4$', *Inorg. Nucl. Chem. Lett.*, 1969, **5**, 887.
223 J. W. Anderson and J. E. Drake, Preparation and properties of some primary silyl- and germyl-arsines, *J. Chem. Soc., A: Inorg. Phys. Theor.*, 1970, 3131.
224 A. Kashizadeh, R. Basnet, A. Liu, Z. Yang, L. Black, C. Sun, W. Han, Y. Wang and D. Macdonald, High Quality Antimony–Doped n–Type Silicon Wafers for Solar Cell Applications, *Sol. RRL*, 2025, **9**, e2500335.
225 E. Amberger and H. Boeters, Notizen: Darstellung und Eigenschaften von Trisilylstiban, *Z. Naturforsch., B*, 1963, **18**, 157.
226 M. Ohring, *Materials Science of Thin Films*, Elsevier, 2002.
227 C. M. Hessel, E. J. Henderson and J. G. C. Veinot, Hydrogen Silsesquioxane: A Molecular Precursor for Nanocrystalline $Si–SiO_2$ Composites and Freestanding Hydride-Surface-Terminated Silicon Nanoparticles, *Chem. Mater.*, 2006, **18**, 6139.
228 A. Stock, C. Somieski and R. Wintgen, Siliciumwasserstoffe. III: Disiloxan, $(SiH_3)_2O$; zur Kenntnis des Tetrachlor monosilans, $SiCl_4$, und des Hexachlor–disiloxans, $(SiCl_3)_2O$, *Ber. Dtsch. Chem. Ges.*, 1917, **50**, 1754.
229 H. J. Emeléus, A. G. MacDiarmid and A. G. Maddock, Sulphur and selenium derivatives of monosilane, *J. Inorg. Nucl. Chem.*, 1955, **1**, 194.
230 W. A. Kriner, A. G. MacDiarmid and E. C. Evers, The Interaction of Disiloxane with Aluminum Halides 1, *J. Am. Chem. Soc.*, 1958, **80**, 1546.
231 L. G. L. Ward and A. G. MacDiarmid, The Preparation and Properties of Disilanyl Iodide and Bis-disilanyl Ether 1, *J. Am. Chem. Soc.*, 1960, **82**, 2151.
232 B. Sternbach and A. G. MacDiarmid, The Preparation and Properties of Silyl Methyl Ether 1, *J. Am. Chem. Soc.*, 1961, **83**, 3384.
233 M. Onyszchuk, The interaction of disiloxane with boron trifluoride and trichloride, *Can. J. Chem.*, 1961, **39**, 808.
234 C. H. van Dyke and A. G. MacDiarmid, The Reaction of 1,2-Disilyldisiloxane, 1-Silyldisiloxane, and 1,1,1-Trimethyldisiloxane with Boron Trichloride, *Inorg. Chem.*, 1964, **3**, 747.
235 C. H. van Dyke, The interaction of disiloxane and methoxysilane with phosphorus(III) halides, *J. Inorg. Nucl. Chem.*, 1968, **30**, 81.
236 C. Glidewell and D. W. H. Rankin, Germyl and silyl derivatives of phenol and thiophenol, *J. Chem. Soc. A*, 1969, 753.
237 J. E. Drake, H. E. Henderson and R. T. Hemmings, Silyl and germyl derivatives of trifluoroacetic and trichloroacetic acid, *Inorg. Chem.*, 1977, **16**, 1682.
238 C. Glidewell, Reaction of silyl bromide with some group VI hydrido-anions, *J. Chem. Soc. A*, 1971, 823.
239 F. Fehér, I. Fischer and D. Skrodzki, Beiträge zur Chemie des Siliciums und Germaniums. XXXI [1]. Die photochemische Darstellung neuer Isopropoxyderivate des Tri–, n–Tetra–, iso–Tetra– und n–Pentasilans und deren saure Hydrolyse zu Bis–Silanyl–Äthern, *Z. Anorg. Allg. Chem.*, 1980, **466**, 29.
240 X. Li, W. Zhang, X. Guo, C. Lu, J. Wei and J. Fang, Constructing heterojunctions by surface sulfidation for efficient inverted perovskite solar cells, *Science*, 2022, **375**, 434.
241 A. J. Downs and E. A. V. Ebsworth, 705. Silyl trifluoromethyl sulphide, *J. Chem. Soc.*, 1960, 3516.
242 B. Sternbach and A. G. MacDiarmid, The preparation and properties of silyl methyl sulphide, *J. Inorg. Nucl. Chem.*, 1961, **23**, 225.
243 M. Schmeißer and H. Frouzanfar, Darstellung von Mercaptosilanen, *Z. Chem.*, 1968, **8**, 254.
244 E. A. V. Ebsworth, C. Glidewell and G. M. Sheldrick, Some reactions of trisilylphosphine, *J. Chem. Soc. A*, 1969, 352.
245 J. E. Drake and C. Riddle, Electric discharge reactions of silane and germane with some volatile group VI species, *J. Chem. Soc. A*, 1970, 3134.

Open Access Article. Published on 24 April 2026. Downloaded on 5/15/2026 8:48:04 PM. This article is licensed under a Creative Commons Attribution 3.0 Unported Licence.

246 J. W. Anderson and J. E. Drake, A. high yield synthesis of methylthio and methylseleno derivatives of silicon, germanium, and tin, *Inorg. Nucl. Chem. Lett.*, 1971, **7**, 1007.
247 S. Cradock, E. A. V. Ebsworth and H. F. Jessep, Ammonium salts of silanethiol and silaneselenol, *J. Chem. Soc., Dalton Trans.*, 1972, 359.
248 S. Cradock, E. A. V. Ebsworth, H. Moretto, D. W. H. Rankin and W. J. Savage, Lithium Derivatives of Silanol and Related Compounds, *Angew. Chem., Int. Ed. Engl.*, 1973, **12**, 317.
249 M. A. Finch and C. H. van Dyke, Mixed silyl germyl Group VIA derivatives, *Inorg. Chem.*, 1975, **14**, 136.
250 A. Haas and M. Vongehr, Darstellung und Eigenschaften von Cyclotrisilathian sowie Trifluormethylchalkogenylsilanen $(CF_3X)_nSiH_{4(n}$ (X = S, Se und n = 1, 2, 3, 4), *Z. Anorg. Allg. Chem.*, 1978, **447**, 119.
251 A. Haas, R. Hitze, C. Krüger and K. Angermund, Darstellung und Charakterisierung von Silathia- und Silasela-Grundkörpern/Synthesis and Characterisation of Silathia and Silasela Basic Compounds, *Z. Naturforsch., B*, 1984, **39**, 890.
252 A. Haas, R. Süllentrup and C. Krüger, Synthese und Charakterisierung neuer Cyclischer und acyclischer Silachalkogenane mit Disilanyleinheiten, *Z. Anorg. Allg. Chem.*, 1993, **619**, 819.
253 (*a*) J. Kang, S. Tongay, J. Zhou, J. Li and J. Wu, Band offsets and heterostructures of two-dimensional semiconductors, *Appl. Phys. Lett.*, 2013, **102**, 012111; (*b*) M. Madhubalan, S. Sathish, M. Mahivardhan, P. Thandapani, K. K. Abimanyu, R. Kumar, J.-H. Seo, B.-W. Gu, S. M. Prabhu and B.-H. Jeon, Advances in Selenium–Based Materials for Supercapacitors: Chemistry, Interaction Mechanisms, and Practical Applications, *Small Struct.*, 2025, **7**, e202500715; (*c*) C. Wang, J. Guo, D. Liu, Z. Lin, S. Guo, S. Cai, J. Yan, B. He, Z. Zhang, M. Zhang and Y. Chai, Band-hybridized selenium contact for p-type semiconductors, *Nat. Nanotechnol.*, 2026, **21**, 207.
254 E. A. V. Ebsworth, H. J. Emeléus and N. Welcman, 440. Perfluoroalkyl silyl selenides, *J. Chem. Soc.*, 1962, 2290.
255 S. Cradock, E. A. V. Ebsworth and D. W. H. Rankin, Studies in germyl chemistry. Part VIII. Digermyl selenide and digermyl telluride, *J. Chem. Soc. A*, 1969, 1628.
256 G. K. Barker, J. E. Drake and R. T. Hemmings, Methylseleno-derivatives of Group IV. Part II. Hydrides, *J. Chem. Soc., Dalton Trans.*, 1974, 450.
257 J. E. Drake and R. T. Hemmings, Silyl and germyl derivatives of selenophenol and related species, *J. Chem. Soc., Dalton Trans.*, 1976, 1730.
258 J. E. Drake, B. M. Glavinčevski and R. T. Hemmings, Studies of silyl and germyl Group VI species. Part IV. Dimethyl- and tetramethyl-disilyl chalcogenides and related species, *Can. J. Chem.*, 1980, **58**, 2161.
259 A. Haas and R. Hitze, Preparation and Characterisation of Cyclotri(silaselane) $(H_2Si\text{-}Se)_3$, *Z. Naturforsch., B*, 1981, **36**, 1069.
260 (*a*) J. Zha, D. Dong, H. Huang, Y. Xia, J. Tong, H. Liu, H. P. Chan, J. C. Ho, C. Zhao, Y. Chai and C. Tan, Electronics and Optoelectronics Based on Tellurium, *Adv. Mater.*, 2024, **36**, e2408969; (*b*) S. Siddique, C. Chowde Gowda, S. Demiss, R. Tromer, S. Paul, K. K. Sadasivuni, E. F. Olu, A. Chandra, V. Kochat, D. S. Galvão, P. Kumbhakar, R. Mishra, P. M. Ajayan and C. S. Tiwary, Emerging two-dimensional tellurides, *Mater. Today*, 2021, **51**, 402; (*c*) J. Y. Kim, S. H. Park, H. J. Yang, M. W. Kim, D. H. Kim, S.-J. Choi and Y. J. Lee, Tellurium-based materials for nanoelectronics: applications, challenges, and outlooks, *Microstructures*, 2026, **6**, 2026006.
261 H. Bürger and U. Goetze, Disilyltellurid, *Inorg. Nucl. Chem. Lett.*, 1967, **3**, 549.
262 J. E. Drake and R. T. Hemmings, Studies of silyl and germyl Group 6 species. 5. Silyl and germyl derivatives of methane- and benzenetellurols, *Inorg. Chem.*, 1980, **19**, 1879.
263 (*a*) E. J. A. Pope and C. L. Hill, US8987402B2, 2015; (*b*) M. Bauer and S. G. Thomas, US8367528B2, 2013; (*c*) P. Tomasini and N. Cody, US7772097B2, 2010; (*d*) P. Tomasini, C. Arena, M. Bauer, C. Nyles, R. Betrram, W. Jianqing and M. D. Stephens, US2008026149A, 2008.
264 (*a*) W. Kim, N. Hwang and Y. Lee, US2021222300A1, 2021; (*b*) T. Ying and Y. N. Sharad, WO2020123907A1, 2020.
265 H. J. Emeléus and A. G. Maddock, 77. Derivatives of monosilane. Part III. The fluoromonosilanes, *J. Chem. Soc.*, 1944, 293.
266 D. Solan and A. B. Burg, Cocondensation reaction of difluorosilene with diborane. New polyfluoropolysilanes, *Inorg. Chem.*, 1972, **11**, 1253.
267 G. R. Langford, D. C. Moody and J. D. Odom, Reaction of silicon difluoride with phosphine, *Inorg. Chem.*, 1975, **14**, 134.
268 K. G. Sharp and J. F. Bald, Redistribution processes in mixed halodisilanes. Reaction of silicon difluoride with hydrogen bromide, *Inorg. Chem.*, 1975, **14**, 2553.
269 K. G. Sharp and J. L. Margrave, Silicon-fluorine chemistry. VII. Reaction of silicon difluoride with hydrogen sulfide, *Inorg. Chem.*, 1969, **8**, 2655.
270 J. J. D'Errico and K. G. Sharp, A new synthetic route to fluorodisilanes via selective reduction of halofluorodisilanes, *Inorg. Chem.*, 1989, **28**, 2886.
271 J. E. Drake and N. Goddard, Halogenodisilanes, *J. Chem. Soc. A*, 1970, 2587.
272 J. E. Drake, N. Goddard and N. P. C. Westwood, Halogenosilanes. Part III. Fluoro-, chloro-, and bromo-derivatives of trisilane, *J. Chem. Soc. A*, 1971, 3305.
273 K. Hassler and W. Köll, Synthese und eigenschaften von 1,1,2,2-Tetrachlorund 1,1,2,2-Tetrafluordisilan, *J. Organomet. Chem.*, 1995, **487**, 223.
274 H. Stüger, Synthese 1,4-disubstituierter tetrasilane durch selektive spaltung von Si-phenyl-bindungen, *J. Organomet. Chem.*, 1992, **433**, 11.
275 F. Höfler and R. Jannach, Zur darstellung fluorierter siliciumwasserstoffe, *Inorg. Nucl. Chem. Lett.*, 1974, **10**, 711.

 This journal is © the Partner Organisations 2026

Open Access Article. Published on 24 April 2026. Downloaded on 5/15/2026 8:48:04 PM. This article is licensed under a Creative Commons Attribution 3.0 Unported Licence.

276 J. E. Drake and N. P. C. Westwood, Halogenosilanes. Part II. Electrical discharge production of halogenodisilanes, *J. Chem. Soc. A*, 1971, 3300.
277 C. Ramírez-Márquez, Solar-Grade Silicon in the Energy Transition: A Strategic Commodity for the Global Photovoltaic Market, *Commodities*, 2025, **4**, 18.
278 (*a*) F. Chigondo, From Metallurgical-Grade to Solar-Grade Silicon: An Overview, *Silicon*, 2018, **10**, 789; (*b*) S. Yadav, K. Chattopadhyay and C. V. Singh, Solar grade silicon production: A review of kinetic thermodynamic and fluid dynamics based continuum scale modeling, *Renewable Sustainable Energy Rev.*, 2017, **78**, 1288.
279 R. K. Agarwal, J. F. Lehmann, C. G. Coe and D. J. Tempel, US8206676B2, 2012.
280 R. P. Hollandsworth, W. M. Ingle and M. A. Ring, Halogenation of silanes by silver chloride and silver bromide, *Inorg. Chem.*, 1967, **6**, 844.
281 G. Fritz and D. Kummer, Reaktionen der Phenylsilane mit Halogen und Halogenwasserstoffen, *Z. Anorg. Allg. Chem.*, 1961, **308**, 105.
282 C. H. van Dyke and A. G. MacDiarmid, Formation of diborane by the interaction of disilane with boron trichloride, *J. Inorg. Nucl. Chem.*, 1963, **25**, 1503.
283 J. E. Drake and N. Goddard, The formation and identification of chlorodisilanes and monochlorotrisilane, *Inorg. Nucl. Chem. Lett.*, 1968, **4**, 385.
284 R. P. Hollandsworth and M. A. Ring, Chlorodisilanes. Preparation and silicon-hydrogen stretching frequencies, *Inorg. Chem.*, 1968, **7**, 1635.
285 (*a*) R. P. Hollandsworth, W. M. Ingle and M. A. Ring, Halogenation of silanes by silver chloride and silver bromide, *Inorg. Chem.*, 1967, **6**, 844; (*b*) A. J. Vanderwielen and M. A. Ring, Chlorination of silanes by silver chloride, *Inorg. Chem.*, 1972, **11**, 246.
286 M. Abedini, C. H. van Dyke and A. G. MacDiarmid, Preparation of disilanyl chloride and disilanyl bromide by the reaction of disilane with hydrogen halide, *J. Inorg. Nucl. Chem.*, 1963, **25**, 307.
287 F. Fehér and F. Ocklenburg, Beiträge zur Chemie des Siliciums und Germaniums. XXXV. Halogenierung von höheren Silanen mit Zinn(IV) – chlorid bzw. Quecksilber (II)–chlorid, *Z. Anorg. Allg. Chem.*, 1984, **515**, 36.
288 F. Fehér, P. Plichta and R. Guillery, Chemistry of silicon and germanium. XII. Transformation of disilane, trisilane, and n-tetrasilane with elementary bromine and chlorine in Freon, *Inorg. Chem.*, 1971, **10**, 606.
289 A. J. Vanderwielen and M. A. Ring, Chlorination of silanes by silver chloride, *Inorg. Chem.*, 1972, **11**, 246.
290 H. Stueger, T. Mitterfellner, R. Fischer, C. Walkner, M. Patz and S. Wieber, Partial halogenation of cyclic and branched perhydropentasilanes, *Inorg. Chem.*, 2012, **51**, 6173.
291 T. Lainer, R. Fischer, M. Leypold, M. Holthausen, O. Wunnicke, M. Haas and H. Stueger, Unusually selective synthesis of chlorohydrooligosilanes, *Chem. Commun.*, 2020, **56**, 13812.
292 F. Höfler, R. Jannach and W. Raml, Darstellung und Eigenschaften einiger Hochchlorierter Oligosilane, *Z. Anorg. Allg. Chem.*, 1977, **428**, 75.
293 A. Gupper and K. Hassler, Synthesis and Properties of 1,2-Dichlorodisilane and 1,1,2-Trichlorodisilane, *Eur. J. Inorg. Chem.*, 2001, **2001**, 2007.
294 K. Hassler and W. Köll, Chlor-, Brom- und Iodtrisilane: Synthesen und ^{29}Si-Kernresonanzspektren, *J. Organomet. Chem.*, 1997, **540**, 113.
295 H. Söllradl and E. Hengge, Vergleichende ^{29}Si-NMR-untersuchungen an verschiedenen disilanderivaten, *J. Organomet. Chem.*, 1983, **243**, 257.
296 W. Uhlig, Synthese funktionell substituierter Disilane auf der Basis von Triflatderivaten, *Z. Anorg. Allg. Chem.*, 1993, **619**, 1479.
297 (*a*) J. C. Schuhmacher, *The production of solar-cell-grade silicon from bromosilanes*, Washington, DC, 1979; (*b*) J. C. Schuhmacher, EP0114876B1, 1990.
298 N. S. Hosmane, Stannic bromide: A selective brominating agent for silanes, *Inorg. Nucl. Chem. Lett.*, 1974, **10**, 1077.
299 L. G. L. Ward, A. D. Norman, S. K. Gondal and A. G. MacDiarmid, in *Inorganic Syntheses*, ed. W. L. Jolly, Wiley, 1968, vol. 11, pp. 159–170.
300 T. C. Geisler, C. G. Cooper and A. D. Norman, Bromination of silanes and germane, *Inorg. Chem.*, 1972, **11**, 1710.
301 H. Stüger and P. Lassacher, Darstellung und spektroskopische charakterisierung verzweigter funktioneller hexasilangerüste, *J. Organomet. Chem.*, 1993, **450**, 79.
302 (*a*) G. Tamizhmani, M. Cocivera, R. T. Oakley and P. Del Bel Belluz, Some physical properties of undoped amorphous silicon prepared by a new CVD process using iodosilanes, *Chem. Mater.*, 1990, **2**, 473; (*b*) G. Kuchenbeiser and B. Lefevre, US9777373B2, 2017.
303 A. G. Maddock, C. Reid and H. J. Emeléus, New Iodine and Fluorine Derivatives of Monosilane, *Nature*, 1939, **144**, 328.
304 B. J. Aylett and I. A. Ellies, The preparation of iodosilanes from phenylchlorosilanes, *J. Chem. Soc.*, 1960, 3415.
305 F. Fehér, B. Mostert, A. G. Wronka and G. Betzen, Präprative Darstellung von Disilanyl- und Trisilanyljodiden, *Monatsh. Chem.*, 1972, **103**, 959.
306 F. Fehér, P. Plichta and R. Guillery, Beiträge zur Chemie des Siliciums und Germaniums, XI. Darstellung und Untersuchung neuer Jodderivate des Disilans, Trisilans und n–Tetrasilans, *Chem. Ber.*, 1970, **103**, 3028.
307 (*a*) K. Schenzel and K. Hassler, Bromdisilan: Verbesserte synthese, schwingungsspektren und normalkoordinatenanalyse, *Spectrochim. Acta, Part A*, 1994, **50**, 139; (*b*) K. Hassler, W. Köll and K. Schenzel, Syntheses, infrared and Raman vibrational spectra, normal coordinate analyses and 29Si-NMR-Spectra of halogenated disilanes $X_nSi_2H_{6(n}$ (X = F, Cl, Br, I), *J. Mol. Struct.*, 1995, **348**, 353; (*c*) K. Hassler and M. Pöschl, Synthese und Kernresonanzspektren von Bromdisilanen und Ioddisilanen, *J. Organomet. Chem.*, 1990, **398**, 225.

Open Access Article. Published on 24 April 2026. Downloaded on 5/15/2026 8:48:04 PM. This article is licensed under a Creative Commons Attribution 3.0 Unported Licence.

308 U. Pöschl and K. Hassler, Synthesis and Spectroscopy of Halogenated Cyclopentasilanes, *Organometallics*, 1996, **15**, 3238.
309 K. G. Sharp and J. F. Bald, Redistribution processes in mixed halodisilanes. Reaction of silicon difluoride with hydrogen bromide, *Inorg. Chem.*, 1975, **14**, 2553.
310 J. Emsley, *Nature's building blocks: an A-Z guide to the elements*, Oxford University Press, 2001.
311 R. A. Street, *Hydrogenated Amorphous Silicon*, Cambridge University Press, 2010.
312 J. A. Rossi and R. K. Willardson, *Silicon Epitaxy*, Elsevier textbooks, s.l., 1st edn, 2001, vol. 72.
313 *Springer Handbook of Electronic and Photonic Materials*, ed. S. Kasap and P. Capper, Springer US, Boston, MA, 2007.
314 P. Sutter, *Introduction to semiconductors : from materials to devices*, Springer, Cham, 2025.
315 *Charge Transport in Disordered Solids with Applications in Electronics*, ed. S. Baranovski, Wiley, Chichester, England, 2006.
316 (*a*) M. K. K. Takahashi, *Amorphous silicon solar cells*, Wiley, New York, 1986; (*b*) J. Nelson, *The Physics of Solar Cells*, Published by Imperial College Press and distributed by World Scientific Publishing Co, 2003; (*c*) A. J. McEvoy, L. Castañer and T. Markvart, *Solar cells : materials, manufacture and operation*, ed. A. McEvoy, L. Castaner and T. Markvart, Elsevier, Waltham, MA, 2nd edn, 2013; (*d*) S. K. Sharma, H. Im, D. Y. Kim and R. M. Mehra, Review on Se-and S-doped hydrogenated amorphous silicon thin films, *Indian J. Pure Appl. Phys.*, 2014, 293.
317 A. Vora, PhD, Dissertation, Michigan Technological University, 2015.
318 (*a*) *Solution Processing of Inorganic Materials*, ed. D. B. Mitzi, Wiley, Hoboken, New Jersey, 2008; (*b*) M. Mews, C. Mader, S. Traut, T. Sontheimer, O. Wunnicke, L. Korte and B. Rech, Solution-processed amorphous silicon surface passivation layers, *Appl. Phys. Lett.*, 2014, 105.
319 T. Bronger, P. H. Wöbkenberg, J. Wördenweber, S. Muthmann, U. W. Paetzold, V. Smirnov, S. Traut, Ü. Dagkaldiran, S. Wieber, M. Cölle, A. Prodi-Schwab, O. Wunnicke, M. Patz, M. Trocha, U. Rau and R. Carius, Solution–Based Silicon in Thin–Film Solar Cells, *Adv. Energy Mater.*, 2014, **4**, 1301871.
320 M. Allendorf, From Bunsen to VLSI, *Electrochem. Soc. Interface*, 1998, **7**, 36.
321 K. Choy, Chemical vapour deposition of coatings, *Prog. Mater. Sci.*, 2003, **48**, 57.
322 H. Katsui and T. Goto, in *Multi-dimensional Additive Manufacturing*, ed. S. Kirihara and K. Nakata, Springer Singapore, Singapore, 2021, pp. 75–95.
323 L. Sun, G. Yuan, L. Gao, J. Yang, M. Chhowalla, M. H. Gharahcheshmeh, K. K. Gleason, Y. S. Choi, B. H. Hong and Z. Liu, Chemical vapour deposition, *Nat. Rev. Methods Primers*, 2021, **1**, 1–20.
324 E. C. Nnadozie, K. I. Ogunwa, V. I. Chukwuike, O. O. Nnadozie and C. Ehikhase, Synthesis and Characterization of Carbonaceous Materials for Medical Applications: A Comprehensive Review, *BioMed*, 2024, **4**, 464.
325 H. C. Theuerer, Epitaxial Silicon Films by the Hydrogen Reduction of $SiCl_4$, *J. Electrochem. Soc.*, 1961, **108**, 649.
326 C. H. Lewis, H. C. Kelly, M. B. Giusto and S. Johnson, Preparation of High-Purity Silicon from Silane, *J. Electrochem. Soc.*, 1961, **108**, 1114.
327 W. O. Filtvedt, A. Holt, P. A. Ramachandran and M. C. Melaaen, Chemical vapor deposition of silicon from silane: Review of growth mechanisms and modeling/scaleup of fluidized bed reactors, *Sol. Energy Mater. Sol. Cells*, 2012, **107**, 188.
328 K. Tonokura and M. Koshi, Reaction kinetics in silicon chemical vapor deposition, *Curr. Opin. Solid State Mater. Sci.*, 2002, **6**, 479.
329 (*a*) M. T. Swihart and S. L. Girshick, Thermochemistry and Kinetics of Silicon Hydride Cluster Formation during Thermal Decomposition of Silane, *J. Phys. Chem. B*, 1999, **103**, 64; (*b*) P. Zhang, J. Duan, G. Chen, J. Li and W. Wang, Production of polycrystalline silicon from silane pyrolysis: A review of fines formation, *Sol. Energy*, 2018, **175**, 44.
330 C. W. Liu and J. C. Sturm, Low temperature chemical vapor deposition growth of β-SiC on (100) Si using methylsilane and device characteristics, *J. Appl. Phys.*, 1997, **82**, 4558.
331 S. Madapura, A. J. Steckl and M. Loboda, Heteroepitaxial Growth of SiC on Si(100) and (111) by Chemical Vapor Deposition Using Trimethylsilane, *J. Electrochem. Soc.*, 1999, **146**, 1197.
332 R. Hazbun, J. Hart, R. Hickey, A. Ghosh, N. Fernando, S. Zollner, T. N. Adam and J. Kolodzey, Silicon epitaxy using tetrasilane at low temperatures in ultra-high vacuum chemical vapor deposition, *J. Cryst. Growth*, 2016, **444**, 21.
333 D.-S. Byeon, C. Cho, D. Yoon, Y. Choi, K. Lee, S. Baik and D.-H. Ko, Epitaxial Growth of Si and SiGe Using High-Order Silanes without a Carrier Gas at Low Temperatures via UHVCVD and LPCVD, *Coatings*, 2021, **11**, 568.
334 G. Dhanaraj, Y. Chen, M. Dudley and H. Zhang, Growth and Surface Morphologies of 6H SiC Bulk and Epitaxial Crystals, *Mater. Sci. Forum*, 2006, **527–529**, 67.
335 O. Sneh, M. L. Wise, A. W. Ott, L. A. Okada and S. M. George, Atomic layer growth of SiO_2 on Si(100) using $SiCl_4$ and H_2O in a binary reaction sequence, *Surf. Sci.*, 1995, **334**, 135.
336 J. Gumpher, W. Bather, N. Mehta and D. Wedel, Characterization of Low-Temperature Silicon Nitride LPCVD from Bis(tertiary-butylamino)silane and Ammonia, *J. Electrochem. Soc.*, 2004, **151**, G353.
337 B. B. Burton, S. W. Kang, S. W. Rhee and S. M. George, SiO 2 Atomic Layer Deposition Using Tris(dimethylamino) silane and Hydrogen Peroxide Studied by in Situ Transmission FTIR Spectroscopy, *J. Phys. Chem. C*, 2009, **113**, 8249.
338 M. A. Todd, US2002173113A1, 2002.

Open Access Article. Published on 24 April 2026. Downloaded on 5/15/2026 8:48:04 PM. This article is licensed under a Creative Commons Attribution 3.0 Unported Licence.

339 *Chemical vapour deposition. Precursors, processes and applications*, ed. A. C. Jones and M. L. Hitchman, Royal Society of Chemistry, Cambridge, UK, 2009.
340 F. Wang and J. Wu, in *Modern Ion Plating Technology*, Elsevier, 2023, pp. 247–285.
341 R. Murri, *Silicon Based Thin Film Solar Cells*, Bentham Science Publishers, 2013.
342 H. F. Sterling and R. Swann, Chemical vapour deposition promoted by r.f. discharge, *Solid-State Electron.*, 1965, **8**, 653.
343 M. H. Brodsky, Plasma preparations of amorphous silicon films, *Thin Solid Films*, 1978, **50**, 57.
344 W. E. Spear and P. G. Le Comber, Substitutional doping of amorphous silicon, *Solid State Commun.*, 1975, **17**, 1193.
345 P. G. Le Comber, W. E. Spear and A. Ghaith, Amorphous-silicon field-effect device and possible application, *Electron. Lett.*, 1979, **15**, 179.
346 A. Matsuda, Formation kinetics and control of microcrystallite in μc-Si:H from glow discharge plasma, *J. Non-Cryst. Solids*, 1983, **59–60**, 767.
347 K. Pokhodnya, K. J. Anderson and P. R. Boudjouk, in 2014 IEEE 40th Photovoltaic Specialist Conference (PVSC), IEEE, 2014, 2014, pp. 3065–3067.
348 W.-J. Lee and Y.-H. Choa, Highly conformal carbon-doped SiCN films by plasma-enhanced chemical vapor deposition with enhanced barrier properties, *Thin Solid Films*, 2018, **657**, 32.
349 (*a*) H. Keppner, J. Meier, P. Torres, D. Fischer and A. Shah, Microcrystalline silicon and micromorph tandem solar cells, *Appl. Phys. A*, 1999, **69**, 169; (*b*) A. Shah, J. Meier, E. Vallat-Sauvain, N. Wyrsch, U. Kroll, C. Droz and U. Graf, Material and solar cell research in microcrystalline silicon, *Sol. Energy Mater. Sol. Cells*, 2003, **78**, 469.
350 (*a*) W. J. Soppe, C. Devilee, M. Geusebroek, J. Löffler and H.-J. Muffler, The effect of argon dilution on deposition of microcrystalline silicon by microwave plasma enhanced chemical vapor deposition, *Thin Solid Films*, 2007, **515**, 7490; (*b*) W. J. Soppe, A. C. W. Biebericher, C. Devilee, H. Donker and H. Schlemm, High-rate growth of microcrystalline silicon by microwave-PECVD, Proc. 3rd World Conf. Photovolt. Energy Convers., 2003.
351 (*a*) B. Rech, J. Müller, T. Repmann, O. Kluth, T. Roschek, J. Hüpkes, H. Stiebig and W. Appenzeller, Amorphous and Microcrystalline Silicon Based Solar Cells and Modules on Textured Zinc Oxide Coated Glass Substrates, *MRS Proc.*, 2003, **762**, 439–447; (*b*) T. Roschek, T. Repmann, J. Müller, B. Rech and H. Wagner, Comprehensive study of microcrystalline silicon solar cells deposited at high rate using 13.56 MHz plasma-enhanced chemical vapor deposition, *J. Vac. Sci. Technol., A*, 2002, **20**, 492.
352 (*a*) B. Rech and H. Wagner, Potential of amorphous silicon for solar cells, *Appl. Phys. A*, 1999, **69**, 155; (*b*) A. V. Shah, H. Schade, M. Vanecek, J. Meier, E. Vallat-Sauvain, N. Wyrsch, U. Kroll, C. Droz and J. Bailat, Thin–film silicon solar cell technology, *Prog. Photovolt. Res. Appl.*, 2004, **12**, 113.
353 *Coating materials. Computational aspects, applications and challenges*, ed. A. Verma, S. K. Sethi and S. Ogata, Springer, Singapore, 2023.
354 C. A. Dorval Dion and J. R. Tavares, Photo-initiated chemical vapor deposition as a scalable particle functionalization technology (a practical review), *Powder Technol.*, 2013, **239**, 484.
355 T. Saitoh, S. Muramatsu, T. Shimada and M. Migitaka, Optical and electrical properties of amorphous silicon films prepared by photochemical vapor deposition, *Appl. Phys. Lett.*, 1983, **42**, 678.
356 T. Inoue, M. Konagai and K. Takahashi, Photochemical vapor deposition of undoped and n -type amorphous silicon films produced from disilane, *Appl. Phys. Lett.*, 1983, **43**, 774.
357 T. F. Deutsch, D. J. Ehrlich and R. M. Osgood, Laser photodeposition of metal films with microscopic features, *Appl. Phys. Lett.*, 1979, **35**, 175.
358 Research progress of laser-assisted chemical vapor deposition, https://www.oejournal.org/oee/en/article/id/621efb7e99d88174c21c44a1, (accessed 2 March 2026).
359 H. Matsumura, H. Umemoto and A. Masuda, Cat-CVD (hot-wire CVD): how different from PECVD in preparing amorphous silicon, *J. Non-Cryst. Solids*, 2004, **338–340**, 19.
360 R. E. Schropp, Hot Wire Chemical Vapor Deposition: Recent Progress, Present State of the Art and Competitive Opportunities, *ECS Trans.*, 2009, **25**, 3.
361 (*a*) H. Wiesmann, A. K. Ghosh, T. McMahon and M. Strongin, a-Si : H produced by high-temperature thermal decomposition of silane, *J. Appl. Phys.*, 1979, **50**, 3752; (*b*) M. Strongin, A. K. Ghosh, H. J. Wiesmann, E. B. Rock and H. A. Lutz III, US4237151A, 1980.
362 (*a*) H. Matsumura, Catalytic Chemical Vapor Deposition (CTC–CVD) Method Producing High Quality Hydrogenated Amorphous Silicon, *Jpn. J. Appl. Phys.*, 1986, **25**, L949; (*b*) H. Matsumura, Study on catalytic chemical vapor deposition method to prepare hydrogenated amorphous silicon, *J. Appl. Phys.*, 1989, **65**, 4396.
363 J. Doyle, R. Robertson, G. H. Lin, M. Z. He and A. Gallagher, Production of high-quality amorphous silicon films by evaporative silane surface decomposition, *J. Appl. Phys.*, 1988, **64**, 3215.
364 A. H. Mahan, J. Carapella, B. P. Nelson, R. S. Crandall and I. Balberg, Deposition of device quality, low H content amorphous silicon, *J. Appl. Phys.*, 1991, **69**, 6728.
365 R. E. I. Schropp and M. Zeman, *Amorphous and Microcrystalline Silicon Solar cells: Modeling, Materials and Device Technology*, Springer US, 1998.
366 T. Suntola, Atomic layer epitaxy, *Thin Solid Films*, 1992, **216**, 84.
367 M. Leskelä and M. Ritala, Atomic layer deposition chemistry: recent developments and future challenges, *Angew. Chem., Int. Ed.*, 2003, **42**, 5548.
368 F. Hirose, M. Suemitsu and N. Miyamoto, Silane gas-source atomic layer epitaxy, *Appl. Surf. Sci.*, 1992, **60–61**, 592.

Open Access Article. Published on 24 April 2026. Downloaded on 5/15/2026 8:48:04 PM. This article is licensed under a Creative Commons Attribution 3.0 Unported Licence.

369 H. Matsunami and T. Kimoto, Step-controlled epitaxial growth of SiC: High quality homoepitaxy, *Mater. Sci. Eng., R*, 1997, **20**, 125.

370 H. Pedersen, S. Leone, A. Henry, F. C. Beyer, V. Darakchieva and E. Janzén, Very high growth rate of 4H-SiC epilayers using the chlorinated precursor methyltrichlorosilane (MTS), *J. Cryst. Growth*, 2007, **307**, 334.

371 (*a*) S. Nishino, T. Miyanagi and Y. Nishio, Epitaxial Growth of SiC on α-SiC Using Si_2Cl_6+C_3H_8+H_2 System, *Mater. Sci. Forum*, 1998, **264–268**, 139; (*b*) T. Rana, M. Chandrashekhar and T. S. Sudarshan, Vapor phase surface preparation (etching) of 4H–SiC substrates using tetrafluorosilane (SiF_4) in a hydrogen ambient for SiC epitaxy, *J. Cryst. Growth*, 2013, **380**, 61.

372 S. Kamiyama, T. Miura and Y. Nara, Comparison between SiO_2 films deposited by atomic layer deposition with $SiH_2[N(CH_3)_2]_2$ and $SiH[N(CH_3)_2]_3$ precursors, *Thin Solid Films*, 2006, **515**, 1517.

373 T. Faraz, M. van Drunen, H. C. M. Knoops, A. Mallikarjunan, I. Buchanan, D. M. Hausmann, J. Henri and W. M. M. Kessels, Atomic Layer Deposition of Wet-Etch Resistant Silicon Nitride Using Di(sec-butylamino) silane and N_2 Plasma on Planar and 3D Substrate Topographies, *ACS Appl. Mater. Interfaces*, 2017, **9**, 1858.

374 (*a*) J. D. Ferguson, E. R. Smith, A. W. Weimer and S. M. George, ALD of SiO_2 at Room Temperature Using TEOS and H_2O with NH_3 as the Catalyst, *J. Electrochem. Soc.*, 2004, **151**, G528; (*b*) V. Y. Vasilyev, Evaluation of Low Temperature TEOS-Ozone Silicon Dioxide Thin Film CVD under Sub-Atmospheric Pressure Using Consecutively Pulsed Reactant Injection, *ECS J. Solid State Sci. Technol.*, 2015, **4**, N3164–N3167.

375 (*a*) D. B. Mitzi, Solution Processing of Chalcogenide Semiconductors via Dimensional Reduction, *Adv. Mater.*, 2009, **21**, 3141; (*b*) D. B. Mitzi, L. L. Kosbar, C. E. Murray, M. Copel and A. Afzali, High-mobility ultrathin semiconducting films prepared by spin coating, *Nature*, 2004, **428**, 299.

376 M. Gerwig, A. S. Ali, D. Neubert, S. Polster, U. Böhme, G. Franze, M. Rosenkranz, A. Popov, I. Ponomarev, M. P. M. Jank, C. Viehweger, E. Brendler, L. Frey, P. Kroll and E. Kroke, From Cyclopentasilane to Thin–Film Transistors, *Adv. Electron. Mater.*, 2021, **7**, 2000422.

377 A. R. Wolff and R. West, Photoinitiation of vinyl polymerization by polysilanes, *Appl. Organomet. Chem.*, 1987, **1**, 7.

378 R. D. Miller and J. Michl, Polysilane high polymers, *Chem. Rev.*, 1989, **89**, 1359.

379 (*a*) T. Shimoda, *Nanoliquid Processes for Electronic Devices*, Springer Singapore, Singapore, 2019; (*b*) T. Masuda, Y. Matsuki and T. Shimoda, Pyrolytic transformation from polydihydrosilane to hydrogenated amorphous silicon film, *Thin Solid Films*, 2012, **520**, 6603.

380 T. Shimoda and T. Masuda, Liquid silicon and its application in electronics, *Jpn. J. Appl. Phys.*, 2014, **53**, 02BA01.

381 M. Trifunovic, T. Shimoda and R. Ishihara, Solution-processed polycrystalline silicon on paper, *Appl. Phys. Lett.*, 2015, 106.

382 H. Frey, R. Lauth, H. Khan, N. Eisenreich and A. Koleczko, Deposition of Silicon Films from Liquid Cyclopentasilane Precursors Using High Pressure Spray System, *Phys. Sci. Int. J.*, 2017, **14**, 1.

383 T. Masuda, M. Nakayama, K. Saito, H. Katayama and A. Terakawa, Inkjet Printing of Liquid Silicon, *Macromol. Rapid Commun.*, 2020, **41**, e2000362.

384 T. Masuda, H. Takagishi, K. Yamazaki and T. Shimoda, Direct Imprinting of Liquid Silicon, *ACS Appl. Mater. Interfaces*, 2016, **8**, 9969.

385 Z. Shen, T. Masuda, H. Takagishi, K. Ohdaira and T. Shimoda, Fabrication of high-quality amorphous silicon film from cyclopentasilane by vapor deposition between two parallel substrates, *Chem. Commun.*, 2015, **51**, 4417.

386 G. R. S. Iyer, E. K. Hobbie, S. Guruvenket, J. M. Hoey, K. J. Anderson, J. Lovaasen, C. Gette, D. L. Schulz, O. F. Swenson, A. Elangovan and P. Boudjouk, Solution-based synthesis of crystalline silicon from liquid silane through laser and chemical annealing, *ACS Appl. Mater. Interfaces*, 2012, **4**, 2680.

387 (*a*) A. P. Cádiz Bedini, B. Klingebiel, M. Luysberg and R. Carius, Sonochemical synthesis of hydrogenated amorphous silicon nanoparticles from liquid trisilane at ambient temperature and pressure, *Ultrason. Sonochem.*, 2017, **39**, 883; (*b*) A. P. Cádiz Bedini, S. Muthmann, J. Allgaier, K. Bittkau, F. Finger and R. Carius, Liquid hydridosilane precursor prepared from cyclopentasilane via sonication at low temperatures without the action of light, *Ultrason. Sonochem.*, 2017, **34**, 289; (*c*) *TechConnect briefs 2017*, ed. M. Laudon and B. Romanowicz, TechConnect, Danville, CA, U.S.A., 2017, vol. 1.

388 F. Haase, B. Lim, A. Merkle, T. Dullweber, R. Brendel, C. Günther, M. H. Holthausen, C. Mader, O. Wunnicke and R. Peibst, Printable liquid silicon for local doping of solar cells, *Sol. Energy Mater. Sol. Cells*, 2018, **179**, 129.

389 (*a*) M. Holthausen, M. Roccaro, A. Pougin, D. Schmitt, J. Zoellner, C. Daeschlein and O. Wunnicke, EP3702397B1, 2021; (*b*) M. Holthausen, M. Roccaro, A. Pougin, D. Schmitt, J. Zöllner, C. Däschlein and O. Wunnicke, EP3702397A1, 2020; (*c*) H. Stüger, V. S. Christopoulos, M. Haas, O. Wunnicke, M. Roccaro and M. Holthausen, WO2022063680A1, 2022; (*d*) H. Stüger, M. Haas, O. Wunnicke, M. D. Malsch and M. Holthausen, EP3590889A1, 2020.

390 T. Masuda, A. Iwasaka, H. Takagishi and T. Shimoda, Polymeric precursor for solution-processed amorphous silicon carbide, *J. Mater. Chem. C*, 2015, **3**, 12212.

 This journal is © the Partner Organisations 2026